EVALUATION OF PRACTICE-ORIENTED NONLINEAR ANALYSIS METHODS FOR SEISMIC PERFORMANCE ASSESSMENT

by

Göktürk ÖNEM

B.S., Civil Engineering, Yıldız Technical University, 1997

M.S., Earthquake Engineering, Boğaziçi University, 2002

Submitted to the Kandilli Observatory and
Earthquake Research Institute in partial fulfillment of
the requirements for the degree of
Doctor of Philosophy

Graduate Program in Earthquake Engineering
Boğaziçi University
2008

EVALUATION OF PRACTICE-ORIENTED NONLINEAR ANALYSIS METHODS FOR SEISMIC PERFORMANCE ASSESSMENT

APPROVED BY:

Prof. M. Dr. Nuray AYDINOĞLU (Thesis Supervisor)	.....
Prof. Dr. Mustafa ERDİK	.....
Prof. Dr. Atilla ANSAL	.....
Prof. Dr. Erkan ÖZER	.....
Assoc. Prof. Dr. Eser DURUKAL	.....

DATE OF APPROVAL: 18.07.2008

To my dear wife Didem Zeynep ÖNEM

ACKNOWLEDGEMENTS

I would like to express my deepest gratitude to my academic advisor, Prof. Dr. M. Nuray Aydınoğlu for his personal and academic support during my years at Boğaziçi University. It has been a great privilege to be his student and to work with him under his great engineering vision. I would like to thank to him for his understanding and guidance during all stages of this study.

My sincere appreciation is due to my dear wife Zeynep who supported me all the way through by undertaking many responsibilities in our life. My sincere thanks are also due to my parents for their encouragement and support through my whole educational life.

I would like to express my special thanks to my friend Umut Utku Celep for our valuable technical discussions with him, which have contributed to this dissertation.

I would like to also thank Yavuz Kaya and Cüneyt Tüzün, my colleagues from Earthquake Engineering Department of Boğaziçi University, for their friendship and assistance.

ABSTRACT

EVALUATION OF PRACTICE-ORIENTED NONLINEAR ANALYSIS METHODS FOR SEISMIC PERFORMANCE ASSESSMENT

In the last decade, nonlinear static analyses based on pushover analysis have been developed as a simplified nonlinear analysis tool within the context of performance based design approach (ATC 40 and FEMA 356). Since nonlinear static analyses provide designers a practical analysis approach in estimating inelastic seismic demands, these methods have been widely used in engineering practice. On the other hand, recent research have clearly shown that simplified nonlinear static analyses, which consider single mode behavior of the structures, have serious limitations for high-rise buildings or buildings irregular in plan, where higher modes effects become important. In order to overcome these limitations and to enhance the feasibility of the pushover analysis in practice, a number of multi-mode pushover analysis methods have been developed. It should be noted that pushover analysis has not been provided with a firm theoretical basis and those methods are therefore based on various assumptions.

In this study, development and codification of nonlinear static analysis as a tool for performance based assessment have been summarized. *Piecewise linear representation of single-mode pushover analysis*, which provides a non-iterative pushover analysis technique with an adaptive load or displacement pattern, has been presented in detail.

A number of multi-mode pushover analysis methods have been investigated in detail and classified with respect to their assumptions. The emphasis of this study is to evaluate the validity of those assumptions and their limitations in terms of practical applicability. In addition, a parametric study is carried out in order to evaluate and understand the limitations of single-mode and multi-mode pushover analysis methods based on various assumptions.

It has been observed that some multi-mode pushover analysis methods deal with estimating only structural capacity, resulting in a conventional pushover curve where higher modes effects are somehow considered. Thus these multi-mode pushover analysis methods can be regarded only as capacity estimation tools. However, the main objective of the nonlinear static analysis should be the estimation of the seismic demands under a given earthquake ground motion. It is interesting to observe that the number of multi-mode pushover analysis methods achieving this objective is very limited. Determination of relative modal contributions at each pushover step with an appropriate modal scaling procedure is a critical point in a multi-mode pushover analysis As a result of the investigation of multi-mode pushover analysis methods, it has been observed that there are mainly two types of modal scaling procedures generally adopted: (a) scaling based on instantaneous inelastic spectral displacements, (b) scaling based on instantaneous elastic spectral displacements or pseudo-accelerations. It has been identified that multi-mode pushover methods adopting modal scaling procedure based on instantaneous elastic spectral quantities would not work when P-delta effects are considered.

The effectiveness of multi-mode pushover analyses has been tested for reinforced concrete frame and dual systems by comparing the results obtained from inelastic time history analysis (ITHA). Analysis results indicated that multi-mode pushover analyses, which combine multi-mode effects at each pushover step, provides relatively good estimates of inter-story drift and plastic rotation demands in the lower and middle stories of taller frames. At the upper story levels, where higher mode effects are significant, Incremental Response Spectrum Analysis (IRSA) developed by Aydınoğlu (2003) and Modal Pushover Analysis (MPA) developed by Chopra and Goel (2001) give more accurate results as compared to the other methods. It has been observed that when P-delta effects are included in the analyses, the discrepancy between the results obtained from ITHA and all pushover analyses tends to increase as compared to the case without P-delta effects.

For dual systems, multi-mode pushover analyses, which combine multi-mode effects at each pushover step, predicts reasonably well the changing height-wise variation of plastic rotation demands in the beams with building height, particularly for dual systems with smaller wall shear ratio. IRSA significantly predicts much more accurate plastic

rotation estimates with respect to all other multi-mode pushover methods. Single-run multi-mode pushover analysis methods with single-load or single-displacement patterns based on combined multi-mode loading significantly underestimate shear force demands in the shear wall elements. Additionally, it has been observed that multi-mode pushover analysis methods provide much more accurate estimate of plastic hinge rotations and their locations at the base of the shear walls as compared to FEMA 356 lateral load distributions. Single-mode adaptive pushover analysis can predict plastic rotation demands accurately at the base of the shear walls in spite of the fact that only single mode was considered, whereas invariant single-mode pushover analysis cannot predict. This shows that adaptive pushover analysis provides a more reliable analysis technique, which is able to capture changing dynamic characteristics of dual systems and eventually plastic rotation demands at the base of the shear walls.

ÖZET

DEPREM PERFORMANS ANALİZLERİ İÇİN UYGULAMAYA YÖNELİK NONLİNEER ANALİZ METODLARININ DEĞERLENDİRİLMESİ

Son on yılda, performansa dayalı tasarım çerçevesi içerisinde itme analizine (pushover) dayalı basitleştirilmiş nonlineer statik analiz yöntemleri geliştirilmiştir (ATC 40 ve FEMA 356). Nonlineer statik yöntemler mühendislerin nonlineer deprem istemlerini pratik bir yaklaşımla tahmin edebilmelerini sağladığı için bu yöntemler pratik mühendislikte yaygın olarak kullanılmışlardır. Diğer taraftan son yıllarda yapılan araştırmalar tek bir titreşim modunu dikkate alan basitleştirilmiş itme analizi yönteminin çok modlu davranışın etkin olduğu çok katlı binalarda ve planda düzensizliği bulunan binalarda uygulanmasının sakıncalı olduğunu açıkça ortaya koymaktadır. Bu nedenle artımsal itme analizinin sakıncalarını aşmak ve pratik mühendislikte uygulanabilirliğini geliştirmek amacı ile yüksek modların etkisini dikkate alan çok modlu itme analizi yöntemleri geliştirilmiştir. Diğer yandan, itme analizinin teorik temelleri tam manası ile henüz ortaya konulmamıştır ve bu nedenle bu yöntemler farklı varsayımlar içermektedirler.

Bu çalışmada, itme analizi yönteminin gelişimi ve deprem yönetmeliklerine girmiş itme analizi yöntemleri özetlenmiştir. Değişken eşdeğer deprem yükü veya yerdeğiştirmeler altında ardışık bir yaklaşım içermeyen tek modlu bir itme analizi metodu ayrıntılı bir biçimde sunulmuştur.

Birden fazla çok modlu itme analizi metodu detaylı bir şekilde incelenmiş ve kabul ettikleri varsayımlara göre sınıflandırılmıştır. Bu çalışmada, çok modlu itme analizi yöntemlerinde kabul edilen varsayımların geçerliliği ve uygulamadaki sakıncaları üzerinde durulmuştur. Ayrıca, değişik varsayımlar içeren çok modlu ve tek modlu itme analizi yöntemlerini değerlendirmek ve sakıncalarını anlamak amacıyla parametrik bir çalışma yürütülmüştür.

Görülmüştür ki bazı çok modlu itme analizi yöntemleri sadece yüksek modların etkisini içeren *global itme eğrisini* elde etmeyi amaçlamaktadırlar. Ancak, nonlineer statik analiz yöntemlerinin temel hedefi deprem istemlerini verilen bir deprem kaydı için tahmin etmek olmalıdır. İlginçtir ki bu hedefe ulaşmayı amaçlayan çok modlu itme analizi yöntemlerinin sayısı çok kısıtlıdır. Çok modlu itme analizi yönteminde önemli noktalardan bir tanesi modal katkıların göreli oranlarının her itme adımında belirli bir *modal ölçeklendirme* yöntemine göre belirlenmesidir. Çok modlu itme analizlerinde genel olarak benimsenen iki farklı modal ölçeklendirme metodu olduğu görülmüştür. Bunlar nonlineer spektral yerdeğiştimeye göre ve elastik spektral yerdeğiştirme ya da sözde-ivmeye göre modal ölçeklendirme yöntemleridir. Tespit edilmiştir ki elastik spektral değerlere göre modal ölçeklendirme metodunu kullanan yöntemlerin P-delta etkisi dikkate alındığında analizleri gerçekleştirilememektedir.

Göz önüne alınan çok modlu itme analizi yöntemlerinin yeterlilikleri iki boyutlu betonarme çerçeve ve betonarme perde/çerçeveli yapısal sistemler için zaman tanım alanında doğrusal olmayan analizlerden elde edilen sonuçlara göre test edilmiştir. Analiz sonuçları göstermiştir ki her itme analizi adımında modal katkıları birleştiren çok modlu artımsal itme analizi yöntemleri çok katlı çerçeve sistemlerde alt ve orta katlarda maksimum göreli kat ötelemeleri ve kirişlerdeki plastik dönme istemlerini daha iyi tahmin etmektedirler. Yüksek modların etkin olduğu üst katlarda ise Aydınoğlu (2003) tarafından geliştirilen *Artımsal Mod Birleştirme Analizi* (ARSA) ve Chopra ve Goel (2001) tarafından geliştirilen *Modal Pushover Analizi* (MPA) diğer yöntemlere göre daha iyi sonuçlar vermektedir. Yapılan analizlerde P-delta etkisi dikkate alındığında, bütün itme analizi yöntemlerinin hata oranları P-delta etkisinin dikkate alınmadığı duruma göre artmaktadır.

Perde/çerçeve sistemlerde, her itme analizi adımında modal katkıları birleştiren çok modlu itme analizi yöntemleri özellikle perde taban kesme kuvveti oranı düşük olan perde/çerçeve sistemlerde kirişlerdeki plastik dönme istemlerini ve bina boyunca değişimini oldukça iyi tahmin edebilmektedirler. ARSA metodu diğer çok modlu itme analizi yöntemlerine göre plastik dönme değerlerini önemli ölçüde daha doğru tahmin etmektedir. Modal eşdeğer deprem yüklerinin kombinasyonu sonucunda elde edilen tek deprem yükü dağılımı ya da tek yerdeğiştirme dağılımı altında yapılan çok modlu itme

analizleri perde boyunca kesme kuvveti istemlerini tahmin edememektedirler. Ayrıca, görülmüştür ki çok modlu itme analizleri perde duvarlarda plastik dönme değerlerini ve bina boyunca yerlerini FEMA 356'ya uygun yatay yük dağılımları altında yapılan itme analizlerine göre daha iyi tahmin etmektedirler. Değişken yük dağılımına göre yapılan tek modlu itme analizi, perde tabanında plastik dönme istemlerini tek mod dikkate alınmasına rağmen kabul edilebilir bir hassasiyetle tahmin edebilirken sabit yük dağılımıyla yapılan itme analizi tahmin edememektedir. Bu durum değişken yük altında yapılan itme analizinin perde/çerçeve sistemlerde değişen dinamik karakteristikleri yakalayabilen ve plastik dönme değerlerini tahmin edebilen daha güvenilir bir itme analizi tekniği olduğunu göstermektedir.

TABLE OF CONTENTS

LIST OF FIGURES

LIST OF TABLES

LIST OF SYMBOLS

$a_1^{(i)}$	Modal pseudo-acceleration for the first mode at the end of (i)'th pushover step
$a^{(i)}$	Spectral acceleration at the end of (i)'th pushover step
b	Thickness of shear wall
C_0	Modification factor that relates the roof displacement of MDOF system and the equivalent SDOF displacement
C_1	Modification factor that represents the relation between the elastic spectral displacement and inelastic spectral displacement of an equivalent SDOF system
C_2	Modification factor to represent the effect of pinched hysteresis shape, cyclic stiffness degradation and strength deterioration on maximum displacement response
C_3	Modification factor that takes into account the displacement amplification caused by the P-delta effects
$d_1^{(i)}$	Modal displacement for the first mode at the end of (i)'th pushover step
$d^{(i)}$	Spectral displacement at the end of (i)'th pushover step
EI_{eff}	Effective flexural stiffness of the structural elements
EI_{gross}	Gross section flexural stiffness of the structural elements
$\tilde{F}^{(i)}$	Cumulative scale factor at the end of (i)'th pushover step
$\mathbf{I}_x$	Influence vector
l_w	Length of shear wall
$\mathbf{M}$	Mass matrix
$M_{\text{eff}}^{(i)}$	Effective modal mass for the single-combined mode at the (i)'th pushover step
$\bar{M}_{x1}^{(1)}$	Participating mass for the first mode in x direction at the first pushover step
$M_1^{(1)}$	Participating mass for the first mode at the first pushover step

$M_{j,1}^{(i)}$	Moment acting on section (j) for the first mode at the (i)'th pushover step
M_{jp}	Yield bending moment of section (j)
$\bar{\mathbf{m}}_1^{(i)}$	Participating modal masses for the first mode at the (i)'th pushover step
N_{jp}	Axial force corresponding to M_{jp}
$N_{j,1}^{(i)}$	Axial force acting on section (j) for the first mode at the (i)'th pushover step
N_D	Axial force acting on a column due to gravity loads
N_C	Axial force capacity of a column
R	Strength reduction factor
$\tilde{r}^{(i)}$	Incremental response quantity for $\Delta d_1^{(i)} = 1$ at the (i)'th pushover step
$\bar{r}^{(i)}$	Incremental response quantity for $\Delta a_1^{(i)} = 1$ at the (i)'th pushover step
$r^{(i)}$	Cumulative response quantity at the end of the (i)'th pushover step
$\bar{r}$	Sample mean value
$S_{aen}^{(i)}$	Instantaneous elastic spectral pseudo-acceleration for the n'th mode
$S_{aen}^{(1)}$	Initial elastic spectral pseudo-acceleration for the n'th mode
S_{ay}	Yield spectral pseudo-acceleration
$S_{di,1}$	Inelastic spectral displacement for the first mode
$S_{de,1}$	Elastic spectral displacement for the first mode
$S_{den}^{(i)}$	Instantaneous elastic spectral displacement for the n'th mode
$S_{den}^{(1)}$	Initial elastic spectral displacement for the n'th mode
S_{dy}	Yield spectral displacement
T_1	The first natural vibration period of structural system at the first pushover step

T_S	Characteristic period of smoothed elastic response spectrum
T_e	Effective fundamental period of structural system
$\bar{u}_{k,1}^{(i)}$	Displacement component at the k'th degree-of-freedom
$\mathbf{u}^{(i)}$	Displacement vector of MDOF system at the (i)'th pushover step
$\tilde{\mathbf{u}}_n^{(i)}$	Instantaneous modal displacement vector at the (i)'th pushover step for the n'th mode
$\alpha_{j,s}$	Coefficients defining the yield line (s) for section (j)
α_s	The ratio between shear force at the base of shear wall and total base shear force
$\beta_{j,s}$	Coefficients defining the yield line (s) for section (j)
$\Delta a_1^{(i)}$	Modal pseudo-acceleration increment for the first mode at the (i)'th pushover step
$\Delta a_n^{(i)}$	Modal pseudo-acceleration increment for the n'th mode at the (i)'th pushover step
$\Delta d_1^{(i)}$	Modal displacement increment for the first mode at the (i)'th pushover step
$\Delta d_1^{(p)}$	Modal displacement increment for the first mode at the last pushover step
$\Delta d_n^{(i)}$	Modal displacement increment for the n'th mode at the (i)'th pushover step
$\Delta F^{(i)}$	Incremental scale factor at the (i)'th pushover step
$\Delta \tilde{F}^{(i)}$	Incremental scale factor at the (i)'th pushover step
$\mathbf{\Delta f}_1^{(i)}$	Incremental force vector for the first mode at the (i)'th pushover step
$\mathbf{\Delta f}_1^{(1)}$	Incremental invariant force vector for the first mode
$\mathbf{\Delta f}_n^{(i)}$	Incremental force vector for the n'th mode at the (i)'th pushover step
$\mathbf{\Delta u}_n^{(i)}$	Incremental displacement vector for the n'th mode at the (i)'th pushover step
$\Delta r^{(i)}$	Generic incremental response quantity at the (i)'th pushover

	step
$\Delta u_{N,1}^{(i)}$	Roof displacement increment for the first mode at the (i)'th pushover step
$\mathbf{\Delta u}_1^{(i)}$	Incremental displacement vector for the first mode at the (i)'th pushover step
$\Delta V_{x1}^{(i)}$	Base shear increment for the first mode at the (i)'th pushover step in x direction
δ_t	Target displacement at the roof level of MDOF system
$\mathbf{\Phi}_1^{(i)}$	Instantaneous mode shape vector for the first mode
$\mathbf{\Phi}_n^{(i)}$	Instantaneous mode shape vector for the n'th mode
$\Gamma_{x1}^{(i)}$	Participation factor for the first mode at the (i)'th pushover step
$\Gamma_{xn}^{(i)}$	Participation factor for the n'th mode at the (i)'th pushover step
$\Gamma^{(i)}$	Participation factor at the (i)'the pushover step based on single-combined mode shape
μ	Ductility factor
$\mathbf{\Psi}^{(i)}$	Instantaneous single-combined mode shape vector of MDOF system
σ	Standard deviation
$\omega_1^{(i)}$	Instantaneous natural circular frequency for the first mode at the (i)'th pushover step

1. INTRODUCTION

1.1. Motivation for This Study

The design objectives of the current seismic design codes aim at providing no structural damage in minor earthquakes, damage control in moderate earthquakes and life safety and collapse prevention in major earthquakes. The design criterion is defined by a strength limit associated with a given overall ductility capacity of a specified type of structure. As a result of such a design procedure, expected damage cannot be quantified and therefore it is obscure whether the building satisfies the design objective. It is observed that although buildings designed according to present seismic codes satisfy the life safety performance objective in major earthquakes, the level of damage, cost of repair and eventually business interruption causes significant economic losses. Thus, there is a widely accepted agreement among the researchers and practitioners that future seismic design codes should be based on explicit design objectives that can be quantified, considering multiple performance and hazard levels. Accordingly, seismic design codes have been under revision in recent years, with the emphasis changing from strength-based design to deformation-based design.

Deformation-based design has gain a great prominence together with the extensive research in recent years. Now it has become clear that seismic performance of structures depends on the inelastic deformation capacity of the structural systems, rather than strength capacity, hence definition of performance criteria through displacement and deformation limits is more effective way to control damage state of the structures. *Performance-based design* concept provides a suitable framework for this purpose. Performance-based design describes quantitative performance levels that are essentially defined in terms of deformation limit states corresponding to each performance level. In order to evaluate inelastic deformation demands, such as inter-story drifts and plastic rotations at the component levels, it is clear that there is a need for a nonlinear analysis tool. However, recognizing the limitation of today's knowledge and practice, a simple but reliable nonlinear analysis tool is needed. Accordingly, nonlinear static analysis based on pushover

analysis has become a preferred analysis method in engineering practice due to its simplicity compared to the nonlinear time history analysis.

Pushover analysis is based on the assumption that structural response can be represented by the equivalent single-degree-of-freedom (SDOF) system. Nonlinear static procedure presented in the pioneering documents ATC40 (1996), FEMA 273 (1997) and FEMA 356 (2000) is essentially based on a single-mode pushover analysis. However, pushover analysis based on single-mode response can be used only for low-rise and mid-rise structures where structural behavior can be represented dominantly by a fundamental mode behavior. Thus, for the buildings where higher modes are significant, single-mode pushover analysis cannot be implemented. In the last decade many researchers have proposed advanced pushover analysis procedures, which take into account the higher mode effects (Gupta and Kunnath, 2000, Aydınoğlu, 2003, Chopra and Goel, 2001, Elnashai, 2001, Antoniou *et al*., 2002, Antoniou and Pinho, 2004[a,b], Casarotti and Pinho, 2007). Since pushover analysis has not been provided with a firm theoretical base, those methods are based on various assumptions. The existence of several methods with different assumptions requires a detailed comparative evaluation in order to understand their applicability in different conditions. This is the basic motivation for this study.

1.2. Objectives and Scope

The primary objective of this study is to classify the multi-mode pushover methods with respect to the assumptions inherent in these methods and to evaluate the validity of those assumptions and their limitations in terms of practical applicability. In addition, a parametric study is carried out in order to evaluate and understand the limitations of single-mode and multi-mode pushover analysis methods based on various assumptions. Specifically the objectives are to

- present a piecewise linear representation of invariant and adaptive single-mode pushover analysis,
- summarize multi-mode pushover procedures developed by several researchers in detail and identify and discuss underlying assumptions in these procedures,

- conduct a parametric study in accordance with common engineering practice; for this purpose design two-dimensional reinforced concrete frame and dual systems in accordance with Turkish Seismic Design Code (2007) so as to obtain structural systems with realistic strength and stiffness distribution,
- evaluate single-mode and multi-mode pushover methods with respect to nonlinear time history analysis for regular reinforced concrete frame systems in estimating seismic demands for a wide range of building heights and strength levels,
- evaluate single-mode and multi-mode pushover methods with respect to nonlinear time history analysis for reinforced concrete dual systems with different heights and wall shear ratios.

In Chapter 2, development and codification of Nonlinear Static Procedure is summarized. In addition, a piecewise linear representation of adaptive and invariant single-mode pushover analysis developed by Aydınoğlu (2003) is presented. Multi-mode pushover methods proposed by Gupta and Kunnath (2000), Aydınoğlu (2003), Chopra and Goel (2001), Elnashai (2002), Antoniou *et al*. (2002), Antoniou and Pinho (2004[a,b]) and Casarotti and Pinho (2007) have been explained in detail and discussed in terms of their essential assumptions.

Chapter 3 focuses on structural systems and ground motions used for the comparative evaluation of nonlinear static procedures and inelastic time history analysis. For this purposes, mathematical models and design of regular frame and dual systems that are used in the comparative evaluation are presented in Chapter 3. In addition, selection and scaling of ground motions in order to obtain response spectrum compatible ground motions are explained.

Chapter 4 covers the evaluation of single-mode and multi-mode nonlinear static analyses for frame systems. Story displacements profiles, inter-story drift profiles and plastic rotations at the central beams obtained from the non-linear static analyses with or without P-delta effects are compared with those obtained from inelastic time history analyses. A similar comparative evaluation study is carried out in Chapter 5 for dual systems. In addition to the story displacement profiles, inter-story drifts profiles and plastic rotation demands, wall shear force demands and wall plastic rotation demands obtained

from the nonlinear static analyses and inelastic time history analyses are compared. In Chapter 6, conclusions obtained from the comparative study for frame and dual systems considered in this study are summarized.

2. DEVELOPMENT OF NONLINEAR STATIC ANALYSIS AS A TOOL FOR PERFORMANCE BASED ASSESSMENT

2.1. Inception of Deformation-Based Seismic Assessment Procedure

Recent earthquakes, such as 1994 U.S. Northridge, 1995 Japan Hyogo-ken Nambu and 1999 Turkey Kocaeli earthquakes have demonstrated that seismic performance of a considerable amount of existing structures is unsatisfactory. Evaluation and upgrading of existing buildings have become a primary concern in engineering communities. Moreover, it has been observed in the past earthquakes that structural and non-structural damage are directly related to displacements (or drift) and deformations imposed by the earthquake on structures. Therefore, it is widely recognized that structural damage can be controlled efficiently by displacement and deformation limits rather than strength limits as adopted in conventional strength-based design.

In conventional strength-based design, required strength level to be resisted by the inelastic system is obtained directly by reducing the elastic strength by a constant factor. This factor, referred to as strength reduction factor, R, is determined through the assumption that the structure has a given global displacement ductility capacity, which can be related to the strength reduction factor based on the equal displacement rule. This approach permits the designers to use simple linear analysis providing demand/capacity check only in terms of strength. Lateral displacements obtained from the linear analysis under reduced seismic forces are amplified to account for the reduction of applied forces and compared with the acceptable limits. This procedure has the following drawbacks in assessing the performance of existing structures:

- Available strength and ductility capacity of an existing structure cannot be accurately predicted by a presumed strength reduction factor, R, given in seismic codes.
- Inelastic deformation demands on the structural components beyond their elastic limits cannot be estimated quantitatively.

- Force and story drift distribution may change considerably due to the yielding of structural elements. This change cannot be estimated by a linear elastic analysis and a strength reduction factor.
- Excessive deformation demands in the critical regions of a structure that may cause a story mechanism in the first or the upper floors cannot be determined by an elastic analysis.

Obviously, in order to assess the performance of existing structures, there is a need for a reliable and practical evaluation procedure. Particularly for the evaluation of existing building stock, where behavioral information obtained from the conventional strength-based design is limited, deformation-based approach provides a more transparent assessment methodology that enables the practicing engineers to understand the available inelastic capacity of the existing buildings. However this requires a nonlinear analysis tool to quantify the inelastic deformation and force demands. In the last decade, a number of guidelines providing seismic evaluation and retrofit design procedures for engineering practice have been published, such as Vision 2000 (SEAOC, 1995), ATC 40 (1996) and FEMA 273 (1997). These publications involve performance-based assessment procedures based on explicit and quantifiable performance criteria considering multiple performance and hazard levels. Performance criteria have been defined in terms of deformation (damage) limit states, which are expected to be achieved when the structure is subjected to an earthquake of a specified intensity. In addition, these documents present alternative analysis methods providing explicit consideration of expected seismic demands associated with the available capacities of the structural members. Thus, these documents have promoted deformation-based evaluation and design procedures and hence use of nonlinear analysis tools to evaluate the seismic performance of buildings expected to deform in the nonlinear range.

Nonlinear dynamic analysis appears to be the best choice as a tool for the quantification of inelastic behavior of structural systems as long as earthquake ground motion records are available. Implementation of this analysis method requires a rigorous selection of earthquake ground motions that account for the differences in frequency characteristics, severity, ground motion duration and fault distance. Furthermore, this analysis requires the capability to model cyclic load-deformation characteristics of the

structural components. Selection of appropriate hysteretic model is an important issue that may significantly affect the analysis results particularly when the strength deterioration and P-delta effects are considered in the analysis (Priestley, 1995, Gupta and Krawinkler, 1998, Medina and Krawinkler, 2003). In addition, complexities in the definition of damping and the computational effort associated with the numerical integration process are some of the major factors that make this method difficult to perform in practice. Besides, interpretation of results at the end of the analyses requires a statistical evaluation considering variability of the records. Hence, there is a wide spread recognition in engineering community that nonlinear dynamic analysis is not matured enough for engineering practice (Priestley, 2000). These drawbacks of nonlinear dynamic analysis invite a simpler but a reliable nonlinear analysis tool. In this regard, Nonlinear Static Procedure (NSP), commonly referred to as pushover analysis, is the most preferable and widely accepted nonlinear analysis method among design engineers since it avoids the complexity of the nonlinear dynamic analysis. Representation of design earthquake using smoothed response spectra rather than ground motions is the preferred choice in engineering practice. Utilization of pushover analysis in conjunction with the response spectra to estimate the seismic demands enhance the practical applicability of pushover analysis for design engineers who are familiar with the Response Spectrum Analysis based on elastic response spectra. Furthermore, available documents *e.g*., ATC40 (1996), FEMA 356 (2000) and structural analysis programs with nonlinear capabilities encourage the use of NSP for performance based assessment with its comparative simplicity.

2.2. Early Development and Codification of Nonlinear Static Procedures

From the original definition, pushover analysis has been particularly referred to as a nonlinear capacity estimation tool and generally called as “capacity analysis”, which is performed under an invariant load pattern consistent with the fundamental mode. Under this load pattern, the structure is pushed until a selected control point (generally located at the roof level of a building) reaches a predetermined displacement value, which may eventually correspond to a collapse state. Thus, available capacity of the structure in terms of both displacement and strength can be estimated. With the introduction of the Capacity Spectrum Method (CSM) developed by Freeman (1978, 1998), pushover analysis can also be used as a demand estimation tool. In this method, seismic demand represented by the

response spectra and the capacity obtained from the pushover analysis are compared in the same graph plotted with acceleration on the vertical axis and displacement on the horizontal axis, where capacity is represented by an inelastic equivalent single degree of freedom (SDOF) system. In order to evaluate inelastic displacement demand, elastic response spectrum is reduced by an equivalent viscous damping ratio approximately estimated from the hysteretic energy dissipated by an equivalent inelastic SDOF system. A similar method proposed by Fajfar and Fischinger (1988), called the N2 method, has also utilized pushover analysis, but using inelastic response spectra related to the displacement ductility demand. The N2 method is a variant of the CSM with a sound physical basis of inelastic demand spectra (Fajfar, 2000). A study conducted by Chopra and Goel (1999) has shown that displacement demand estimation using inelastic response spectra provides more accurate results with respect to Capacity Spectrum Method, particularly for acceleration- and displacement-sensitive regions of the design response spectrum.

ATC 40 (Seismic Evaluation and Retrofit of Concrete Buildings, 1996) has been published to provide an assessment and rehabilitation methodology for reinforced concrete buildings in California, U.S. This document emphasized the use of pushover analysis based on Capacity Spectrum Method. Pushover analysis described in ATC 40 consists of lateral load distribution proportional to the fundamental mode shape. As a result of the analysis carried out under the invariant lateral load distribution, nonlinear force-displacement relation of a multi-degree-of-freedom (MDOF) system is obtained and then converted to the so-called capacity diagram of an equivalent single-degree-of-freedom (SDOF) system in order to estimate inelastic displacement demand with a graphical representation as implemented in CSM.

FEMA 273/274 (NEHRP Guidelines for Seismic Rehabilitation of Buildings, 1997) presents a prescriptive evaluation and design procedure in the framework of performance based approach. These documents are evolved later into a pre-standard (FEMA 356, 2000) by the American Society of Civil Engineers (ASCE). Nonlinear static procedure described in FEMA 356 consists of two groups of vertical load distribution. In the first group three different load distributions are prescribed. One of these distributions is proportional with the fundamental mode shape. The other distribution is consistent with code-based seismic force distributions. These two distributions are recommended when at least 75% mass

participation is provided in the first mode. The third load distribution results from story shear forces, which are obtained from a linear response spectrum analysis (RSA) with sufficient modes to capture 90% modal mass participation. The last one is recommended for the structures whose fundamental period is longer than 1 second. In the second group of lateral load distribution, there is a uniform load pattern, which presumably accounts for soft-story mechanism. The aim of using at least two types of vertical load distributions is to capture a probable variation of lateral force distribution during an earthquake. Pushover analysis is performed with the invariant load patterns mentioned above until the roof displacement reaches to a displacement value called *target displacement*, which is estimated through *Displacement Coefficient Method*. This method utilizes inelastic displacement response spectrum defined through C_1 coefficient, which represents the relation between the elastic spectral displacement and inelastic spectral displacement of an equivalent SDOF system, depending on the initial period and the strength level of the SDOF system.

$$\begin{aligned} C_1 &= 1 && T_e \geq T_S \\ C_1 &= \left[1+(R-1)T_S/T_e\right]/R && T_e < T_S \end{aligned} \tag{2.1}$$

in which, T_e denotes the effective fundamental period of the structural system in the direction of interest determined based on bilinear idealization of the pushover curve. T_s is the characteristic period of the response spectrum. Target displacement corresponding to the displacement at the roof level is given in the following equation.

$$\delta_t = C_0 C_1 C_2 C_3 S_a \frac{T_e^2}{4\pi^2} g \tag{2.2}$$

where C_0 represents the modification factor that relates the roof displacement and the equivalent SDOF displacement. In addition to the modification factor of C_1, hysteresis characteristics of the members, such as pinching effect, stiffness and/or strength degradation, are approximately considered in the estimation of target displacement through C_2 coefficient. Finally, C_3 coefficient is the modification factor, which takes into account the displacement amplification caused by the P-delta effects.

Following the publication of ATC 40, FEMA 273/274 and FEMA 356, the use of NSP has accelerated particularly in the U.S., where both Displacement Coefficient Method (FEMA 356) and Capacity Spectrum Method (ATC 40) are applied. However it was immediately made clear that for the same equivalent SDOF system and the same ground motion, different inelastic displacements are estimated with those two methods. ATC 55 project was initiated in order to evaluate the accuracy of these methods in estimating the inelastic demand of SDOF systems and to improve these approaches. The findings of the project are reported in FEMA 440 report, where displacement coefficients defined in Equation (2.2) have been modified. Improved relationships are proposed for C_1 and C_2. Instead of defining C_3 coefficient, strength limits are given to account for P-delta effects and strength deterioration. According to FEMA 440, the new expression for the target displacement is given by the following equation.

$$\delta_t = C_0 C_1 C_2 S_a \frac{T_e^2}{4\pi^2} g \tag{2.3}$$

The ASCE 41-06 (Seismic Rehabilitation of Existing Buildings, 2007) is the latest generation of a performance-based seismic rehabilitation standards, which was developed from the pre-standard FEMA 356. This new standard includes a simplified pushover procedure based on a single load pattern consistent with the fundamental mode shape instead of several different load patterns as recommended in FEMA 356. In addition, the improved procedure for displacement coefficient method based on the recommendation contained in FEMA 440 has been adopted by ASCE 41-06.

Performance based seismic engineering has also been adopted in Europe in Eurocode 8 (2005) and in the new version of the Turkish Seismic Design Code (TSC, 2007). In Eurocode 8, NSP has been recommended for both the evaluation of existing buildings (EN 1998-3, 2005) and the design of new buildings (EN 1998-1, 2005). N2 method (Fajfar and Fischinger, 1988) forms the basis of NSP implemented in Eurocode 8. At least two types of vertical load distributions are suggested, similar to the recommendations of FEMA 356. One is a uniform load distribution proportional to story masses and the other is modal load patterns, which are consistent with fundamental mode shape of the structure or story shear forces obtained from response spectrum analysis. All load patterns are applied to the

structure in an invariant manner. Target spectral displacement is estimated from the inelastic displacement response spectrum as implemented in N2 method (Fajfar, 2000). Initial period of the equivalent SDOF system is determined based on the elasto-plastic idealization of the pushover curve. Inelastic spectral displacement corresponding to the initial period is estimated based on the relation between the elastic spectral displacement and the inelastic spectral displacement, which is identical to relationship in Equation (2.1) (FEMA 356, 2000).

In Turkish Seismic Design Code (TSC 2007), non-linear static procedures are used for seismic evaluation and retrofit of existing buildings. According to TSC (2007), pushover analysis is performed under the invariant or adaptive load patterns consistent with the fundamental mode shape of a structure. Pushover analysis based on single-mode load pattern is permitted for structures with no or slight irregularity in plan and where at least 70% percent mass participation is provided in the first mode. Pushover curve obtained from the analysis is converted to the capacity curve to estimate seismic demands. Inelastic spectral displacement demand is estimated based on the relationship between the elastic and inelastic spectral displacement as defined in Equation (2.1). For structures where higher mode effects are significant, a multi-mode pushover analysis method called Incremental Response Spectrum Analysis (IRSA - Aydınoğlu, 2003) is recommended. Different from FEMA 356, ASCE 41-06 and Eurocode 8, TSC (2007) is the only code presenting a multi-mode pushover analysis (IRSA) algorithm explicitly in an appendix.

2.3. Single-Mode Pushover Analysis

The purpose of the pushover analysis is to evaluate force and deformation demands and compare them with the limit states corresponding to the performance level associated with the level of ground motion intensity considered. In general, with the exception of high-rise buildings and buildings having irregularity in plan, pushover analysis under load pattern consistent with single-mode can predict inelastic seismic demands in a reasonable accuracy (Lawson *et al*., 1994, Krawinkler and Seneviratna, 1998). Furthermore, pushover analysis exposes the design weaknesses in structures that cannot be predicted by an elastic analysis. These weaknesses may be listed as;

- Story mechanisms due to formation of plastic hinges.
- Excessive deformation demands on the structural components where flexural behavior is dominant.
- Excessive force demands on potentially brittle elements, such as shear force demands on reinforced concrete columns, deep beams and beam-column connections.
- Strength deterioration of the structural components and their effect on the behavior of a structural system.
- Excessive inter-story drift demands at the first or upper stories due to strength and stiffness discontinuities, which may lead to collapse due to P-delta effects.

Nonlinear static procedures proposed in ATC 40, FEMA 356, ASCE 41-06, Eurocode 8 are essentially based on two main assumptions: (a) The first one is that the seismic response is fully dominated by a single mode behavior (b) The equivalent seismic load distribution is invariant. NSPs based on these two assumptions are suitable for structures where single mode is indeed dominant in their structural response, such as mid-rise and low-rise regular buildings. However, for structures where higher mode contributions are important, such as high-rise buildings or buildings irregular in plan, NSP based on single mode response may not be appropriate. Moreover, progressively changing structural properties during the earthquake due to yielding of structural components cannot be accurately estimated by an invariant load pattern throughout the pushover analysis. Therefore, it has been recognized that NSP, which is essentially based on invariant single-mode pushover analysis, has serious shortcomings.

Results of the study presented by Seneviratna (1995) clearly point out that conventional pushover analysis is not capable of capturing seismic demands for taller frame and wall structures where higher mode effects become important. Therefore, improved non-linear static procedures considering higher mode effects are needed to enhance the effectiveness and the range of applicability of the nonlinear static analysis.

Since no single invariant load patterns can capture the variations in the local demands expected in a design earthquake, the use of at least two load patterns that are expected to bound inertia force distribution is recommended (Lawson *et al.*, 1994). For instance, use of at least two load pattern has been recommended in FEMA 356 and

Eurocode 8 so as to bound likely redistribution of inertia force during seismic excitation. Clearly, none of these invariant load patterns can capture the variation in the dynamic characteristics of a building due to the formation of plastic hinges. An adaptive pushover technique has been proposed by Bracci *et al*. (1997) to account for changes in inelastic dynamic characteristics. In this method, pushover analysis is initiated by an inverted triangular load pattern and the load patterns to be applied at the next steps are modified so that story loads are proportional to story shear resistances at the previous pushover step. This adaptive pushover procedure considers only single-mode behavior of structures.

2.3.1. Piecewise Linear Representation of Single Mode Pushover Analysis

As it is stated above, single mode pushover analysis can be employed for structures, in which seismic response is governed by the first mode behavior throughout the seismic excitation. In the analysis, variation in the first mode due to yielding of structural components may be considered in an adaptive manner. For practical purposes, a constant lateral load pattern based on the initial structural properties can also be adopted, as given in ATC 40 and FEMA 356.

Piecewise linear representation of the pushover analysis, which provides a non-iterative pushover analysis technique with an adaptive load or displacement pattern, has been introduced by Aydınoğlu (2003, 2007). At each pushover step in between the formation of two consecutive plastic hinges, structural system can be considered to be linear. Accordingly, incremental seismic load vector acting on the MDOF system at (i)'th pushover step associated with the first mode response can be expressed as in the following equation:

$$\Delta \mathbf{f}_1^{(i)} = \underbrace{\mathbf{M}\boldsymbol{\Phi}_1^{(i)}\Gamma_{x1}^{(i)}}_{\bar{\mathbf{m}}_1^{(i)}} \Delta a_1^{(i)} \quad \Rightarrow \quad \Delta \mathbf{f}_1^{(i)} = \bar{\mathbf{m}}_1^{(i)} \Delta a_1^{(i)} \tag{2.4}$$

where $\mathbf{M}$ is the diagonal mass matrix, $\boldsymbol{\Phi}_1^{(i)}$ represents the instantaneous mode shape vector for the first mode and $\Gamma_{x,1}^{(i)}$ denotes the participation factor for the first mode at the (i)'th step for an earthquake in x direction, which is expressed as

$$\Gamma_{x1}^{(i)} = \frac{L_{x1}^{(i)}}{\boldsymbol{\Phi}_1^{(i)T}\mathbf{M}\boldsymbol{\Phi}_1^{(i)}} \quad ; \quad L_{x1}^{(i)} = \boldsymbol{\Phi}_1^{(i)T}\mathbf{M}\mathbf{I}_x \tag{2.5}$$

In Equation (2.4), $\bar{\mathbf{m}}_1^{(i)}$ and $\Delta a_1^{(i)}$ represent the participating modal mass vector and pseudo acceleration increment for the first mode at the (i)'th pushover step, respectively. Mode shape vector and modal participation factor at the current step are updated based on continuously changing structural properties due to formation of plastic hinges at the previous steps. In a similar way, displacement increment of the MDOF system for the first mode, which is compatible with lateral force increment at the same step, can be given as follows:

$$\Delta\mathbf{u}_1^{(i)} = \underbrace{\boldsymbol{\Phi}_1^{(i)}\Gamma_{x1}^{(i)}}_{\bar{\mathbf{u}}_1^{(i)}}\Delta d_1^{(i)} \quad \Rightarrow \quad \Delta\mathbf{u}_1^{(i)} = \bar{\mathbf{u}}_1^{(i)}\Delta d_1^{(i)} \tag{2.6}$$

where $\Delta d_1^{(i)}$ represents modal displacement increment at the (i)'th step, which can be related to modal pseudo-acceleration increment as follows

$$\Delta a_1^{(i)} = (\omega_1^{(i)})^2\,\Delta d_1^{(i)} \tag{2.7}$$

in which $(\omega_1^{(i)})^2$ represents the instantaneous natural frequency at the (i)'th pushover step.

Note that modal displacement increment and compatible lateral seismic load increments at the (i)'th step yield the same results in terms of the structural response quantities, such as section forces, inter-story drift ratios and plastic rotations, if pushover procedure carried out in an adaptive manner.

In the case of a pushover analysis under invariant load pattern, mode shape vector is assumed to be constant throughout the analysis. Participating modal mass vector is defined at the first step as $\bar{\mathbf{m}}_1^{(1)}$ and kept constant at each pushover step. Thus, invariant incremental seismic load vector can be expressed as

$$\Delta \mathbf{f}_1^{(i)} = \underbrace{\mathbf{M}\boldsymbol{\Phi}_1^{(1)}\Gamma_{x1}^{(1)}}_{\bar{\mathbf{m}}_1^{(1)}} \Delta a_1^{(i)} \quad \Rightarrow \quad \Delta \mathbf{f}_1^{(i)} = \bar{\mathbf{m}}_1^{(1)} \Delta a_1^{(i)} \tag{2.8}$$

2.3.2. Identification of Modal Coordinates by Piecewise Linear Pushover Analysis

Utilizing plastic hinge model, through which nonlinear response of the structural elements is assumed to be concentrated at the critical sections, pushover analysis can be performed as a series of piecewise linear static analyses. Since structural system is assumed to be linear between two consecutive plastic hinges, incremental structural response quantities, $\Delta r^{(i)}$, at each piecewise linear step, such as section forces, story drifts or plastic rotations of previously yielded hinges, can be obtained for incremental seismic load vector, $\mathbf{\Delta f}_1^{(i)}$ as follows:

$$\Delta r^{(i)} = \bar{r}^{(i)} \Delta a_1^{(i)} \tag{2.9}$$

in which $\Delta r^{(i)}$ denotes the generic incremental response quantity at the (i)'th step and $\bar{r}^{(i)}$ represents the same response quantity for $\Delta a_1^{(i)} = 1$ under the adaptive lateral load pattern, $\bar{\mathbf{m}}_1^{(i)}$, given by Equation (2.4) or invariant load pattern, $\bar{\mathbf{m}}_1^{(1)}$, given by Equation (2.8). Hence, the cumulative response quantity, $r^{(i)}$ at the end of (i)'th step can be expressed by the following equation.

$$r^{(i)} = r^{(i-1)} + \Delta r^{(i)} = r^{(i-1)} + \bar{r}^{(i)} \Delta a_1^{(i)} \tag{2.10}$$

where $r^{(i-1)}$ is the response quantity obtained at the end of the previous step. At the initial pushover step, $r^{(i-1)}$ is equal to the response from the gravity load case and can be denoted by $r^{(0)}$. Subsequently, the above given generic expression is specialized for the response quantities that define the coordinates of the yield surfaces of all potential plastic hinges. As part of the piecewise linearization process of pushover analysis as well as to avoid iterative operations in hinge identification process, yield surface are linearized by a number of lines or planes, considering two- or three-dimensional behavior of the structural components. Approximation in the definition of linearized yield surface can be reduced by increasing

the number of lines (or planes). As an example, planar yield surfaces (lines) of a reinforced concrete section (j) is illustrated in Figure 2.1 where a typical line (s) can be expressed as

$$\alpha_{j,s} M_{jp} + \beta_{j,s} N_{jp} = 1 \tag{2.11}$$

in which M_{jp} and N_{jp} denotes yield bending moment and corresponding axial force, respectively, at section (j). $\alpha_{j,s}$ and $\beta_{j,s}$ represent coefficients defining the yield lines. Equation (2.10) is specialized for bending moment and axial force acting on a critical section (j) of a column at the (i)'th pushover step as in the following equations;

$$M_j^{(i)} = M_j^{(i-1)} + \bar{M}_j^{(i)} \Delta a_1^{(i)} \quad ; \quad N_j^{(i)} = N_j^{(i-1)} + \bar{N}_j^{(i)} \Delta a_1^{(i)} \tag{2.12}$$

and then substituting these equation into the Equation (2.11) yields required $(\Delta a_1^{(i)})_{j,s}$ for the yield line (s) at section (j) as given in Equation (2.13). $(\Delta a_1^{(i)})_{j,s}$ is determined for each yield line at all critical sections in the structural system and minimum positive of them identifies the plastic hinge formation and required $\Delta a_1^{(i)}$ at the (i)'th pushover step.

$$(\Delta a_1^{(i)})_{j,s} = \frac{1 - \alpha_{j,s} M_j^{(i-1)} + \beta_{j,s} N_j^{(i-1)}}{\alpha_{j,s} \bar{M}_j^{(i)} + \beta_{j,s} \bar{N}_j^{(i)}} \tag{2.13}$$

At each pushover step, investigation of minimum modal pseudo-acceleration increment can be performed without any iterative process based on the piecewise linear representation of the yield surface of the structural components as presented above.

Once $\Delta a_1^{(i)}$ is determined, any response quantity of interest developed at the end of that step can be obtained from the generic expression of Equation (2.10). As the formation of the new hinge is identified, the current global stiffness matrix of the structure is locally modified such that only the element stiffness matrix that affected by the new hinge is replaced with a new one for the next pushover step. Normality criterion is enforced in columns and walls for the coupling of internal forces as well as plastic deformation components of the newly formed plastic hinge.

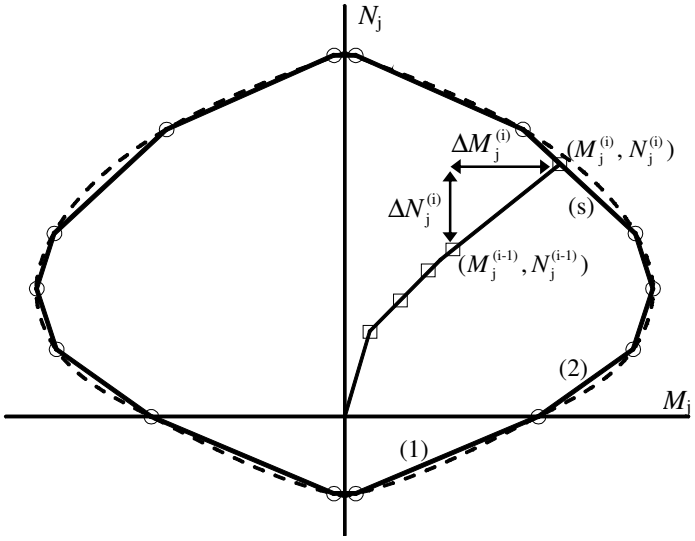

Figure 2.1. Typical piecewise linear yield surface for reinforced concrete section and illustration of the incremental response at the (i)'th step when yielding occurs

When adaptive load pattern is used in the pushover analysis, lateral load increments are always compatible with the displacement increments. Thus, after the modal acceleration increment is calculated at the current step, modal displacement increment can be found easily through Equation (2.7):

If piecewise linear pushover analysis is performed under the displacement pattern based on Equation (2.6), response increments are related to modal displacement increment at each step, hence Equation (2.9) can be rewritten as follows.

$$\Delta r^{(i)} = \tilde{r}^{(i)} \Delta d_1^{(i)} \tag{2.14}$$

Accordingly, Equation (2.10) is specialized for bending moment and axial force acting on section (j) at the (i)'th pushover step under the displacement pattern, $\Delta d_1^{(i)}$, as in the following equations;

$$M_j^{(i)} = M_j^{(i-1)} + \tilde{M}_j^{(i)} \Delta d_1^{(i)} \quad ; \quad N_j^{(i)} = N_j^{(i-1)} + \tilde{N}_j^{(i)} \Delta d_1^{(i)} \tag{2.15}$$

Substituting of these equation into the Equation (2.14) yields required $(\Delta d_1^{(i)})_{j,s}$ for the yield line (s) at section (j) as given in Equation (2.16). Using above-mentioned procedure, minimum modal displacement increments that lead to a plastic hinge formation at each critical section are calculated based on Equation (2.16) and minimum of them yields modal displacement increment at the current pushover step.

$$(\Delta d_1^{(i)})_{j,s} = \frac{1 - \alpha_{j,s} M_j^{(i-1)} + \beta_{j,s} N_j^{(i-1)}}{\alpha_{j,s} \tilde{M}_j^{(i)} + \beta_{j,s} \tilde{N}_j^{(i)}} \tag{2.16}$$

When displacement pattern is used in the pushover analysis, corresponding modal acceleration increment at the (i)'th pushover step can be extracted from Equation (2.7) for a known modal displacement increment.

In the case of an invariant load pattern, however, modal lateral loads and resulting displacement increments are not compatible. Therefore, modal displacement increment of the equivalent inelastic SDOF system is estimated based on the following equation as implemented in ATC 40 and FEMA 356.

$$\Delta d_1^{(i)} = \frac{\Delta u_{N,1}^{(i)}}{\boldsymbol{\Phi}_{N,1}^{(1)} \Gamma_{x1}^{(1)}} \tag{2.17}$$

in which $\Delta u_{N,1}^{(i)}$ and $\boldsymbol{\Phi}_{N,1}^{(1)}$ represent the roof displacement increment at the (i)'th pushover step and the corresponding mode shape vector at the first pushover step for the first mode, respectively.

In addition, an approximate method has been proposed by Aydınoğlu (2005, 2007) to calculate the instantaneous eigenvalue, $(\omega_1^{(i)})^2$, as a Rayleigh quotient and then to determine incremental modal displacement increment at each step by using Equation (2.7).

$$(\omega_1^{(i)})^2 \cong \frac{\sum_k \bar{m}_{k,1}^{(1)} \bar{u}_{k,1}^{(i)}}{\sum_k m_k \bar{u}_{k,1}^{(i)2}} \tag{2.18}$$

in which $\bar{u}_{k,1}^{(i)}$ represents the displacement component at the k'th DOF under equivalent seismic loads, $\bar{m}_{k,1}^{(1)}$, with invariant pattern that are defined through Equation (2.8) for $\Delta a_1^{(i)}$=1. Thus, modal displacement increment, $\Delta d_1^{(i)}$, can be obtained by using Equation (2.18) and Equation (2.7).

It should be noted that above-described single-mode pushover analysis can be performed without any need to plot pushover curve in terms of base-shear versus roof displacement as implemented in conventional approach (ATC 40 and FEMA356). Since modal acceleration increments are already defined by Equation (2.13), converting base shear increments to the modal acceleration increments is not required. In fact, the same modal acceleration increment can be obtained even if conventional pushover analysis is applied. In this case, base shear increment at each pushover step can be calculated by summing up the equivalent seismic loads given by Equation (2.8) in x direction as follows

$$\Delta V_{x1}^{(i)} = \mathbf{I}_x^T \Delta \mathbf{f}_1^{(i)} = \mathbf{I}_x^T \bar{\mathbf{m}}_1^{(1)} \Delta a_1^{(i)} \tag{2.19}$$

Modal participating mass for the first mode of the MDOF system in x direction can be expressed as

$$\bar{M}_{x1}^{(1)} = \mathbf{I}_x^T \bar{\boldsymbol{m}}_1^{(1)} = \frac{L_{x1}^{(1)2}}{M_1^{(1)}} \tag{2.20}$$

Modal pseudo-acceleration increments corresponding to the base shear increments given in Equation (2.19) is calculated from the following equation.

$$\Delta a_1^{(i)} = \frac{\Delta V_{x1}^{(i)}}{\bar{M}_{x1}^{(1)}} \tag{2.21}$$

After the determination of modal acceleration and modal displacement increments at each pushover step, cumulative modal displacement and acceleration at the end of the each step can be determined by using the following equations, which define the coordinates of the modal capacity curve for the first mode.

$$\begin{aligned} d_1^{(i)} &= d_1^{(i-1)} + \Delta d_1^{(i)} \\ a_1^{(i)} &= a_1^{(i-1)} + \Delta a_1^{(i)} \end{aligned} \tag{2.22}$$

As a result of the procedure presented above, coordinates of the modal capacity diagrams for the first mode can be determined as shown in Figure 2.2. In this figure, modal capacity diagram for the first mode obtained from the adaptive pushover analysis including P-delta effects of 8-story frame building (properties of the 8-story building will be given in detail in the next chapter) is presented. The circles on the capacity diagram represent plastic hinge formations at the end of each piecewise linear step. Between consecutive plastic hinge formations, instantaneous slope of the capacity diagram is equal to the eigenvalue of the structural system at that step.

It should be noted that instantaneous slope in the modal capacity diagram as depicted in Figure 2.2 turns into negative at a certain step due to the P-delta effects. At this step, stiffness matrix of the structural system is negative-definite stiffness matrix. Thus, pushover analysis under incremental load pattern can not be implemented. This is a well-known limitation of force-controlled pushover analysis when P-delta effects are included. However, Aydınoğlu (2004, 2007) revealed that adaptive pushover analysis is not influenced by a negative instantaneous slope of the capacity diagram. Because of the negative eigenvalue, natural frequency is equal to an imaginary value. Although, a negative natural frequency has no physical meaning, the corresponding mode shape represents post-buckling deformation state of the structure and can be routinely calculated by matrix transformation methods of eigenvalue analysis, such as the well-known Jacobi Method (Aydınoğlu, 2004, 2007). Thus, it is clear that displacement-controlled pushover analysis should be performed when P-delta effects are considered. In this case, piecewise linear pushover analysis with displacement pattern, as summarized above, provides an explicit pushover analysis technique that manage to overcome the limitation of force-controlled pushover analysis.

It is worth noting that as a result of the piecewise linear representation of single-mode pushover analysis above, modal capacity diagram can be determined directly without any need to plot the pushover curve.

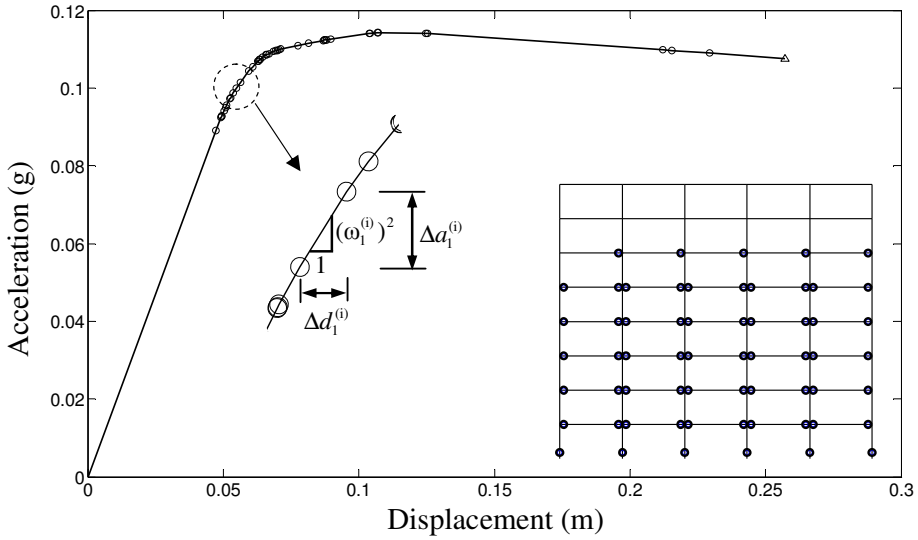

Figure 2.2. Modal capacity for the first mode obtained from the adaptive pushover analysis for 8-story frame building

2.3.3. Evaluation of Seismic Demand: Estimation of Maximum Inelastic Modal Displacement

Pushover analysis as summarized above is continued until the cumulative modal displacement defined in Equation (2.22) reaches the inelastic spectral displacement demand. As can be seen from Figure 2.3, modal displacement increment at the last step can be calculated using the following equation.

$$\Delta d_1^{(p)} = S_{di,1} - d_1^{(p-1)} \tag{2.23}$$

where $S_{di,1}$ represents inelastic spectral displacement for the first mode.

Estimation of peak modal displacement of an inelastic equivalent SDOF system and corresponding peak response quantities at the level of structural components is the ultimate phase of the performance based assessment utilizing a nonlinear static procedure. Utilizing an appropriate hysteretic model, inelastic spectral displacement can be estimated by performing nonlinear time history analysis for a given earthquake. However, implementation of nonlinear static procedure into the structural engineering practice

requires a simplified analysis procedure to estimate inelastic displacement demand. For this purposes, a number of approximate methods have been proposed by many researchers (Nassar and Krawinkler, 1991, Vidic, Fajfar and Fischinger, 1994, Miranda, 2000, 2001, Aydınoğlu and Kaçmaz, 2002, Chopra and Chintanapakdee, 2003 and Ruiz-Garcia and Miranda, 2003) to compute the maximum inelastic displacement based on the relation between the inelastic spectral displacement and the elastic spectral displacement. A simplified relation to estimate inelastic spectral displacement has been presented in FEMA 356 through C_1 coefficient, as given in the following equation.

$$S_{\mathrm{di},1} = C_{\mathrm{R},1} S_{\mathrm{de},1} \tag{2.24}$$

where $S_{\mathrm{de},1}$ represents the elastic spectral displacement of the equivalent linear SDOF system. Its first natural vibration period is equal to the initial natural vibration period of the inelastic SDOF system. $C_{\mathrm{R},1}$ denotes the inelastic displacement ratio coefficient and depends on the initial period of the inelastic SDOF system as expressed in the following equation.

$$\begin{aligned} C_{\mathrm{R},1} &= 1 && T_1 \geq T_{\mathrm{S}} \\ C_{\mathrm{R},1} &= \frac{1+(R_{\mathrm{y},1}-1)T_1/T_{\mathrm{S}}}{R_{\mathrm{y},1}} \geq 1 && T_1 < T_{\mathrm{S}} \end{aligned} \tag{2.25}$$

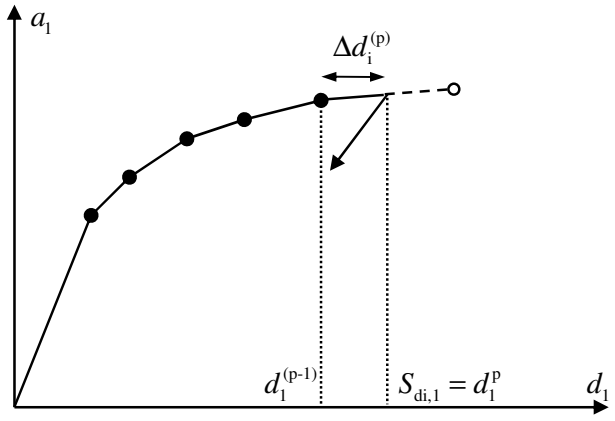

Figure 2.3. Modal capacity diagram for the first mode

For practical purposes, elastic natural vibration period of the structure, $T_{1,}$ which corresponds to the initial slope of the modal capacity diagram, can be determined accurately based on the cracked section rigidity of the structural components.

In Equation (2.25), T_S is the characteristic period defining the transition period from the constant acceleration region to the constant velocity region in the elastic response spectrum. As can be seen from the equation above, equal displacement rule is valid for the system whose elastic natural vibration period is equal to or larger than the characteristic period. However in the constant acceleration region, $C_{R,1}$ depends on the relative strength, $R_{y,1}$, which is defined by the ratio of elastic strength and yield strength of the SDOF system. Consequently, bilinear idealization of the modal capacity diagram is needed to calculate yield strength. Once inelastic spectral displacement demand is determined by using the initial slope of the modal capacity diagram as depicted in Figure 2.4, bilinear idealization can be done easily. However, calculation of inelastic spectral displacement is dependent on $R_{y,1}$. Therefore, iterative procedure should be carried out to estimate spectral displacement demand of an inelastic SDOF system, of which initial period is in the constant acceleration region (Figure 2.4a). On the other hand, bilinear idealization is not necessary for the system, whose first natural vibration period is longer than the characteristic period of the response spectrum.

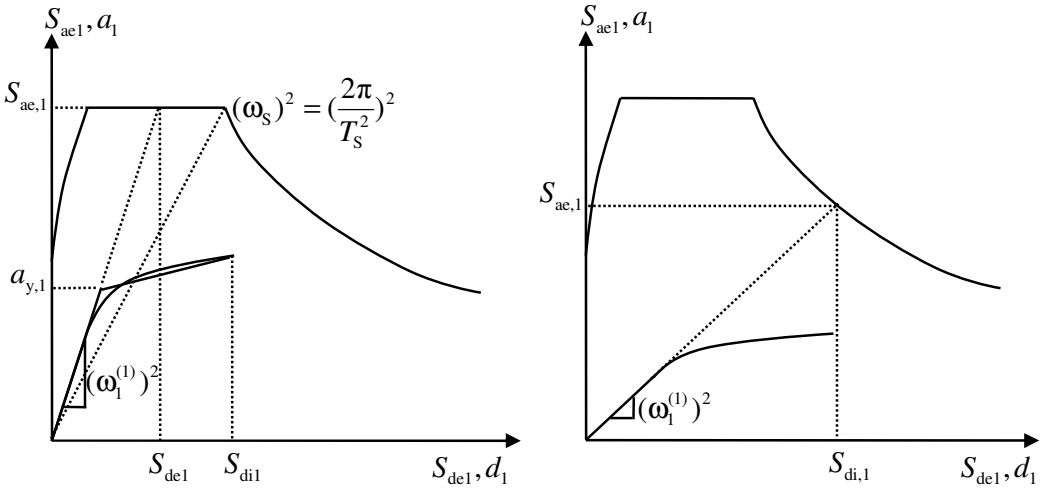

Figure 2.4. Estimation of spectral displacement demand

2.4. Multi-Mode Pushover Analysis

In order to overcome the limitations of single mode pushover analysis for MDOF systems, where higher mode effects have considerable contributions to the seismic response, multi-mode pushover analysis procedures have been proposed by many researchers based on the various assumptions.

Paret *et al*., (1996) and Sasaki *et al*., (1998) have proposed nonlinear static procedures, which are the first attempts taking higher mode effects into account. In these procedures, pushover analyses are performed separately for modes deemed to be excited during earthquake excitation, considering invariant modal load patterns. These methods simply discuss the need for consideration of higher mode contributions in the pushover analysis. More sophisticated pushover analysis procedures have been offered in the last decade (Gupta and Kunnath, 2000, Aydınoğlu, 2003, Chopra and Goel, 2001, Elnashai, 2001, Antoniou *et al*. 2002, Antoniou and Pinho, 2004[a,b], Casarotti and Pinho, 2007) in an attempt to take higher mode effects into account and to propose a practical multi-mode pushover method that can be used in engineering practice. These multi-mode pushover procedures will be explained in detail in the next sections.

Consistent with the notations used in above-presented piecewise linear representation of single-mode pushover analysis, instantaneous modal displacement increment associated with the instantaneous n'th mode shape at each pushover step can be written based on Equation (2.6) as follows

$$\Delta \mathbf{u}_n^{(i)} = \underbrace{\boldsymbol{\Phi}_n^{(i)} \Gamma_{xn}^{(i)}}_{\tilde{\mathbf{u}}_n^{(i)}} \Delta d_n^{(i)} \quad \Rightarrow \quad \Delta \mathbf{u}_n^{(i)} = \tilde{\mathbf{u}}_n^{(i)} \Delta d_n^{(i)} \tag{2.26}$$

and instantaneous modal force vector, compatible with the instantaneous modal displacement for the n'th mode, can be expressed as

$$\Delta \mathbf{f}_n^{(i)} = \underbrace{\mathbf{M} \boldsymbol{\Phi}_n^{(i)} \Gamma_{xn}^{(i)}}_{\bar{\mathbf{m}}_n^{(i)}} \Delta a_n^{(i)} \quad \Rightarrow \quad \Delta \mathbf{f}_n^{(i)} = \bar{\mathbf{m}}_n^{(i)} \Delta a_n^{(i)} \tag{2.27}$$

2.4.1. Modal Scaling

In the case of single mode pushover analysis, response quantities can be evaluated under the first mode consistent load or displacement pattern at each piecewise linear step resulting in a single plastic hinge formation. However, in the case of multi-mode pushover analysis, development of a plastic hinge at the end of the pushover step should be determined by taking into account the contributions from all modes considered and therefore a critical assumption is required to define relative modal contributions at each step to reduce the number of unknown to one. This is called modal scaling procedure, which is the most critical assumption that has to be considered in all multi-mode pushover procedures.

As it can be seen from the Equation (2.26) and (2.27), increments of modal response quantities for each mode are weighted by the modal acceleration or modal displacement increments depending on whether force- or displacement-controlled pushover analysis is performed. Therefore, modal acceleration increment or modal displacement increment for each mode should be determined based on the modal scaling procedure at each pushover step to determine relative modal contributions. Modal scaling procedures adopted in several multi-mode pushover analysis procedures have been summarized in a comprehensive paper by Aydınoğlu (2007). Consistent with the notations used in this paper, some of the modal scaling procedures are presented briefly herein and discussed in the next sections in detail for all multi-mode pushover methods under consideration.

For instance, one of the multi-mode pushover analysis methods is Incremental Response Spectrum Analysis (Aydınoğlu, 2003), in which modal pushovers are performed under instantaneous modal displacement increments simultaneously based on Equation (2.26). In principle, modal displacement increments are scaled in IRSA with respect to inelastic spectral displacement, $S_{\mathrm{din}}^{(\mathrm{i})}$, associated with the instantaneous configuration of the structure. In practical version of IRSA that making use of advantage of well-known equal displacement rule, modal scaling is based on initial elastic spectral displacement, $S_{\mathrm{den}}^{(1)}$, This modal scaling procedure can be expressed as

$$\Delta d_{\mathrm{n}}^{(\mathrm{i})} = S_{\mathrm{den}}^{(1)} \Delta \tilde{F}^{(\mathrm{i})} \tag{2.28}$$

where $\Delta \tilde{F}^{(\mathrm{i})}$ denotes incremental scale factor, which is constant for all modes at each step.

Another modal scaling procedure, which has been adopted in several force-controlled multi-mode pushover analysis methods (Gupta and Kunnath, 2000, Elnashai, 2001 and Antoniou *et al*., 2002) is based on instantaneous elastic spectral pseudo-accelerations. Such a modal scaling procedure can be expressed as follow

$$\Delta a_{\mathrm{n}}^{(\mathrm{i})} = S_{\mathrm{aen}}^{(\mathrm{i})} \Delta \overline{F}^{(\mathrm{i})} \tag{2.29}$$

in which $S_{\mathrm{aen}}^{(\mathrm{i})}$ represents instantaneous elastic spectral pseudo-acceleration for the n'th mode at the (i)'th step and $\Delta \overline{F}^{(\mathrm{i})}$ denotes incremental scale factor, which is independent of the mode number. Modal scaling procedure adopted in other multi-mode pushover methods will be discussed next.

2.4.2. Single-Run Pushover Analysis with Invariant Single-Load Patterns Based on Combined Multi-Mode Loading

Pushover analysis performed with a single-load pattern that account for elastic higher mode effects is one of the pushover analysis procedure recommended in FEMA 356. In this procedure, load pattern to be applied on a structure at each step is proportional to lateral forces, which is calculated from story shears determined by linear response spectrum analysis (RSA) based on linear elastic stiffness state of the structure. In RSA modal response quantities belonging to elastic higher mode effects are combined by SRSS modal combination rule. Resultant load pattern is assumed to be constant throughout the pushover analysis. Since modal load patterns, $\Delta \overline{\mathbf{f}}_{\mathrm{n}}^{(1)}$, used in the linear response spectrum are scaled by the initial elastic spectral pseudo-accelerations as expressed in Equation (2.30), it can be stated that modal scaling is performed on initial elastic spectral accelerations, $S_{\mathrm{aen}}^{(1)}$.

$$\Delta \mathbf{f}_{\mathrm{n}}^{(\mathrm{i})} = \underbrace{\mathbf{M}\boldsymbol{\Phi}_{\mathrm{n}}^{(1)}\Gamma_{\mathrm{xn}}^{(1)}S_{\mathrm{aen}}^{(1)}}_{\Delta \bar{\mathbf{f}}_{\mathrm{n}}^{(1)}} \Delta \bar{F}^{(\mathrm{i})} \tag{2.30}$$

Pushover analysis is performed under the invariant single-load pattern as described above until roof displacement of the MDOF system reaches target displacement, which is defined through *displacement coefficient method* as described in FEMA 356. As stated earlier, target displacement is estimated based on inelastic spectral displacement demand of the equivalent SDOF system. According to displacement coefficient method, relation between displacement of MDOF system and equivalent SDOF system is defined by C_0 coefficient, which is the product of the mode shape vector at the roof level and the modal participation factor. However, it should be noted that displacements obtained from the pushover analysis under the combined multi-mode loading contains higher mode effects. Therefore, an assumption is required to relate displacement coordinate of the MDOF and SDOF system. It is assumed that deflected shape of the MDOF system is treated as a *single-combined mode* shape in order to determine C_0 coefficient. However, it is not a convenient approach to correlate displacement response of MDOF system containing multi-mode effects with that of SDOF system. It should be strongly pointed out that single-load pattern based on combined multi-mode loading enforces to make an above-given controversial assumption in order to evaluate seismic demands.

2.4.3. Single-Run Pushover Analysis with Adaptive Single-Load Patterns Based on Combined Multi-Mode Loading

Similar to above-given invariant single-run pushover procedure, an alternative multi-mode pushover analyses based on adaptive single-load patterns have been proposed by Elnashai (2001), Antoniou *et al*. (2002) and Antoniou and Pinho (2004[a]) to overcome the limitation of invariant pushover analysis. In these pushover procedures, equivalent modal seismic loads, consistent with the instantaneous mode shapes, are calculated at each pushover step based on instantaneous stiffness state of the structure and then scaled with the corresponding instantaneous elastic spectral pseudo-accelerations, $S_{\mathrm{aen}}^{(\mathrm{i})}$, as given in Equation (2.31).

$$\Delta \mathbf{f}_{\mathrm{n}}^{(\mathrm{i})} = \underbrace{\mathbf{M}\boldsymbol{\Phi}_{\mathrm{n}}^{(\mathrm{i})}\Gamma_{\mathrm{xn}}^{(\mathrm{i})}S_{\mathrm{aen}}^{(\mathrm{i})}}_{\Delta \bar{\mathbf{f}}_{\mathrm{n}}^{(\mathrm{i})}} \Delta \bar{F}^{(\mathrm{i})} \quad ; \quad \Delta \mathbf{f}_{\mathrm{n}}^{(\mathrm{i})} = \Delta \bar{\mathbf{f}}_{\mathrm{n}}^{(\mathrm{i})} \Delta \bar{F}^{(\mathrm{i})} \tag{2.31}$$

The modal seismic loads are combined with an appropriate modal combination rule and then applied to the structure at each pushover step (see Figure 2.5) in order to obtain the increments of the pushover curve coordinates and incremental response quantities.

As can be seen from Equation (2.31), relative modal contributions are scaled by instantaneous elastic spectral acceleration and therefore modal scaling procedure adopted in these force-controlled pushover procedures can be expressed as

$$\Delta a_{\mathrm{n}}^{(\mathrm{i})} = S_{\mathrm{aen}}^{(\mathrm{i})} \Delta \bar{F}^{(\mathrm{i})} \tag{2.32}$$

According to Equation (2.32), modal response quantities obtained from the modal force vectors are weighted by the instantaneous elastic spectral accelerations corresponding to current stiffness state of the MDOF system. In fact, this is an intuitive approach so as to consider frequency content of the earthquake ground motion. If the structure reaches its global strength capacity and eventually deforms inelastically beyond its elastic limits, structural response would be directly related to the deformation or displacement demands, not acceleration demand. In this regard, modal scaling procedure based on instantaneous spectral pseudo-acceleration may be inconvenient for inelastic structures.

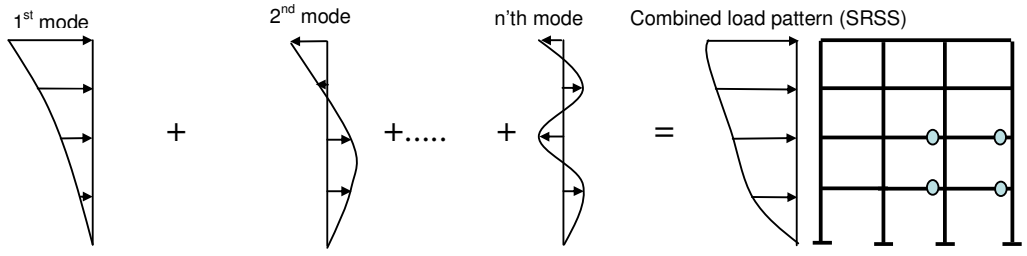

Figure 2.5. Calculation of combined load pattern at each pushover step according to the method by Elnashai (2001)

As presented in ATC 40 and FEMA 356, pushover analysis has been employed to estimate not only *structural capacity* but also *seismic demands* through an equivalent SDOF system by using elastic response spectrum. Therefore, utilization of pushover analysis in conjunction with the response spectra to estimate seismic demands is one of the fundamental tasks that should be completed by a pushover analysis procedure to be used as an assessment tool. However, above-described single-run pushover analysis methods utilizes elastic response spectrum only for scaling modal seismic load patterns, not for estimating seismic demands. In the studies presented by Elnashai (2001), Antoniou *et al.* (2002) and Antoniou and Pinho (2004[a]), target displacements used in the pushover analyses are obtained from the inelastic time history analyses of the MDOF systems. As a result of the pushover analysis, story displacements and inter-story drift distribution are compared with that of inelastic time history analysis for the same target displacement. Accuracy of these methods has been tested in terms of relative story displacements and inter-story drift distribution. Moreover, in order to evaluate seismic demands by using elastic response spectrum, representation of an equivalent SDOF system determined from a pushover curve is needed. However, above-described single-run pushover procedures result in a conventional pushover curve containing multi-mode effects. As stated earlier, conversion of the pushover curve coordinates including higher mode effects to that of an equivalent SDOF system is a controversial point. This situation enforces to make an assumption, which is that instantaneous deflected shape of the structure is treated as an instantaneous mode shape. Unlike the single-run pushover analysis presented in the preceding section, demand estimation based on single-combined mode has not been implemented in these multi-mode pushover procedures. Thus, these multi-mode pushover procedures can be treated as capacity estimation tools, but not demand estimation tools.

When P-delta effects are included in the pushover analysis, it is expected that pushover curve gradually decreases following a certain step (see Figure 2.6). Previously formed plastic hinges and P-delta effects lead to a negative-definite second-order stiffness matrix at that step. Eigenvalue analysis at that step results in a negative eigenvalue and eventually an imaginary natural vibration frequency for the first mode. In fact, there is no physical meaning of an imaginary natural frequency. Thus, natural vibration period for the first mode and corresponding instantaneous spectral acceleration can not be estimated and multi-mode pushover analyses utilizing modal scaling procedure based on instantaneous

spectral quantities may be terminated without reaching to target displacement. This is an important limitation of the modal scaling procedure based on the instantaneous elastic spectral quantities when P-delta effects are considered in the analysis.

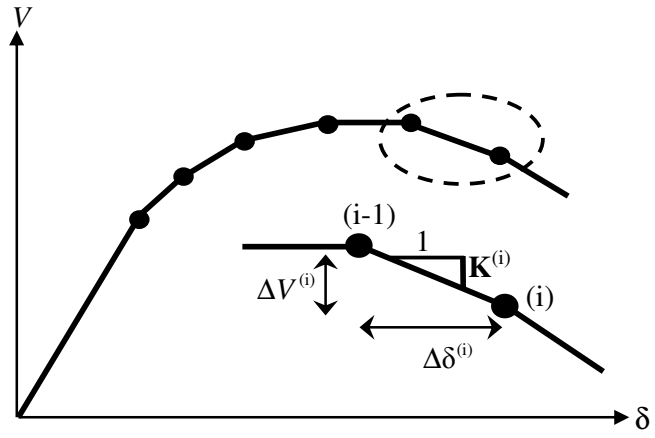

Figure 2.6. Pushover curve in the case including P-delta effects

Modal response contributions obtained from each mode have to be combined to evaluate total seismic response of an inelastic MDOF system. An appropriate modal combination rule, such as Square-Root-of-Sum-of-Squares (SRSS) or Complete Quadratic Combination (CQC) can be used to find individual combined response quantities as implemented in well-known linear response spectrum analysis. Although there is no theoretical basis of using modal combination procedure for inelastic systems, it seems reasonable because it provides results for elastic buildings that are identical to the well-known RSA procedure (Chintanapakdee and Chopra, 2003).

Therefore, modal combination procedure, that is identical to linear response spectrum analysis, forms the basis for the implementation of modal combination procedure in multi-mode pushover analysis. Determination of the combined response quantities under the combined load or displacement vector seems attractive in stead of combining individual modal response quantities. However, it is a pitfall that should be avoided in a modal combination procedure to be used in a multi-mode pushover analysis (Chopra, 2007, p.529, Aydınoğlu, 2003, 2007). It should be noted that according to force-controlled multi-mode pushover analysis procedures proposed by Elnashai (2001), Antoniou *et al*. (2002) and Antoniou and Pinho (2004[a]), incremental modal force vectors are combined to obtain a

single-load pattern. As a result of these procedures, combined response quantities, such as plastic rotations, story drifts and section forces, are obtained from the combined single-load at each incremental step. This is a pitfall pointed out above.

2.4.4. Single-Run Pushover Analysis with Adaptive Single-Displacement Patterns Based on Combined Multi-Mode Loading

Antoniou and Pinho (2004[b]) presented a displacement-controlled adaptive pushover procedure (DAP) instead of force-controlled adaptive pushover procedure (FAP), which was again proposed by them because of FAP limitations. According to DAP, single-displacement pattern based on combined multi-mode effects are applied to a structure at each step. Inter-story drift-based scaling technique is employed to determine single-displacement pattern. At each story, inter-story drift values for each mode, which are the product of the mode shape and corresponding modal participation factor, are scaled by an elastic spectral displacement corresponding to instantaneous period of the structure and then combined using SRSS rule to obtain combined inter-story drifts. Displacement pattern to be imposed on the structure is obtained by summing up combined inter-story drifts at each story. This process (see Figure 2.7) is repeated at each pushover step progressively.

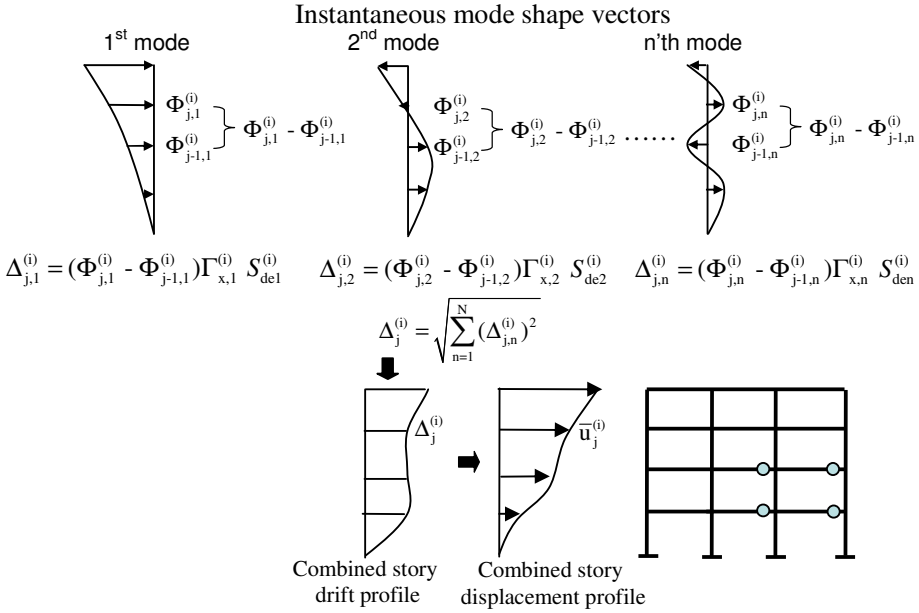

Figure 2.7. Displacement pattern at each pushover step determined by inter-story drift-based scaling according to DAP (Antoniou and Pinho, 2004[b])

Incremental response quantities are computed from the combined displacement pattern and therefore relative modal contributions are determined based on a modal scaling procedure utilizing instantaneous elastic spectral displacements. Modal scaling procedure used in this method can be expressed as

$$\Delta d_{\mathrm{n}}^{(\mathrm{i})} = S_{\mathrm{den}}^{(\mathrm{i})} \Delta \tilde{F}^{(\mathrm{i})} \tag{2.33}$$

where $S_{\mathrm{den}}^{(\mathrm{i})}$ denotes instantaneous elastic spectral displacement for the n'th mode. In this method, similar to the single-run pushover analysis described in the previous section, elastic response spectrum is utilized only for modal scaling procedure, but not for demand estimation. Therefore, DAP can also be treated as a capacity estimation tool, but not a demand estimation tool. Note that since modal scaling procedure based on instantaneous elastic spectral displacements is used in the DAP, the same shortcoming pointed out in the preceding section can also be observed when P-delta effects are included in the analysis. Consequently, it can be concluded that multi-mode pushover analysis procedures utilizing modal scaling procedure based on instantaneous spectral quantities have a serious drawback in case P-delta effects are considered.

Incremental response quantities at each pushover step in DAP are computed from the combined displacement pattern, which is a pitfall in terms of the application of modal combination as pointed out in the previous section.

It should be noted that single-run pushover analyses with single-load patterns or single-displacement patterns (Elnashai, 2001, Antoniou *et al*., 2002 and Antoniou and Pinho, 2004[a,b]) can estimate seismic demands if they assume that deflected shape of the MDOF system at each pushover step is treated as a *single-combined* mode shape, which is proposed by Casarotti and Pinho (2007). These two researchers are the only appliers of this proposition. In this method, single pushover curve obtained from an adaptive pushover analysis is converted to the capacity diagram of the equivalent SDOF system based on the assumption that deformed shape of the structure at each pushover step is treated as an instantaneous mode shape of the structural system as follows

$$\boldsymbol{\Psi}^{(i)} \cong \mathbf{u}^{(i)} \tag{2.34}$$

in which $\mathbf{u}^{(i)}$ represents displacement vector of MDOF system at the (i)'th pushover step obtained from a single-run adaptive pushover analysis, such as DAP method (see Figure 2.8). $\boldsymbol{\Psi}^{(i)}$ refers to instantaneous mode shape of the MDOF system. In fact it is a controversial assumption as stated earlier because deflected shape of the MDOF system obtained from a multi-mode pushover analysis contains higher mode effects. Moreover, theoretically, it is doubtful that mode shape vector derived from the deflected shape of the MDOF system confirms the modal orthogonality conditions.

Equation 2.34 leads to the following equations according to above-given assumption

$$\mathbf{u}^{(i)} = \boldsymbol{\Psi}^{(i)}\Gamma^{(i)}d^{(i)} \quad ; \quad d^{(i)} = \frac{1}{\Gamma^{(i)}} \tag{2.35}$$

where $\Gamma^{(i)}$ and $d^{(i)}$ represent participation factor based on the deformed shape of the structure and spectral displacement at the (i)'th step, respectively. Hence, spectral displacement coordinates of the capacity diagram of an equaivalent SDOF system can be expressed as

$$d^{(i)} = \frac{\sum_{n=j}^{N} m_j (\Psi_j^{(i)})^2}{\sum_{n=j}^{N} m_j \Psi_j^{(i)}} \tag{2.36}$$

where m_j denotes the mass at the j'th node and N refers to the number of degree of freedom. Spectral acceleration coordinates corresponding to the (i)'th pushover step is defined in the following equation.

$$M_{eff}^{(i)} = \frac{(\sum_{n=j}^{N} m_j \Psi_j^{(i)})^2}{\sum_{n=j}^{N} m_j \Psi_j^{(i)2}} \quad ; \quad a^{(i)} = \frac{V_b^{(i)}}{M_{eff}^{(i)}} \tag{2.37}$$

As a result of the derivation of the modal capacity diagram, single pushover curve containing higher mode effects is utilized in estimating seismic demands.

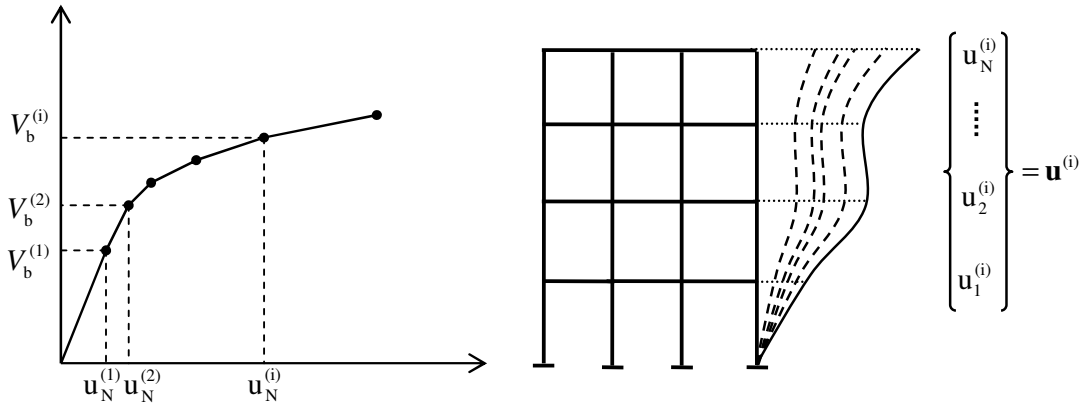

Figure 2.8. Pushover curve (Base shear vs. Roof displacement) and corresponding story displacements at each pushover step

2.4.5. Simultaneous Multi-Mode Pushover Analysis with Adaptive Multi-Modal Load Patterns

One of the pushover analysis methods that takes into account the higher mode effects in adaptive fashion has been proposed by Gupta and Kunnath (2000). In this method, incremental response spectrum analysis associated with the instantaneous configuration of the structure is performed at each pushover step. Eigenvalue analysis is performed at each pushover step based on the current stiffness state in order to compute equivalent modal lateral forces. Then, these forces are scaled by instantaneous elastic spectral pseudo-accelerations as given in the following equation.

$$\Delta\mathbf{f}_n^{(i)} = \underbrace{\mathbf{M}\boldsymbol{\Phi}_n^{(i)}\Gamma_{xn}^{(i)}S_{aen}^{(i)}}_{\Delta\bar{\mathbf{f}}_n^{(i)}}\Delta\bar{F}^{(i)} \quad ; \quad \Delta\mathbf{f}_n^{(i)} = \Delta\bar{\mathbf{f}}_n^{(i)}\Delta\bar{F}^{(i)} \tag{2.38}$$

Static analysis is carried out under the scaled modal lateral forces for each mode separately. Contributions of modal response quantities at each step are combined using SRSS rule to obtain incremental responses, such as story drift, plastic rotations or section forces. The procedure is repeated progressively for each predefined number of uniform

step until target roof displacement obtained from inelastic time history analysis or specified building base shear is reached. As a result of this pushover procedure, resultant pushover curve including higher mode effects has been obtained. In the case of seismic demand estimation by using elastic response spectrum, representation of an equivalent SDOF system based on the pushover curve is needed. However, demand estimation based on single-combined mode has not been implemented in this procedure.

It should be pointed out that unlike the single-run pushover analyses with combined multi-mode loadings patterns described above, in this force-controlled pushover procedure, incremental response quantities are computed from the combination of modal response quantities, not from combined seismic load. The use of the instantaneous values of the elastic spectral pseudo-accelerations to scale relative modal response contributions is identical to the modal scaling procedure proposed by Elnashai (2001). Therefore, when P-delta effects cause a negative post-yield stiffness in the pushover curve, pushover analysis can not be performed due to the limitation of modal scaling procedure based on instantaneous spectral quantities as stated earlier.

2.4.6. Simultaneous Multi-Mode Pushover Analysis with Adaptive Multi-Modal Displacement Patterns

The multi-mode pushover analysis procedure IRSA (Incremental Response Spectrum Analysis) has been introduced recently to enable the two- and three-dimensional nonlinear analyses of buildings in a practical manner (Aydınoğlu, 2003). Incremental Response Spectrum Analysis (IRSA) is a multi-mode pushover procedure, in which the incremental response is assumed *piecewise linear* at each pushover step in between the formation of two consecutive plastic hinges. Linear response spectrum analysis associated with the instantaneous configuration of the structure is performed at each step. Modal capacity diagrams develop simultaneously during the pushover analysis. Relative modal displacement increments are scaled by the instantaneous inelastic spectral displacement demands to determine relative modal contributions and hence plastic hinge formation at each step. Adopting an appropriate hysteretic model based on the bilinear idealization of modal capacity diagrams developed from the first step to the end of the current step, inelastic spectral displacement demands for a given earthquake can be obtained through a

time history analysis or inelastic displacement response spectra. At each step, this analysis procedure is repeated based on the bilinear idealization of the updated modal capacity diagrams until the cumulative modal displacement values reach peak modal displacements. Physically, such an analysis corresponds to a series of analyses with gradually scaled earthquakes, which is similar to the concept of incremental dynamic analysis (IDA). For practical purposes, a simpler approach has been proposed in the practical version of IRSA instead of the demanding analysis procedure mentioned above. The practical version of IRSA utilizes well-known equal displacement rule for each mode to estimate corresponding inelastic spectral displacement as depicted in Figure 2.9 and this approximation leads to the following equations.

$$\Delta d_{\mathrm{n}}^{(\mathrm{i})} = \Delta \tilde{F}^{(\mathrm{i})} S_{\mathrm{den}}^{(1)} \tag{2.39}$$

where $\Delta \tilde{F}^{(\mathrm{i})}$ is an incremental scale factor, which is applicable to all modes at the (i)'th pushover step. $S_{\mathrm{den}}^{(1)}$ represents n'th mode initial elastic spectral displacement defined at the first step. Cumulative modal displacement at the end of the same pushover step can be written as

$$d_{\mathrm{n}}^{(\mathrm{i})} = d_{\mathrm{n}}^{(\mathrm{i}-1)} + \Delta d_{\mathrm{n}}^{(\mathrm{i})} \quad ; \quad d_{\mathrm{n}}^{(\mathrm{i})} = \tilde{F}^{(\mathrm{i})} S_{\mathrm{den}}^{(1)} \tag{2.40}$$

in which $\tilde{F}^{(\mathrm{i})}$ represents the *cumulative scale factor* with a maximum value of unity:

$$\tilde{F}^{(\mathrm{i})} = \tilde{F}^{(\mathrm{i}-1)} + \Delta \tilde{F}^{(\mathrm{i})} \leq 1 \tag{2.41}$$

Thus, main stages of IRSA can now be described as follows and summarized in Figure 2.10.

1. A standard linear response spectrum analysis (RSA) is performed at each incremental pushover step for the unit value of the unknown incremental scale factor ($\Delta \tilde{F}^{(\mathrm{i})} = 1$) by considering instantaneous mode shapes that are compatible with the current stiffness state of the structure and the initial elastic spectral displacements $S_{\mathrm{den}}^{(1)}$ taken as seismic input. Thus, any response quantity of interest, which is

represented by a generic response quantity, $\tilde{r}^{(i)}$, is obtained for the unit value of the unknown incremental scale factor. Now, the increment of the generic response quantity, $\Delta r^{(i)}$, is expressed as

$$\Delta r^{(i)} = \tilde{r}^{(i)} \Delta \tilde{F}^{(i)} \tag{2.42}$$

and the generic response quantity at the end of the (i)'th pushover step can be written as

$$r^{(i)} = r^{(i-1)} + \Delta r^{(i)} = r^{(i-1)} + \tilde{r}^{(i)} \Delta \tilde{F}^{(i)} \tag{2.43}$$

in which $r^{(i)}$ and $r^{(i-1)}$ are the generic response quantities to develop at the end of current and previous pushover steps, respectively. In the first pushover step (i=1), response quantities due to gravity loading are considered as $r^{(0)}$.

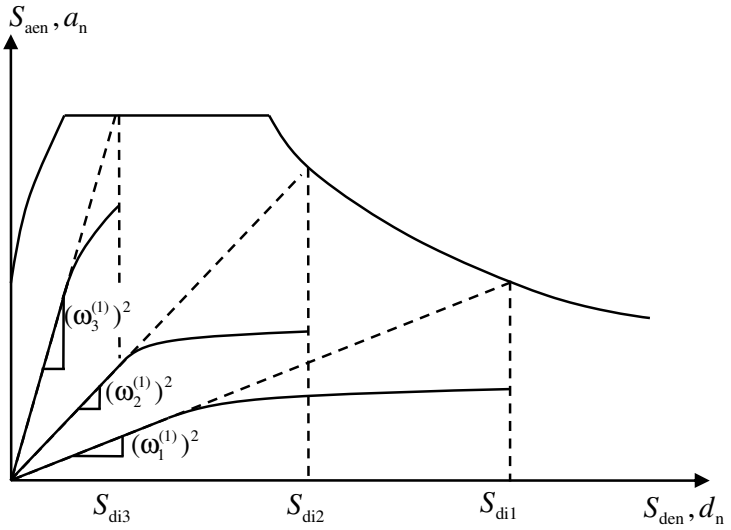

Figure 2.9. Modal capacity diagrams and corresponding inelastic spectral displacement demand

2. Equation (2.43) is specialized for the internal force components defining the yield surfaces of potential plastic hinges to develop in the structural system. The minimum $\Delta \tilde{F}^{(i)}$ identifies the location of the new hinge developed at the end of (i)'th pushover step.

3. Cumulative scale factor, $\tilde{F}^{(i)}$, is calculated from Equation (2.41) and checked if it exceeded unity. If unity is not exceeded, the remainder of this stage can be skipped and the analysis proceeds with the next stage. If exceeded, incremental scale factor in the last step, $\Delta\tilde{F}^{(p)}$, is re-calculated as

$$\Delta\tilde{F}^{(p)} = 1 - \tilde{F}^{(p-1)} \tag{2.44}$$

and in the last pushover step modal displacement increment is redefined as

$$\Delta d_n^{(p)} = S_{den}^{(1)} \Delta\tilde{F}^{(p)} \tag{2.45}$$

4. All response quantities of interest developed at the end of the pushover step are calculated from the generic expression of Equation (2.43). If the final pushover step has been reached, the analysis is terminated. If not, it is continued with the next stage.
5. The current stiffness matrix is modified by considering the last yielded hinge identified at Stage (2) and it is returned to Stage (1) for the next pushover step.

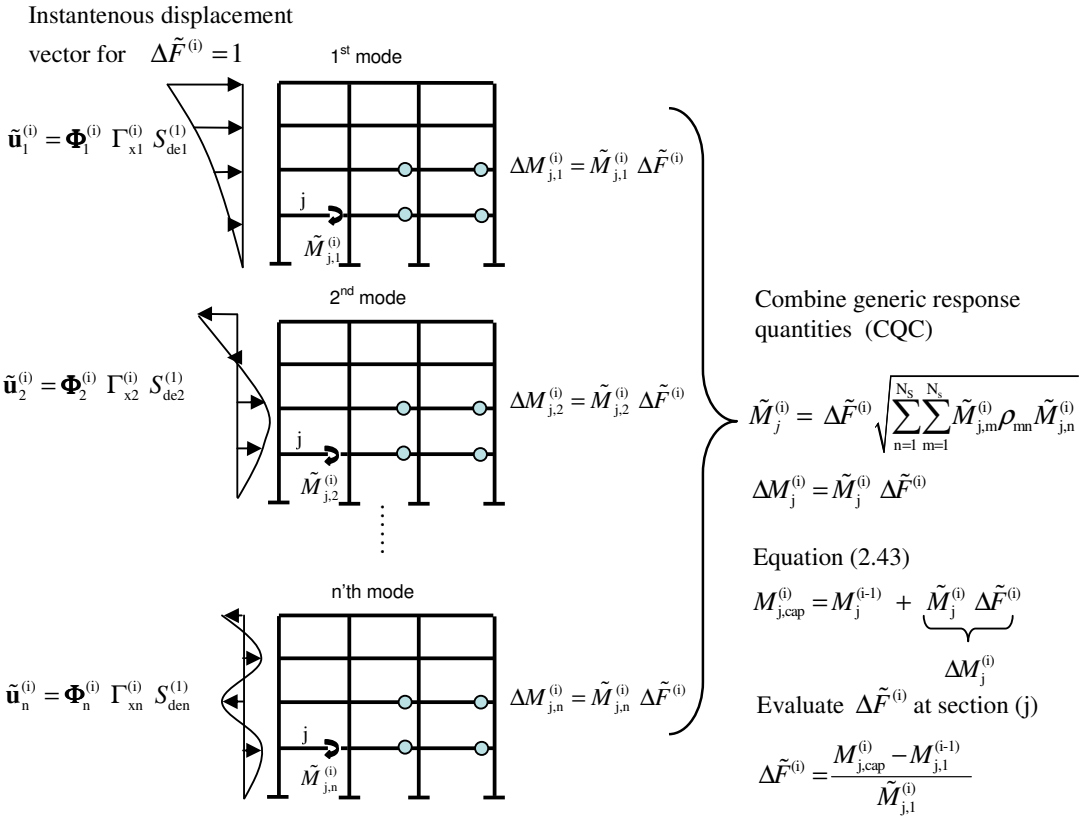

Figure 2.10. Piecewise linear pushover analysis procedure according to IRSA (Aydınoğlu, 2003)

2.4.7. Individual Multi-Mode Pushover Analysis with Invariant Multi-Mode Load Patterns

One of the improved pushover procedures proposed by Chopra and Goel (2001), the so-called modal pushover analysis (MPA) is taking into account the higher mode effects through pushover analysis assuming invariant load pattern. Performing modal pushover analyses under the invariant load patterns, which are consistent with the initial elastic mode shapes, is the most serious assumption inherent in this procedure. Pushover analysis for each mode is performed independently. Therefore, contributions from all modes to the incremental response quantities are neglected in the course of pushover analysis. In other words, it is assumed that modal response contributions to the inelastic behavior of the structure are uncoupled. A comparative study presented by Chintanapakdee and Chopra

(2003) shows that MPA manages to estimate story drift distribution for frame systems in a acceptable accuracy compared to that of FEMA-356. Analysis procedure in MPA are summarized in the following steps

1. Gravity load analysis is carried out before the pushover analysis for each mode. Pushover analysis is performed separately for as many modes as required for sufficient accuracy of the seismic response under invariant load patterns in accordance with the mode shapes based on initial elastic stiffness state of the structure as follows

$$\Delta\bar{\mathbf{f}}_n^{(1)} = \mathbf{M}\boldsymbol{\Phi}_n^{(1)} \tag{2.46}$$

   where $\Delta\bar{\mathbf{f}}_n^{(1)}$ denotes invariant load pattern for the n'th mode. **M** is diagonal mass matrix and $\boldsymbol{\Phi}_n^{(1)}$ represents the mode shape vector based on initial elastic stiffness state for the n'th mode.
2. Pushover curve for each mode is converted to modal capacity diagram of the equivalent SDOF system by using the modal conversion parameters based on the mode shapes at the first step.
3. Bilinear idealization is implemented to the modal capacity diagram of the equivalent SDOF system to evaluate inelastic spectral displacement demand under a given earthquake record or through inelastic displacement spectrum. Empirical equations for the ratio of deformations of inelastic and elastic systems developed by Chintanapakdee and Chopra (2003) can also be used.
4. Peak modal response quantities are calculated for each mode and gravity load effects are extracted from the peak response quantities to obtain modal response contributions as given in the following equation.

$$r_n^{(p)} = r_{n+g}^{(p)} - r_g \tag{2.47}$$

   where $r_{n+g}^{(p)}$ denotes peak response quantity obtained at the end of the modal pushover analysis for n'th mode and r_g represents gravity load response.

5. Modal response contributions obtained at Stage (4) are combined by using SRSS modal combination rule and then gravity load responses are added to the combined responses to obtain total response as follows.

$$r^{(p)} = r_g \pm \sqrt{\sum_{n=1}^{N} r_n^{(p)}} \tag{2.48}$$

According to modal pushover analysis method (MPA) proposed by Chopra and Goel (2001), pushover analysis for each mode is conducted independently and peak modal displacement demand for each mode is evaluated independently at the end of the modal pushover analysis. Thus, modal scaling procedure cannot be implemented in this procedure due to independent modal pushover analyses.

3. STRUCTURAL SYSTEMS, GROUND MOTIONS AND STATISTICAL EVALUATION PROCEDURE FOR SEISMIC DEMANDS

3.1. Structural Systems Used in This Study

Two types of load resisting systems are used in this study to evaluate performance of single-mode and multi-mode pushover procedures considered in this study. The first type of load resisting system is reinforced concrete frame system, which is predominantly used in the design of new reinforced concrete buildings and commonly observed in the existing building stock. Application of pushover analysis methods has been extensively tested for frame type structures. However, although dual systems are commonly preferred in practice for taller buildings, especially in high seismicity regions, verification studies examining dual systems are rare in the literature. Therefore, dual systems have been also considered in this study for the evaluation of the multi-mode pushover analysis methods. For both types of lateral load resisting systems, two dimensional structural models, which are appropriate for buildings with symmetrical plan in both horizontal directions, are used.

3.1.1. Structural Model Used for Frame Systems

In the study of frame systems, a regular 5-bay planar frame model with five different heights (4, 8, 12, 16 and 20 stories) has been selected as shown in Figure 3.1a. Typical story height of 3.15 m and span length of 5 m have been assumed for all frame systems. Three different ductility levels, *i.e.*, low, medium and high, have been adopted in the design of frames. Therefore, totally 15 different frame systems have been considered in this study.

Columns and beams are modeled by using line elements. Effective flexural stiffnesses of the structural elements are determined based on cracked section bending rigidities of the cross sections. For beams, effective moment of inertia, I_{eff}, which is equal to 40% of moment of inertia of the gross section, is used to determine effective flexural

stiffness. For columns, axial forces due to the gravity loads, N_D, have been considered to determine cracked section bending rigidities. Reduced bending rigidity of the column section is estimated by using Equation (3.1) based on Turkish Seismic Code (TSC, 2007) depending on the ratio between the axial force due to gravity loads and compressive axial force capacity, N_C, of the column section of interest. For intermediate value of the ratio, linear interpolation has been implemented.

$$\begin{aligned} N_D / N_C \le 0.10 \;\Rightarrow\; EI_{eff} &= 0.4 EI_{gross} \\ N_D / N_C \ge 0.40 \;\Rightarrow\; EI_{eff} &= 0.8 EI_{gross} \end{aligned} \tag{3.1}$$

The floor diaphragm at each story level is assumed to be infinitely rigid. All degrees of freedoms at foundation level are assumed to be fixed. To account for inertia forces during dynamic analysis, story masses are calculated in accordance with the combination of dead load and live load (G + 0.3Q). Distributed dead load value of 4.5 kN/m^2 and live load value of 2.0 kN/m^2 are considered. Consistent with the gravity load effects, a total of 102.4 ton mass is lumped at each story level.

Concentrated plastic hinge with zero length is used to account for nonlinear behavior of the reinforced concrete components. Plastic hinge locations are assumed to be at both ends of the columns and the beams. For practical purposes, rigid-plastic moment-rotation relation without strain hardening has been adopted for all plastic hinges (Figure 3.2). P-M hinge model is used in columns to consider the effect of axial force to flexural yield strength.

In inelastic time history analyses, damping effect is considered through proportional (Rayleigh) damping matrix according to 5% modal damping ratio at 1st and the 4th mode with an exception of 4-story frame systems, where 1st and 3rd are selected in the definition of damping matrix. Figure 3.3 shows the variation of damping ratio with respect to the periods for 16-story frame systems.

3.1.2. Structural Model Used for Dual Systems

Lateral load resistance of a dual system is provided by a combination of frames and structural walls. The proportion of resistance shared by the elements is influenced by the relative stiffness of the frames and the walls along the height of the structure. In traditional design, the ratio, α_s, between the shear resistance provided by the shear wall at the base and the total shear force to be resisted is an important design parameter based on the linear behavior of the structure. However, development of plastic hinges during the seismic action changes the hierarchy in the resistance shared by the frames and the walls and hence the dynamic characteristics of the system. For instance, when a plastic hinge occurs at the base of the wall, deformation pattern, depending on the relative stiffness of the shear wall with respect to the frames, may change considerably. In this respect, three different wall shear ratio, α_s, have been considered for the design of the dual systems in this study.

Consequently, structural model used for the evaluation of dual system is composed of a 5-bay planar frame with a single wall element and three different heights (8, 16 and 24 stories) as shown in Figure 3.1b. For each model, three different wall shear ratio, α_s, which are 0.50, 0.75 and 0.90, have been used in the design phase and hence a total of 9 different structural models have been considered for the evaluation of dual systems. Typical story height and span length are the same as those used in the frame systems (Section 3.1.1). All structural elements including shear wall are modeled using line elements. Flexural stiffness of the shear wall section is reduced by a factor of 0.45 to obtain cracked section stiffness and assumed to be constant over the height of the wall. Effective flexural stiffnesses of the other members belonging to the frame are determined based on the procedure summarized in Section 3.1.1.

In order to provide deformation compatibility between the frame and the shear wall at each story level, infinitely rigid link element is modeled as shown in Figure 3.4. Accordingly, The story mass is assumed to be lumped at each story level and their values are calculated in accordance with the gravity load combination of G+0.3Q, similar to the frame systems. Weight of structural elements is also considered in the calculation of masses. Calculated story masses are given in Table 3.3, 3.4 and 3.5. At the foundation level, fixed base condition is assumed for all columns and the wall.

In addition to the plastic hinge model used for the frame systems as described in Section 3.1.1, nonlinear behavior of the shear wall is also idealized by means of plastic hinge model with the same moment-rotation relation. In order to take into account distributed plasticity along the wall, plastic hinges are defined at the bottom of the line elements representing the wall at each story level (see Figure 3.4). Effect of axial force on the flexural capacity of the wall section is neglected.

In nonlinear response history analysis, damping effect is considered through proportional (Rayleigh) damping matrix according to 5% modal damping ratio at 1st and the 4th mode.

3.2. Seismic Design of the Structural Systems

3.2.1. Seismic Design of Frame Systems

Each frame system has been designed in accordance with Turkish Seismic Code (2007) provisions and capacity design principles. Three ductility levels (low, medium and high) have been adopted in the design of the frames, for which strength reduction factors, R, are specified as 2, 4 and 6, respectively. However, the initial stiffnesses of the frames remain unchanged, regardless of the strength levels assigned. A code-based smoothed elastic response spectrum with a 5% damping ratio and a probability of exceedance of 10% percent in 50 years is used as a design earthquake. Elastic response spectrum is constructed based on Seismic Zone 1 and site class Z3 according to Turkish Seismic Code (2007) as shown in Figure 3.5.

An iterative design procedure has been adopted for the determination of member dimensions and required reinforcement at the critical sections. Linear Response Spectrum Analysis (RSA) is performed for each frame to determine the elastic design forces corresponding to strength reduction factor of 2, 4 and 6. Elastic response spectrum is reduced by these strength reduction factors to obtain reduced response spectra to be used in the analysis. Contribution of the first four modes of each frame has been taken into account in the analysis. Gravity load effect is also considered in the design of the structural elements with the combination of seismic load effect.

Under the action of design forces, required reinforcement ratio for each structural element has been computed. Accordingly, the flexural yield strength at the critical sections, where plastic hinges are located, have been determined based on characteristic material strength. In order to obtain strength distribution consistent with design forces throughout the structure, required reinforcement ratio of the sections has been selected so that its flexural capacity is approximately equal to the design forces obtained from the analysis. As a result of the design procedure summarized above, geometrical characteristic and modal properties of the frame systems are given in Table 3.1 and 3.2.

Minimum reinforcement requirements control the design of beams at the upper story levels and therefore their flexural strength are larger than the required strength corresponding to the sectional forces obtained from the analysis for R=4 and 6. However, it has been observed that sectional design forces obtained from the analysis for low ductility level (R=2) are dominant in the design of the structural elements throughout the structures. Therefore, strength distribution along the height of the structure is consistent with the earthquake seismic forces for R=2.

3.2.2. Seismic Design of Dual systems

Each dual system has been designed in accordance with Turkish Seismic Code (2007) provisions and capacity design principles. Single ductility level has been adopted in the design of the dual systems, for which strength reduction factors, R, is specified as 4. Code spectrum used in the design of the frame systems is also considered for dual systems (see Figure 3.5).

Linear Response Spectrum Analysis (RSA) is performed for each dual system to determine the elastic design forces corresponding to strength reduction factor of 4. Therefore, elastic design response spectrum is reduced by the strength reduction factor of 4 to be used in the response spectrum analyses. Contribution of the first four modes has been taken into account in the analysis. Gravity load effects are also considered in the design of the structural elements with the combination of seismic load effect.

Design procedure adopted in Section 3.2.1 for columns and beams is also used here for the elements belonging to the frame of the dual systems. Dimensions of the wall sections are tuned so that shear force resisted by the wall at the base section satisfies the wall shear ratios of α_s=0.50, 0.75 and 0.90. Dimensions of the frame elements and the wall elements are listed in Table 3.3, 3.4 and 3.5. Design moment at the base of the wall obtained from the response spectrum analysis is assumed as flexural yield strength of the section and it is assumed to be constant throughout the wall element. Dimensions belonging to the beam and column elements remain unchanged, regardless of the wall shear ratio, α_s, considered in the analysis. Periods and modal participating mass ratios for the first four modes are listed for all dual systems in Table 3.6.

3.3. Ground Motions and Scaling Procedure

All inelastic time history analyses have been performed with an ensemble of 20 ground motion records. In the selection process of ground motions, earthquake records with similar ground motion characteristics, such as distance to fault, earthquake magnitude and site condition, have been selected so as to reduce the scatter in the results obtained from the time history analyses and hence to obtain reliable mean results. Therefore, ground motions with the following characteristics were considered in the selection process:

- Minimum earthquake magnitude of M=6
- Peak ground acceleration (PGA) larger than 0.15g
- Distance to the fault between 13 km – 60 km
- Rock and firm soil condition

As a result of the selection process, selected earthquake records are listed in Table 3.7. Elastic response spectrum with 5% damping ratio of the selected records is shown in Figure 3.6.

In addition to the objective in the selection process of earthquake records, selected records are appropriately scaled to match the target response spectrum, which is the smoothed elastic response spectrum used in the design of the structural systems considered. A suitable scaling method as described in the dissertation presented by Celep,

U.U. (2007) in detail has been adopted in this study. According to this method, pseudo velocity response spectrum of the target response spectrum is divided by the pseudo velocity response spectrum of the original record of interest in frequency domain so as to obtain scale factor as a function of frequency. Then, the fourier transform of the original record is scaled by this scale factor. Inverse fourier transforms of the scaled fourier transform yields the scaled record. This process is repeated until the elastic acceleration response spectrum of the scaled record fairly match target elastic acceleration response spectrum. As a result of scaling procedure, elastic response spectrum of the scaled records and their means are presented in Figure 3.7.

3.3.1. Inelastic Spectral Displacement Demand Characteristics of Selected Ground Motions

Displacement-based evaluation of a structure is concerned with the estimation of maximum inelastic displacement demands consistent with the available global capacity of the existing structure. Utilization of inelastic displacement response spectrum provides a basic methodology in estimating displacement demands for practical purposes.

In the application of nonlinear static analyses for structural systems used in this study, estimation of the inelastic spectral displacement demands is based on the assumption that spectral displacement of an inelastic SDOF system is approximately equal to that of corresponding elastic SDOF system, which is the well kwon *equal displacement rule*. In fact, this is the practical approach adopted in FEMA 356. Therefore, it is important to select ground motion records, which satisfies this approximation as much as possible.

In order to observe inelastic spectral demand characteristics of the scaled ground motions, nonlinear analyses of inelastic SDOF systems are performed by a computer program, KOERINON, which utilizes a unified formulation of Piecewise Exact Method (Aydınoğlu and Fahjan, 2002). Inelastic SDOF systems with non-degrading hysteresis have been evaluated for 0%, 5% and 10% strain hardening ratio and constant strength reduction factors of 2, 4 and 6. Damping ratio is assumed to be equal to 5%. Inelastic spectral displacement for a given initial period can be defined as relative to the corresponding elastic displacement as shown in the following equation.

$$S_{di} = C_R S_{de} \quad ; \quad S_{di} = \frac{\mu}{R_y} S_{de} \tag{3.2}$$

in which S_{di} and S_{de} are inelastic and elastic spectral displacements, respectively, and C_R represents the spectral displacement amplification. As will be seen from Figure 3.8, μ and R_y represent ductility factor and strength reduction factor, respectively, which are defined as

$$\mu = \frac{S_{di}}{S_{dy}} \quad ; \quad R_y = \frac{S_{ae}}{S_{ay}} \tag{3.3}$$

Based on the Equation (3.2), strength-based displacement amplification can be defined as

$$C_R(T, R_y) = \frac{S_{di}(T, R_y)}{S_{de}(T)} = \frac{\mu(T, R_y)_{max}}{R_y} \tag{3.4}$$

Figure 3.9 shows the mean spectral displacement amplification spectra for R=2, 4 and 6. For all strain hardening ratios, spectral amplifications in a short period range result in rapid amplification of inelastic spectral displacements. This rapid amplification is observed for periods smaller than 0.6 s. For 0% strain hardening ratio and R_y=6, spectral amplifications is greater than one between 0.6 s and 2 s, which means that equal displacement rule underestimate inelastic spectral displacement demands. However, equal displacement rule is nearly satisfied in the intermediate- to long-period range for increasing R_y. For increasing strain hardening ratio together with increasing R_y, displacement spectral amplifications decrease in all period range compared to that of 0% strain hardening. Equal displacement rule is nearly satisfied in the periods between 0.6 s and 2 s, but overestimates inelastic spectral displacement demands, especially at longer period range.

As a result, it is expected that seismic demand estimation based on the equal displacement rule leads to conservative demand estimation for the structure where the first mode behavior is dominant in the structural response and their fundamental period is larger than 2 s. For smaller periods and increasing strain hardening ratio, the seismic demands

estimation is much more reliable. This conclusion is drawn in the context of ground motion records used in this study.

3.4. Statistical Evaluation Procedure for Seismic Demands

Seismic demand parameters, such as story displacement, inter story drift ratios and plastic rotations, obtained from the nonlinear time history analysis for each of 20 records have been evaluated based on the statistical study. Two basic methods, which are computed and counted statistic, has been implemented in order to determine central value and measure of dispersion. According to the computed statistic, sample mean value, $\bar{r}$, of the peak response quantity of n (number of record =20) values is calculated based on the following equation.

$$\bar{r} = \frac{1}{n}\sum_{i=1}^{n} r_i \tag{3.5}$$

The standard deviation of the observed peak values is given as follows.

$$\sigma = \frac{1}{n}\sum_{i=1}^{n} (r_i - \bar{r}) \tag{3.6}$$

If counted statistic is considered, the peak values obtained from 20 records are sorted in ascending order and the average of the 10^{th} and 11^{th} values becomes the median. Starting from the lowest value, the 16^{th} percentile and 84^{th} percentile corresponds to 3^{rd} and 17^{th} value, respectively. In this case, the dispersion in the data is estimated based on the difference of the median and 3^{rd} or 17^{th} value as given in the following equation.

$$\sigma = r_{17} - \bar{r} \tag{3.7}$$

Figure 3.10 is presented to observe the differences between the counted and computed statistic. As can be seen from the characteristic example shown in Figure 3.10, the difference between the counted and computed statistic is small. This tendency is generally observed in all data. However, when P-delta effect is included in the time history analyses, structural systems may experience extremely large demands, which physically

corresponds to the collapse state. In this case counted statistic method, which provides complete and consistent statistical evaluation, is used.

Table 3.1. Structural properties of reinforced concrete frame systems

Number of Stories	Floor Levels	Side Columns (cm)	Internal Columns (cm)	Beams (cm)	Story mass (t)
4	1 - 4	50 x 50	50 x 50	30 x 60	102.4
8	1 - 5	45 x 45	50 x 50	30 x 60	102.4
	6 - 8	45 x 45	45 x 45	30 x 60	102.4
12	1 - 3	55 x 55	60 x 60	30 x 60	102.4
	4 - 12	55 x 55	55 x 55	30 x 60	102.4
16	1 - 3	60 x 70	60 x 70	30 x 60	102.4
	4 - 6	60 x 60	60 x 60	30 x 60	102.4
	7 - 9	60 x 50	60 x 50	30 x 60	102.4
	10 - 16	60 x 40	60 x 40	30 x 60	102.4
20	1 - 3	70 x 70	70 x 70	30 x 60	102.4
	4 - 6	60 x 70	60 x 70	30 x 60	102.4
	7 - 9	60 x 60	60 x 60	30 x 60	102.4
	10 - 12	60 x 50	60 x 50	30 x 60	102.4
	13 - 20	60 x 40	60 x 40	30 x 60	102.4

Table 3.2. Modal Properties of frame systems

4 - story			
Mode	Period (s)	M_{eff} (%)	ΣM_{eff} (%)
1	0.74	0.840	0.840
2	0.23	0.107	0.947
3	0.13	0.040	0.987
4	0.09	0.013	1.000

8 - story			
Mode	Period (s)	M_{eff} (%)	ΣM_{eff} (%)
1	1.46	0.802	0.802
2	0.50	0.105	0.907
3	0.29	0.040	0.948
4	0.20	0.021	0.969

12 - story			
Mode	Period (s)	M_{eff} (%)	ΣM_{eff} (%)
1	1.96	0.791	0.791
2	0.65	0.101	0.892
3	0.38	0.039	0.931
4	0.26	0.022	0.952

16 - story			
Mode	Period (s)	M_{eff} (%)	ΣM_{eff} (%)
1	2.55	0.784	0.784
2	0.86	0.101	0.885
3	0.50	0.038	0.923
4	0.34	0.021	0.943

20 - story			
Mode	Period (s)	M_{eff} (%)	ΣM_{eff} (%)
1	3.14	0.776	0.776
2	1.06	0.102	0.877
3	0.62	0.038	0.915
4	0.43	0.020	0.935
5	0.32	0.013	0.948

Table 3.3. Structural properties of 8-story dual systems with α_s= 0.50, 0.75 and 0.90

	Floor Levels	Side Columns	Internal Columns	Beams	Shear wall		Story mass
		(cm)	(cm)	(cm)	l_w (cm)	b (cm)	(t)
α_s=0.50	1 - 5	45 x 45	50 x 50	30 x 60	185	25	106.8
	6 - 7	45 x 45	45 x 45	30 x 60	185	25	106.8
	8	45 x 45	45 x 45	30 x 60	185	25	104.6
α_s=0.75	1 - 5	45 x 45	50 x 50	30 x 60	275	30	109.0
	6 - 7	45 x 45	45 x 45	30 x 60	275	30	109.0
	8	45 x 45	45 x 45	30 x 60	275	30	105.7
α_s=0.90	1 - 5	45 x 45	50 x 50	30 x 60	450	30	113.4
	6 - 7	45 x 45	45 x 45	30 x 60	450	30	113.4
	8	45 x 45	45 x 45	30 x 60	450	30	107.9

Table 3.4. Structural properties of 16-story dual systems with α_s= 0.50, 0.75 and 0.90

.

	Floor Levels	Side Columns	Internal Columns	Beams	Shear wall		Story mass
		(cm)	(cm)	(cm)	l_w (cm)	b (cm)	(t)
α_s=0.50	1 - 3	60 x 70	60 x 70	30 x 60	225	30	107.8
	4 - 6	60 x 60	60 x 60	30 x 60	225	30	107.8
	7 - 9	60 x 50	60 x 50	30 x 60	225	30	107.8
	10 - 16	60 x 40	60 x 40	30 x 60	225	30	105.1
α_s=0.75	1 - 3	60 x 70	60 x 70	30 x 60	375	30	111.4
	4 - 6	60 x 60	60 x 60	30 x 60	375	30	111.4
	7 - 9	60 x 50	60 x 50	30 x 60	375	30	111.4
	10 - 16	60 x 40	60 x 40	30 x 60	375	30	106.9
α_s=0.90	1 - 3	60 x 70	60 x 70	30 x 60	650	30	118.0
	4 - 6	60 x 60	60 x 60	30 x 60	650	30	118.0
	7 - 9	60 x 50	60 x 50	30 x 60	650	30	118.0
	10 - 16	60 x 40	60 x 40	30 x 60	650	30	110.0

Table 3.5. Structural properties of 24-story dual systems with α_s= 0.50, 0.75 and 0.90

.

	Floor Levels	Side Columns	Internal Columns	Beams	Shear wall		Story mass
		(cm)	(cm)	(cm)	l_w (cm)	b (cm)	(t)
α_s=0.50	1 - 6	80 x 80	80 x 80	30 x 60	275	30	109.0
	7 - 12	70 x 70	70 x 70	30 x 60	275	30	109.0
	13 - 18	60 x 60	60 x 60	30 x 60	275	30	109.0
	19 - 24	60 x 40	60 x 40	30 x 60	275	30	105.7
α_s=0.75	1 - 6	80 x 80	80 x 80	30 x 60	500	30	114.4
	7 - 12	70 x 70	70 x 70	30 x 60	500	30	114.4
	13 - 18	60 x 60	60 x 60	30 x 60	500	30	114.4
	19 - 24	60 x 40	60 x 40	30 x 60	500	30	108.4
α_s=0.90	1 - 6	80 x 80	80 x 80	30 x 60	800	30	122.4
	7 - 12	70 x 70	70 x 70	30 x 60	800	30	122.4
	13 - 18	60 x 60	60 x 60	30 x 60	800	30	122.4
	19 - 24	60 x 40	60 x 40	30 x 60	800	30	114.4

Table 3.6. Modal Properties of dual systems

4-story (α_s=0.50)			
Mode	Period (Sec.)	M_{eff} (%)	ΣM_{eff} (%)
1	1.36	0.760	0.760
2	0.43	0.120	0.880
3	0.21	0.052	0.932
4	0.13	0.030	0.962

4-story (α_s=0.75)			
Mode	Period (Sec.)	M_{eff} (%)	ΣM_{eff} (%)
1	1.21	0.718	0.718
2	0.33	0.149	0.867
3	0.14	0.062	0.930
4	0.08	0.033	0.963

4-story (α_s=0.90)			
Mode	Period (Sec.)	M_{eff} (%)	ΣM_{eff} (%)
1	0.95	0.680	0.680
2	0.21	0.185	0.865
3	0.08	0.069	0.934
4	0.05	0.034	0.968

16-story (α_s=0.50)			
Mode	Period (Sec.)	M_{eff} (%)	ΣM_{eff} (%)
1	2.48	0.758	0.758
2	0.80	0.108	0.865
3	0.43	0.044	0.910
4	0.27	0.026	0.936

16-story (α_s=0.75)			
Mode	Period (Sec.)	M_{eff} (%)	ΣM_{eff} (%)
1	2.28	0.720	0.720
2	0.66	0.127	0.847
3	0.31	0.056	0.902
4	0.18	0.031	0.933

16-story (α_s=0.90)			
Mode	Period (Sec.)	M_{eff} (%)	ΣM_{eff} (%)
1	1.85	0.670	0.670
2	0.43	0.168	0.837
3	0.17	0.066	0.903
4	0.10	0.035	0.938

24-story (α_s=0.50)			
Mode	Period (Sec.)	M_{eff} (%)	ΣM_{eff} (%)
1	3.64	0.750	0.750
2	1.19	0.108	0.857
3	0.65	0.043	0.900
4	0.41	0.025	0.925

24-story (α_s=0.75)			
Mode	Period (Sec.)	M_{eff} (%)	ΣM_{eff} (%)
1	3.35	0.708	0.708
2	0.97	0.128	0.837
3	0.45	0.055	0.892
4	0.26	0.031	0.923

24-story (α_s=0.90)			
Mode	Period (Sec.)	M_{eff} (%)	ΣM_{eff} (%)
1	2.87	0.666	0.666
2	0.69	0.162	0.828
3	0.28	0.064	0.892
4	0.15	0.034	0.926

Table 3.7. Selected earthquake records in the study

No	Earthquake Name	M	Station	Distance (km)	Site Condition	PGA (g)	PGV (cm/s)	PGD (cm)
1	Chalfant Valley	6.2	54428 Zack Brothers Ranch	18.7	D	0.45	36.9	7.01
2	Chalfant Valley	6.2	54429 Zack Brothers Ranch	18.7	D	0.40	44.5	8.56
3	Loma Prieta 1989	6.9	APEEL 2 - Redwood City	47.9	D	0.22	34.3	6.87
4	Loma Prieta 1989	6.9	1686 Fremont - Emerson Court	43.4	B	0.19	12.7	5.5
5	Mammoth Lakes 1980	6	54214 Long Valley dam	19.7	A	0.48	14.2	1.77
6	Mammoth Lakes 1980	5.7	54214 Long Valley dam	14.4	A	0.25	18.5	1.56
7	Mammoth Lakes 1980	6	54301 Mammoth Lakes H. S.	14.2	D	0.39	23.9	2.72
8	Morgan Hill 1984	6.2	47380 Gilroy Array #2	15.1	C	0.21	12.6	2.1
9	Morgan Hill 1984	6.2	57382 Gilroy Array #4	12.8	C	0.35	17.4	3.11
10	Northridge 1994	6.7	90074 La Habra - Briarcliff	61.6	C	0.21	12.3	1.23
11	Northridge 1994	6.7	24575 Elizabeth Lake	37.2	C	0.16	7.3	2.7
12	Northridge 1994	6.7	24611 LA - Temple &amp	32.3	B	0.18	20	2.74
13	Northridge 1994	6.7	90061 Big Tujunga, Angeles Nat F	24	B	0.25	12.7	1.12
14	Northridge 1994	6.7	90021 LA - N Westmoreland	29	B	0.40	20.9	2.29
15	Whittier Narrows 1987	6	Brea Dam (Downstream)	23.3	D	0.31	14.5	0.77
16	Whittier Narrows 1987	6	108 Carbon Canyon Dam	26.8	A	0.22	8.7	0.64
17	Whittier Narrows 1987	6	90034 LA - Fletcher Dr	14.4	C	0.21	12.6	1.45
18	Whittier Narrows 1987	6	90063 Glendale - Las Palmas	19	C	0.30	17.1	1.82
19	Whittier Narrows 1987	6	90021 LA - N Westmoreland	16.6	B	0.21	9.7	0.98
20	Whittier Narrows 1987	6	24461 Alhambra, Fremont Sch	13.2	B	0.33	22	2.42

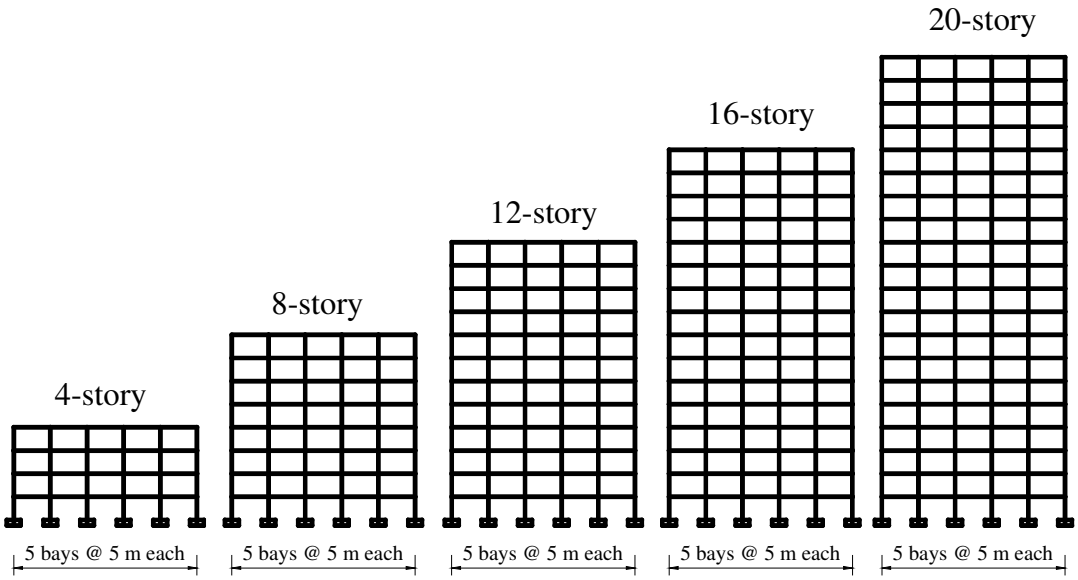

Typical story height =3.15 m

(a)

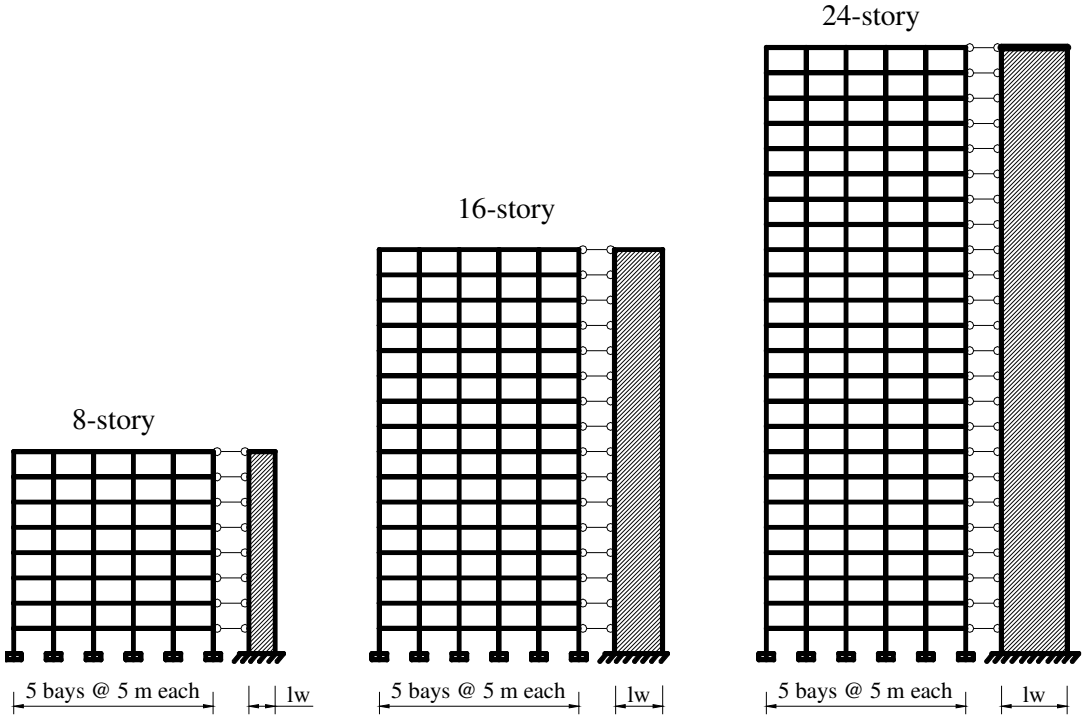

Typical story height =3.15 m

(b)

Figure 3.1. Reinforced concrete (a) frame systems and (b) dual systems used in this study

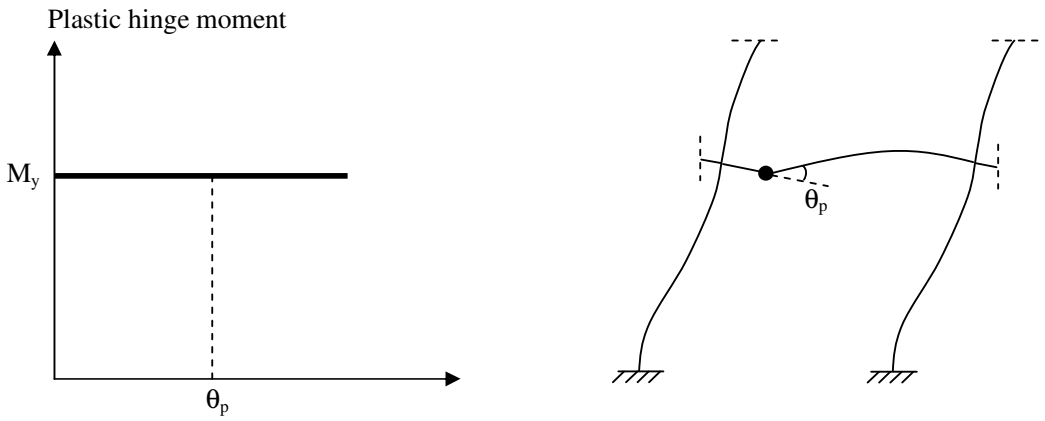

Figure 3.2. Moment-rotation relationship for plastic hinges

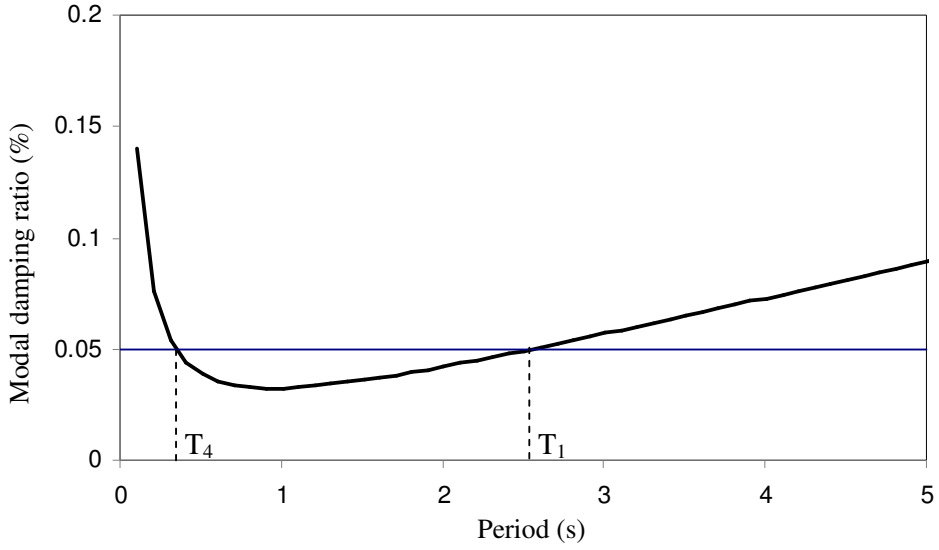

Figure 3.3. Definition of modal damping ratio for 16-story frame system

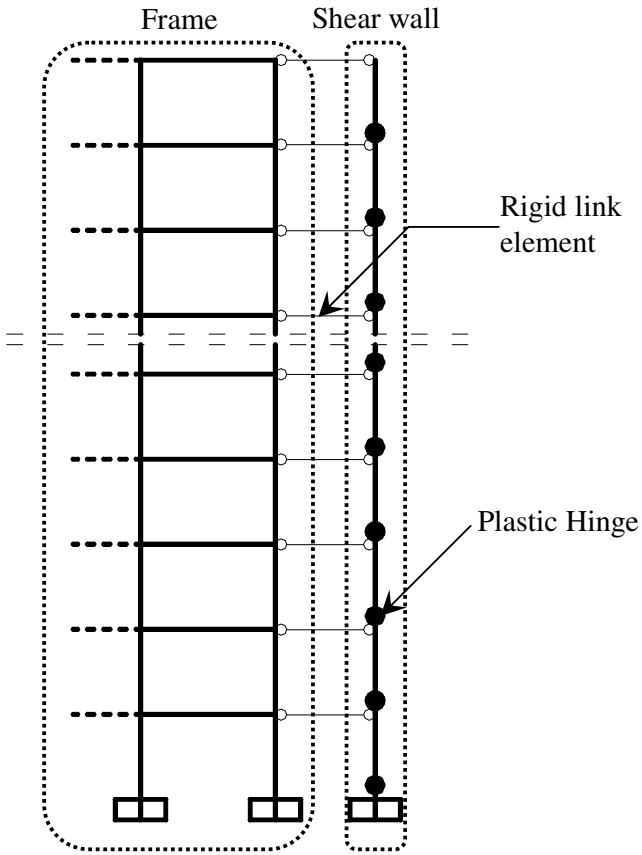

Figure 3.4. Plastic hinge locations defined for shear wall

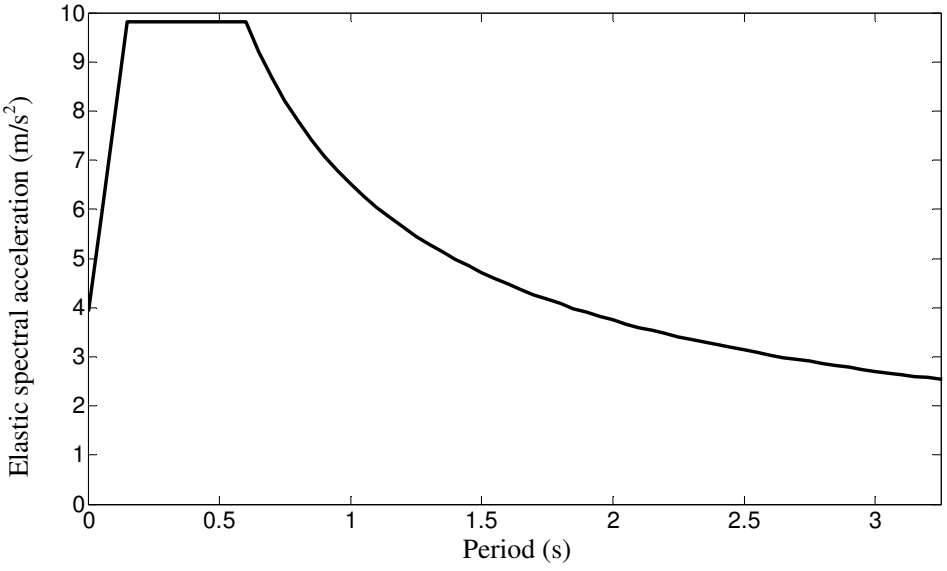

Figure 3.5. Elastic acceleration response spectrum with 5% damping ratio according to Turkish Seismic Code (2007)

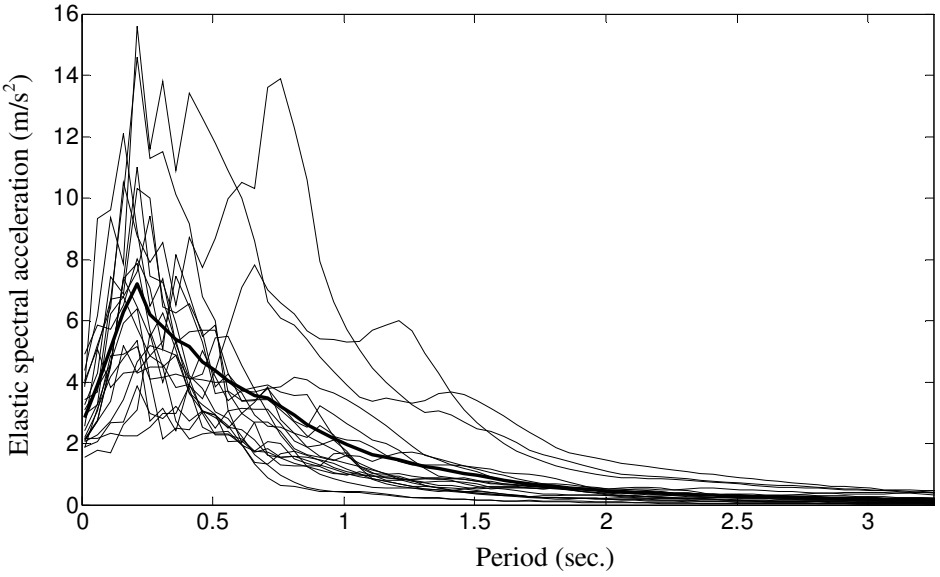

Figure 3.6. Acceleration response spectra of selected records and their mean with 5% damping ratio

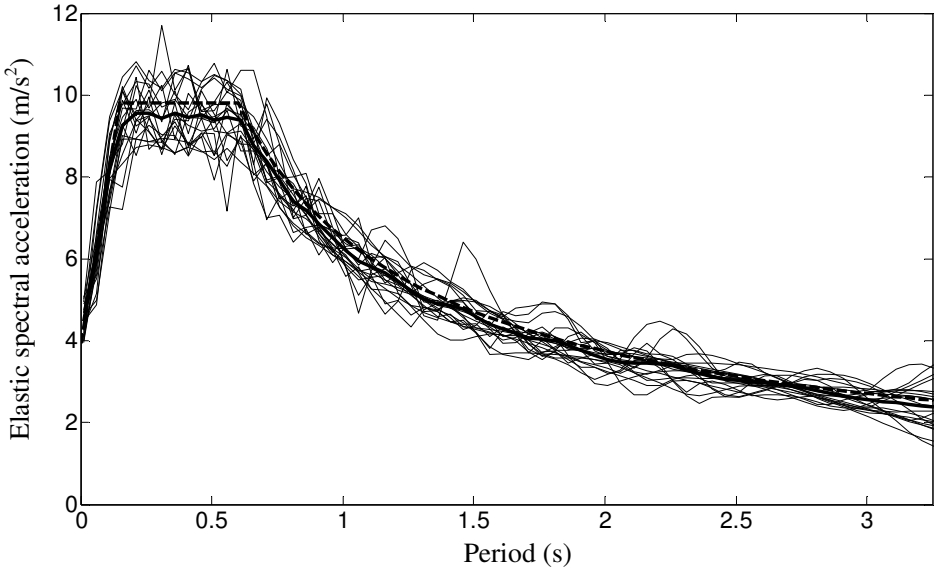

Figure 3.7. Acceleration response spectra of the scaled records and their mean superimposed on code response spectrum with 5% damping ratio

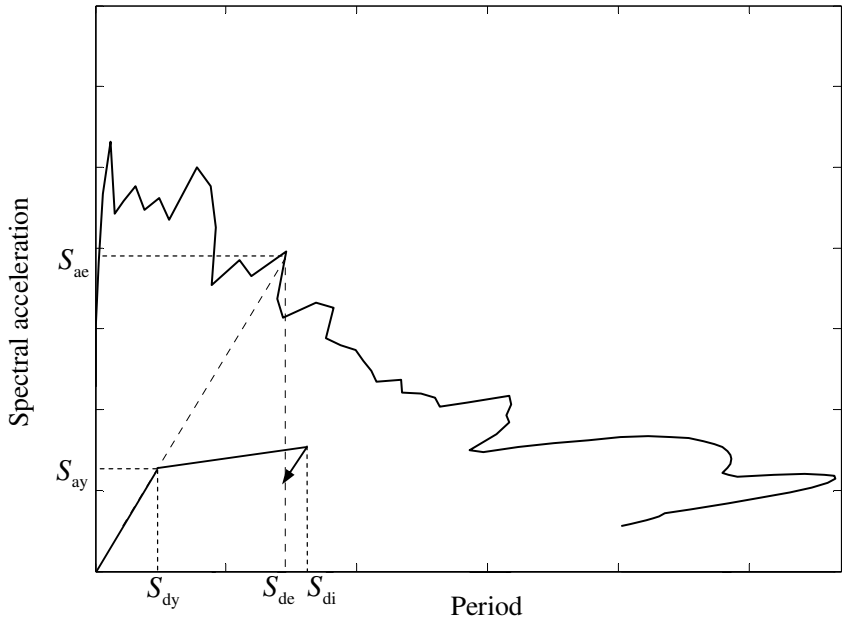

Figure 3.8. Bilinear representation of an inelastic SDOF system and elastic demand response spectrum of an earthquake

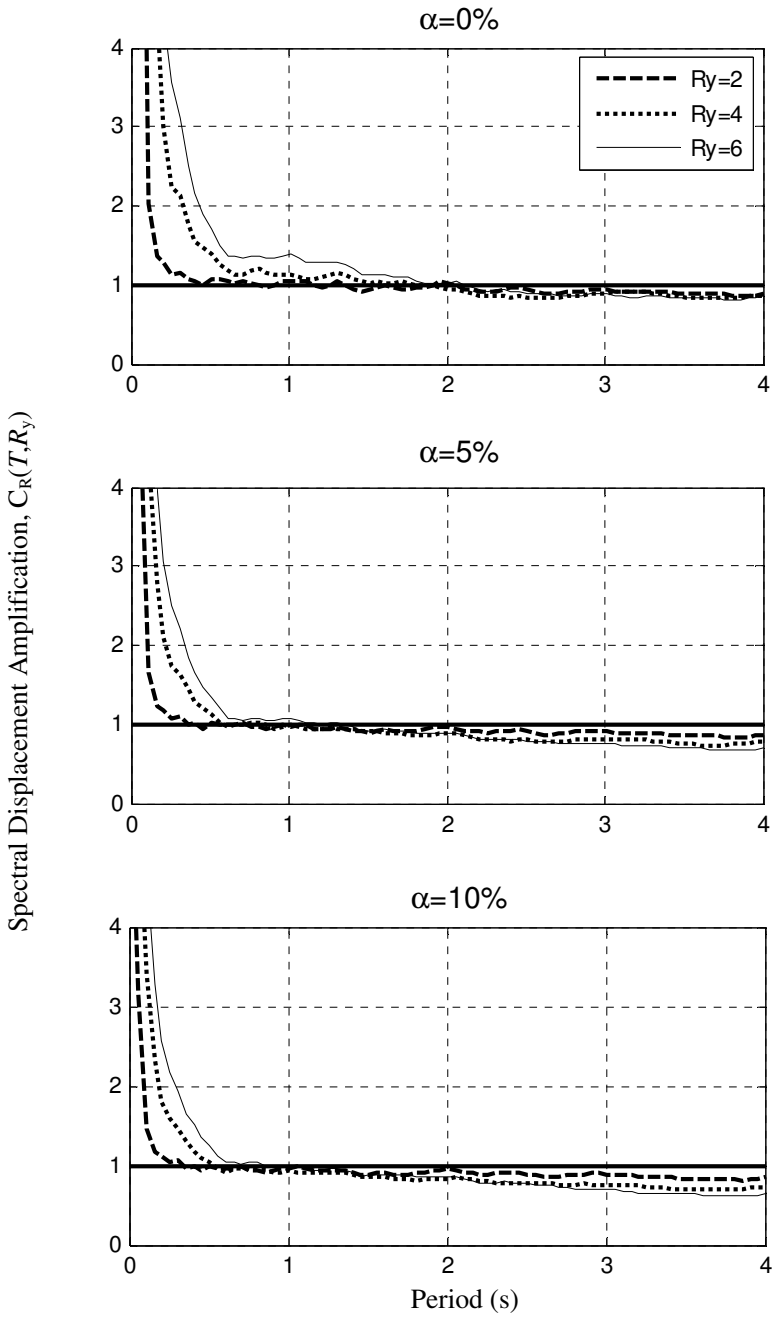

Figure 3.9. Mean strength-based displacement amplification spectra of 20 scaled ground motions for R_y=2, 4 and 6 and α=0%, 5%, 10% strain hardening, 5% damping ratio

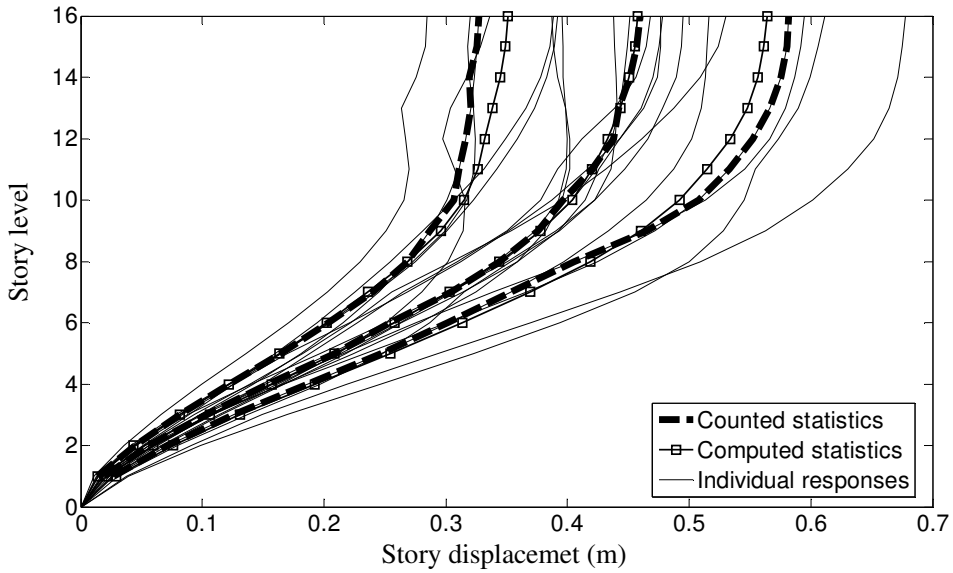

Figure 3.10. Mean and mean $\pm \sigma$ story displacements based on counted and computed statistic for 16-story frame system of medium ductility level (R=4)

4. EVALUATION OF SINGLE-MODE AND MULTI-MODE PUSHOVER PROCEDURES FOR FRAME SYSTEMS

In this chapter, a comparative study for frame systems is conducted to evaluate performance of the multi-mode pushover analysis methods proposed by Gupta and Kunnath (2000), Chopra and Goel (2001), Aydınoğlu (2003), Antoniou and Pinho, (2004[b]) and Casarotti and Pinho (2007) in estimating seismic demands. Additionally, nonlinear static procedures with four different lateral load distributions as specified in FEMA 356 (FEMA, 2000) are considered.

The structural systems analyzed in this chapter are two dimensional frame systems with five different heights (4, 8, 12, 16 and 20 stories) and with three different strength levels (R=2, 4 and 6), as described in Chapter 3. Inelastic response of each frame system to 20 earthquake records is determined by using inelastic time history analysis (ITHA).

Representation of seismic input by a smoothed elastic response spectrum and estimating seismic demands by using elastic response spectrum are the preferred choice in engineering practice. Therefore, in order to carry out a study in a manner consistent with engineering practice, single elastic response spectrum, which is the mean response spectrum of 20 scaled earthquake records (see Figure 3.7), is used for each nonlinear static methods. Seismic demands obtained from each pushover analysis method are compared with the mean values of seismic demands from ITHA.

As a seismic demand parameter, inter-story drift ratio obtained from the nonlinear static analyses at each story level, which is a useful indicator related to damage and higher modes responses, are presented. However, for design and assessment purposes, definition of performance levels requires more detailed damage measures for structural members such as plastic rotations. Therefore, plastic rotations are also presented. Additionally, story displacement results have been analyzed for each frame system. In this study, plastic rotation and inter-story drift ratio, which are the demand parameters related to damage, are emphasized in the evaluation of the practice-oriented nonlinear static procedures. Consequently, maximum story displacements, maximum inter-story drift ratios and

maximum plastic rotations at the central beam along the height of the structure are presented.

4.1. Application of Nonlinear Static Procedures Considered in This Study

4.1.1. Single-Mode and Multi-Mode Pushover Analysis Methods Considered in This Study

Multi-mode pushover procedures in this study are classified based on the assumptions inherent in these methods, as presented in Chapter 2. In order to check the performance of these methods, hence their assumptions, mainly four different multi-mode pushover procedures have been considered as follows:

- Adaptive Spectra-Based Pushover Procedure (ASBP-Gupta and Kunnath, 2000)
- Modal Pushover Analysis (MPA-Chopra and Goel, 2001)
- Incremental Response Spectrum Analysis (IRSA - Aydınoğlu, 2003)
- Displacement-Based Adaptive Pushover (DAP - Antoniou and Pinho, 2004[b])

Additionally, four different lateral load distributions as described in FEMA 356 are considered. According to FEMA 356, it is suggested that at least two types of lateral load distributions should be applied to the structure. One of them should be selected from the following:

- Lateral load distribution consistent with the fundamental mode shape and assumed to be invariant throughout the pushover analysis (SMI).
- Lateral load distribution proportional to seismic force defined through distribution factor, C_{vx}, in FEMA 356 (section 3.3.1.3.2 – FEMA 356) (SME).
- Lateral load distribution proportional to story forces, which is calculated from story shears obtained from linear response spectrum analysis (SRSS).

The second lateral load distribution is uniform distribution or adaptive distribution, which takes into account changing structural properties following yielding. Adaptive load distribution, consistent with the fundamental mode shape (SMA), is used in this study. As

stated above, four lateral load distributions except uniform distribution are considered in accordance with FEMA 356. Figure 4.1 illustrates normalized lateral load distributions recommended in FEMA 356, except adaptive load pattern.

Consequently, eight different pushover analysis procedures have been performed for each frame system in this study. Five of them are multi-mode pushover analysis procedures that take into account higher mode effects (ASBP, IRSA, MPA, DAP and SRSS) and the others are single mode pushover analysis methods (SMI, SME and SMA).

4.1.2. Assumptions and Methodology in the Application of Nonlinear Static Analysis

The following assumptions are made in the application of single-mode and multi-mode pushover procedures.

- *Piecewise linear pushover analysis* technique is used for all pushover analysis methods. As stated earlier, structural system is assumed to be linear in between two consecutive plastic hinge formations. Accordingly, capacities of the structural members are represented by a piecewise linearised yield surface.
- In the analyses of multi-mode pushover methods, the first four modes of each frame system are included in the analyses to take into account higher mode effects. Accordingly, lateral load distribution for SRSS is calculated from the linear response spectrum analysis considering the first four modes.
- The P-delta effects due to gravity loads are included in the pushover analyses. However, when P-delta effects are included, pushover analysis for ASBP and DAP cannot be performed due to the limitation of the modal scaling procedures adopted in these method, as mentioned earlier in Chapter 2. Therefore, nonlinear static analyses including P-delta effects have been carried out only for MPA, IRSA and pushover analyses under the lateral load distributions of FEMA 356.
- In this study, for the purpose of conducting a practice-oriented study, smoothed elastic response spectrum is used in estimating seismic demands, which is the preferred choice in engineering practice. However, some of pushover analysis methods analyzed in this study are incapable of estimating seismic demands by using elastic response spectrum. These methods are ASBP and DAP, which can be

regarded as only capacity estimation tools, as indicated in Chapter 2. In order to estimate seismic demands for these two methods, it is assumed that each pushover curve obtained from ASBP and DAP are converted to the capacity diagram of the corresponding SDOF system in accordance with the procedure proposed by Casarotti and Pinho (2007). In fact, this procedure has not been implemented in ASBP. Therefore, it should be pointed out that application of this procedure for ASBP is the assumption made in this study so as to evaluate ASBP.

- Target inelastic spectral displacements for FEMA 356 and the other multi-mode pushover procedures are estimated according to well-known equal displacement rule to eliminate the discrepancy in terms of the evaluation of inelastic spectral displacements. Accordingly, elastic spectral displacement corresponding to the period determined from the first step of the capacity curve is assumed equal to inelastic spectral displacement demand.

A computer program has been coded in MATLAB (The MathWorks Inc., 2004) in order to perform multi-mode and single-mode pushover analysis procedures under consideration. The program is capable of performing piecewise linear pushover analyses for two dimensional frame systems. Accordingly, piecewise linear moment-axial force yield surface are used for column elements. Nonlinear behavior of the structural component is considered through plastic hinge model including normality condition for column elements. P-delta effects can be considered in the program.

Mainly two groups of nonlinear static analyses have been performed. In Group 1, 15 different frame systems have been analyzed for eight different pushover procedures excluding P-delta effects whereas Group 2 includes P-delta effects. Because of the limitation of the modal scaling procedure adopted in ASBP and DAP, six of eight different pushover procedures have been executed for the frame systems in Group 2. Totally, 210 nonlinear static analyses have been performed.

4.2. Inelastic Time History Analysis for Frame Systems

Statistical findings obtained from the inelastic time history analyses are assumed to be exact solutions and forms the basis for the comparative evaluation of the multi-mode pushover procedures in estimating seismic demand. The analyses have been performed by using RUAUMOKO (Carr, 2000) structural analysis program. Step-by-step integration based on average acceleration method (β=0.25, α=0.5) is used in the program for the solution of incremental equation of motion. In order to obtain acceptable accuracy, the time interval of a given acceleration records has been used.

In order to be consistent with the structural models used for nonlinear static analyses, nonlinear behavior of the structural components are represented by plastic hinge models in the time history analyses. Two different hysteretic models are used for plastic hinges, which are elasto-plastic and peak oriented hysteretic models. Figure 4.2 illustrates the hysteresis rule of both models. In addition to various hysteresis types, seismic demands of the frame systems have been investigated for the case including P-delta effects.

Consequently, four groups of time history analyses have been performed to study the sensitivity of the seismic demand parameter and the behavior of the frame systems in terms of P-delta effects and hysteresis models. These analysis groups are given as follows:

- Group 1 analyses with elasto-plastic hysteresis and without P-delta effects.
- Group 2 analyses with elasto-plastic hysteresis and P-delta effects.
- Group 3 analyses with peak-oriented hysteresis and without P-delta effects.
- Group 4 analyses with peak-oriented hysteresis and P-delta effects.

4.3. Inelastic Time History Analysis Results

Since time history analysis forms the basis of comparative evaluation, before presenting results of the non-linear static procedures, inelastic time history analyses will be examined in detail below. Figure 4.3 will be used as a guide to analyze inelastic time history analysis results.

Figure 4.3 presents the mean inter-story drift ratio profiles determined by inelastic time history analyses with or without P-delta effects for 4, 8, 12, 16 and 20-story frame systems with ductility factor of 4. As shown in Figure 4.3a, mean inter-story drift results obtained from the analyses for elasto-plastic and peak-oriented hysteresis rules are similar for all buildings. When P-delta effects are included in the analyses, inter-story drift demands increase especially for taller frames as expected. It should be noted that, the difference between the results for both type of hysteresis rules increases as the number of stories are increased (Figure 4.3b). At the lower and middle story levels of 16 and 20-story frames, where it is expected that the first mode behavior is dominant, the discrepancy due to the influence of different hysteresis characteristics is large. As can be seen from the Figure 4.2b reloading stiffness of the peak-oriented hsyteresis is less than that of elasto-plastic hysteresis and gradually decreases at each cycle. Therefore, resistance of the plastic hinges to the flexural force demand that may cause reloading in the reverse direction is lower than that of the elasto-plastic hysteretic rule. Thus, it may reduce or prevent the residual deformation in contrast to the elasto-plastic hysteresis. This phenomenon can be clearly observed in the analysis results, including P-delta effects, obtained from 20-story frame building for Mammoth Lake 1980 – A-LUL record as illustrated in Figure 4.4. In this figure, hysteretic behavior of a plastic hinge located at the right end of the central beam in the 8^{th} story level have been presented for elasto-plastic and peak-oriented model at the different time instant. After the plastic hinges for both hysteresis models experience the first cycle (t=5.21 s) causing a plastic deformation, it is observed that residual plastic rotation for elasto-plastic hysteresis is larger than that of peak-oriented hysteresis. Since reloading branch of the elasto-plastic hysteresis is much stiffer than that of the peak-oriented hysteresis, closing of the plastic hinge for elasto-plastic hysteresis is prevented. In the case of the second cycle (t=7.40 s), the similar trend can be observed. Progressively increasing residual plastic rotation at each cycle in elasto-plastic hysteresis eventually leads to a larger plastic rotation demand at the end of the analysis (t=42 s) relative to the plastic rotation demand for peak-oriented model. The similar trends have been also investigated in the frame systems with ductility level of 2 and 6.

4.4. Comparative Evaluation of Nonlinear Static Analyses and Inelastic Time History Analysis Results

4.4.1. Story Displacements

Figure 4.5 and Figure 4.6 present mean story displacement profiles obtained from the inelastic time history analyses (ITHA) and nonlinear static analyses for 15 different frame systems without P-delta effects. It is observed that the story displacements obtained from ITHA and all nonlinear static analyses match fairly well in low to mid-height buildings and begin to divert as the number of stories and the ductility levels are increased, especially for 16 and 20-story frame systems. This is attributed to approximation of equal displacement rule and the uneven distribution of damping effect through Rayleigh damping matrix.

As it is stated before, target inelastic spectral displacement demands for all nonlinear static procedures are determined based on the equal displacement rule. As can be seen in Figure 3.9, displacement amplification spectra shows that equal displacement rule overestimates the spectral displacements at long period range. It should be noted that these period ranges correspond to the first natural vibration periods of 16- and 20-story frame systems. Consequently, it is expected that overestimation of the nonlinear static procedures for the structures with long period partially comes from the approximation of equal displacement rule.

As can be seen in Figure 4.5, multi-mode adaptive pushover methods (ASBP, IRSA, DAP, SRSS) and single-mode adaptive method (SMA) give almost identical displacement profiles for all story levels as well as ductility levels. The same situation can also be observed between the single mode (SMI) and multi-mode (MPA) non-adaptive analyses. It can be concluded that pushover analysis based on single mode is sufficient in estimating story displacements response, which helps to explain the discrepancy as stated above between the story displacement results of ITHA and nonlinear static analyses. Additionally, it should be noted that non-adaptive single-mode and multi-mode pushover procedures, SMI and MPA, give more conservative results compared to the adaptive single-mode and multi-mode pushover methods, respectively, for all buildings.

Figures 4.7 and Figure 4.8 plot mean story displacement profiles obtained from the inelastic time history analyses and nonlinear static analyses with P-delta effects for 15 different frame systems. It is worth repeating that nonlinear static analyses including P-delta effects for DAP and ASBP have not been performed due to the limitation of the modal scaling procedures adopted in these methods. When P-delta effects due to the gravity load are included, story displacements obtained from all nonlinear static procedures for all buildings get closer to the results of ITHA with elasto-plastic hysteresis as compared to the results of analyses without P-delta effects. However, discrepancy between ITHA with peak-oriented hysteresis (ITHA(p.o.)) and the nonlinear static procedures still persists as observed in the case without P-delta effects. This can be attributed to the effect of peak-oriented hysteresis rule as discussed in Section 4.3.

4.4.2. Inter-story Drifts

Figures 4.9 and Figures 4.10 show mean inter-story drift ratio profiles obtained from the inelastic time history analyses and nonlinear static analyses without P-delta effects for 15 different frame systems. Mean inter-story drift profiles obtained from the ITHA in all buildings for R=2 have a uniform distribution in middle stories as compared to the results for R=4 and 6. This is in part a consequence of designing the structures. Elastic design forces for R=2 control the design of the structural elements at almost every story level followed by the consistency of the strength distribution with the design lateral forces. However, under the design of reduced seismic forces for R=4 and 6, strength level in upper stories are dominated by the minimum reinforcement conditions that lead to conservative flexural strength relative to that corresponding to the seismic design forces.

It is observed that height-wise distribution of inter-story drift ratios for low- to mid-rise buildings obtained from almost all nonlinear static analyses are similar to the exact solution (ITHA). However, the results begin to divert as the number of stories as well as the ductility level are increased at particularly lower and middle story levels. The bias in the inter-story drift results is mainly stemmed from the overestimation of equal displacement rule for taller buildings as indicated in the preceding section.

IRSA, DAP and SRSS give better results as compared to MPA in lower and middle stories of all buildings, where the largest inter-story drift ratio value is observed along the height of the structures (see Figures 4.9 and 4.10). Particularly in all stories of structures for R=2, the differences between MPA and other multi-mode pushover analyses except ASBP are clear. As mentioned earlier, pushover analysis for each mode is performed independently in MPA, neglecting the coupling of modal contributions at each pushover step, which is the main difference between the MPA and the other multi-mode pushover methods. The discrepancy between MPA and the other multi-mode pushover methods in Figures 4.9 and 4.10 indicates influence of combination of multi-mode effects at each pushover step. Moreover, result of SRSS for R=2 clearly support this finding because pushover analysis with SRSS is carried out in invariant manner as implemented in MPA. Therefore, it can be concluded that multi-mode pushover methods, which combine multi-mode effects at each pushover step give more accurate results in the lower and middle story levels for all frame systems.

Note that although modal response quantities are combined at the end of each pushover step in ASBP, ASBP excessively overestimates inter-story drift demands in lower and upper stories of 16- and 20-story buildings, where higher modes responses are expected to be significant. As can be seen from Figures 4.9 and 4.10, the differences between ASBP and IRSA indicates that modal scaling procedure based on instantaneous spectral acceleration as adopted in ASBP fails for taller frames for all ductility levels.

At the upper story levels, where higher mode responses are significant, IRSA and particularly MPA present much more accurate estimation for R=4 and 6 compared to the other nonlinear static procedures. It may be expected that DAP, as a multi-mode pushover analysis method, may manage to capture higher mode responses at the upper story levels. However, results of SMA and DAP are similar at the upper story levels. This similarity can also be observed between SRSS and SMI distributions. These results imply that multi-mode pushover analysis with single-load or single-displacement pattern based on multi-mode loading, such as DAP and SRSS, cannot estimate inter-story drift demands accurately at the upper story levels of taller frames.

The discrepancy between the ITHA and SME distribution is small in 4-story buildings. However, SME overestimates inter-story drift demands at the upper stories, but underestimates at the lower stories as the number of story and ductility level are increased. The discrepancy arises from the characteristic of load distribution of SME given in Figure 4.1a, which exaggerates story forces corresponding to upper story levels relative to that of lower stories, hence the responses at the upper stories.

FEMA 356 (FEMA, 2000) suggests two types of lateral distributions so as to bound the possible response due to the variety of the earthquake characteristics. When the envelope inter-story drift distribution obtained from load distributions of FEMA 356 (SMI, SME and SRSS) is traced along the height of the structures, it is observed that the difference between ITHA and the envelope result increases. However, SRSS alone provides more consistent results for all frames compared to the other lateral load distributions of FEMA 356.

When P-delta effects due to the gravity load are included (see Figures 4.11 and 4.12), it is observed that almost all nonlinear static procedures overestimate the inter-story drift result in the lower stories of buildings for R=2, especially in taller buildings. Because of P-delta effects, the story drift estimates tend to decrease in the upper stories, be unaffected in the middle stories, and increase in the lower stories. The decrease in drift of middle stories is due to unloading (or "backing up") of upper stories as the drift concentration occurs in the lower stories (Gupta and Krawinkler, 1999 and Goel and Chopra, 2004). Clearly, a drift concentration at the first story level arises from the largest gravity load at the first story and the early development of plastic hinges at the base of the first story columns, which lead to stiffness degradation in the first story relative to the upper stories.

Mean inter-story drift demands obtained from IRSA, SRSS and SMA for R=4 and 6 at the lower and middle story levels, where the first mode behavior is dominant, match well with the results of ITHA with elasto-plastic hysteresis. (see Figures 4.11). However, MPA and SMI slightly overestimate inter-story drift demands at these story levels. On the other hand, at the upper story levels, MPA and IRSA approach the exact results (ITHA) when compared to the inter-story distributions obtained from SRSS, SMI and SMA. The similar trend can be observed for the frames with peak-oriented hysteresis model as shown

in Figure 4.12. The accuracy of MPA at the upper story level is much more satisfactory than IRSA, as observed in the case without P-delta effects. Note that SRSS distribution and single-mode pushover analyses (SMI, SME and SMA) give identical inter-story drift estimates at the upper story level in taller frames. This situation point out that single-load pattern based on multi-mode loading, as implemented in SRSS, give inaccurate estimate of drift demands at the upper story levels for taller buildings.

It should be noted that inter-story drift distributions obtained from ITHA for peak-oriented model tend to be unaffected when P-delta effects are considered as stated in Section 4.3. Therefore, the discrepancy between ITHA (p.o.) and the all nonlinear static analyses for R=4 and 6 tend to increase as the number of story increases as shown in Figures 4.12, similar to the case without P-delta effects. Although all pushover analysis methods include this discrepancy, IRSA gives much more approximate inter-story drift estimates at the lower half of all frames as compared to the other nonlinear static methods. At the upper story levels in 16- and 20-story buildings, superiority of IRSA and MPA is still persist relative to other pushover analysis methods (SRSS, SMI, SME and SMA)

As a result of the analyses with P-delta effects, it can be concluded that IRSA and MPA are conservative at the lower and middle story level for taller buildings for R=4 and 6. MPA overestimates inter-story drift demand excessively at these story levels compared to IRSA. Another important observation is that P-delta effects uniformly magnify the error rate in the inter-story drift distributions – relative to the estimates without P-delta effects – throughout the structures obtained from IRSA and MPA.

4.4.3. Plastic Rotations

In this study, for the family of frame systems designed according to the strong-column and weak beam concept, the distribution of plastic hinge rotations is consistent with the distribution of the inter-story drift ratios obtained from ITHA and nonlinear static analyses. Therefore, accuracy of the nonlinear static procedures in estimating plastic rotation demands is expected to be similar to that of inter-story drift demands and discussed in the following paragraphs.

Figure 4.13 and Figure 4.14 show the maximum mean plastic rotations of the central beams estimated by ITHA and all pushover analysis procedures without P-delta effects. Similar to the inter-story drift ratios, plastic rotations obtained from almost all nonlinear static procedures are consistent with the exact solutions (ITHA) in buildings up to 8 stories. However, the results begin to divert as the number of story level and ductility level increase. In all buildings for R=2, superiority of IRSA, DAP and SRSS are still valid as observed in the inter-story drift results, since these analysis procedures take into account combined multi-mode effects at each pushover step as opposed to *individual multi-mode pushover analysis procedure*, MPA. In addition, it should be noted that single-mode pushover analyses (SMI and SMA) and MPA give identical plastic rotation estimates for 16- and 20-story buildings for R=2 where higher modes responses become important. This situation strongly emphasizes the shortcomings of individual multi-mode pushover analysis procedure. Consistent with this conclusion, multi-mode pushover analysis methods, ASBP, IRSA, DAP and SRSS distribution provide more reliable results at the lower half of buildings for R=4 and 6 as compared to MPA. However, in the upper story levels, IRSA and MPA give better results, especially for taller buildings.

It should be noted that at the upper story levels, ASBP gives more reliable plastic rotation estimate in buildings up to 12 stories relative to the other methods. However, it does not persist as the number of story levels and the ductility levels increase, similar to the observation in inter-story drift demands. As can be seen from Figure 4.13 and Figure 4.14, compared to other nonlinear static procedures, mean plastic rotation distributions obtained from IRSA give much more accurate results for the structures in all 16- and 20-story buildings. For a fixed frame height, error rate of IRSA in upper story levels reduces as the ductility level increases.

Figure 4.15 confirms the preceding predictions by comparing the inter-story drift demands computed by nonlinear static analyses and ITHA with P-delta effects. Plastic rotation estimates in lower stories for low- and mid-height buildings obtained from multi-mode pushover analyses, MPA, IRSA and SRSS, are similar to that obtained from ITHA with acceptable accuracy, thanks to elasto-plastic hysteresis rule. However, relative differences tend to increase in the upper stories in all frames due to P-delta effects. For a fixed frame height, the discrepancy between ITHA and nonlinear static procedures

decreases as the ductility level increases. As can be seen from Figure 4.16, all nonlinear static methods with respect to the ITHA (p.o.) overestimate the plastic rotation demands at the middle stories, where the maximum plastic rotations are observed, due to the influence of the peak oriented hysteresis.

It should be noted that the discrepancy between plastic rotation results obtained from ITHA and nonlinear static analyses with P-delta effects tends to increase for taller frames for R=2 as the contribution from higher mode effects become significant. This underestimation is similar to the trend found by almost all nonlinear static procedures in estimating inter-story drift for buildings for R=2. The differences arise from the drift concentration due to P-delta effects as discussed in the preceding section. It is worth noting that the degree of the discrepancy observed in plastic rotation estimates is larger than that of the inter-story drift estimate.

It can be concluded that multi-mode nonlinear static procedures overestimate the plastic rotation at the lower stories for 16- and 20-story buildings, but underestimate in the upper stories, where higher mode contributions are significant. IRSA and SRSS distribution give more approximate results that are much more close to ITHA (p.o.) in the lower and middle stories relative to the other pushover analysis methods. At the upper story levels, IRSA and MPA are more reliable as compared to SRSS although an underestimation of ITHA results still exists.

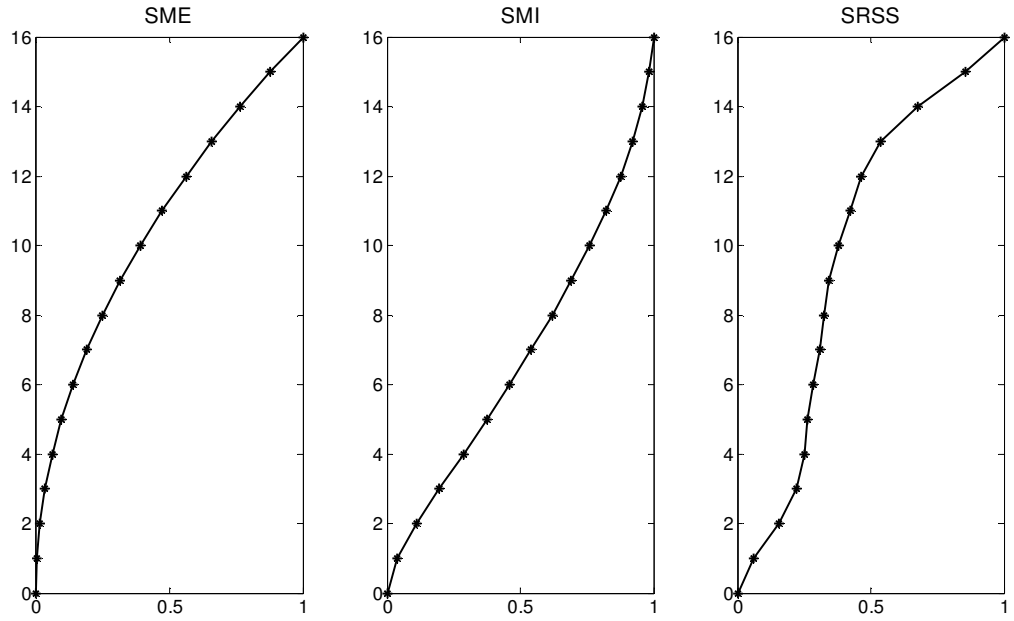

Figure 4.1. FEMA lateral load distributions for 16-story frame: (a) equivalent seismic force according to FEMA 356, SME, (b) single mode (1st mode) invariant, SMI, (c) combined story shear, SRSS

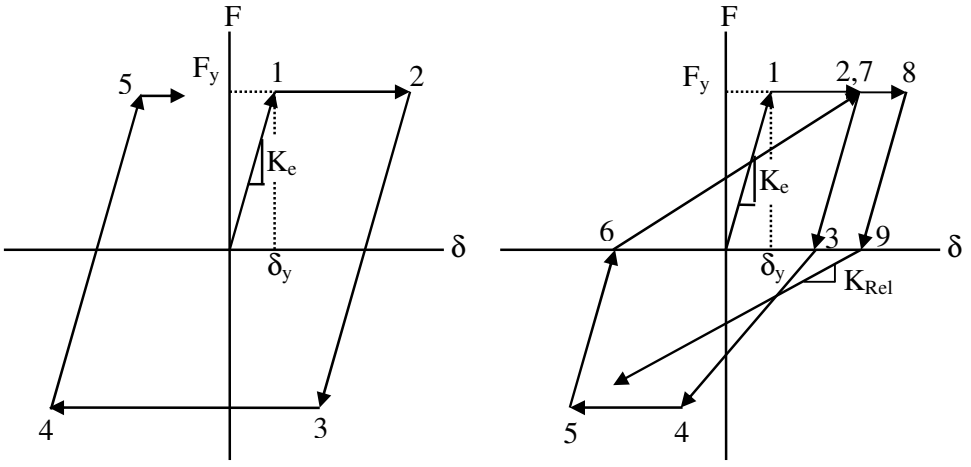

(a) Elasto-plastic hysteresis rule (b) Peak-oriented hysteresis rule

Figure 4.2. General force-deformation relation for (a) elasto-plastic and (b) peak-oriented hysteresis

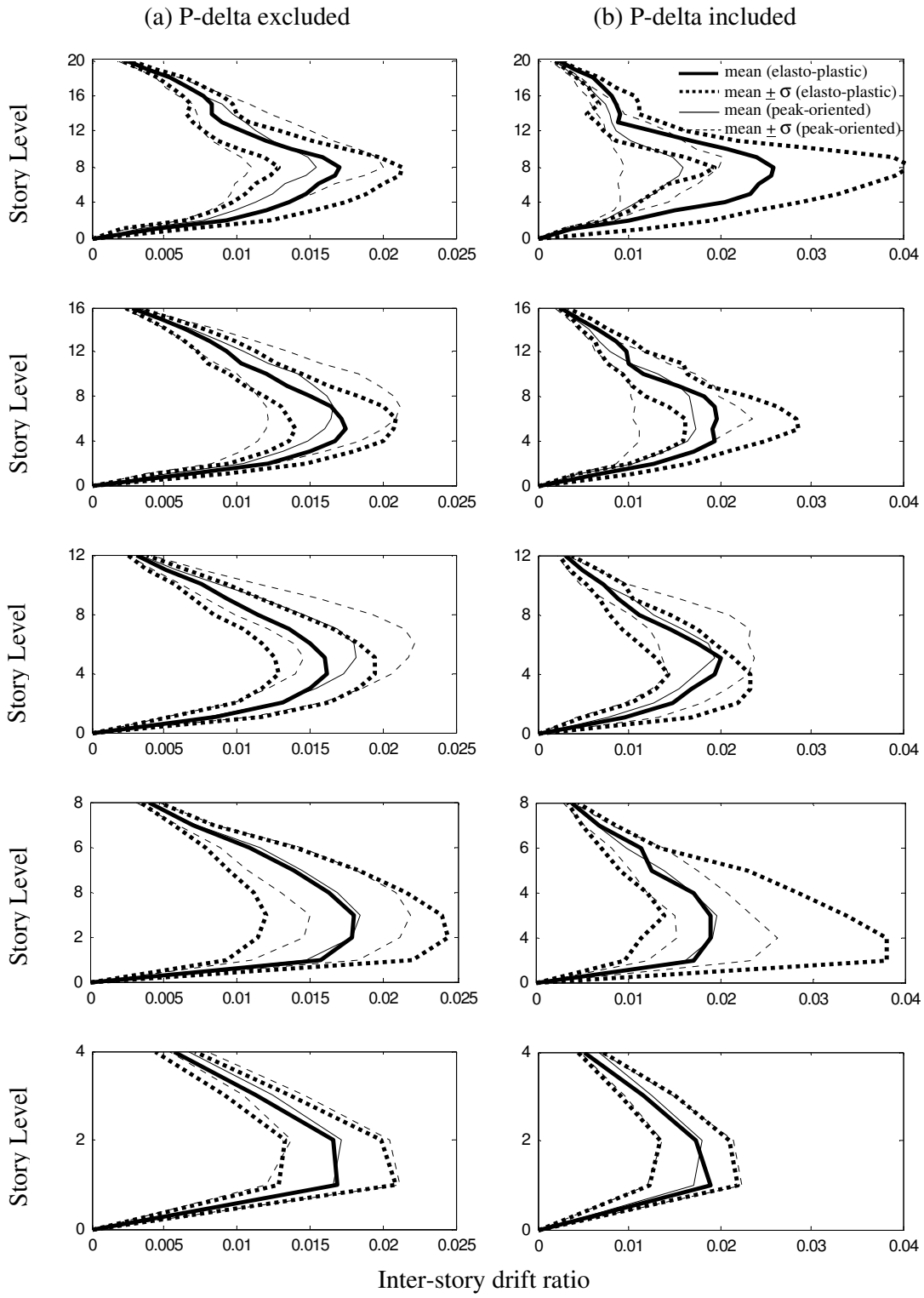

Figure 4.3. Mean inter-story drift ratios estimated by inelastic time history analyses (ITHA) with elasto-plastic and peak-oriented hysteresis rules for 4,8,12,16 and 20-story frame systems of medium ductility level (R=4), (a) P-delta excluded (b) P-delta included

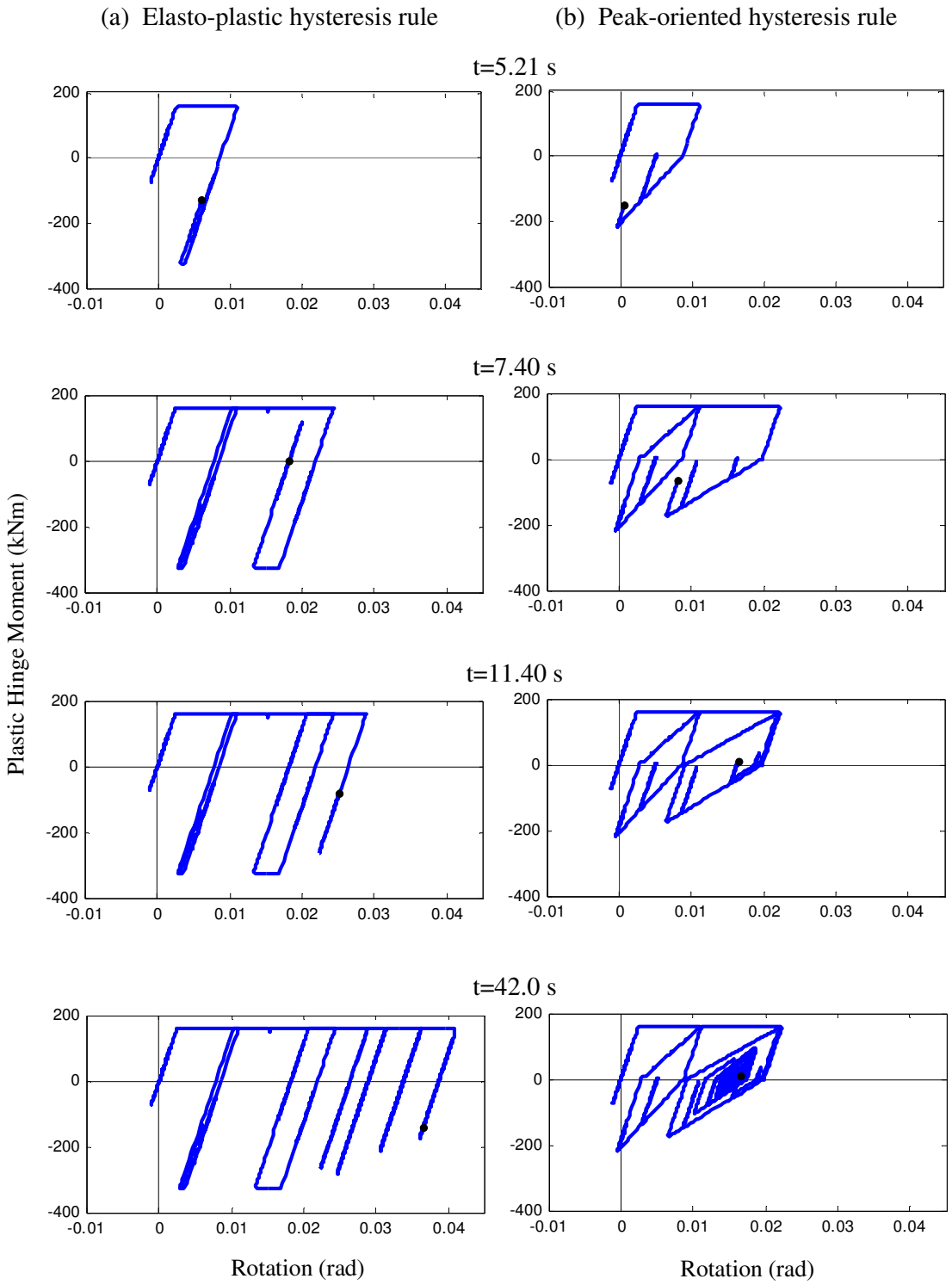

Figure 4.4. Hysteretic behavior for (a)elasto-plastic and (b)peak-oriented model of a beam hinge at different time instant

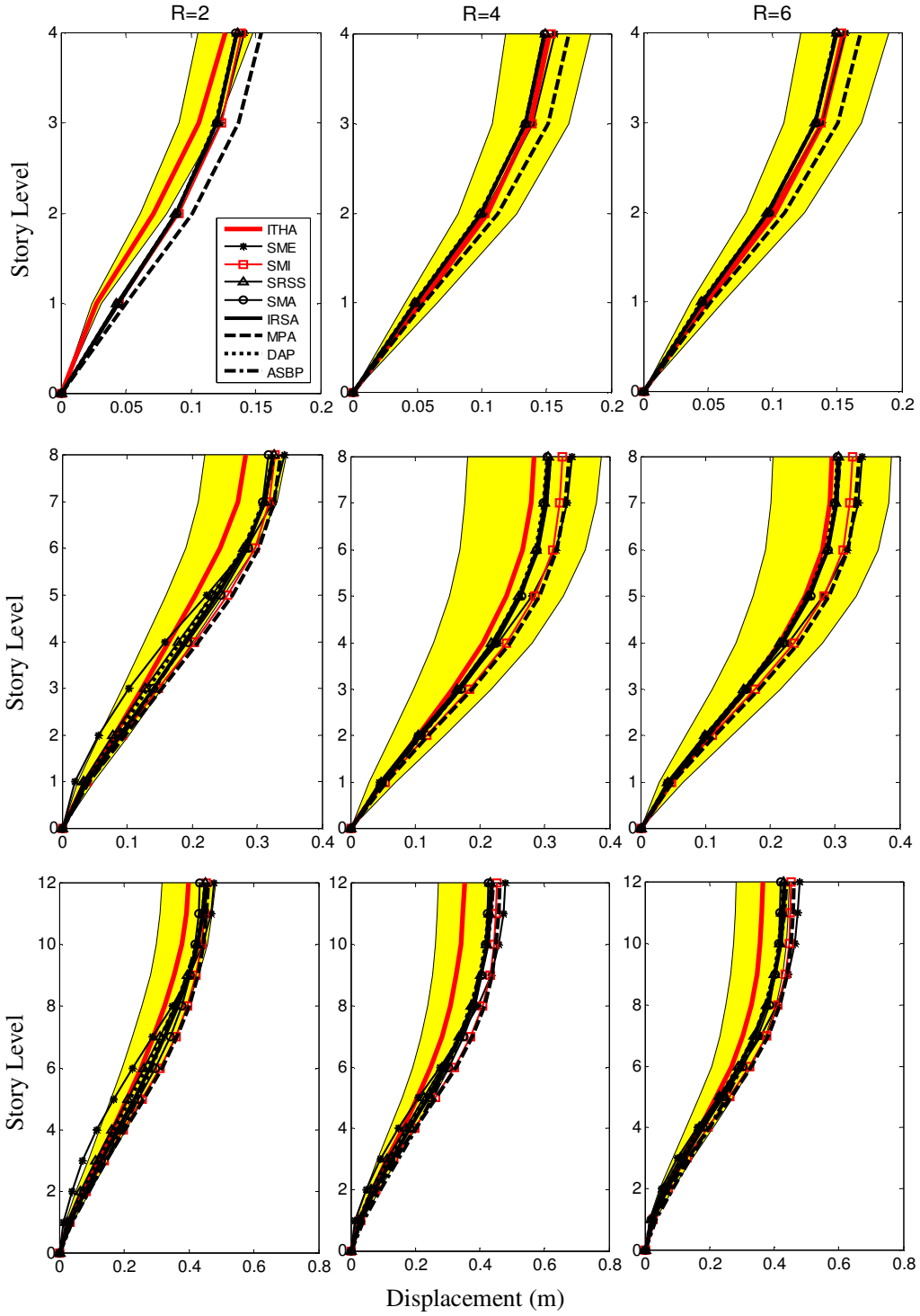

Figure 4.5. Mean story displacements estimated by inelastic time history analyses (ITHA) with elasto-plastic hysteresis rule and nonlinear static procedures (IRSA, MPA, DAP, ASBP and four FEMA load distributions) for 4, 8, 12, 16 and 20-story frame systems, each designed for R=2, 4 and 6, P-delta excluded

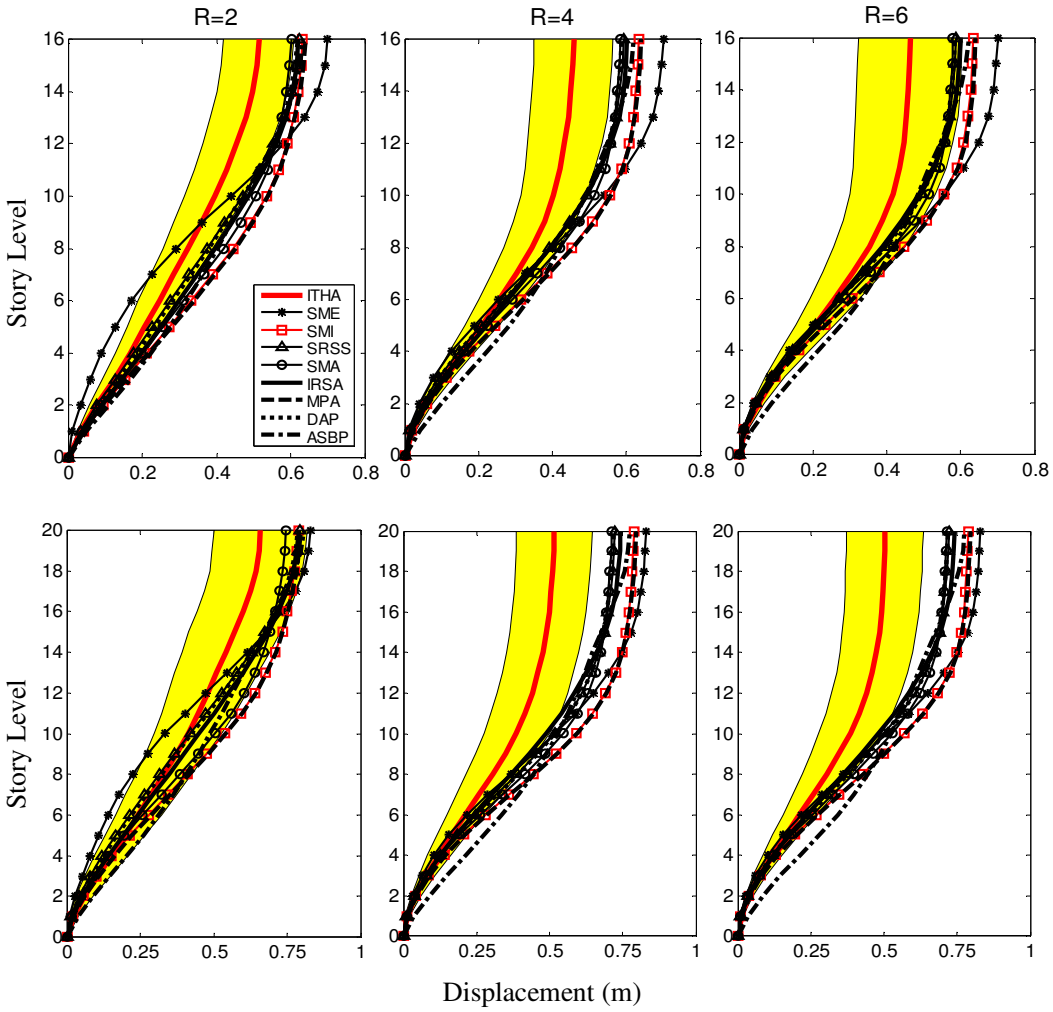

Figure 4.5(contn'd). Mean story displacements estimated by inelastic time history analyses (ITHA) with elasto-plastic hysteresis rule and nonlinear static procedures (IRSA, MPA, DAP, ASBP and four FEMA load distributions) for 4, 8, 12, 16 and 20-story frame systems, each designed for R=2, 4 and 6, P-delta excluded

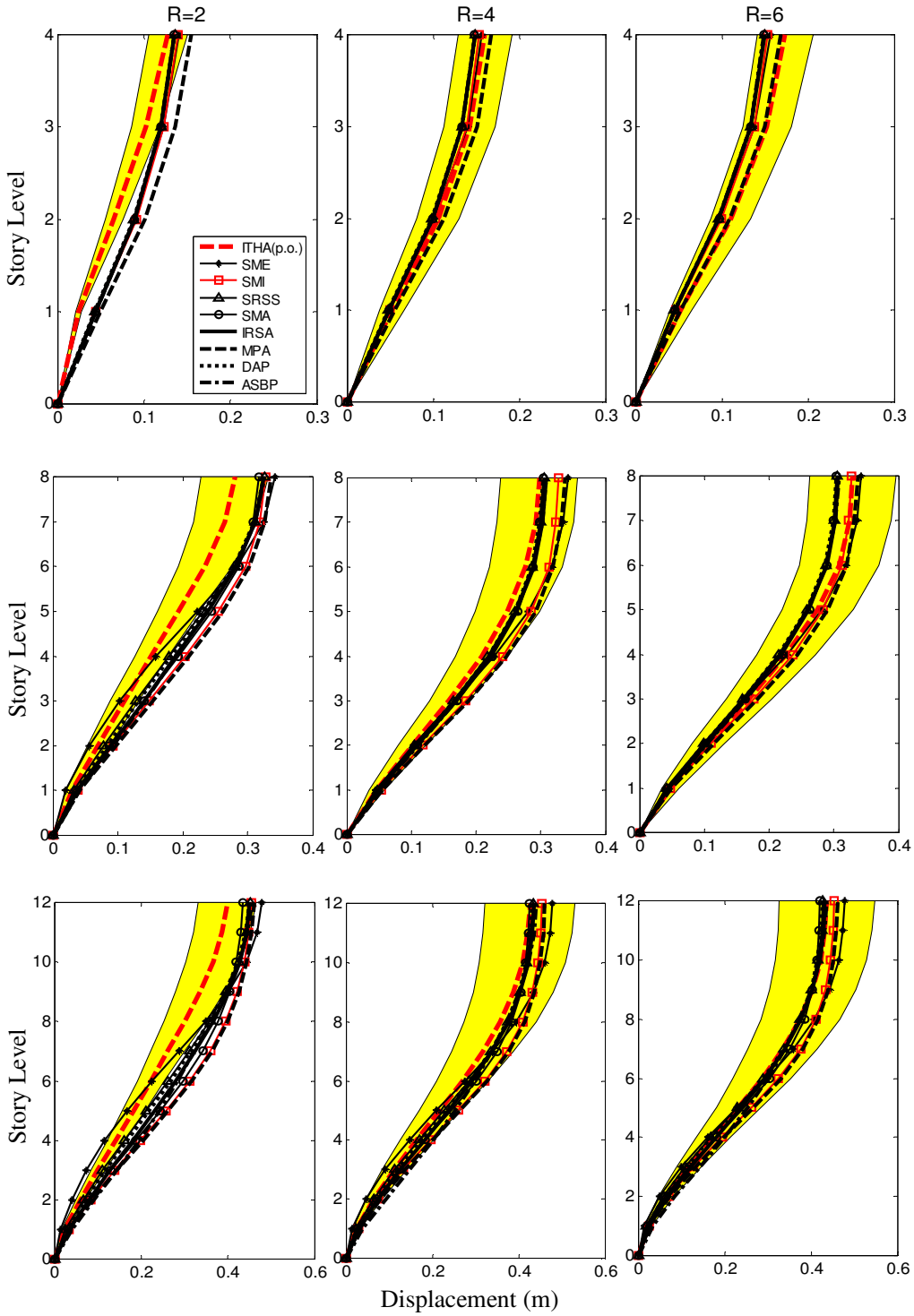

Figure 4.6. Mean story displacements estimated by inelastic time history analysis (ITHA) with peak-oriented hysteresis rule and nonlinear static procedures (IRSA, MPA, DAP ASBP and four FEMA load distributions) for 4, 8, 12, 16 and 20-story frame systems, each designed for R=2, 4 and 6, P-delta excluded

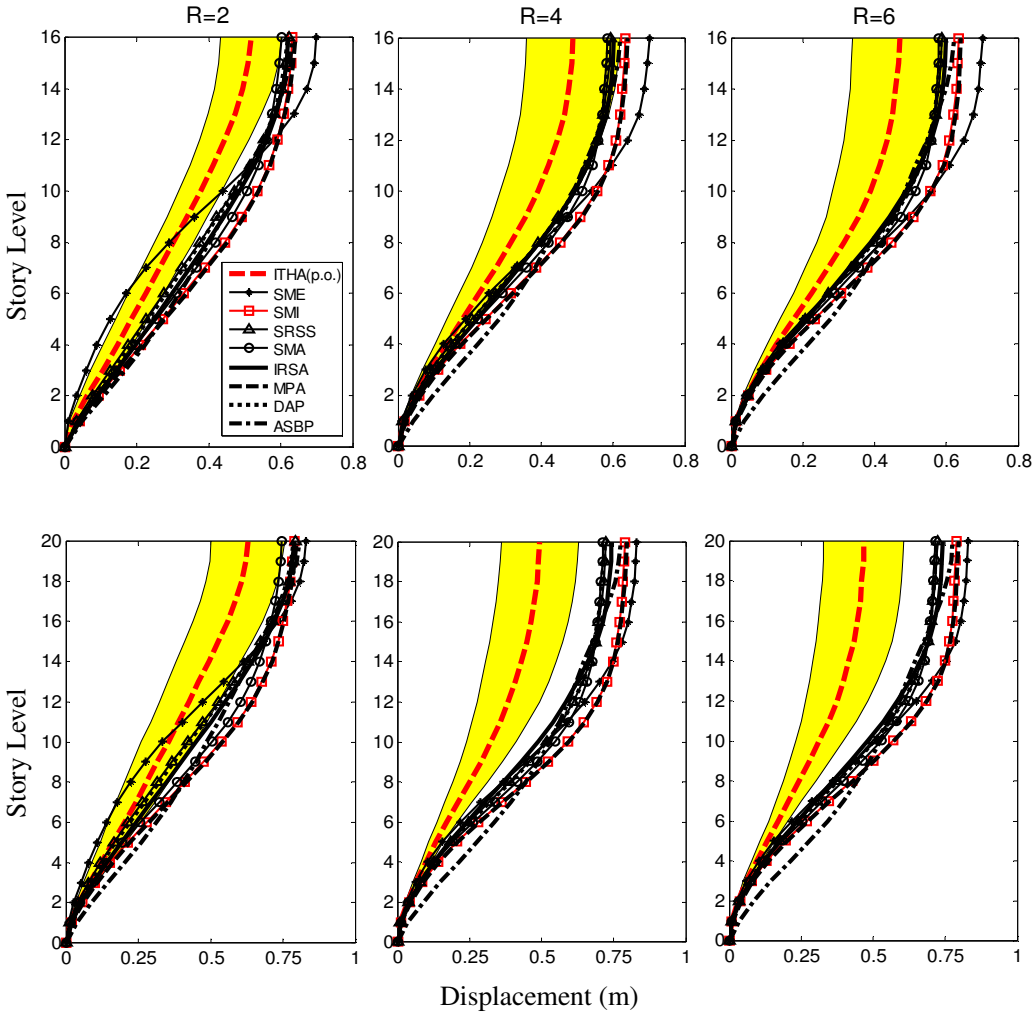

Figure 4.6(contn'd). Mean story displacements estimated by inelastic time history analysis (ITHA) with peak-oriented hysteresis rule and nonlinear static procedures (IRSA, MPA, DAP, ASBP and four FEMA load distributions) for 4, 8, 12, 16 and 20-story frame systems, each designed for R=2, 4 and 6, P-delta excluded

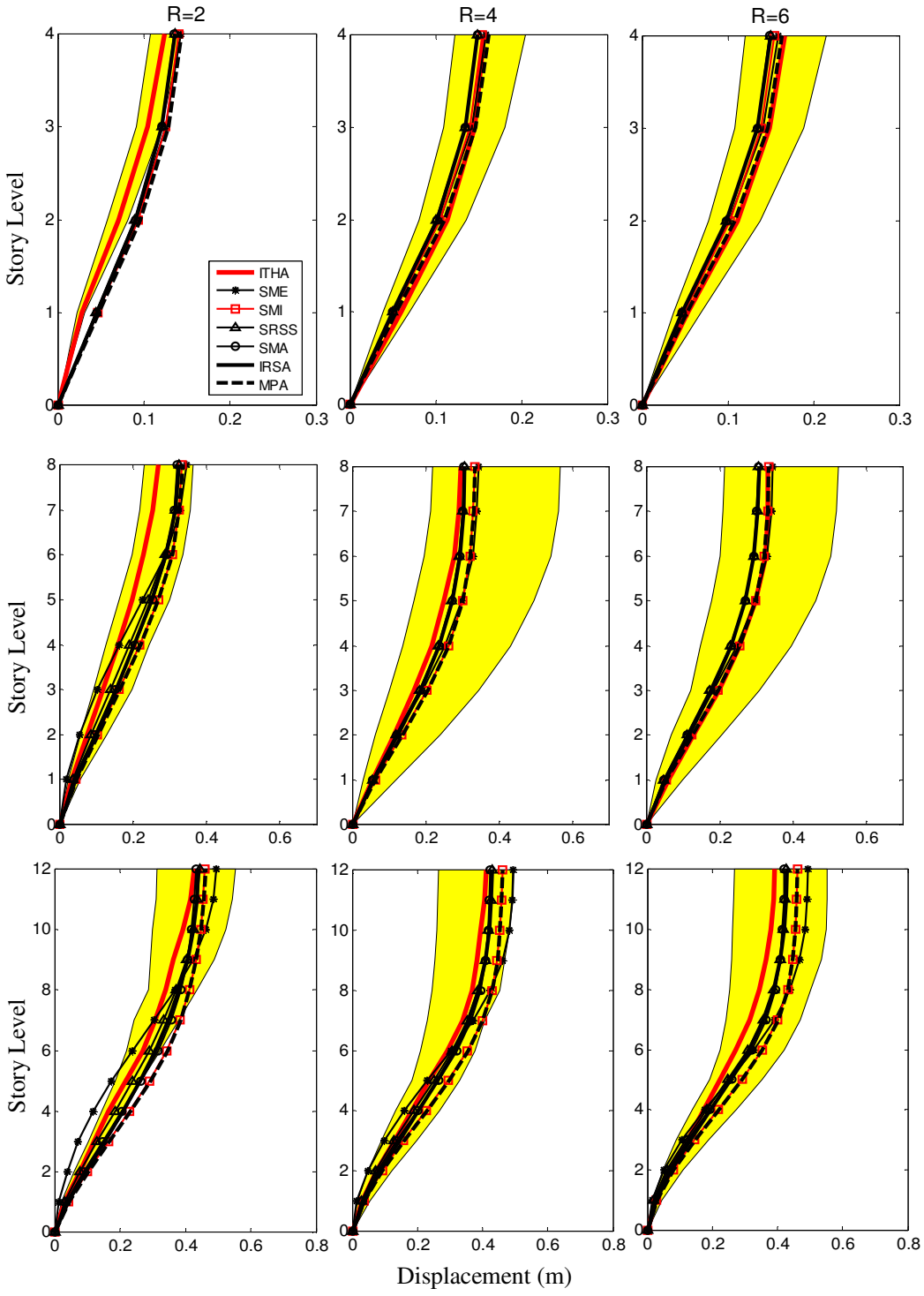

Figure 4.7. Mean story displacements estimated by inelastic time history analysis (ITHA) with elasto-plastic hysteresis rule and nonlinear static procedures (IRSA, MPA and four FEMA load distributions) for 4, 8, 12, 16 and 20-story frame systems, each designed for R=2, 4 and 6, P-delta included

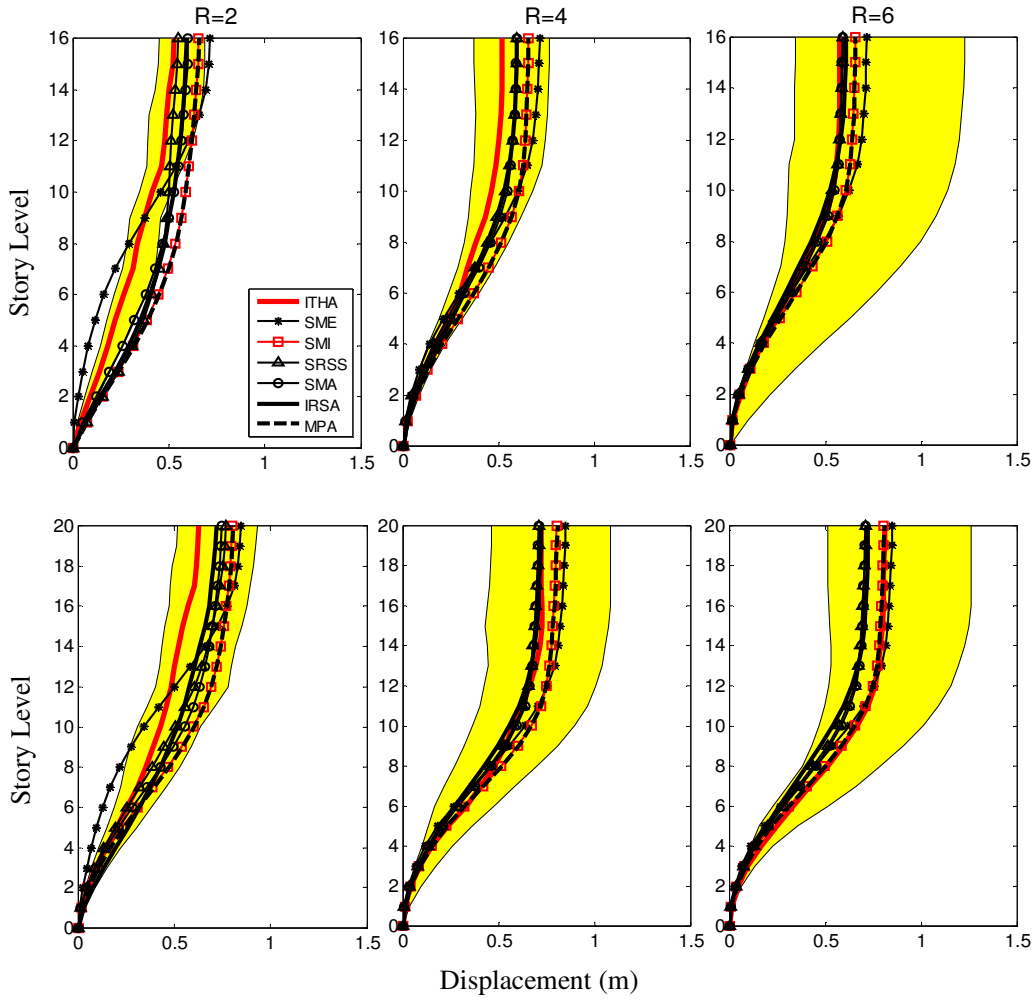

Figure 4.7(contn'd). Mean story displacements estimated by inelastic time history analysis (ITHA) with elasto-plastic hysteresis rule and nonlinear static procedures (IRSA, MPA and four FEMA load distributions) for 4, 8, 12, 16 and 20-story frame systems, each designed for R=2, 4 and 6, P-delta included

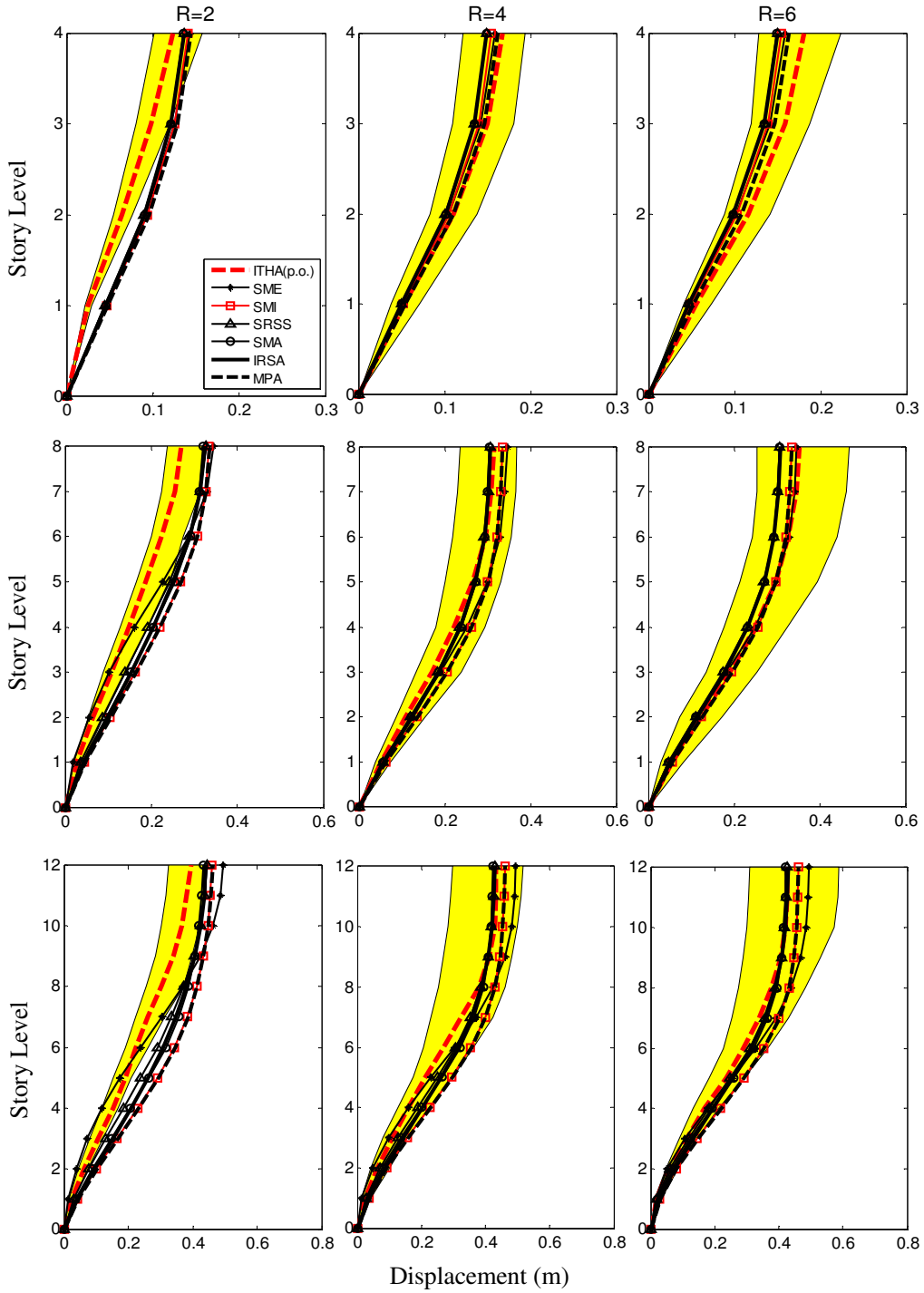

Figure 4.8. Mean story displacements estimated by inelastic time history analysis (ITHA) with peak-oriented hysteresis rule and nonlinear static procedures (IRSA, MPA and four FEMA load distributions) for 4, 8, 12, 16 and 20-story frame systems, each designed for R=2, 4 and 6, P-delta included

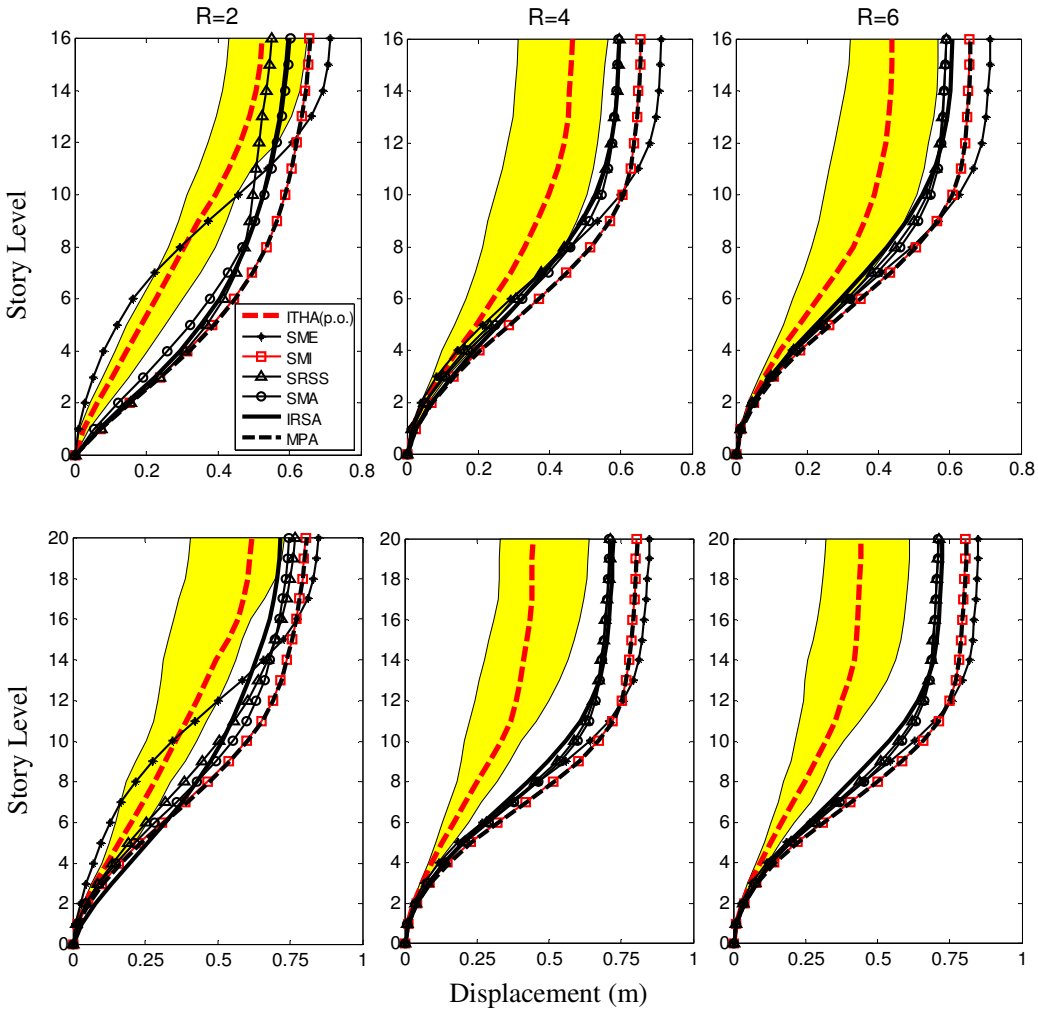

Figure 4.8(contn'd). Mean story displacements estimated by inelastic time history analysis (ITHA) with peak-oriented hysteresis rule and nonlinear static procedures (IRSA, MPA and four FEMA load distributions) for 4, 8, 12, 16 and 20-story frame systems, each designed for R=2, 4 and 6, P-delta included

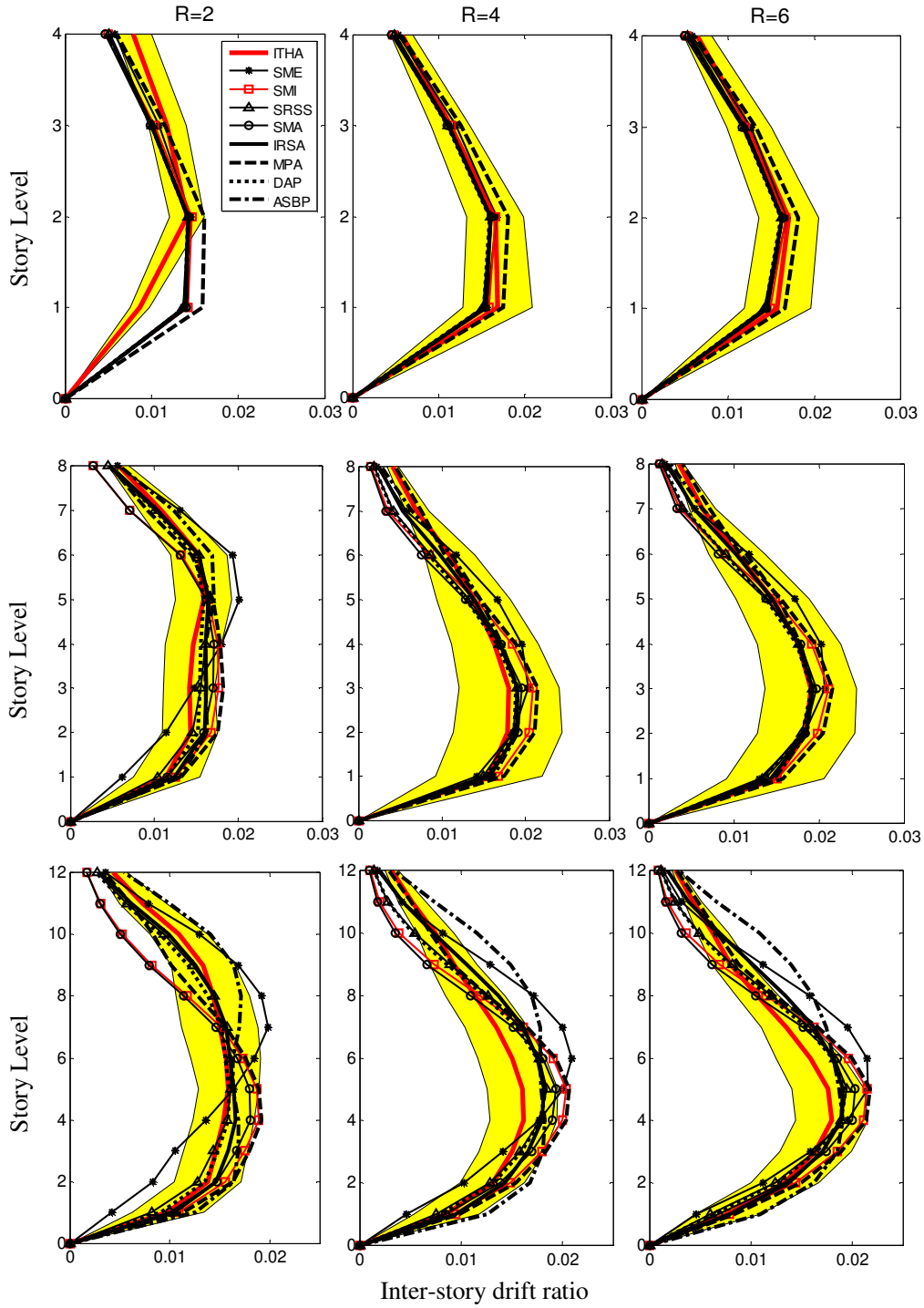

Figure 4.9. Mean inter-story drift ratio estimated by inelastic time history analysis (ITHA) with elasto-plastic hysteresis rule and nonlinear static procedures (IRSA, MPA, DAP, ASBP and four FEMA load distributions) for 4, 8, 12, 16 and 20-story frame systems, each designed for R=2, 4 and 6, P-delta excluded

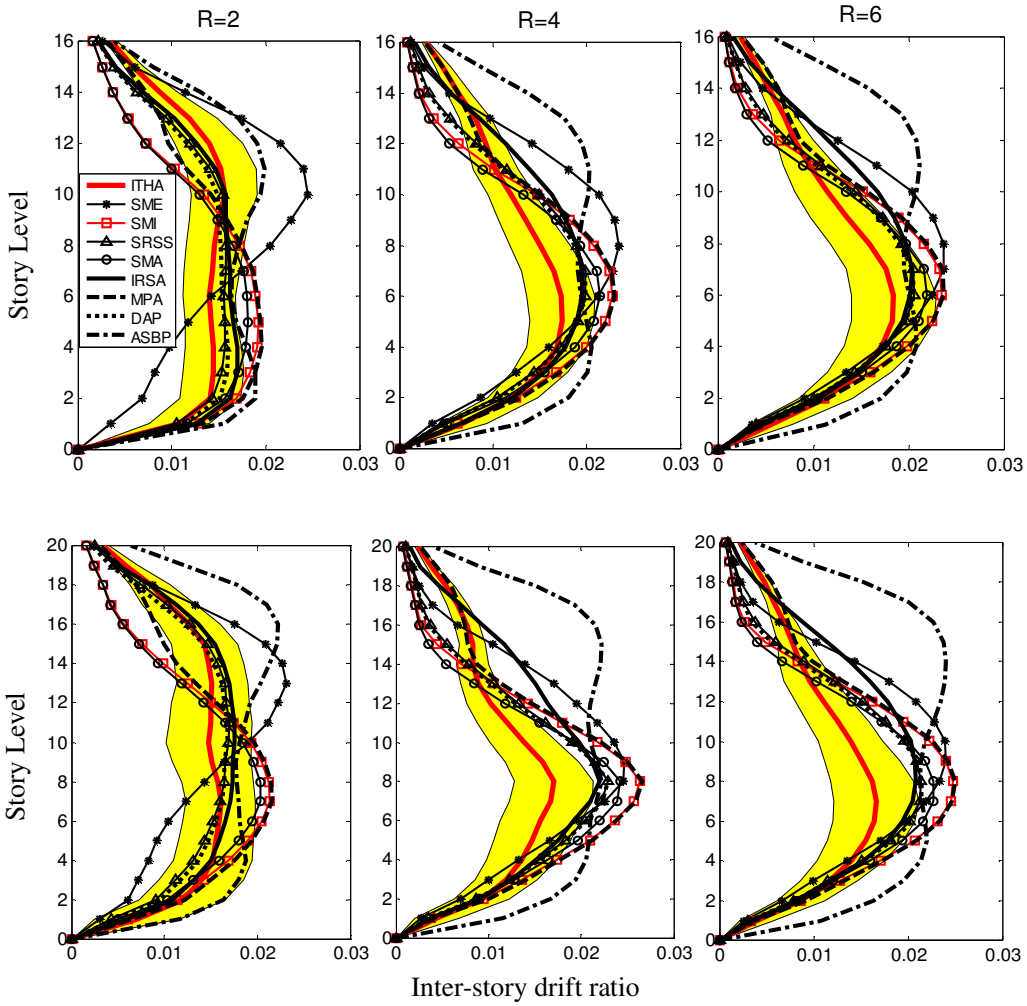

Figure 4.9(contn'd). Mean inter-story drift ratio estimated by inelastic time history analysis (ITHA) with elasto-plastic hysteresis rule and nonlinear static procedures (IRSA, MPA, DAP, ASBP and four FEMA load distributions) for 4, 8, 12, 16 and 20-story frame systems, each designed for R=2, 4 and 6, P-delta excluded

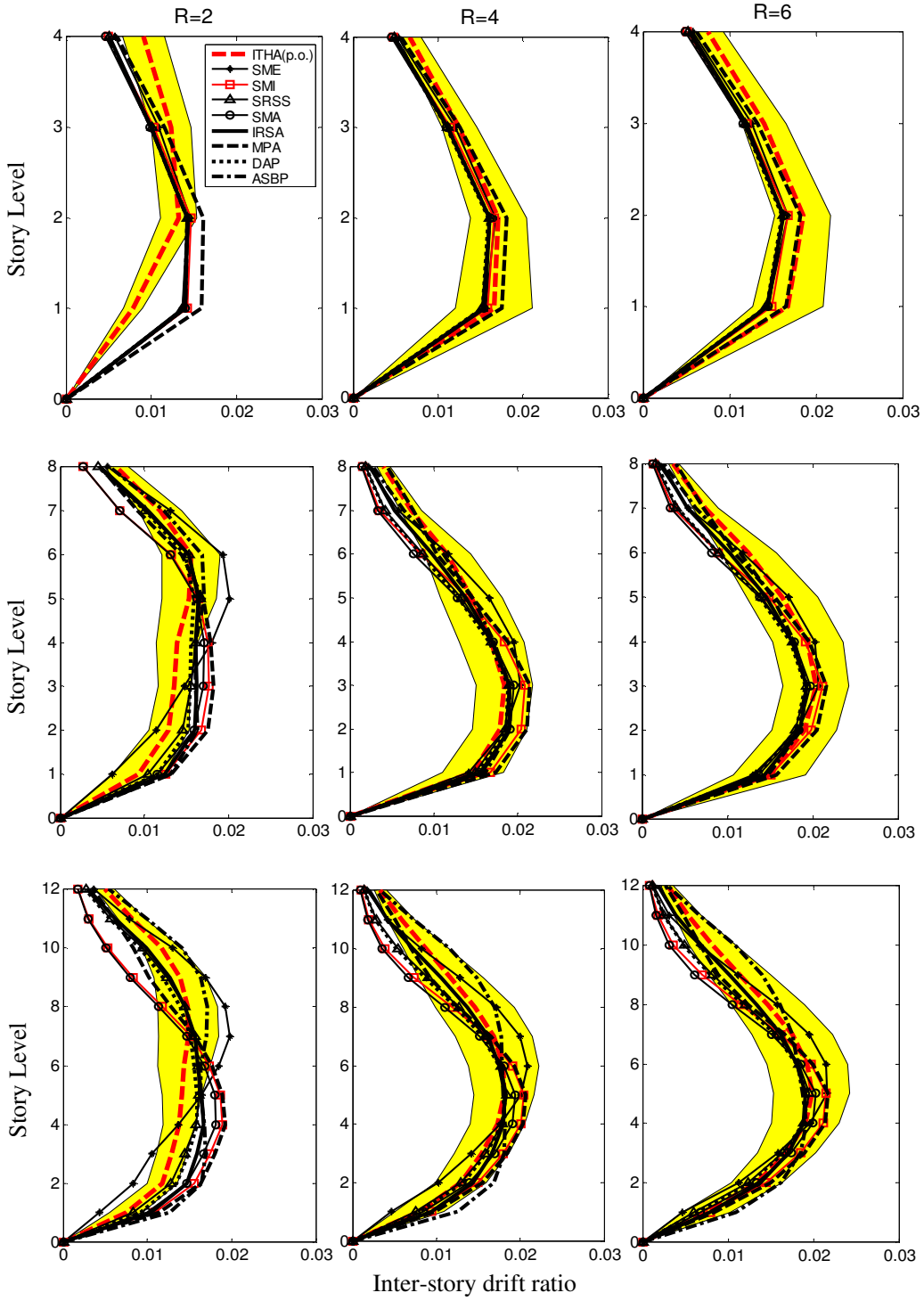

Figure 4.10. Mean inter-story drift ratio estimated by inelastic time history analysis (ITHA) with peak-oriented hysteresis rule and nonlinear static procedures (IRSA, MPA, DAP, ASBP and four FEMA load distributions) for 4, 8, 12, 16 and 20-story frame systems, each designed for R=2, 4 and 6, P-delta excluded

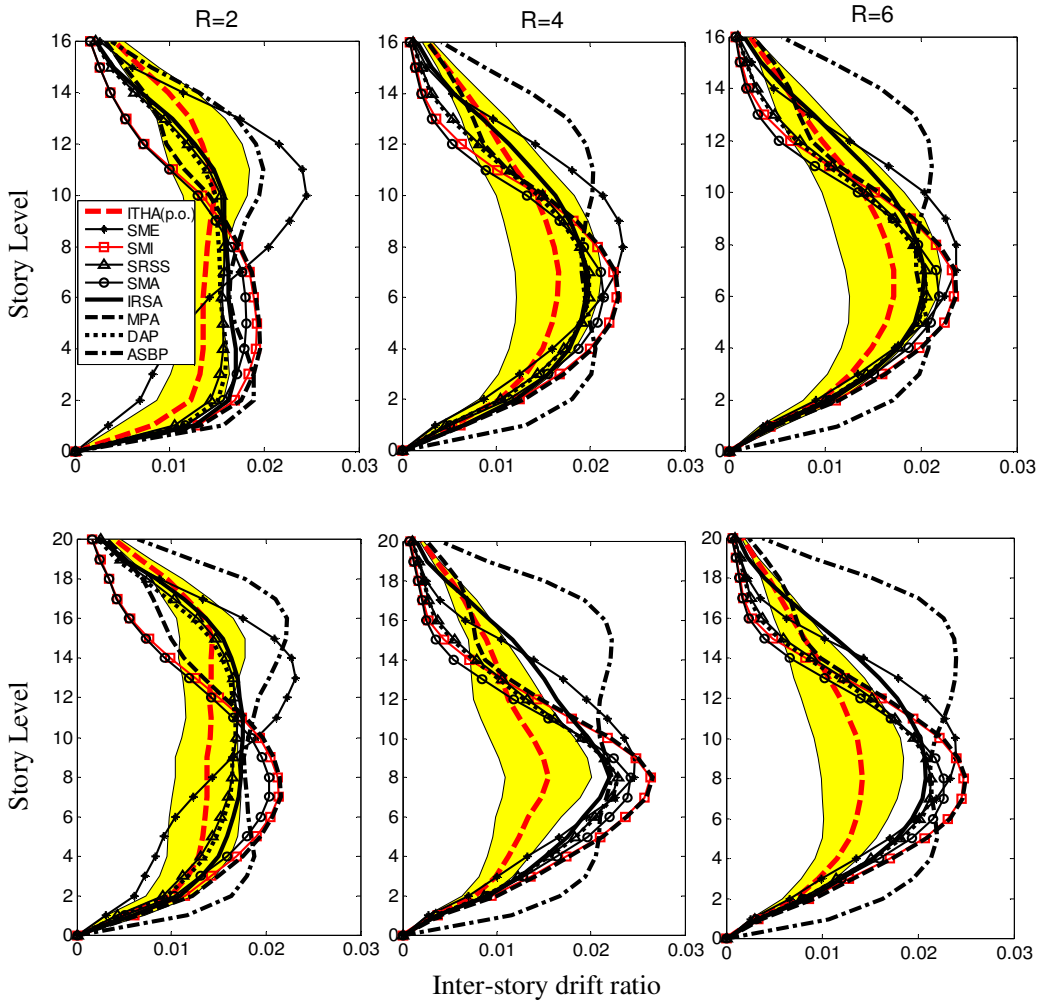

Figure 4.10(contn'd). Mean inter-story drift ratio estimated by inelastic time history analysis (ITHA) with peak-oriented hysteresis rule and nonlinear static procedures (IRSA, MPA, DAP, ASBP and four FEMA load distributions) for 4, 8, 12, 16 and 20-story frame systems, each designed for R=2, 4 and 6, P-delta excluded

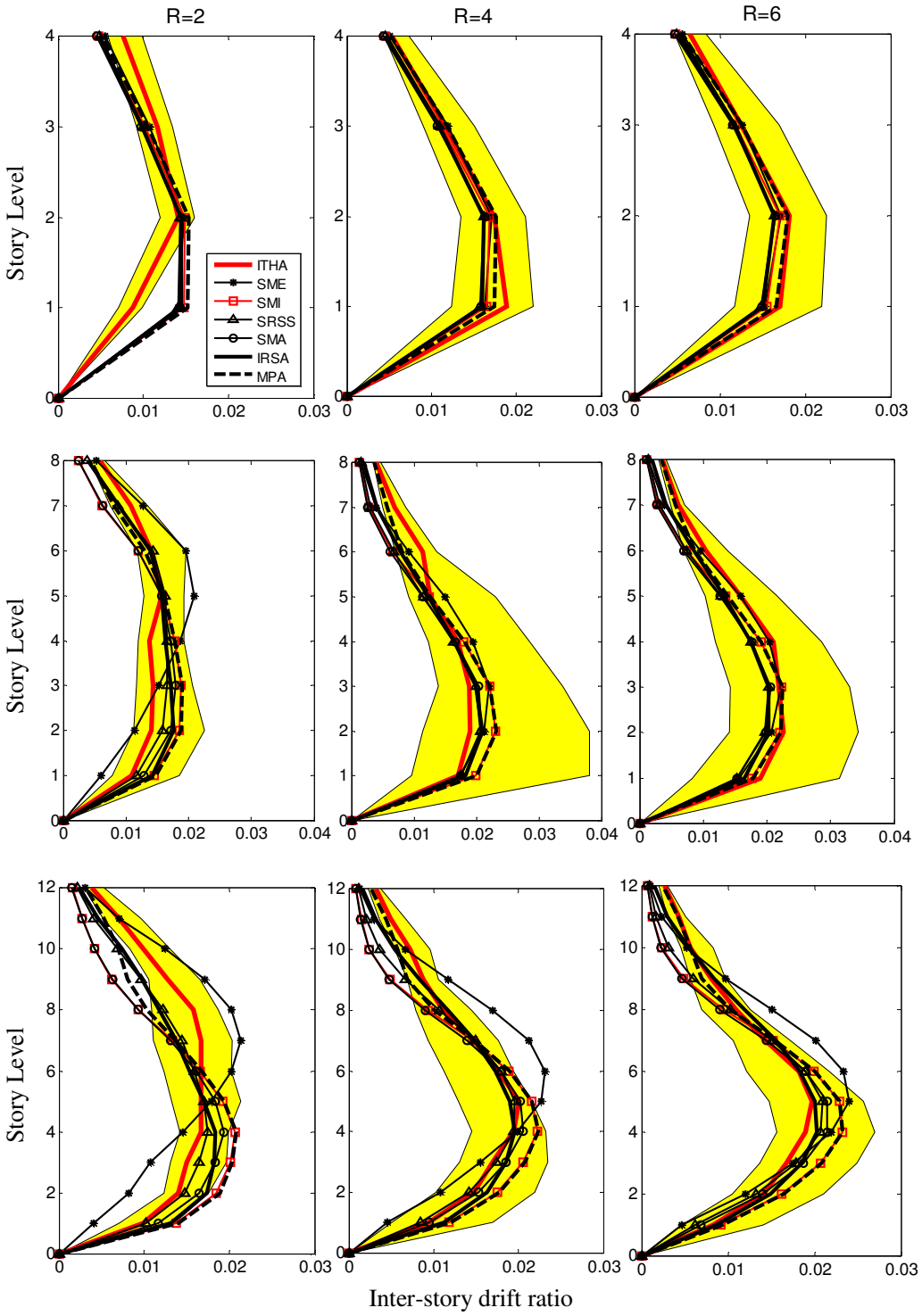

Figure 4.11. Mean inter-story drift ratio estimated by inelastic time history analysis (ITHA) with elasto-plastic hysteresis rule and nonlinear static procedures (IRSA, MPA and four FEMA load distributions) for 4, 8, 12, 16 and 20-story frame systems, each designed for R=2, 4 and 6, P-delta included

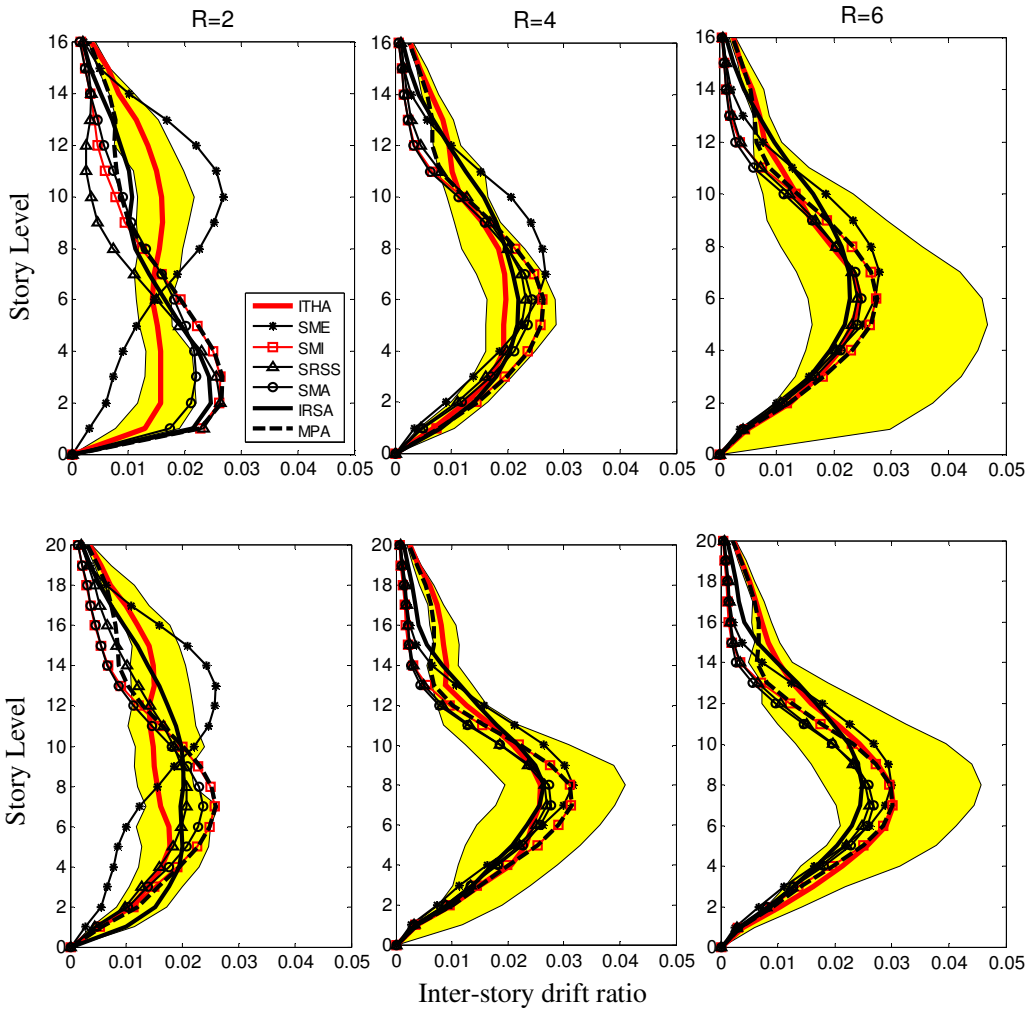

Figure 4.11(contn'd). Mean inter-story drift ratio estimated by inelastic time history analysis (ITHA) with elasto-plastic hysteresis rule and nonlinear static procedures (IRSA, MPA and four FEMA load distributions) for 4, 8, 12, 16 and 20-story frame systems, each designed for R=2, 4 and 6, P-delta included

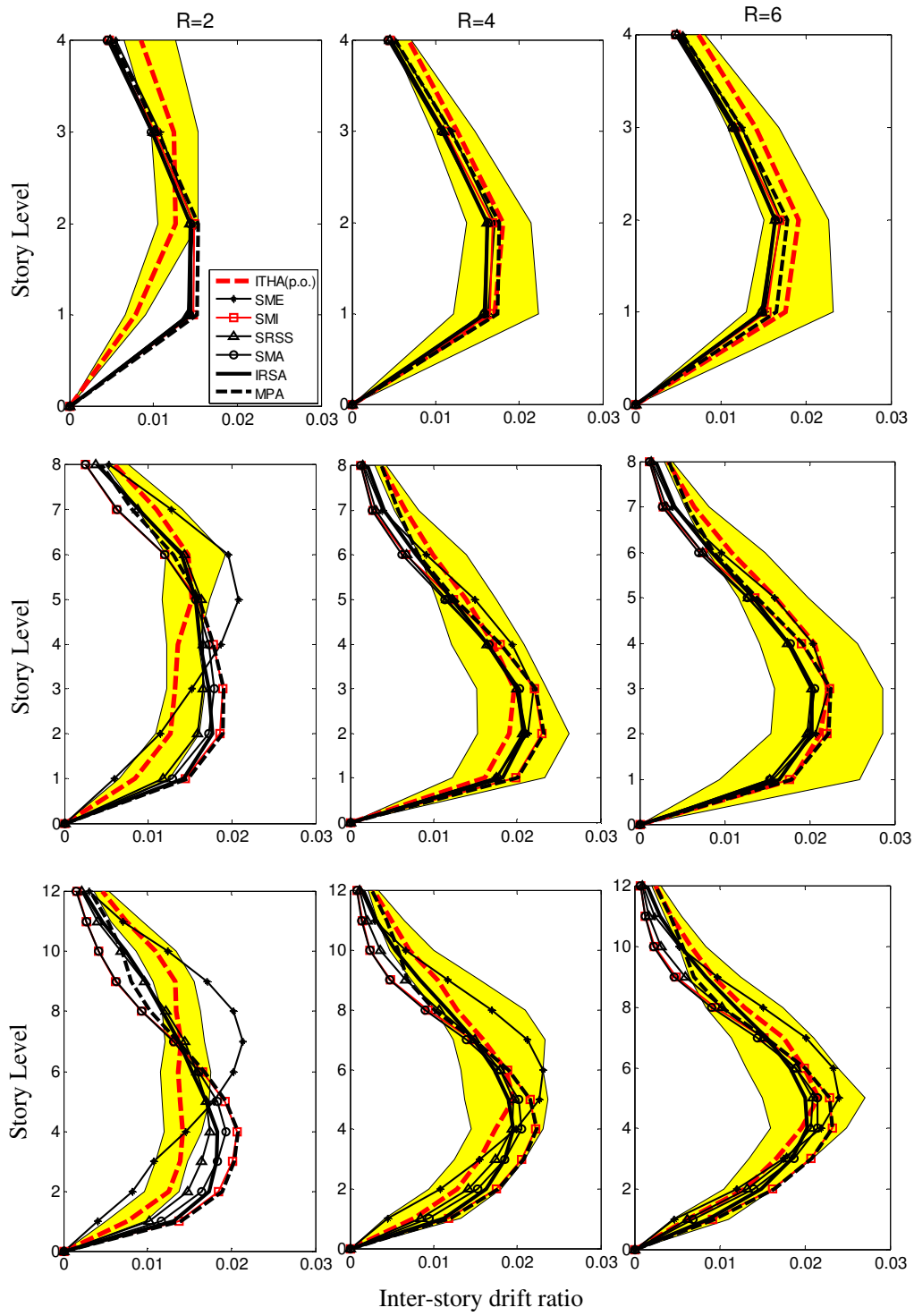

Figure 4.12. Mean inter-story drift ratio estimated by inelastic time history analysis (ITHA) with peak-oriented hysteresis rule and nonlinear static procedures (IRSA, MPA and four FEMA load distributions) for 4, 8, 12, 16 and 20-story frame systems, each designed for R=2, 4 and 6, P-delta included

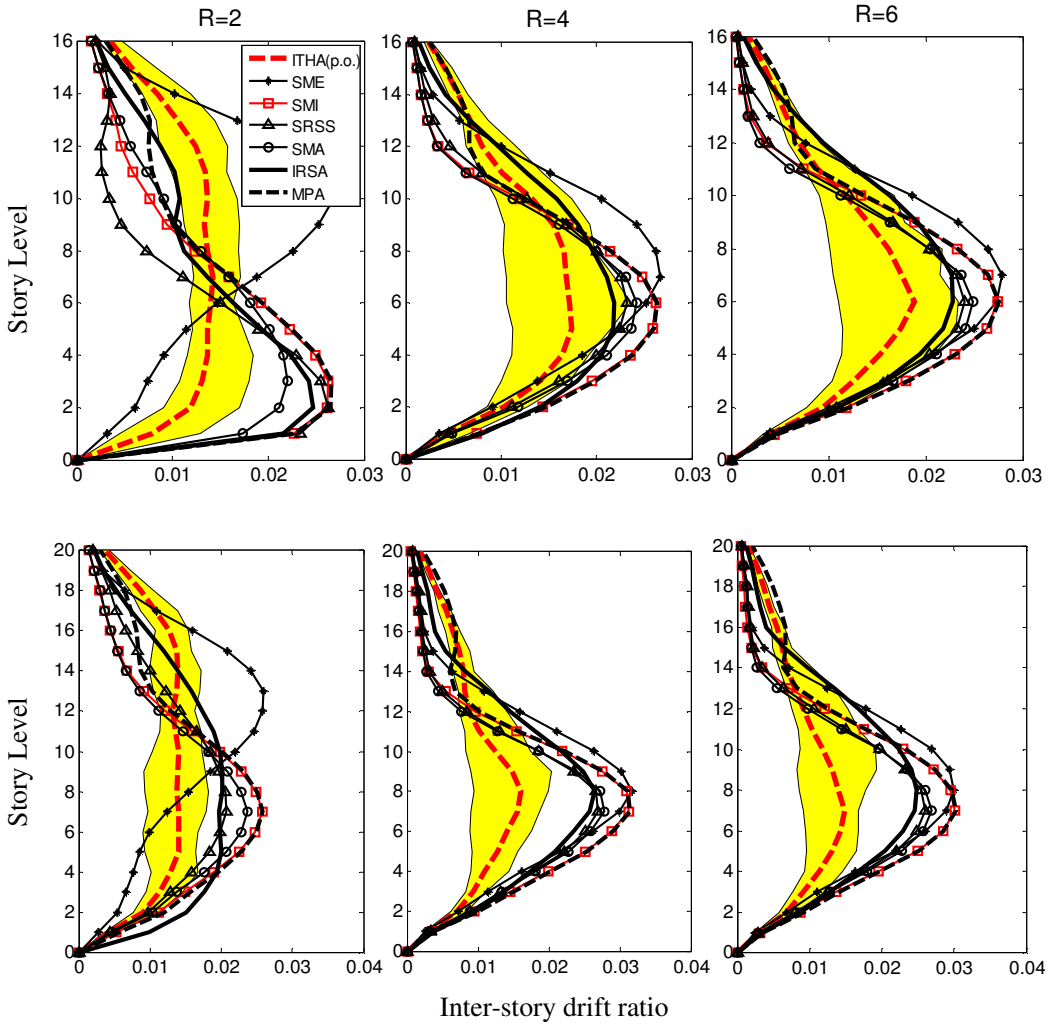

Figure 4.12(contn'd). Mean inter-story drift ratio estimated by inelastic time history analysis (ITHA) with peak-oriented hysteresis rule and nonlinear static procedures (IRSA, MPA and four FEMA load distributions) for 4, 8, 12, 16 and 20-story frame systems, each designed for R=2, 4 and 6, P-delta included

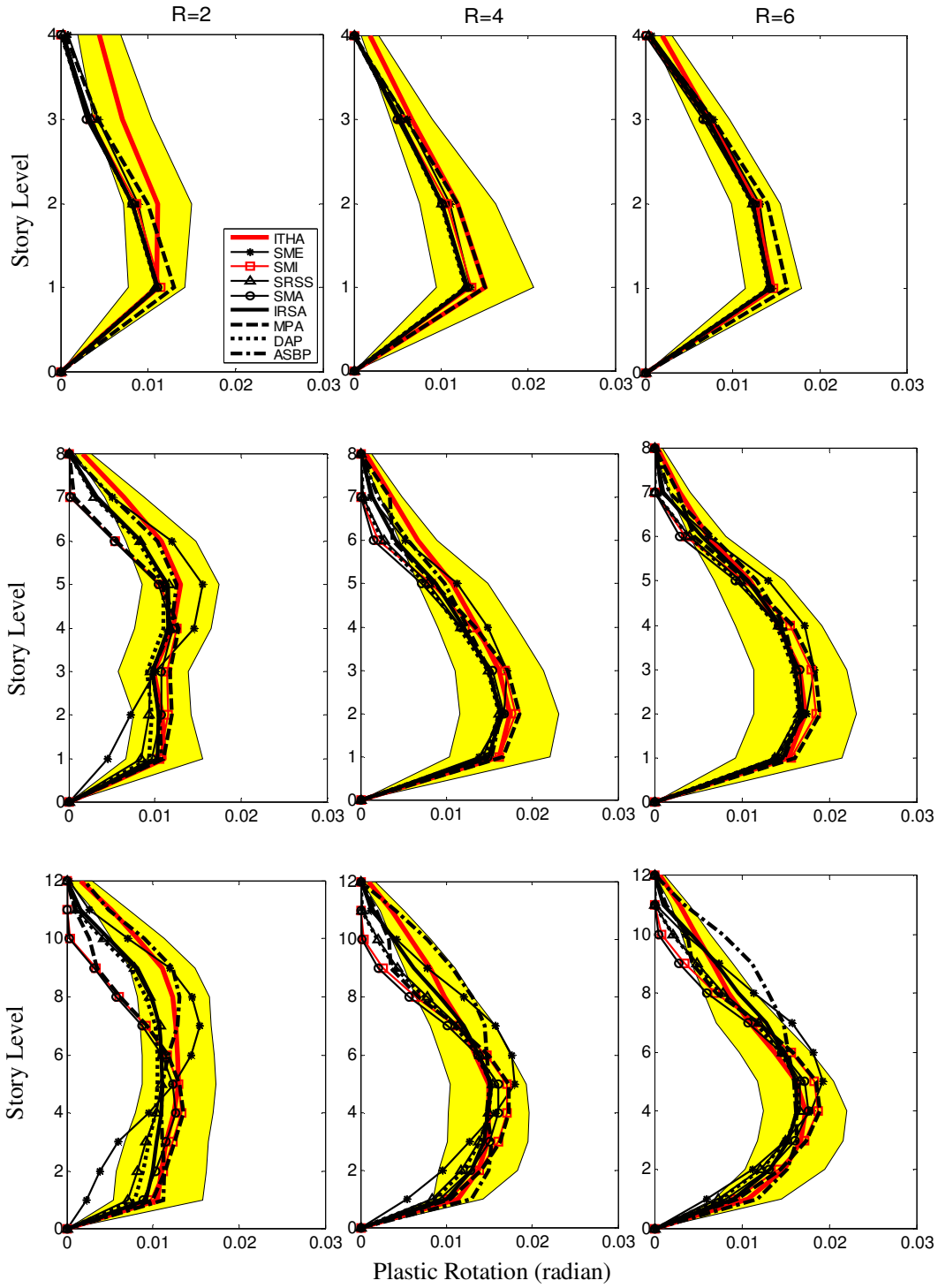

Figure 4.13. Mean plastic rotation at the central beams estimated by inelastic time history analysis (ITHA) with elasto-plastic hysteresis rule and nonlinear static procedures (IRSA, MPA, DAP, ASBP and four FEMA load distributions) for 4, 8, 12, 16 and 20-story frame systems, each designed for R=2, 4 and 6, P-delta excluded

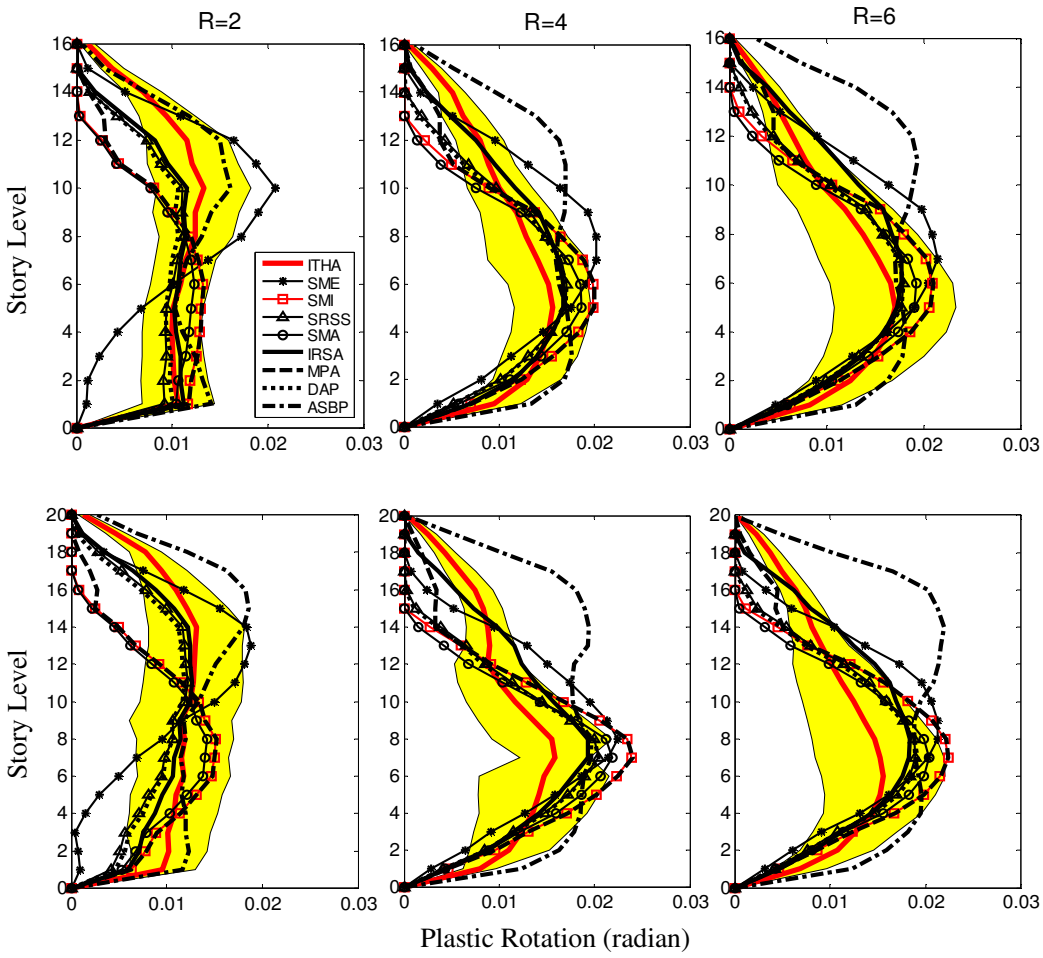

Figure 4.13(contn'd). Mean plastic rotation at the central beams estimated by inelastic time history analysis (ITHA) with elasto-plastic hysteresis rule and nonlinear static procedures (IRSA, MPA, DAP, ASBP and four FEMA load distributions) for 4, 8, 12, 16 and 20-story frame systems, each designed for R=2, 4 and 6, P-delta excluded

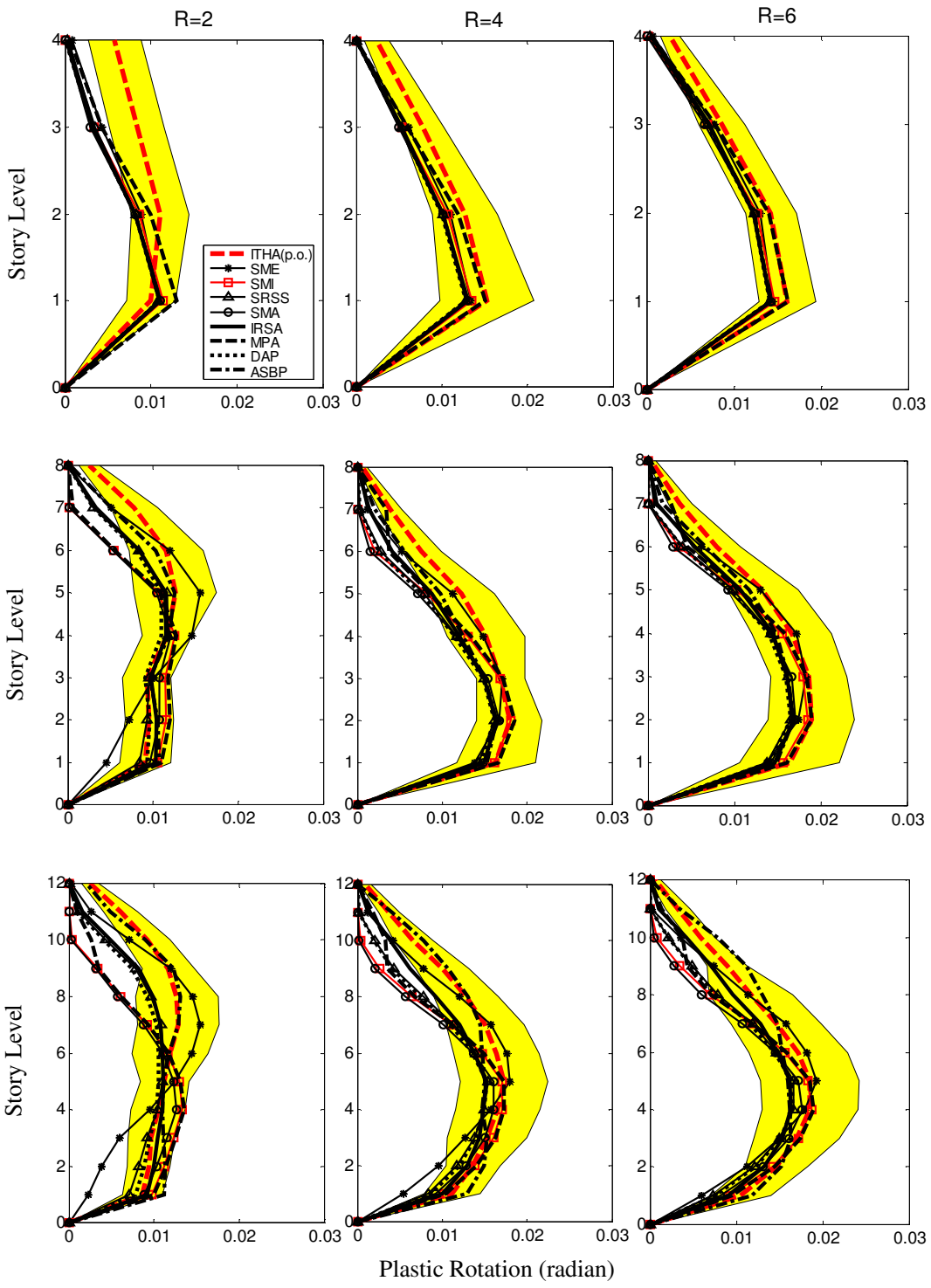

Figure 4.14. Mean plastic rotation at the central beams estimated by inelastic time history analysis (ITHA) with peak-oriented hysteresis rule and nonlinear static procedures (IRSA, MPA, DAP, ASBP and four FEMA load distributions) for 4, 8, 12, 16 and 20-story frame systems, each designed for R=2, 4 and 6, P-delta excluded

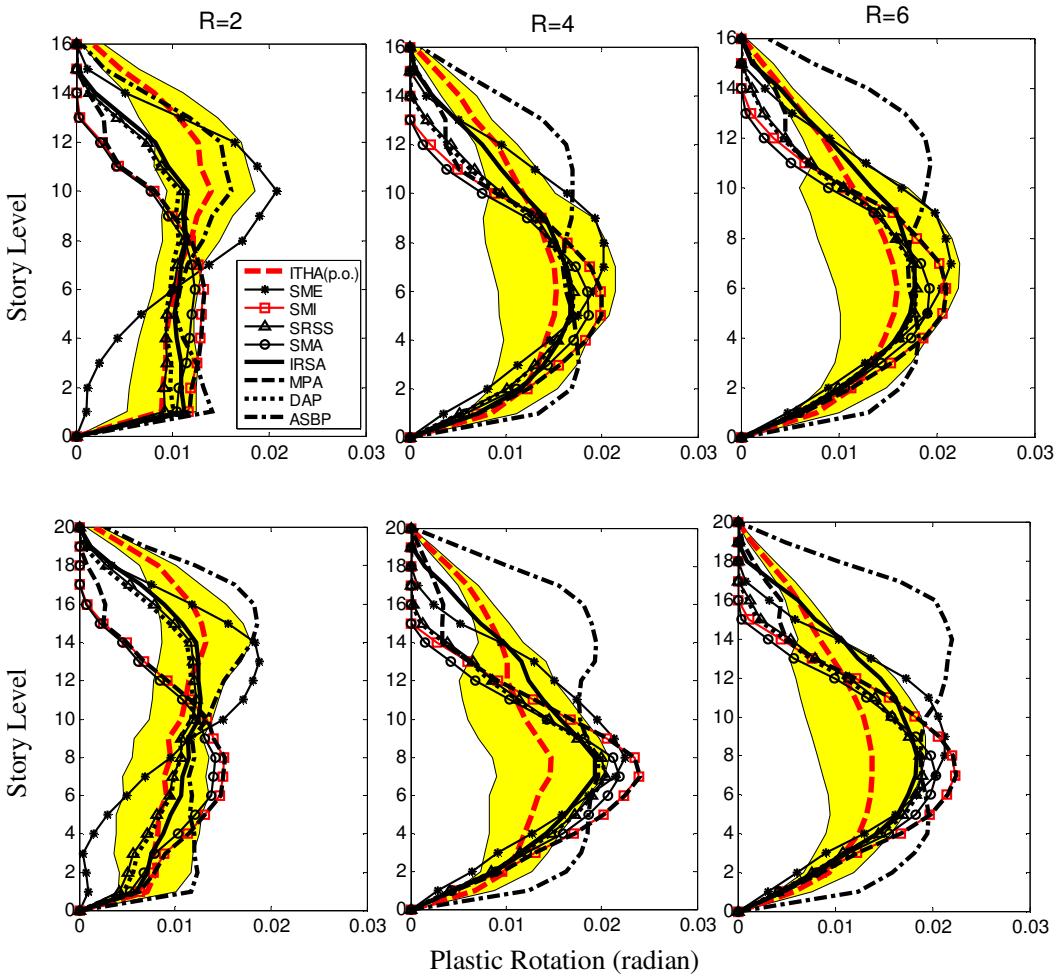

Figure 4.14(contn'd). Mean plastic rotation at the central beams estimated by inelastic time history analysis (ITHA) with peak-oriented hysteresis rule and nonlinear static procedures (IRSA, MPA, DAP, ASBP and four FEMA load distributions) for 4, 8, 12, 16 and 20-story frame systems, each designed for R=2, 4 and 6, P-delta excluded

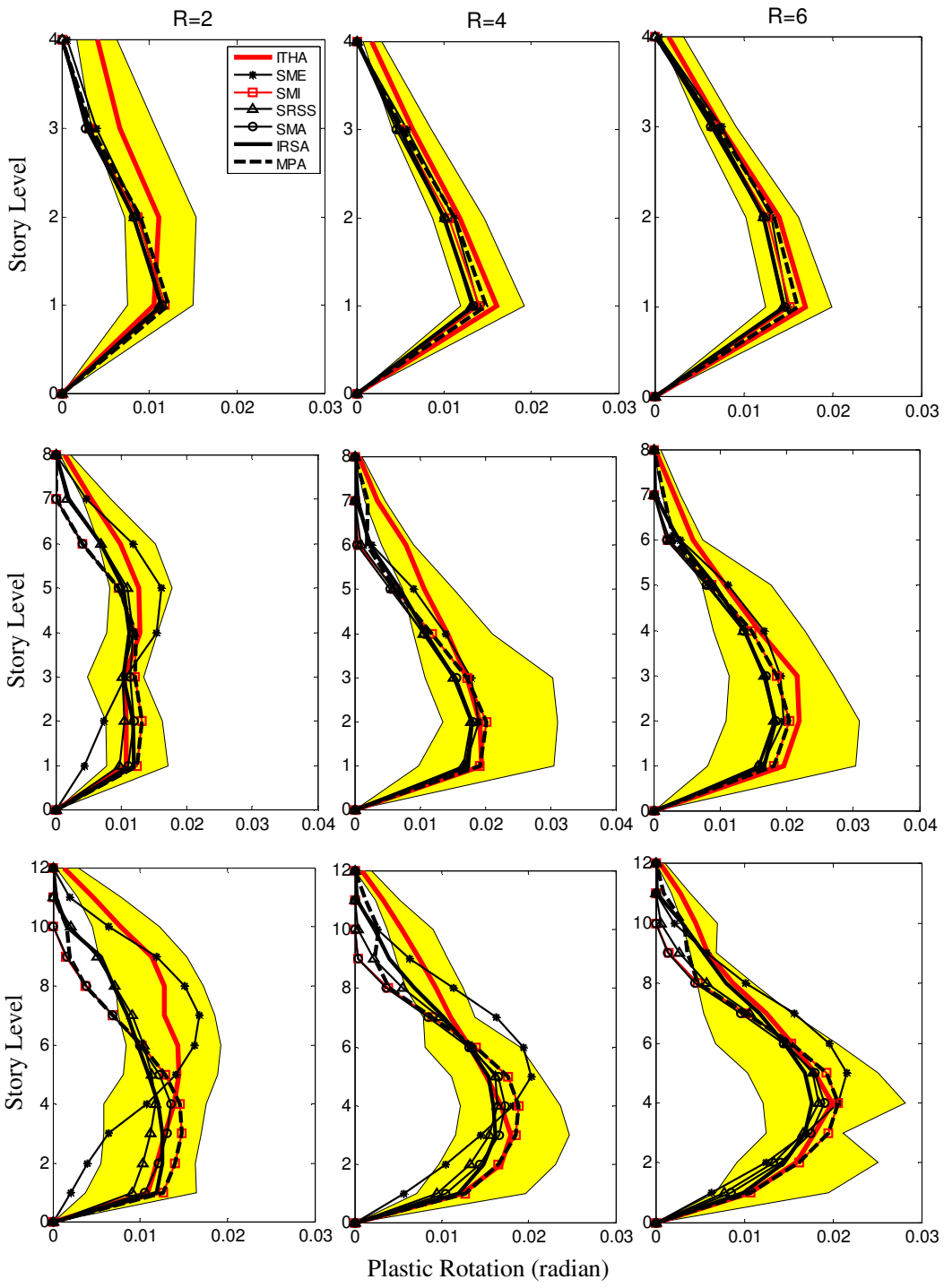

Figure 4.15. Mean plastic rotation at the central beams estimated by inelastic time history analysis (ITHA) with elasto-plastic hysteresis rule and nonlinear static procedures (IRSA, MPA and four FEMA load distributions) for 4, 8, 12, 16 and 20-story frame systems, each designed for R=2, 4 and 6, P-delta included

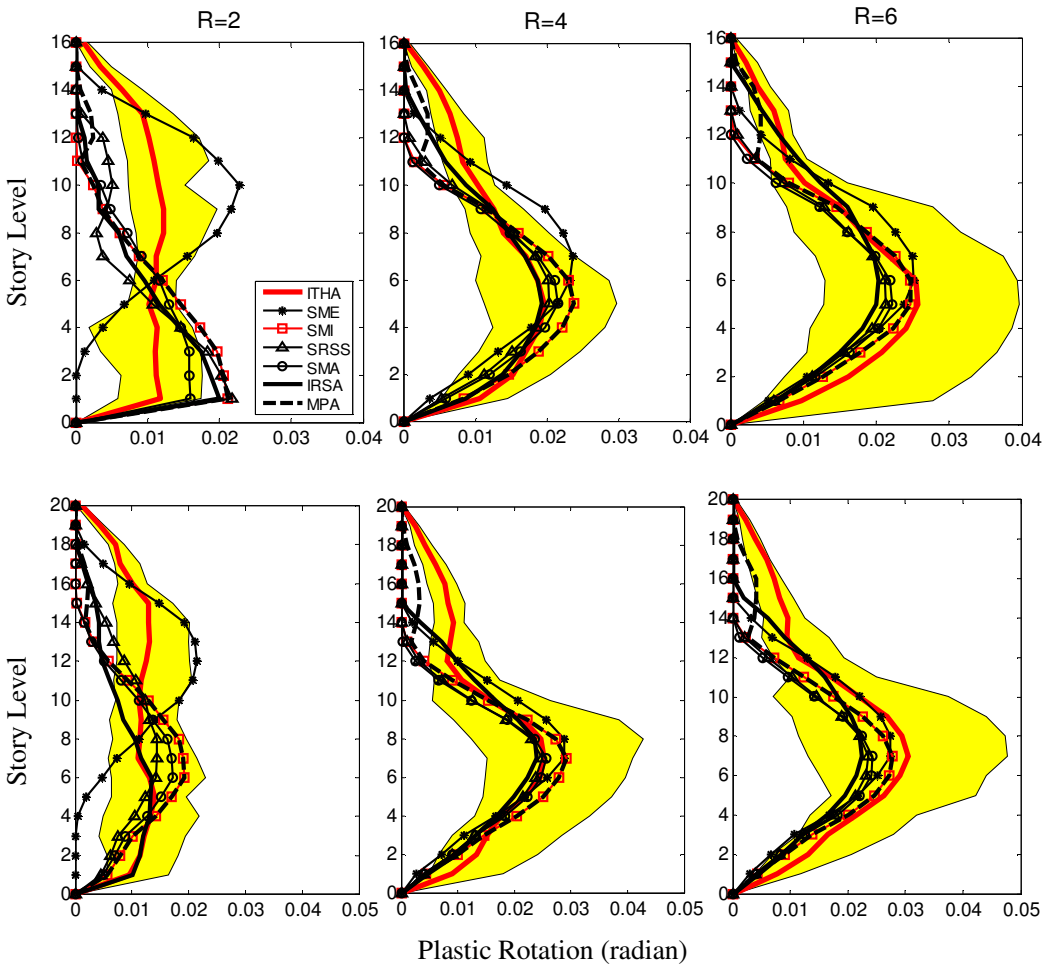

Figure 4.15(contn'd). Mean plastic rotation at the central beams estimated by inelastic time history analysis (ITHA) with elasto-plastic hysteresis rule and nonlinear static procedures (IRSA, MPA and four FEMA load distributions) for 4, 8, 12, 16 and 20-story frame systems, each designed for R=2, 4 and 6, P-delta included

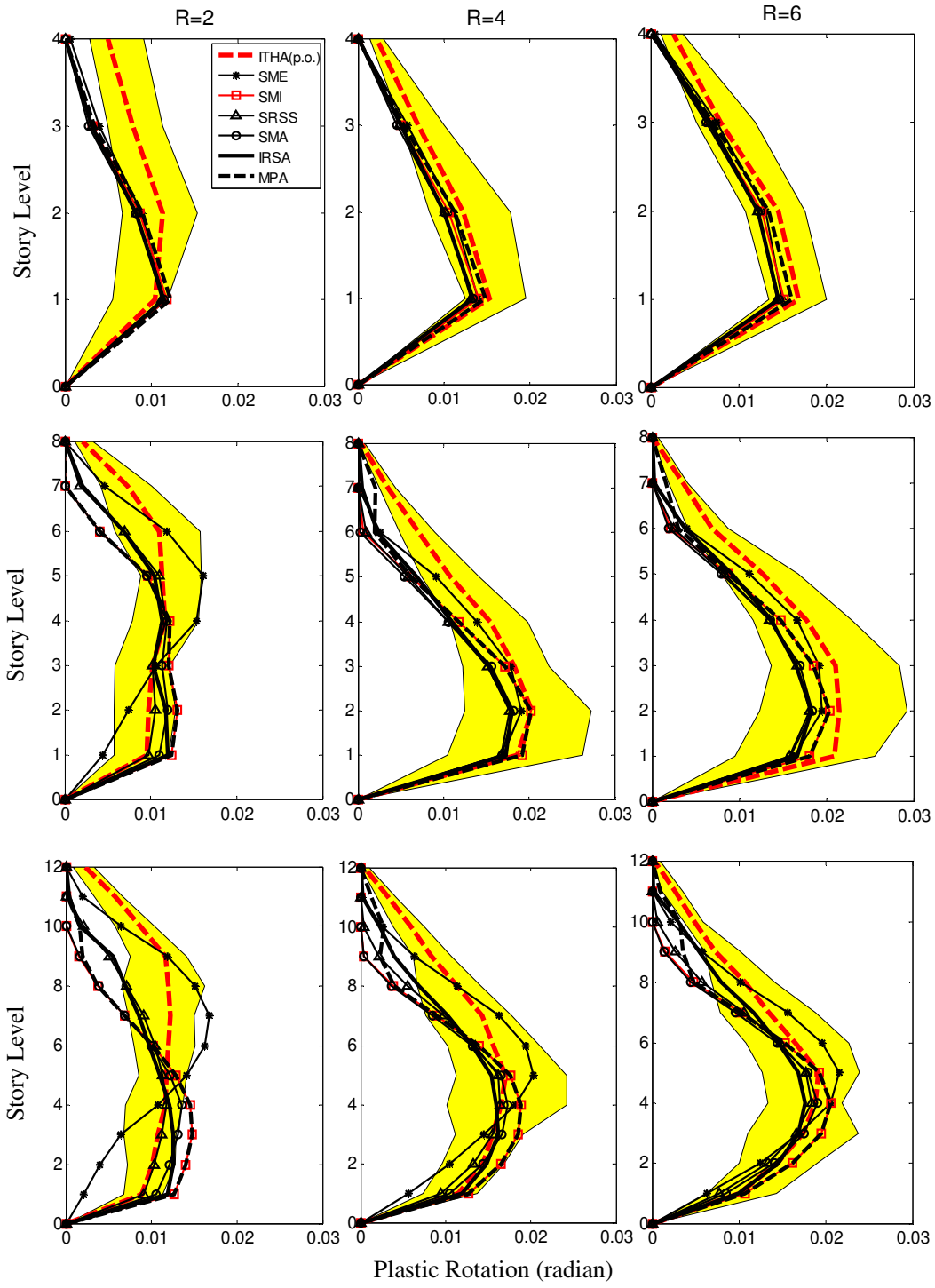

Figure 4.16. Mean plastic rotation at the central beams estimated by inelastic time history analysis (ITHA) with peak-oriented hysteresis rule and nonlinear static procedures (IRSA, MPA and four FEMA load distributions) for 4, 8, 12, 16 and 20-story frame systems, each designed for R=2, 4 and 6, P-delta included

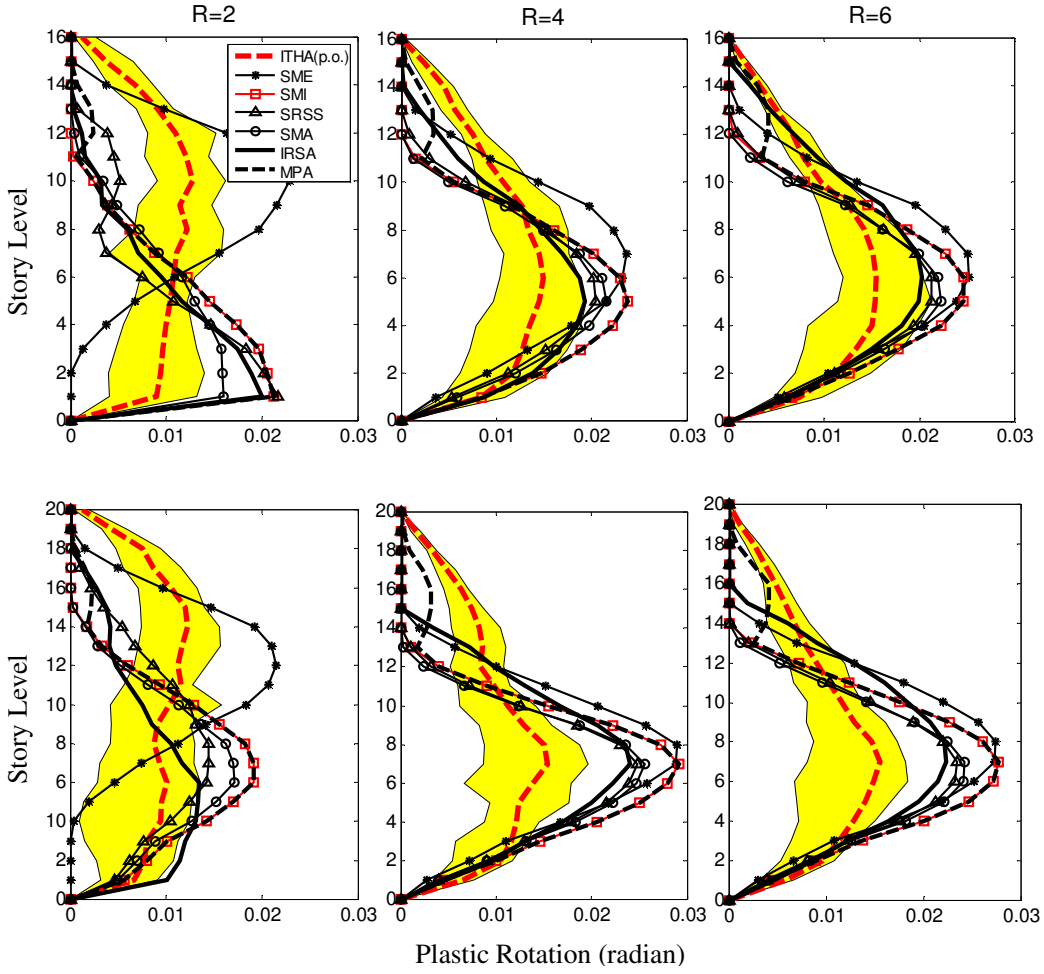

Figure 4.16(contn'd). Mean plastic rotation at the central beams estimated by inelastic time history analysis (ITHA) with peak-oriented hysteresis rule and nonlinear static procedures (IRSA, MPA and four FEMA load distributions) for 4, 8, 12, 16 and 20-story frame systems, each designed for R=2, 4 and 6, P-delta included

5. EVALUATION OF SINGLE-MODE AND MULTI-MODE PUSHOVER PROCEDURES FOR DUAL SYSTEMS

In this chapter a comparative study for dual systems is conducted to evaluate performance of the nonlinear static procedures proposed by Gupta and Kunnath(2000), Chopra and Goel (2001), Aydınoğlu (2003), Antoniou and Pinho (2004[b]) and Casarotti and Pinho (2007) in estimating seismic demands. In addition, nonlinear static procedures with four different lateral load distributions specified in FEMA 356 (FEMA, 2000) are considered.

The structural systems analyzed in this chapter are two dimensional dual systems with three different heights (8, 16 and 24 stories) and with three different wall shear ratios (α_s=0.50, 0.75 and 0.90) for single ductility level (R=4) as described in Chapter 3. Inelastic response of each dual system to 20 earthquake records is determined using inelastic time history analysis (ITHA). Nonlinear static analyses according to the methods proposed by the researchers mentioned above and lateral load patterns described in FEMA 356 have been performed for single elastic response spectrum as implemented in the preceding chapter. Seismic demands from each nonlinear static analysis are compared with the mean values of seismic demands obtained from ITHA.

Story displacement and inter-story drift ratios obtained from the nonlinear static analyses for each story are presented and compared with the results from ITHA. In a similar way, as implemented in the preceding chapter, plastic rotations at the central beams along the height of the buildings are also presented to observe the structural damage distribution in the frames. Shear wall elements are the primary structural components governing the overall structural response and the dynamic characteristics of the structural system depending on their stiffness and strength level relative to the frames, which is represented by wall shear ratio, α_s, in this study. Therefore, variation of the maximum shear demands and maximum plastic rotations along the wall have been presented in addition to the seismic demand parameters mentioned above.

5.1. Application of Nonlinear Static Procedures

The multi-mode and single-mode pushover analysis procedures, which have been evaluated for the frame systems in the preceding chapter are also evaluated for dual systems. Therefore, assumptions made in the application of the nonlinear static analyses for each method in Chapter 4 have been also adopted in this chapter.

P-delta effects due to gravity loads have been included in the nonlinear static analyses for dual systems. A stated in Chapter 2, when P-delta effects are included, ASBP and DAP cannot be performed because of the modal scaling procedures based on instantaneous elastic spectral quantities. Therefore, nonlinear static analyses including P-delta effects have been carried out only for MPA, IRSA and pushover analyses using FEMA 356 load distributions.

The computer program, which has been coded in MATLAB to perform nonlinear static analysis for frame systems, is capable of performing piecewise linear pushover analyses for two dimensional dual systems. Therefore, the same computer program has been also executed for the nonlinear static analyses of dual systems.

In this study, mainly two groups of nonlinear static analyses have been performed. In Group 1, 9 different dual systems have been analyzed for eight different pushover analysis procedures that exclude P-delta effects. In Group 2, there are six different pushover analysis procedures that include P-delta effects. Totally, 126 nonlinear static analyses have been performed for dual systems.

5.2. Inelastic Time History Analysis for Dual Systems

Statistical findings obtained from the inelastic time history analyses are assumed to be exact solutions and forms the basis for the comparative evaluation of the multi-mode pushover procedures in estimating seismic demands. The analyses have been performed by using RUAUMOKO (Carr, 2000) structural analysis program.

Consistent with the structural models used for nonlinear static analyses, nonlinear behavior of the structural components is also represented by concentrated plastic hinge with zero length plastic hinge in the time history analyses. Two different hysteretic models are used for plastic hinges, which are elasto-plastic and peak oriented hysteretic models as described in Chapter 4. In addition to two types of hysteresis models, seismic demands of the dual systems have been investigated for the case including P-delta effects.

Consequently, four groups of time history analyses have been performed to evaluate the sensitivity of the seismic demands and the behavior of the dual systems in terms of P-delta effects and hysteresis models. These analysis groups are given as follows:

- Group 1 analyses with elasto-plastic hysteresis and without P-delta effects.
- Group 2 analyses with elasto-plastic hysteresis and P-delta effects.
- Group 3 analyses with peak-oriented hysteresis and without P-delta effects.
- Group 4 analyses with peak-oriented hysteresis and P-delta effects.

5.3. Inelastic Time History Analysis Results

Because of the vast number of ITHA analyses performed in this study, only mean inter-story drift ratio results for dual systems with α_s=0.75 are presented for the interpretation of ITHA results. Figure 5.1 shows the mean inter-story drift ratios estimated by inelastic time history analyses, including and excluding P-delta effects for 8, 16 and 24-story dual systems. As shown in Figure 5.1a, the differences between results of the analyses with the elasto-plastic and peak-oriented hysteresis increase as the story level increases. Inelastic time history analyses for peak-oriented hysteresis model give larger values due to the gradually degrading stiffness of peak-oriented hysteresis rule at each cycle, as depicted in Figure 4.2.

It should be observed that P-delta effects have little influence on the inter-story drift demand throughout the structure. Results with and without P-delta effects are almost identical. The similar trends have been observed for story displacement and plastic rotation demands at the central beams in the dual systems with wall shear ratio of 0.5 and 0.9.

5.4. Comparative Evaluation of Nonlinear Static Analyses and Inelastic Time History Analysis Results

5.4.1. Story Displacements

Figure 5.2 and Figure 5.3 present mean story displacement results obtained from the inelastic time history analyses and nonlinear static analyses for 9 different dual systems without P-delta effects. It is observed that agreement with ITHA is excellent in 8-story dual systems for all nonlinear static analysis methods. However, the discrepancy tends to increase between ITHA and nonlinear static procedures as the number of story level increases. This is attributed to the approximation of equal displacement rule, as discussed in Chapter 4, and the uneven distribution of damping effect through Rayleigh damping matrix.

Note that for all dual systems and all multi-mode pushover procedures together with single-mode pushover methods give almost identical results. This ephasizes that considering only first mode is sufficient in estimating story displacements response as observed for the frame systems presented in the preceding chapter.

Figure 4.4 and Figure 4.5 show mean story displacement results obtained from the inelastic time history analyses and nonlinear static analyses with P-delta effects for 9 different dual systems. It is observed that P-delta effects have little influence on the story displacements demands as compared to the analyses excluding P-delta effects. The similar tendency has been already observed in comparison of ITHA with and without P-delta effects. Therefore, overestimation of all nonlinear static analyses still persists for 16 and 24-story buildings when P-delta effects are included.

5.4.2. Inter-Story Drifts

Figure 5.6 and Figure 5.7 show mean inter-story drift ratio profiles obtained from the inelastic time history analyses and nonlinear static analyses without P-delta effects for 9 different dual systems. Inter-story drifts obtained from ITHA increase linearly as the number of story level increases for buildings with α_s=0.75 and 0.90. In contrast, inter-story

drift values decrease in the upper stories of dual system with α_s=0.50. These trends imply that inter-story drift distribution throughout the structure depends on the flexural stiffness of the wall relative to the stiffness of the frame.

Inter-story drift ratios obtained from ITHA and all nonlinear static analyses regardless of single-mode or multi-mode effects considered match fairly well in 8-story buildings. This is because, for these structures, the effects of higher modes are negligible. However, the results between the responses estimated by ITHA and nonlinear static methods begin to divert as the number of stories are increased. Similar to the discrepancy as observed in the story displacement result, the divergence arises from the approximation of equal displacement rule.

As can be seen from Figure 5.6 and Figure 5.7, for taller frames with α_s=0.75 and 0.90, almost all nonlinear static procedures give similar results, except ASBP. ASBP overestimates the inter-story drift demand in the lower and upper story levels particularly for 24-story buildings with α_s=0.75 due to the modal scaling procedure based on instantaneous elastic spectral accelerations. For a fixed frame height, the discrepancy between ASBP and ITHA decreases as the wall shear ratio increases. Inter-story drift distribution obtained from IRSA in 24-story building with α_s=0.50 is similar to that of ITHA with a shift by a constant error, which implies the expected error due to the approximation of equal displacement rule. Shape of inter-story drift distribution obtained from IRSA match fairly well with that of ITHA. In the upper story levels, IRSA overestimates story drift demands relative to the other nonlinear static methods. The similar trend can be observed for DAP and SRSS, which are closer to the exact solution (ITHA) in the upper stories as compared to the other methods. However, IRSA provides a good approximation to ITHA with peak-oriented hysteresis throughout the 16-story building with α_s=0.5. The other nonlinear static methods again tend to underestimate inter-story drift demands in the upper stories compared to ITHA. The variation of the response and the location of the largest inter-story drift ratio are estimated reasonably well by the multi-mode pushover methods, IRSA, DAP and SRSS, particularly for taller frames with α_s=0.50.

MPA tends to underestimate the inter-story drift demands in the upper stories for 16 and 24-story buildings, but overestimates in the middle stories as compared to the IRSA, DAP and SRSS. Therefore, it can be concluded that multi-mode pushover procedures, which take into account modal contributions and combine them at each pushover step, provide better estimate of inter-story drift demands in the middle and upper stories of dual systems with smaller shear wall ratio.

As it is stated earlier, FEMA 356 suggests two types of lateral load distributions so as to bound the likely responses. When the envelope inter-story drift distributions obtained from load distribution of FEMA 356 (SMI, SME, SRSS and SMA) are traced along the height of dual systems with α_s=0.5, the discrepancy between the ITHA and the envelope result increases. However, SRSS and SME distributions provide more consistent results with ITHA for all dual systems compared to the single mode invariant or adaptive lateral load distribution (SMI and SMA).

Figure 5.8 and Figure 5.9 show the mean inter-story drift profiles obtained from the inelastic ITHA and nonlinear static analyses with P-delta effects. When P-delta effects due to the gravity load are included, story drift results obtained from both ITHA and nonlinear static procedures tend to be unaffected for all buildings, which is similar to the story displacement results as expected.

5.4.3. Plastic Rotations

Figure 5.10 and Figure 5.11 show mean plastic rotations of central beams estimated by ITHA and nonlinear static procedures without P-delta effects. Similar to the inter-story drift ratio estimates, plastic rotation distributions along the height of each 8-story building obtained from all nonlinear static procedures are almost the same and consistent with the exact solutions (ITHA) in acceptable accuracy. The similar trend can be observed for taller buildings with α_s=0.75 and 0.90. However, ASBP overestimates plastic rotation demands in the lower and the upper story levels, especially for 24-story buildings. Plastic rotations obtained from ASBP tend to increase with respect to the results obtained from ITHA as the wall shear ratio decreases. This result implies shortcoming of modal scaling procedure based on instantaneous elastic spectral acceleration as adopted in ASBP.

IRSA manages to capture variation in plastic rotation demands throughout 16- and 24-story buildings, where the effect of higher modes become important, as compared to the other nonlinear static procedures. In addition, IRSA predicts the location of the largest plastic rotation demand. DAP and SRSS give similar results in the lower and middle stories of 24-story building with α_s=0.50. However both methods underestimate the plastic rotation demands at the upper story levels in comparison with IRSA.

MPA tends to overestimate plastic rotation demands in the lower story level of 16- and 24-story buildings with α_s=0.50 and 0.75 and underestimates in the upper story levels compared to the other multi-mode pushover procedures. This trend indicates again that multi-mode pushover procedures (IRSA, DAP and SRSS), which combine multi-mode effects at each pushover step, provide better estimate of plastic rotation demands in the middle and upper stories of dual systems.

Figure 5.12 and Figure 5.13 show mean plastic rotation obtained from the inelastic time history analyses and nonlinear static analyses with P-delta effects. When P-delta effects due to the gravity load are included, results obtained from both ITHA and nonlinear static procedures tend to be unaffected for all buildings, which is similar to the story displacement and inter-story drift demands as expected.

5.4.4. Wall Shear Force Demands

Shear force demands, which have to be checked in order to assess the brittle behavior in the structural components, is one of the important demand parameters. It is crucial especially for shear wall elements, which govern structural behavior dominantly. In this respect, assessing the ability of the practice-oriented nonlinear static methods in estimating shear force demands in the walls is very important for dual systems. Figure 5.14 shows the variation of shear demands along the height of the shear wall obtained from the inelastic time history analyses and nonlinear static analyses without P-delta effects. Maximum absolute shear force values acting on the wall during the course of analyses have been presented in Figure 5.14.

Maximum shear force demands have been observed in the first and second story level as expected, where it is the most critical region of the wall in terms of the plastic rotation demands. In the upper story levels, variation of the maximum shear force demands are approximately constant, particularly for dual system with α_s=0.5 and 0.75. It should be pointed out that MPA, IRSA and ASBP capture the variation in the shear force demands reasonably well for all buildings compared to the other nonlinear static procedures. Shear force demands predicted by DAP and FEMA 356 load distributions are less than those obtained from the ITHA for all buildings. As shown in Figure 5.15, when P-delta effects are considered in the analyses, the same conclusion can be drawn due to the little influence of P-delta effects to seismic response in dual systems.

Figure 5.16, 5.17, 5.18 and 5.19 present the ratios between the shear demands obtained from ITHA and nonlinear static procedures with or without P-delta effects. If the ratio of responses between ITHA and nonlinear static analysis is less than one, the nonlinear static analysis of interest underestimates the response. If the ratio is larger than one, the method provides an overestimate. Figure 5.16 plots the bias with respect to the ITHA for elasto-plastic hysteresis model. DAP and FEMA load patterns excessively underestimate the shear demands with biased larger than that of MPA, IRSA and ASBP, as mentioned above. MPA, IRSA and ASBP underestimate the shear force demands for 8-story buildings with less than 25 % bias. For 16 and 24-story buildings, IRSA estimates the shear force demands approximately with less than 30% bias. The similar trend can be observed for MPA, but with the bias less than 45%. ASBP generally overestimates the shear force demand for buildings with α_s=0.50 and 0.75 with less than 40% bias. Similar results can be observed in Figure 5.17 for the case of ITHA with peak-oriented hysteresis. As observed in the evaluation of inter-story drifts and plastic rotations results, P-delta effects does not change the shear force demands with respect to the case without P-delta effects.

It should be emphasized that multi-mode pushover procedures, which estimate response quantities at each pushover step under the combined load or displacement vector, such as DAP and SRSS, cannot estimate shear force demands accurately. In fact, it is a crucial inability in terms of the prediction of brittle behavior of shear walls in dual systems.

5.4.5. Wall Plastic Rotations Demands

The sequence of plastic hinges estimated by inelastic time history analysis may be different from that estimated by the nonlinear static analysis due to the random cyclic nature of the earthquake. In fact, one of the main objectives of a pushover analysis is to predict the plastic hinge locations and their magnitudes in order to observe damage distribution throughout the structure. In the line with the objective mentioned above, from Figure 5.20 to Figure 5.25, plastic hinge locations and their magnitude in the wall elements obtained from ITHA and all nonlinear static analyses have been presented. Locations of the plastic hinges in these figures are marked to observe the length of the plasticity along the height of the wall. These markers are scaled depending on the magnitude of plastic hinge rotations. It is clear from the figures that multi-mode pushover procedures can better estimate length of the plasticity at the base of the wall when compared to single-mode pushover analysis. It is interesting that single-mode adaptive pushover analysis (SMA) also manages to capture both the location of the plastic hinges and their magnitudes in spite of the fact that only single mode was considered. In the case of P-delta effects, similar conclusion can be drawn.

In addition, plastic rotation demands, which are estimated by all nonlinear static analyses at the base of the walls, are summarized in Figure 5.26, 5.27 and 5.28. Sum of the plastic rotation values along the height of the wall are presented as if distributed plasticity is represented by single plastic hinge formation at the base of the walls. Similar to the observation above, MPA, IRSA and DAP give more consistent results with the plastic rotation demands predicted by ITHA. However, these methods overestimate the plastic rotation demand for 24 story buildings. For 16- and 8-story buildings, the agreement is excellent for multi-mode pushover procedures, which are ASBP, MPA, IRSA and DAP. In addition to these methods, SMA gives also accurate results, which are consistent with observation made for plastic hinge locations. The other methods, which are invariant pushover procedure of FEMA 356 (SME, SMI and SRSS), underestimate the plastic rotation demands, especially for 8-story buildings as compared to other pushover analysis methods.

It is interesting that invariant pushover methods, such as SME, SMI and SRSS, cannot predict plastic hinge formation at the base of the shear walls in 8-story buildings, where higher mode effects are negligible. However, single-mode adaptive distribution, SMA, is capable of estimating plastic hinge formation at the base of the wall. It is evident that adaptive pushover procedure, even for single mode, is capable of capturing the variation in the dynamic characteristics in dual systems and inelastic action at the base of the wall. This situation emphasizes the superiority of the adaptive pushover technique for dual systems with respect to invariant pushover method. The same trend summarized above for the case without P-delta effects can also be observed when P-delta effects are included as shown in Figure 5.29, 5.30 and 5.31.

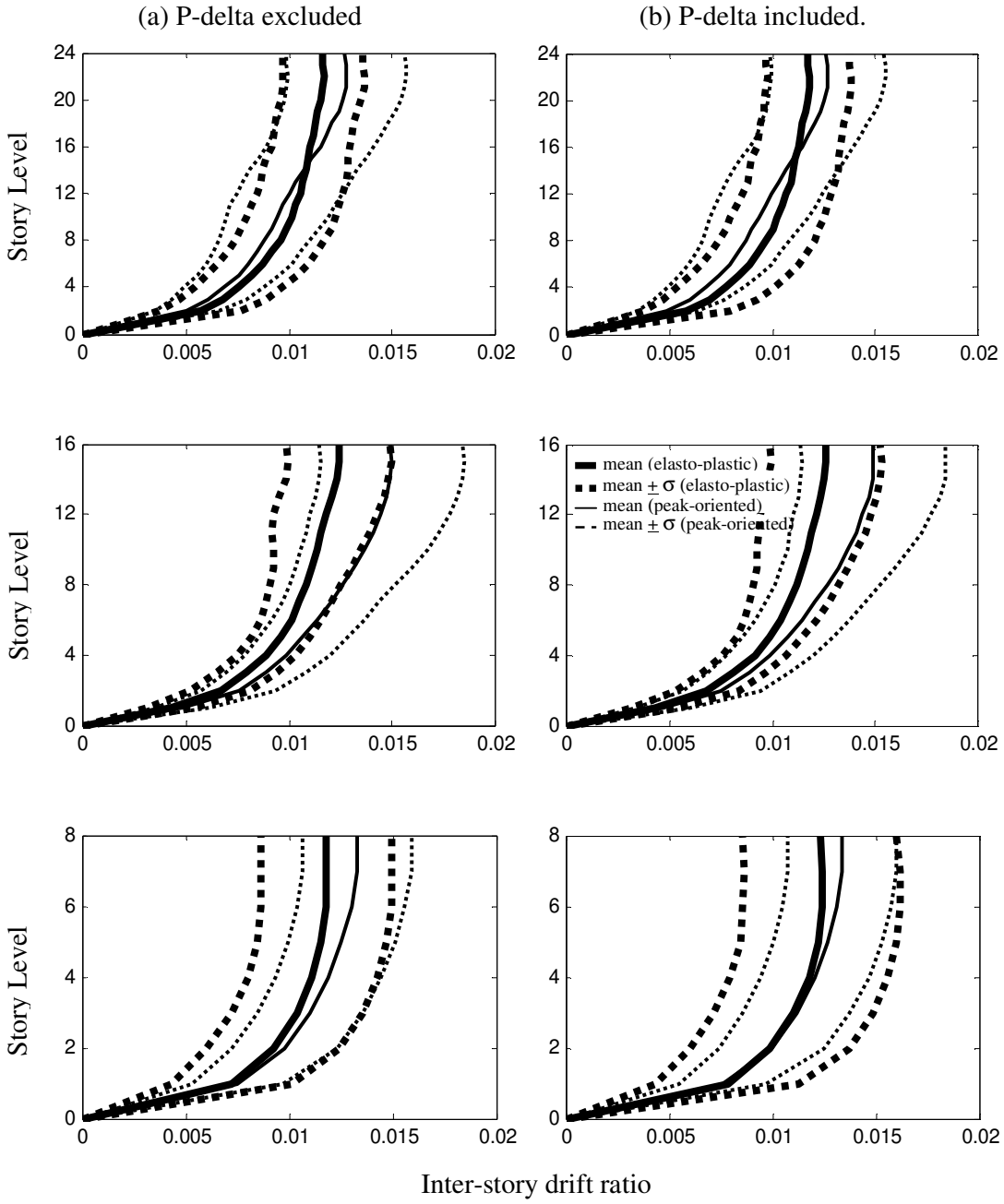

Figure 5.1. Mean inter-story drift ratios estimated by inelastic time history analyses (ITHA) with elasto-plastic and peak-oriented hysteresis rules for 8, 16 and 24-story dual systems with α_s=0.75, (a) P-delta excluded (b) P-delta included

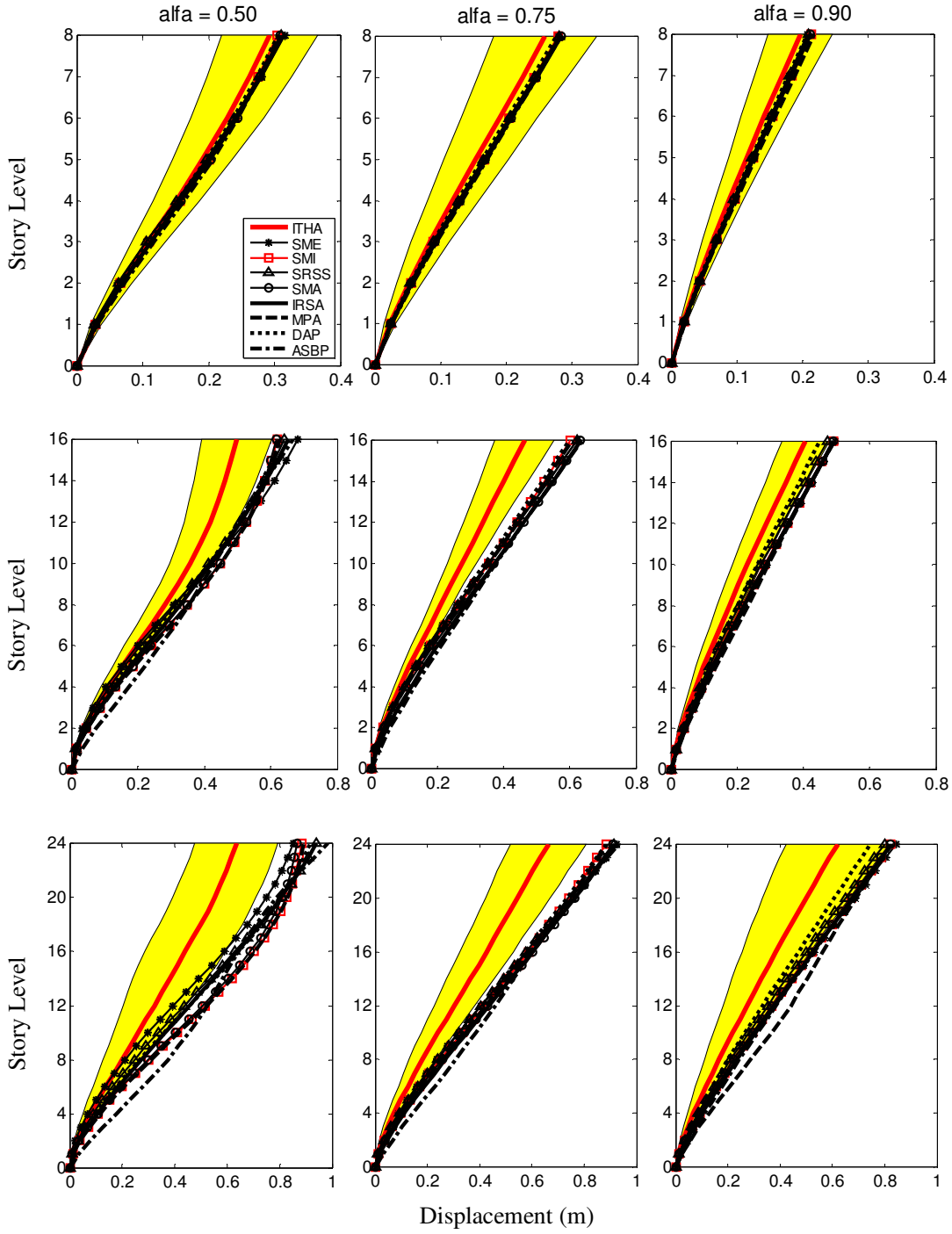

Figure 5.2. Mean story displacements estimated by inelastic time history analysis (ITHA) with elasto-plastic hysteresis rule and nonlinear static procedures (IRSA, MPA, DAP, ASBP and four FEMA load distributions) for 8, 16 and 24-story dual systems, each designed for α_s =0.50, 0.75 and 0.90, P-delta excluded

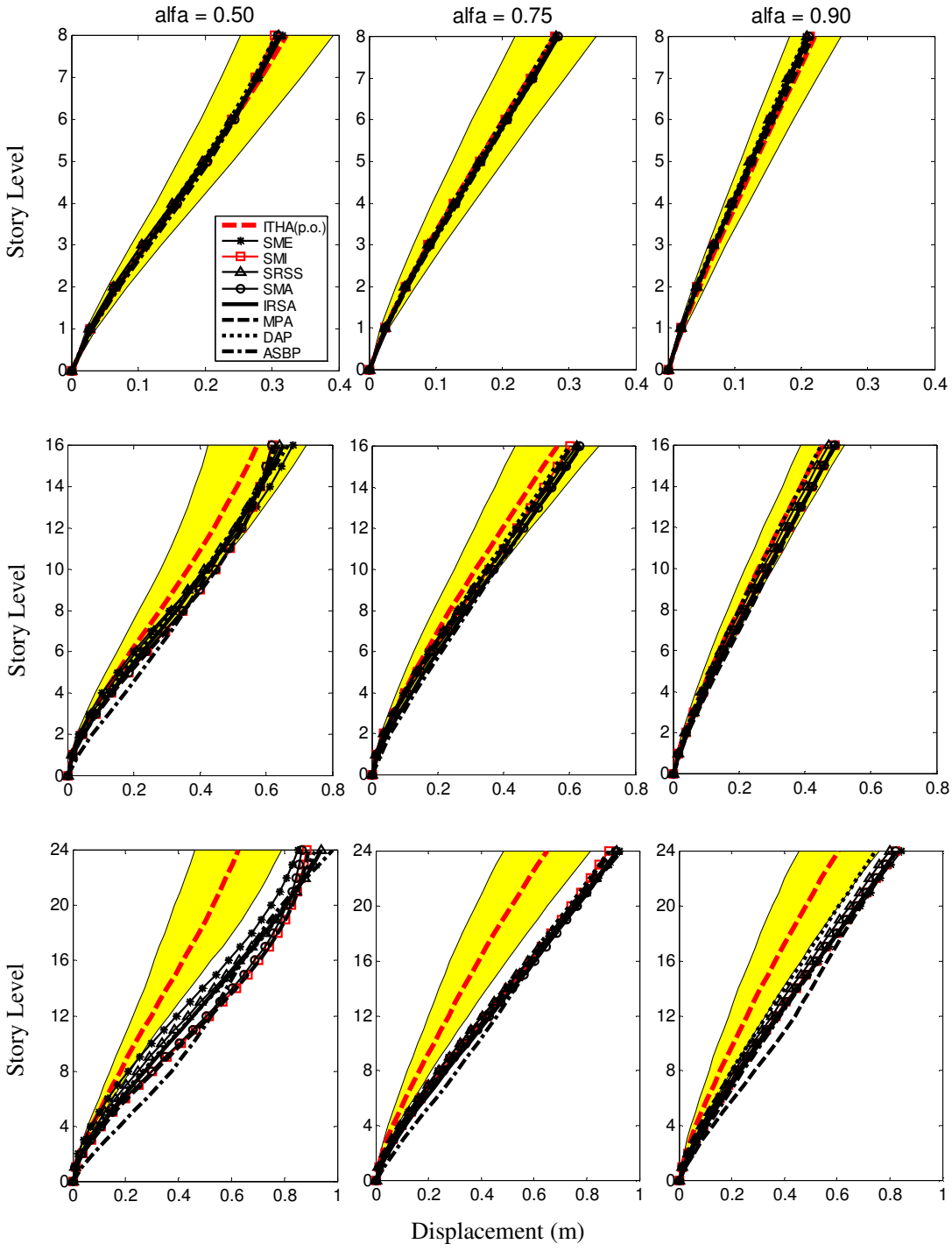

Figure 5.3. Mean story displacements estimated by inelastic time history analysis (ITHA) with peak-oriented hysteresis rule and nonlinear static procedures (IRSA, MPA, DAP, ASBP and four FEMA load distributions) for 8, 16 and 24-story dual systems, each designed for α_s =0.50, 0.75 and 0.90, P-delta excluded

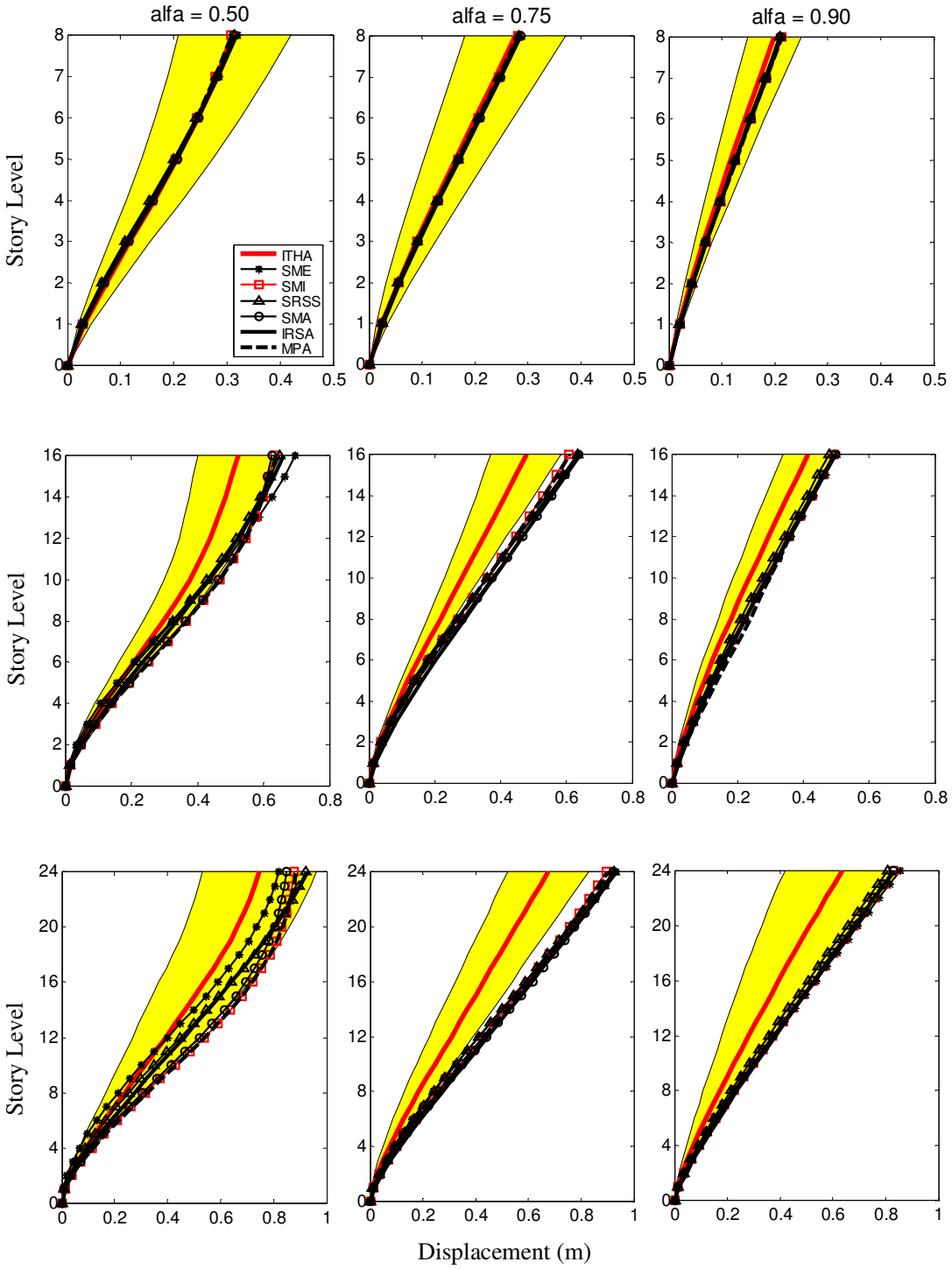

Figure 5.4. Mean story displacements estimated by inelastic time history analysis (ITHA) with elasto-plastic hysteresis rule and nonlinear static procedures (IRSA, MPA and four FEMA load distributions) for 8, 16 and 24-story dual systems, each designed for α_s =0.50, 0.75 and 0.90, P-delta included

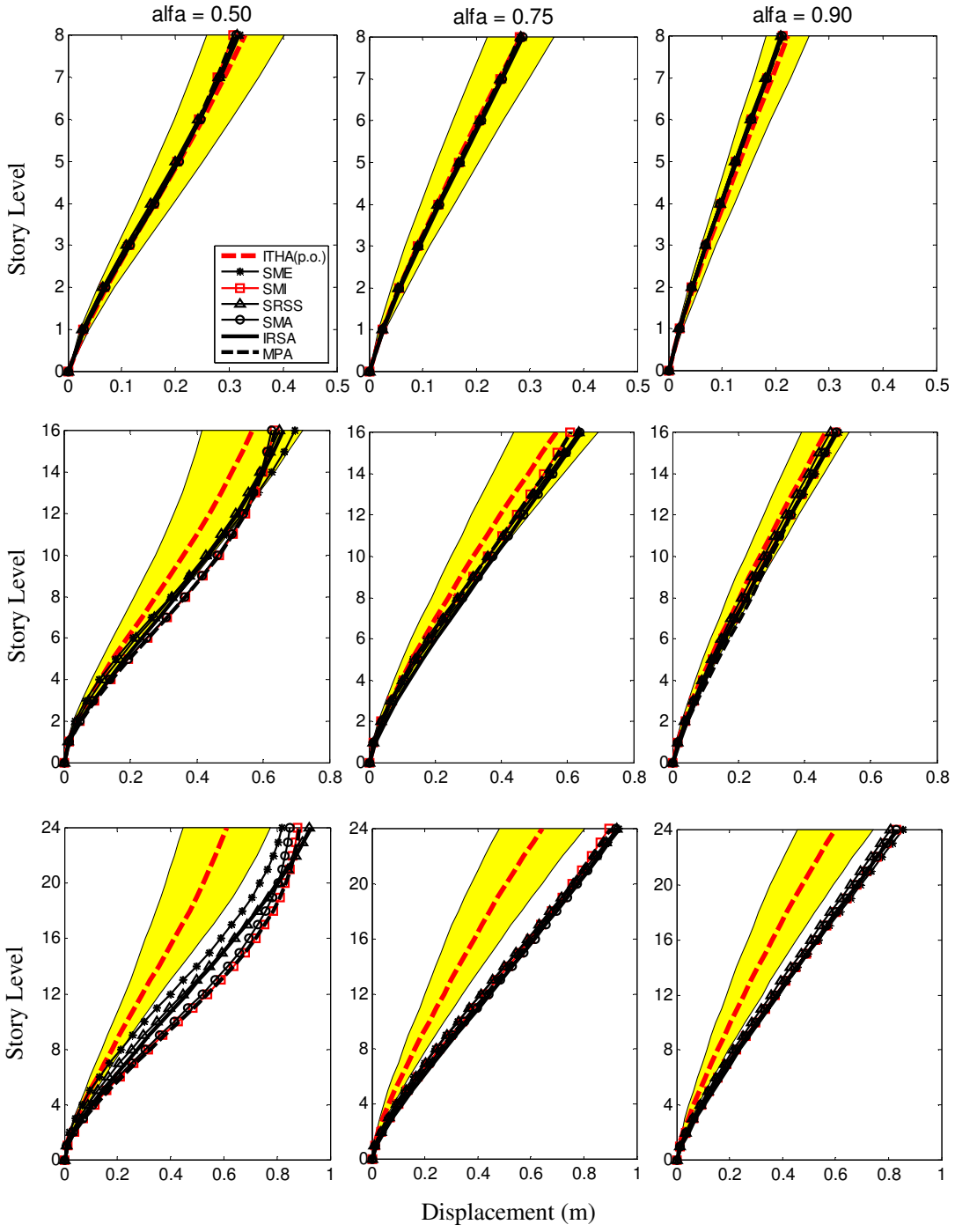

Figure 5.5. Mean story displacements estimated by inelastic time history analysis (ITHA) with peak-oriented hysteresis rule and nonlinear static procedures (IRSA, MPA and four FEMA load distributions) for 8, 16 and 24-story dual systems, each designed for α_s =0.50, 0.75 and 0.90, P-delta included

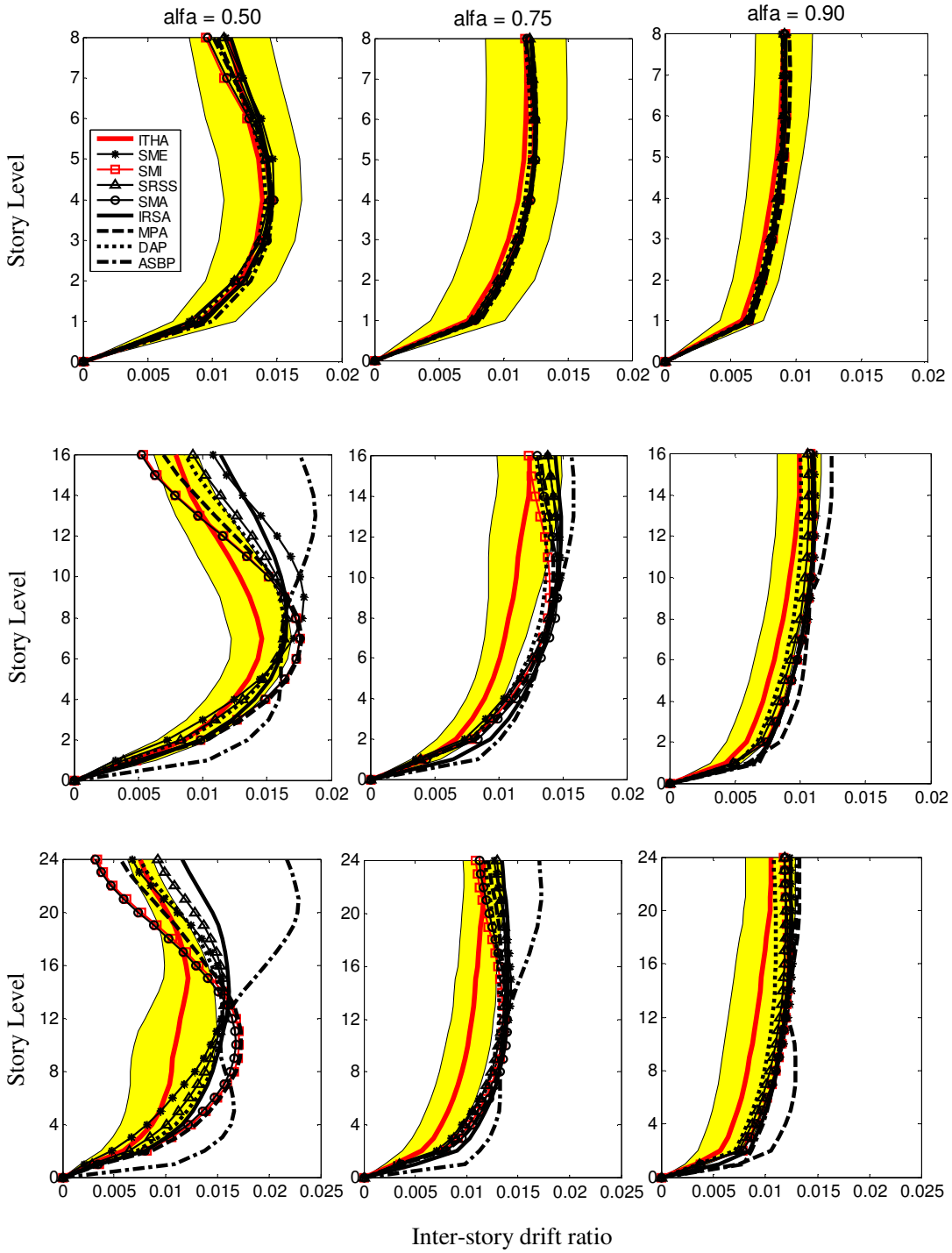

Figure 5.6. Mean inter-story drift ratios estimated by inelastic time history analysis (ITHA) with elasto-plastic hysteresis rule and nonlinear static procedures (IRSA, MPA, DAP, ASBP and four FEMA load distributions) for 8, 16 and 24-story dual systems, each designed for α_s =0.50, 0.75 and 0.90, P-delta excluded

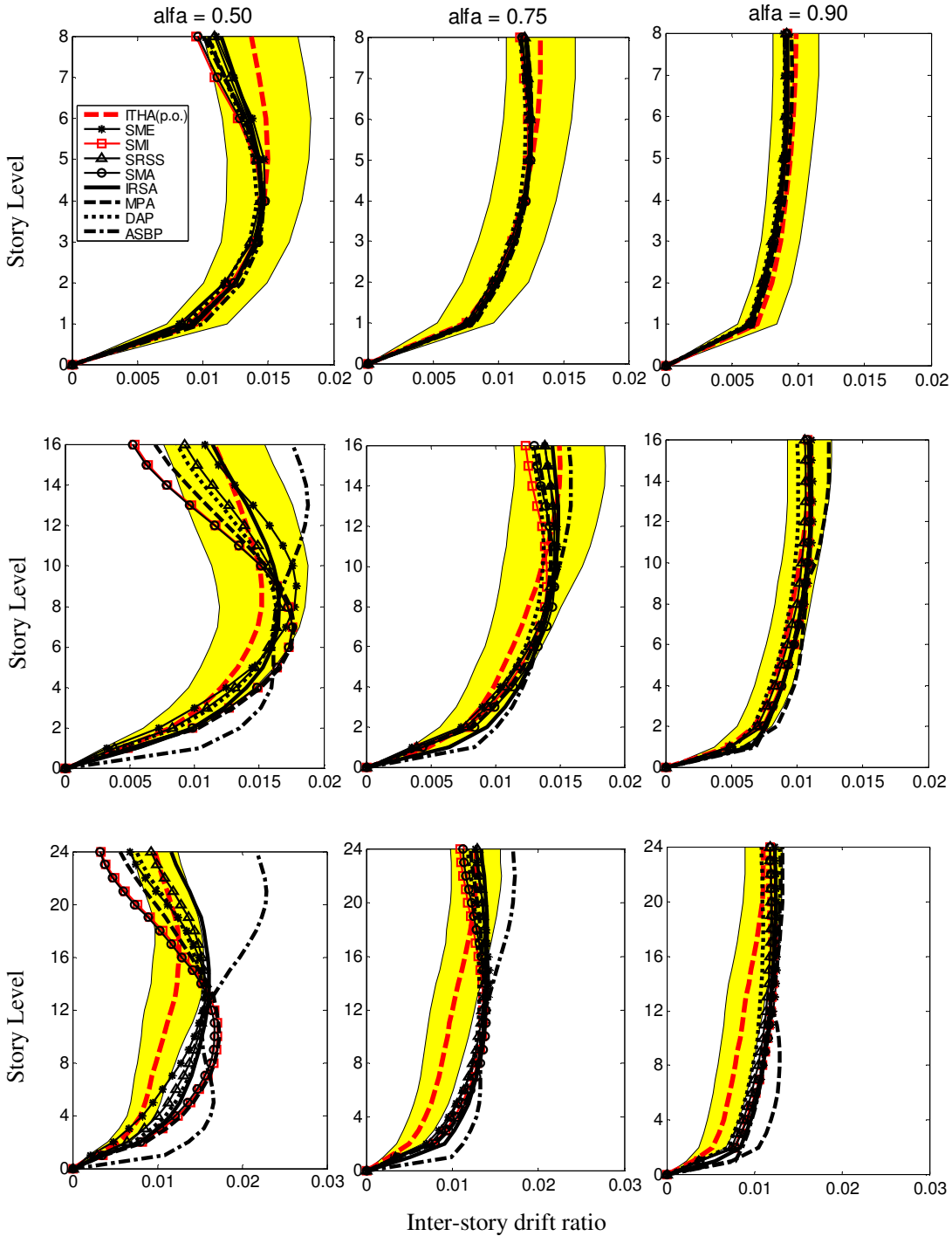

Figure 5.7. Mean inter-story drift ratios estimated by inelastic time history analysis (ITHA) with peak-oriented hysteresis rule and nonlinear static procedures (IRSA, MPA, DAP, ASBP and four FEMA load distributions) for 8, 16 and 24-story dual systems, each designed for α_s =0.50, 0.75 and 0.90, P-delta excluded

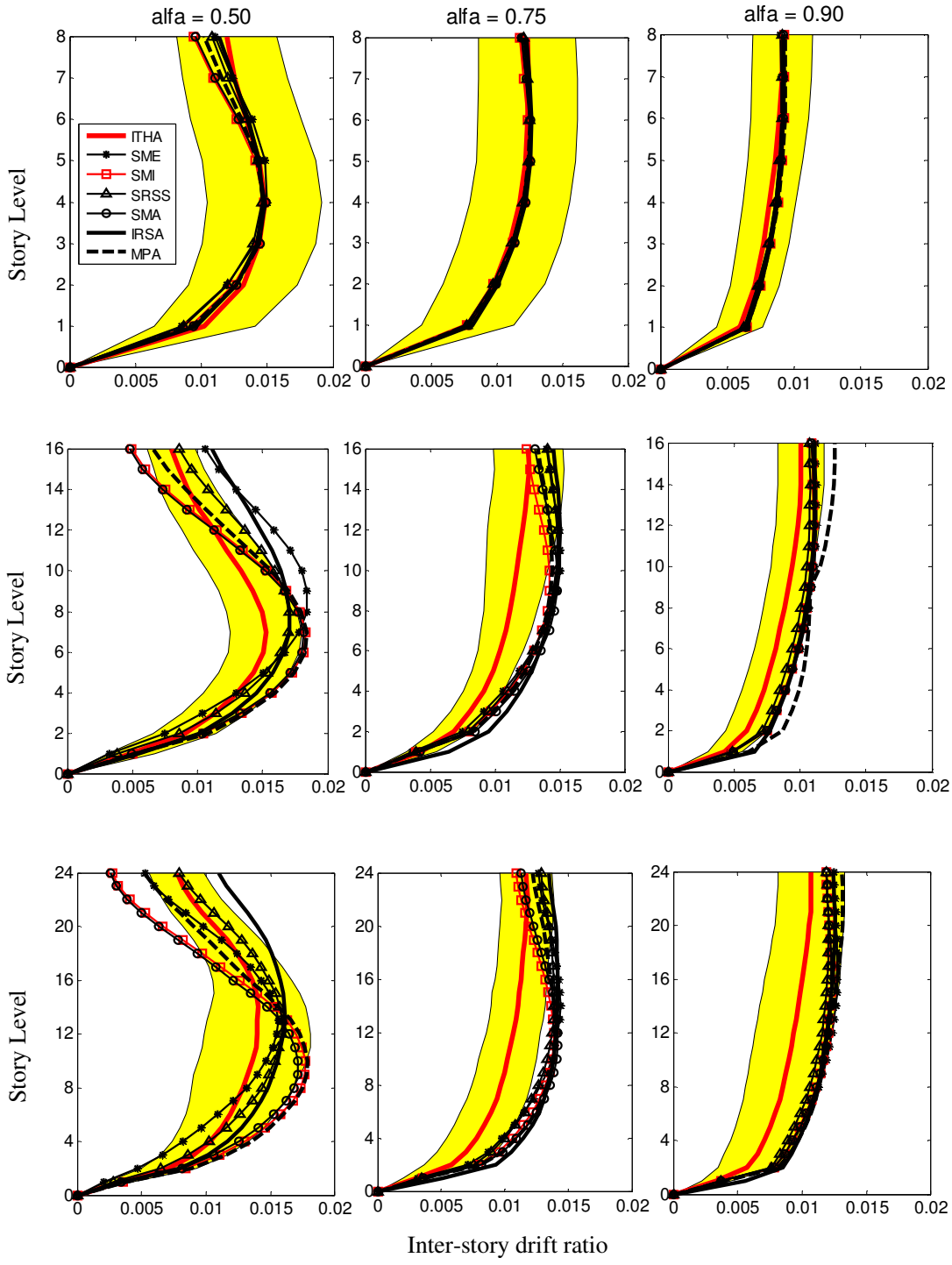

Figure 5.8. Mean inter-story drift ratios estimated by inelastic time history analysis (ITHA) with elasto-plastic hysteresis rule and nonlinear static procedures (IRSA, MPA, and four FEMA load distributions) for 8, 16 and 24-story dual systems, each designed for α_s =0.50, 0.75 and 0.90, P-delta included

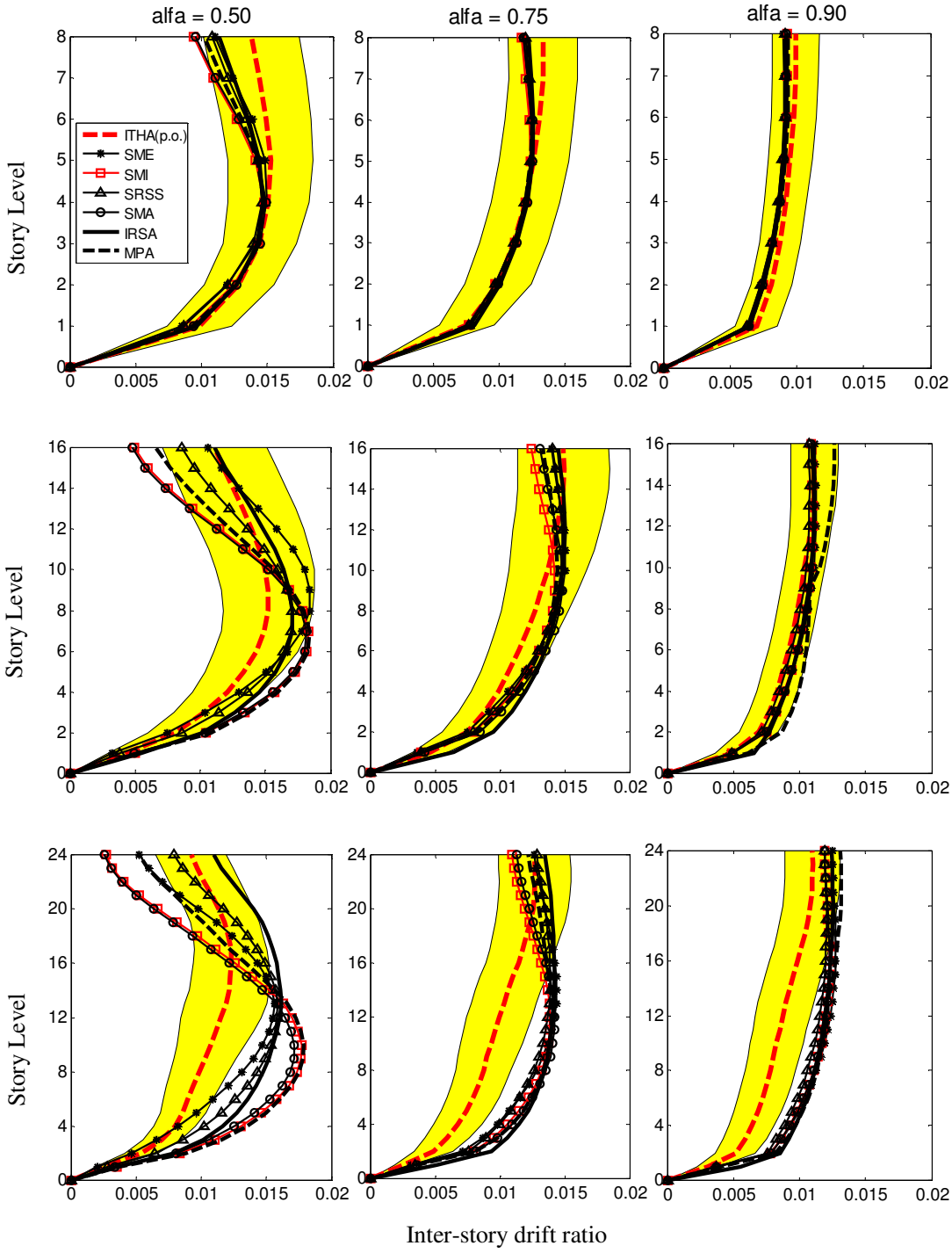

Figure 5.9. Mean inter-story drift ratios estimated by inelastic time history analysis (ITHA) with peak-oriented hysteresis rule and nonlinear static procedures (IRSA, MPA, and four FEMA load distributions) for 8, 16 and 24-story dual systems, each designed for α_s =0.50, 0.75 and 0.90, P-delta included

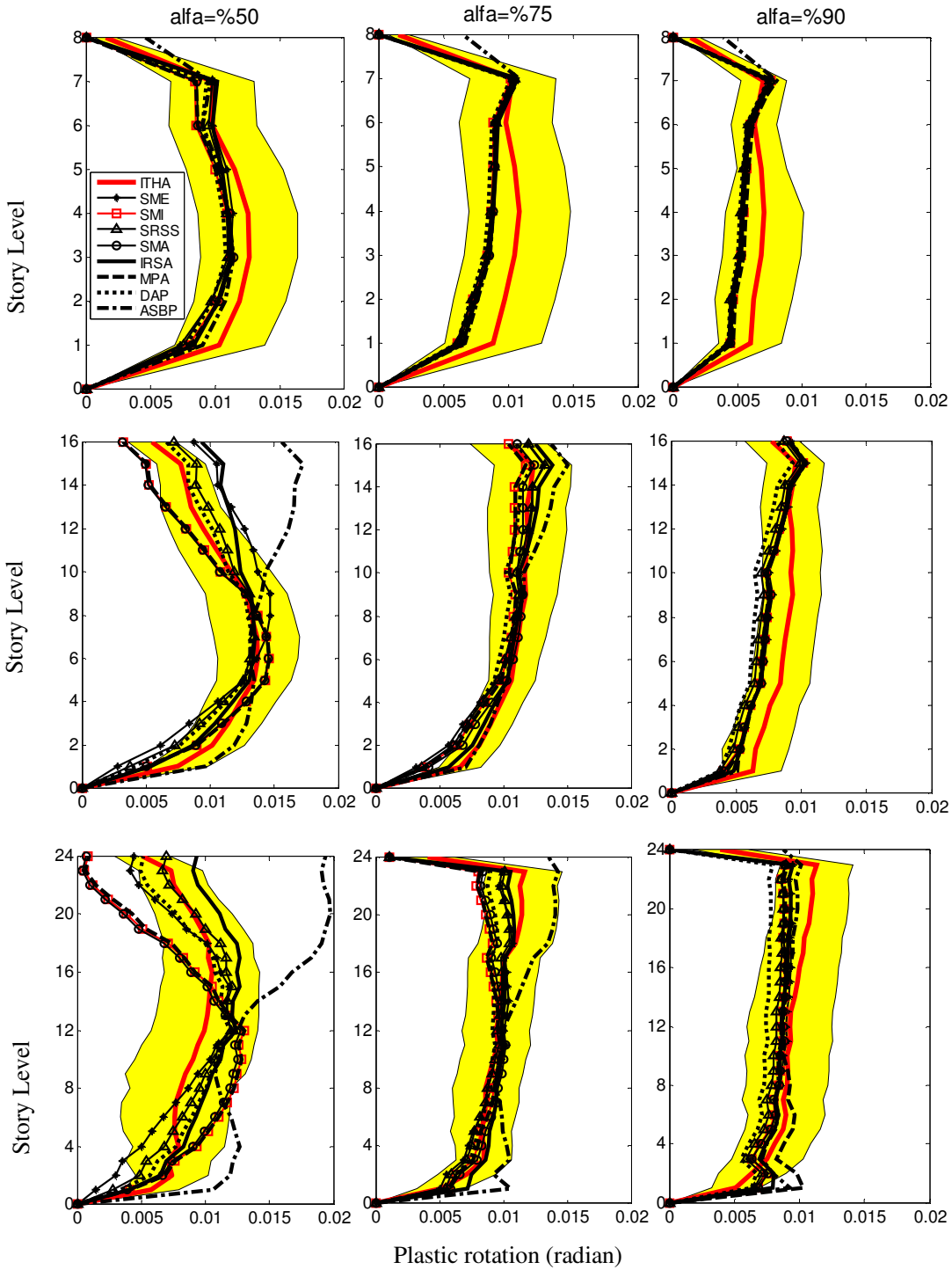

Figure 5.10. Mean plastic rotations at central beams estimated by inelastic time history analysis (ITHA) with elasto-plastic hysteresis rule and nonlinear static procedures (IRSA, MPA, DAP, ASBP and four FEMA load distributions) for 8, 16 and 24-story dual systems, each designed for α_s =0.50, 0.75 and 0.90, P-delta excluded

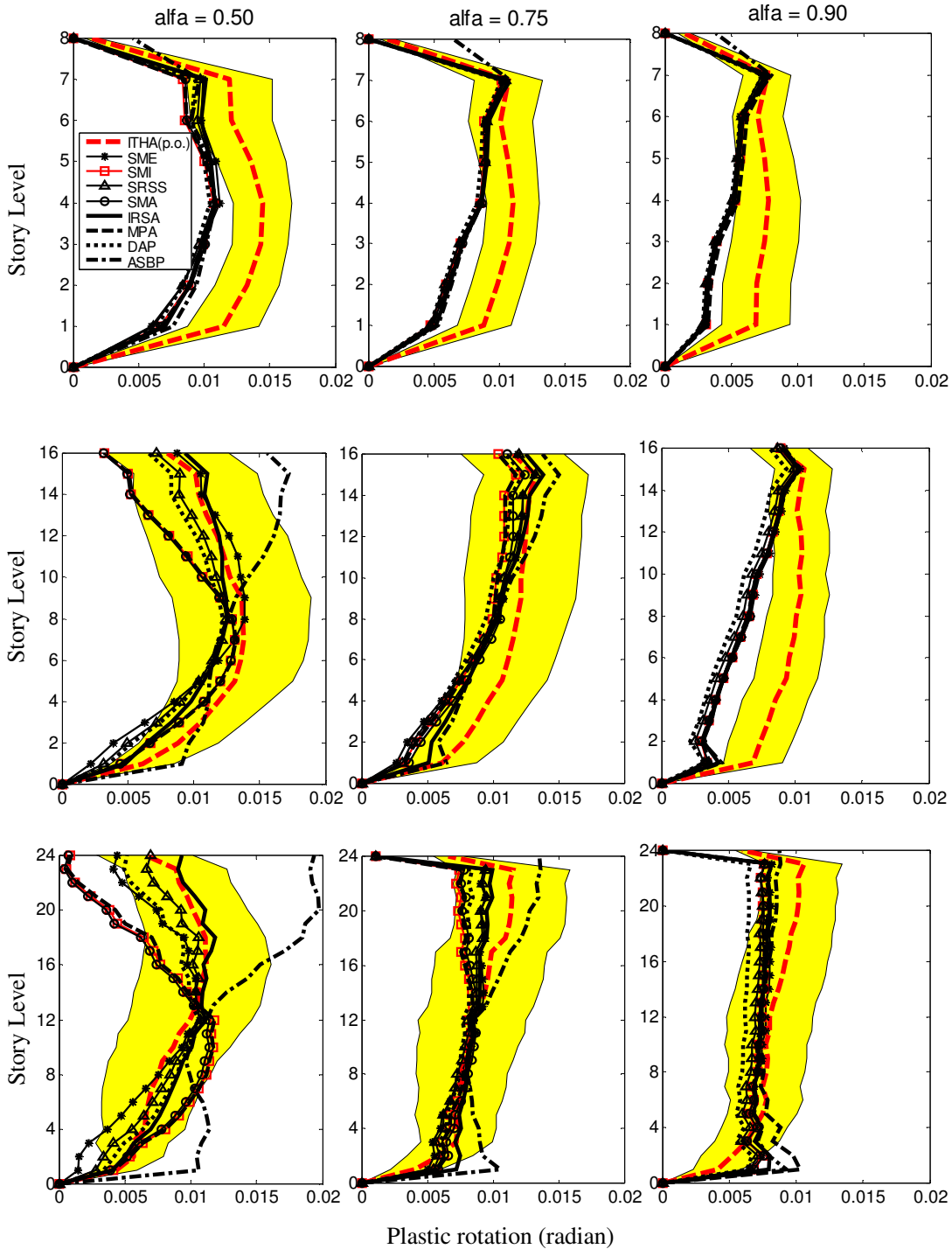

Figure 5.11. Mean plastic rotations at central beams estimated by inelastic time history analysis (ITHA) with peak-oriented hysteresis rule and nonlinear static procedures (IRSA, MPA, DAP, ASBP and four FEMA load distributions) for 8, 16 and 24-story dual systems, each designed for α_s =0.50, 0.75 and 0.90, P-delta excluded

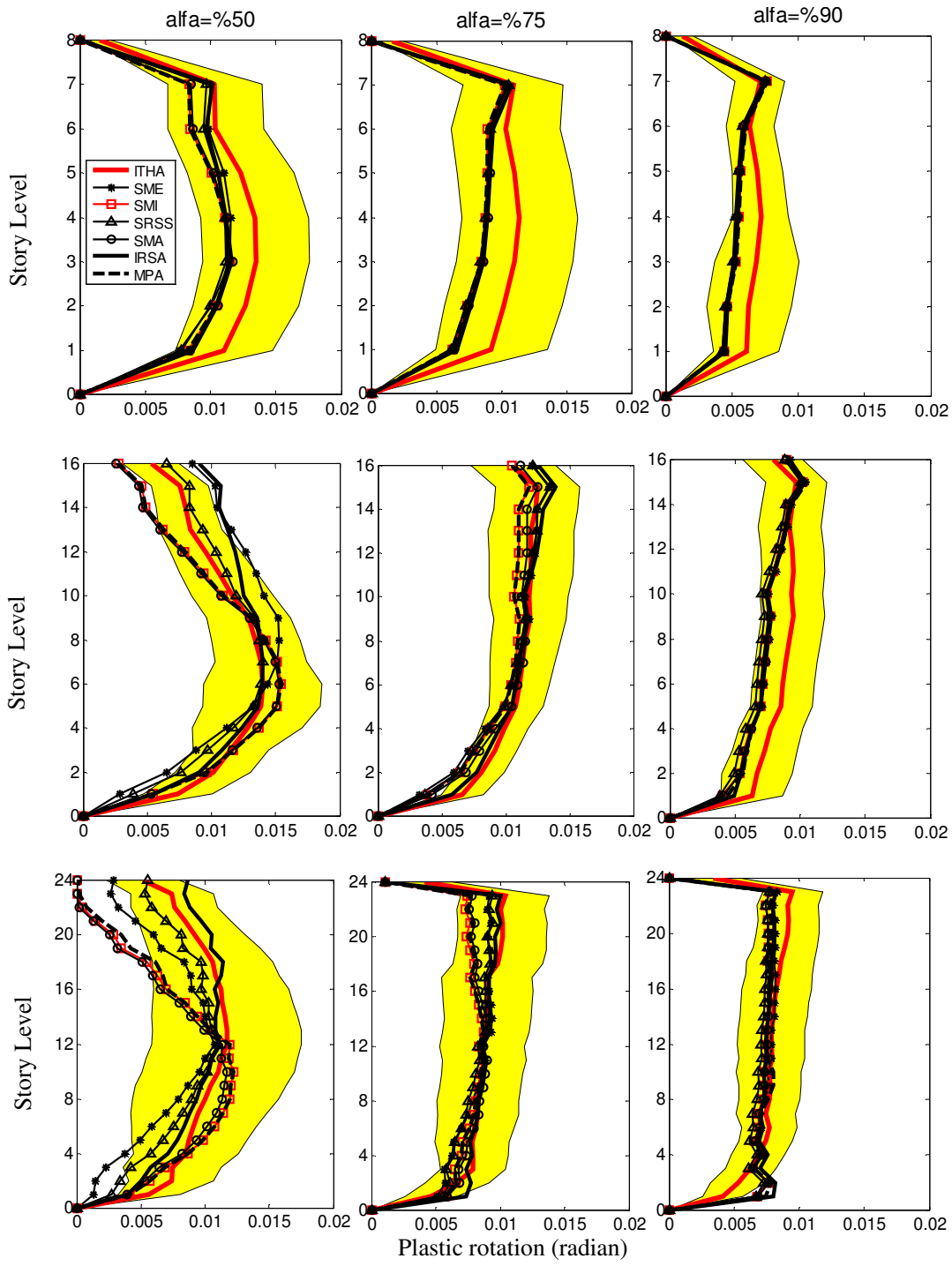

Figure 5.12. Mean plastic rotations at central beams estimated by inelastic time history analysis (ITHA) with elasto-plastic hysteresis rule and nonlinear static procedures (IRSA, MPA and four FEMA load distributions) for 8, 16 and 24-story dual systems, each designed for α_s =0.50, 0.75 and 0.90, P-delta included

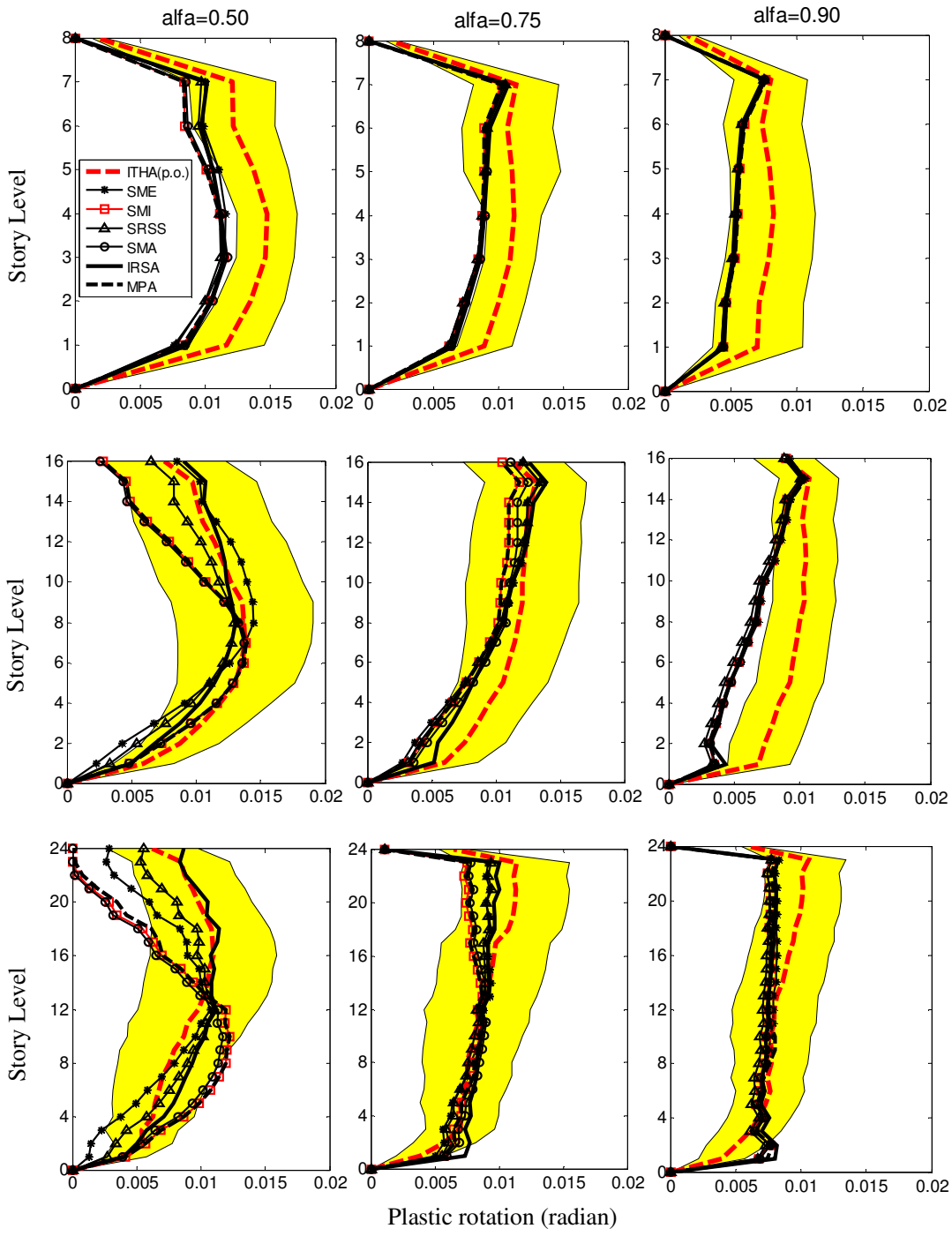

Figure 5.13. Mean plastic rotations at central beams estimated by inelastic time history analysis (ITHA) with peak-oriented hysteresis rule and nonlinear static procedures (IRSA, MPA and four FEMA load distributions) for 8, 16 and 24-story dual systems, each designed for α_s =0.50, 0.75 and 0.90, P-delta included

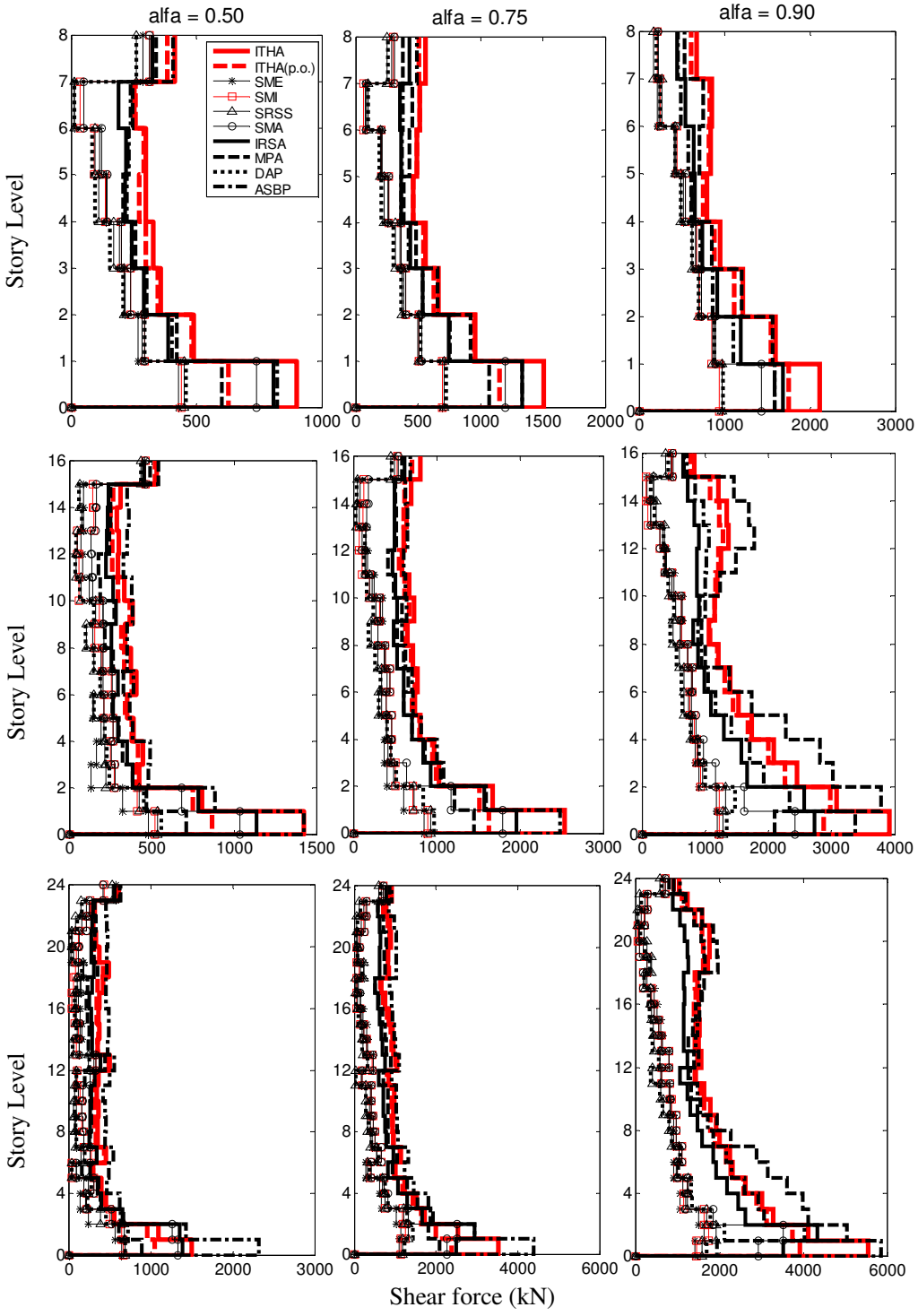

Figure 5.14. Mean shear force profile along the wall estimated by inelastic time history analyses and nonlinear static procedures (IRSA, MPA, DAP, ASBP and four FEMA load distributions) for 8, 16 and 24-story dual systems, each designed for α_s =0.50, 0.75 and 0.90, P-delta excluded

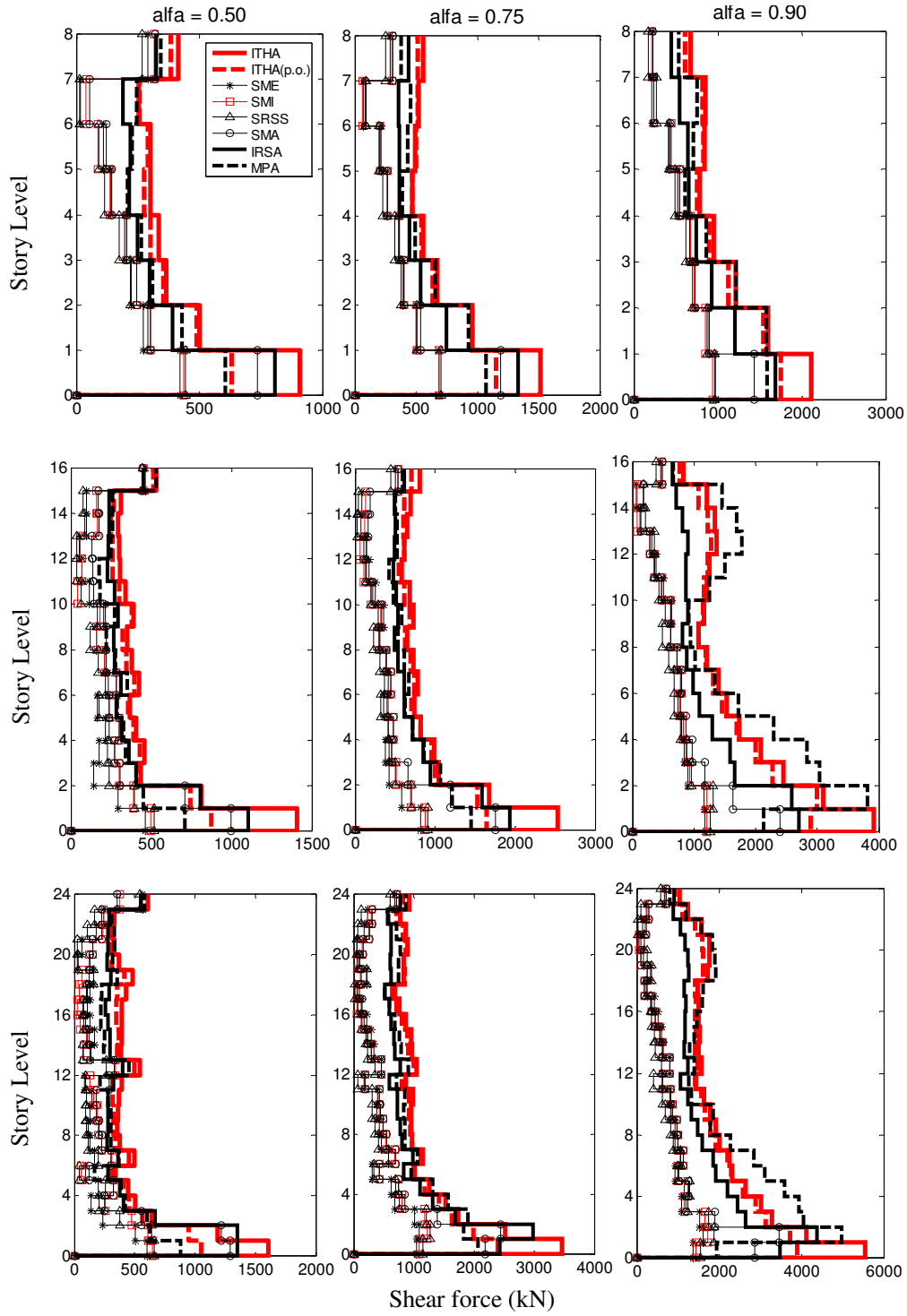

Figure 5.15. Mean shear force profile along the wall estimated by inelastic time history analyses and nonlinear static procedures (IRSA, MPA, and four FEMA load distributions) for 8, 16 and 24-story dual systems, each designed for α_s =0.50, 0.75 and 0.90, P-delta included

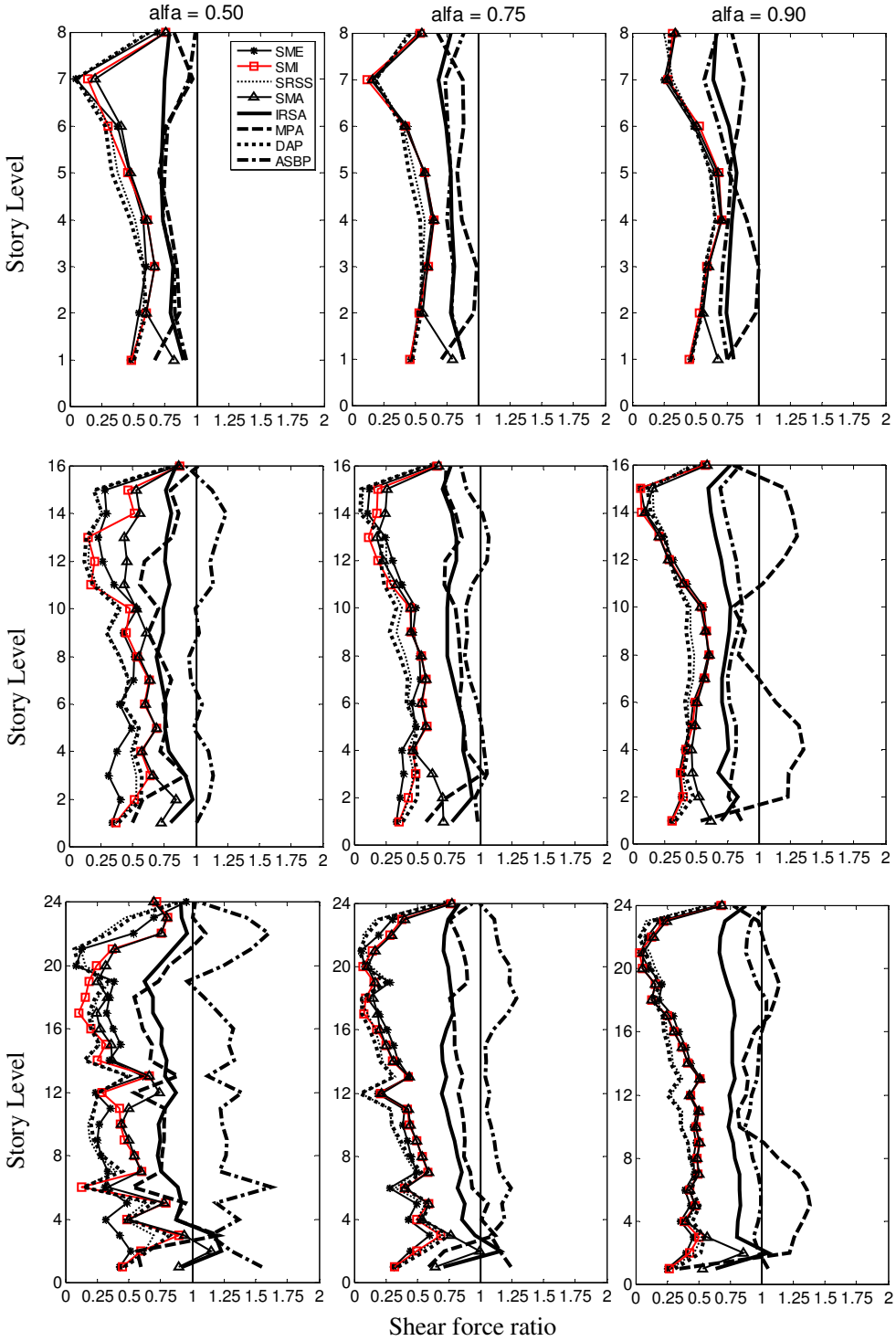

Figure 5.16. Ratio of the mean shear force profile between inelastic time history analyses with elasto-plastic hysteresis and nonlinear static procedures (IRSA, MPA, DAP, ASBP and four FEMA load distributions) for 8, 16 and 24-story dual systems, each designed for α_s =0.50, 0.75 and 0.90, P-delta excluded

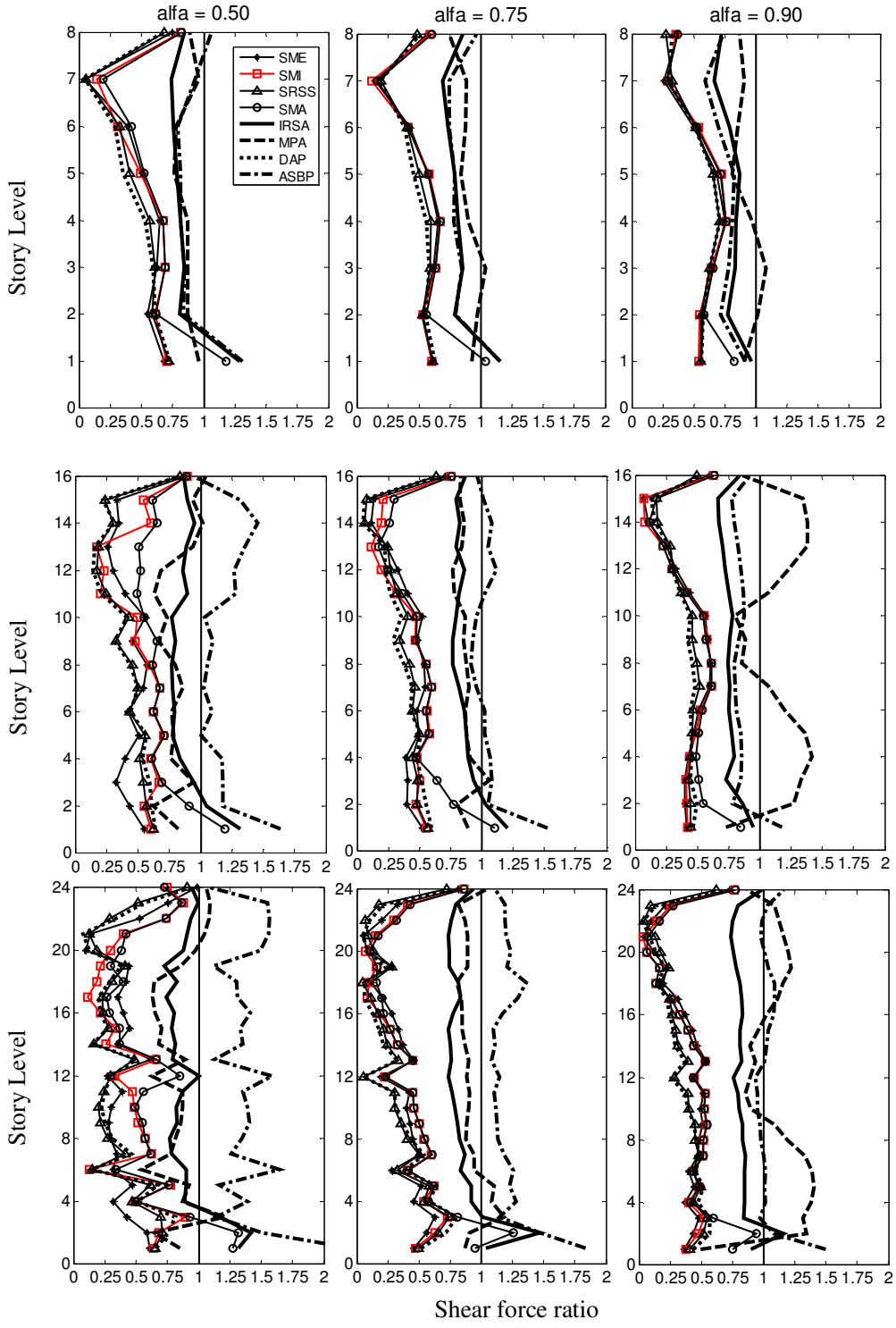

Figure 5.17. Ratio of the mean shear force profile between inelastic time history analyses with peak-oriented hysteresis and nonlinear static procedures (IRSA, MPA, DAP, ASBP and four FEMA load distributions) for 8, 16 and 24-story dual systems, each designed for α_s =0.50, 0.75 and 0.90, P-delta excluded

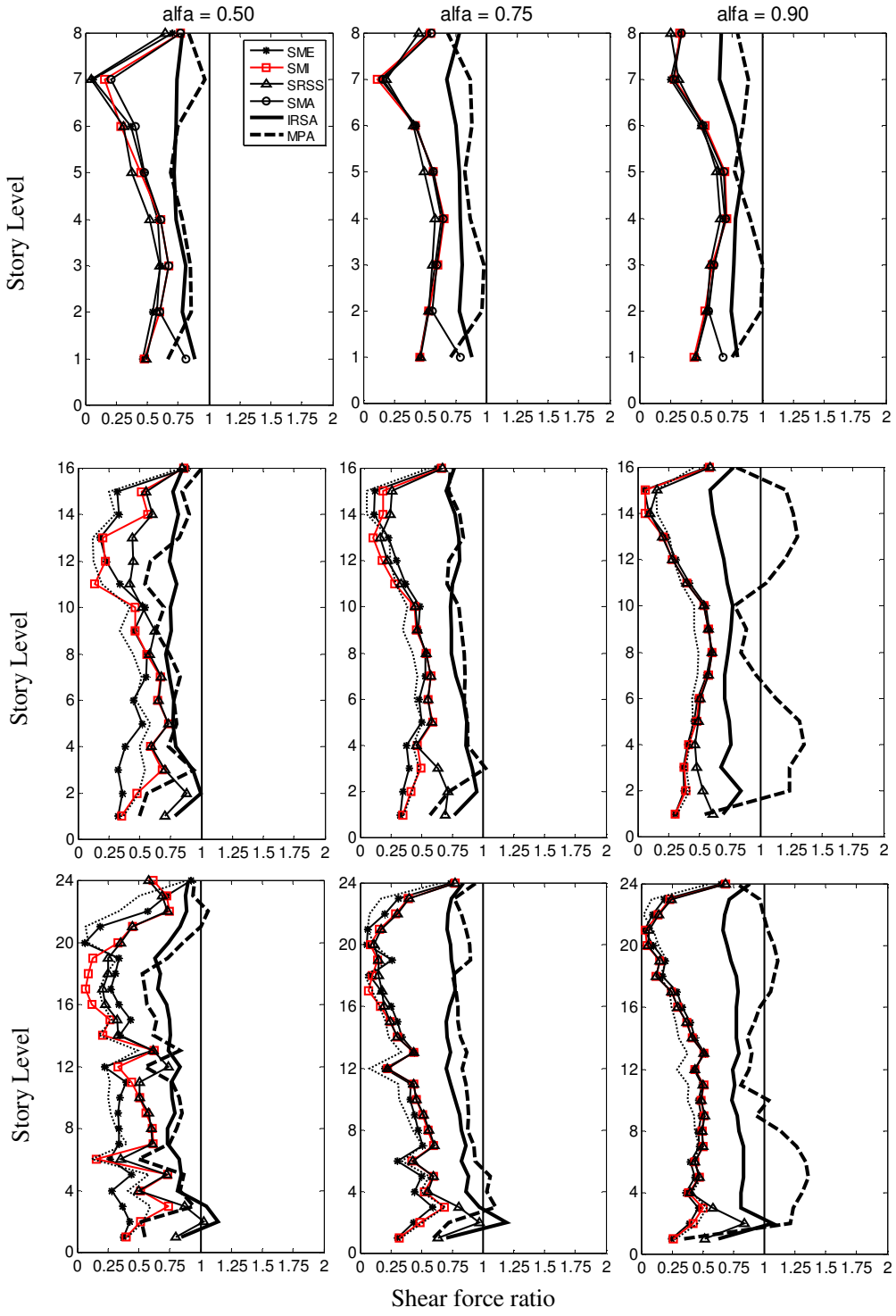

Figure 5.18. Ratio of the mean shear force profile between inelastic time history analyses with elasto-plastic hysteresis and nonlinear static procedures (IRSA, MPA and four FEMA load distributions) for 8, 16 and 24-story dual systems, each designed for α_s =0.50, 0.75 and 0.90, P-delta included

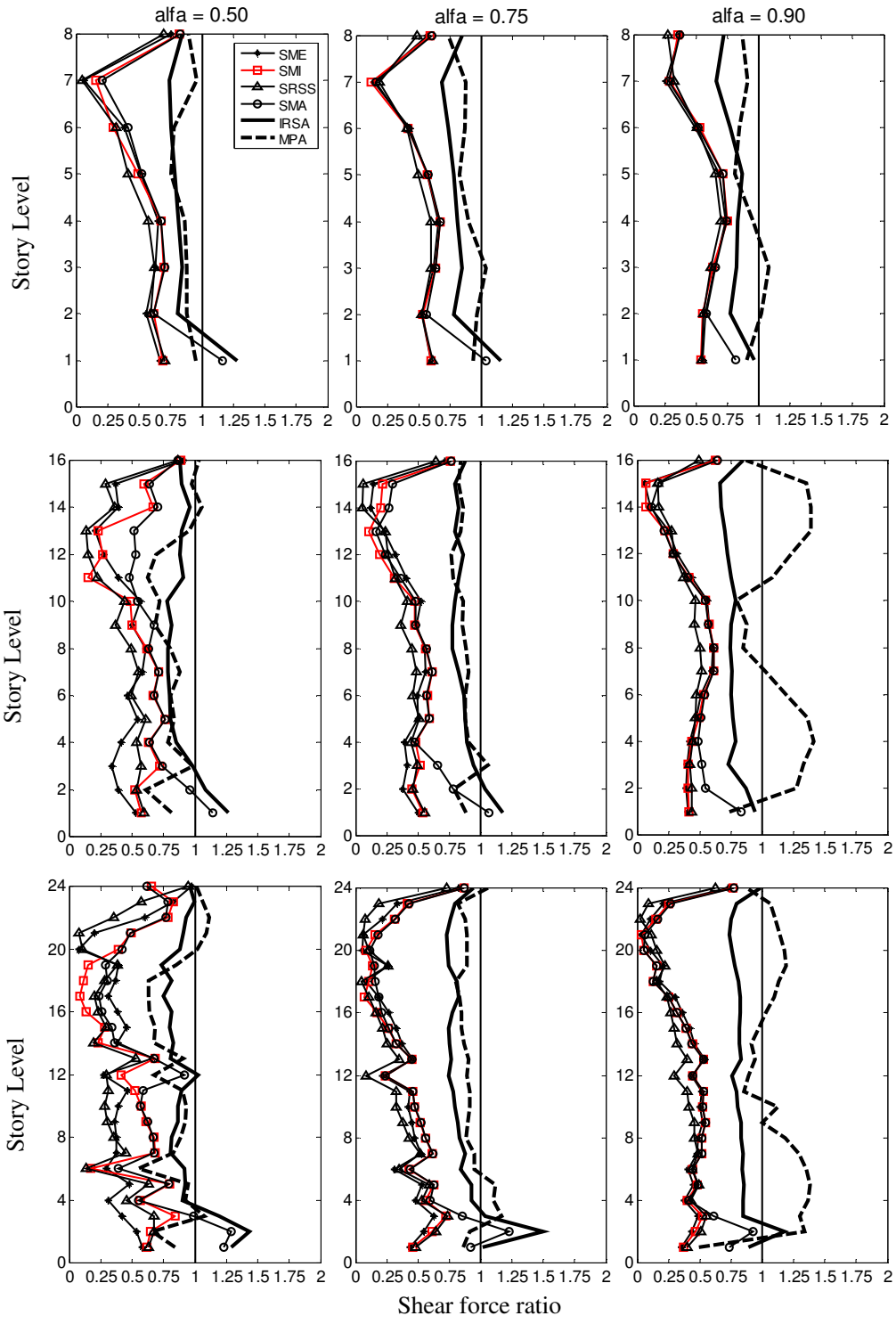

Figure 5.19. Ratio of the mean shear force profile between inelastic time history analyses with peak-oriented hysteresis and nonlinear static procedures (IRSA, MPA and four FEMA load distributions) for 8, 16 and 24-story dual systems, each designed for α_s =0.50, 0.75 and 0.90, P-delta included

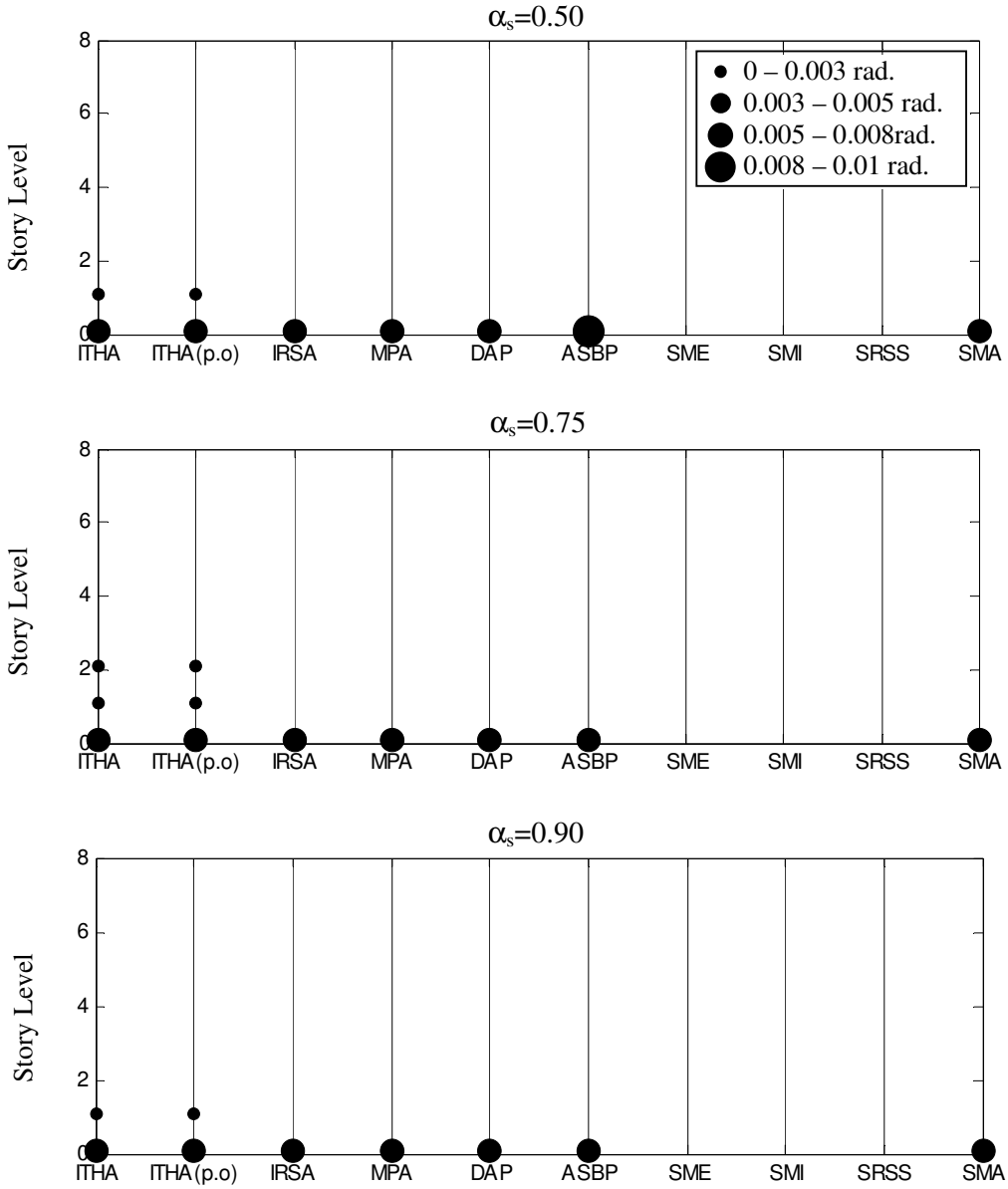

Figure 5.20. Location of plastic hinges and their magnitudes along the wall height estimated by inelastic time history analyses and nonlinear static procedures (IRSA, MPA, DAP, ASBP and four FEMA load distributions) for 8-story dual systems, each designed for α_s =0.50, 0.75 and 0.90, P-delta excluded

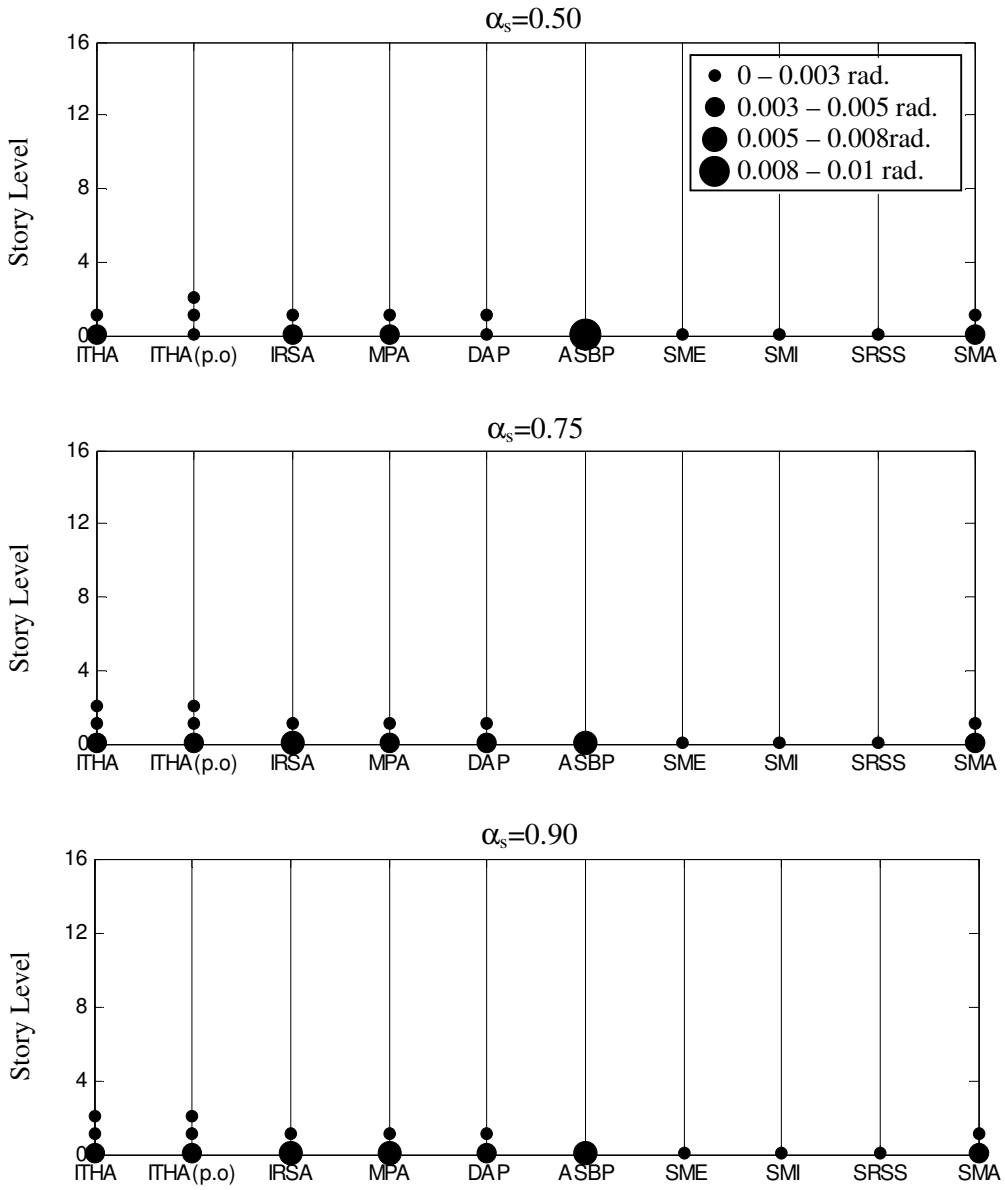

Figure 5.21. Location of plastic hinges and their magnitudes along the wall height estimated by inelastic time history analyses and nonlinear static procedures (IRSA, MPA, DAP, ASBP and four FEMA load distributions) for 16-story dual systems, each designed for α_s =0.50, 0.75 and 0.90, P-delta excluded

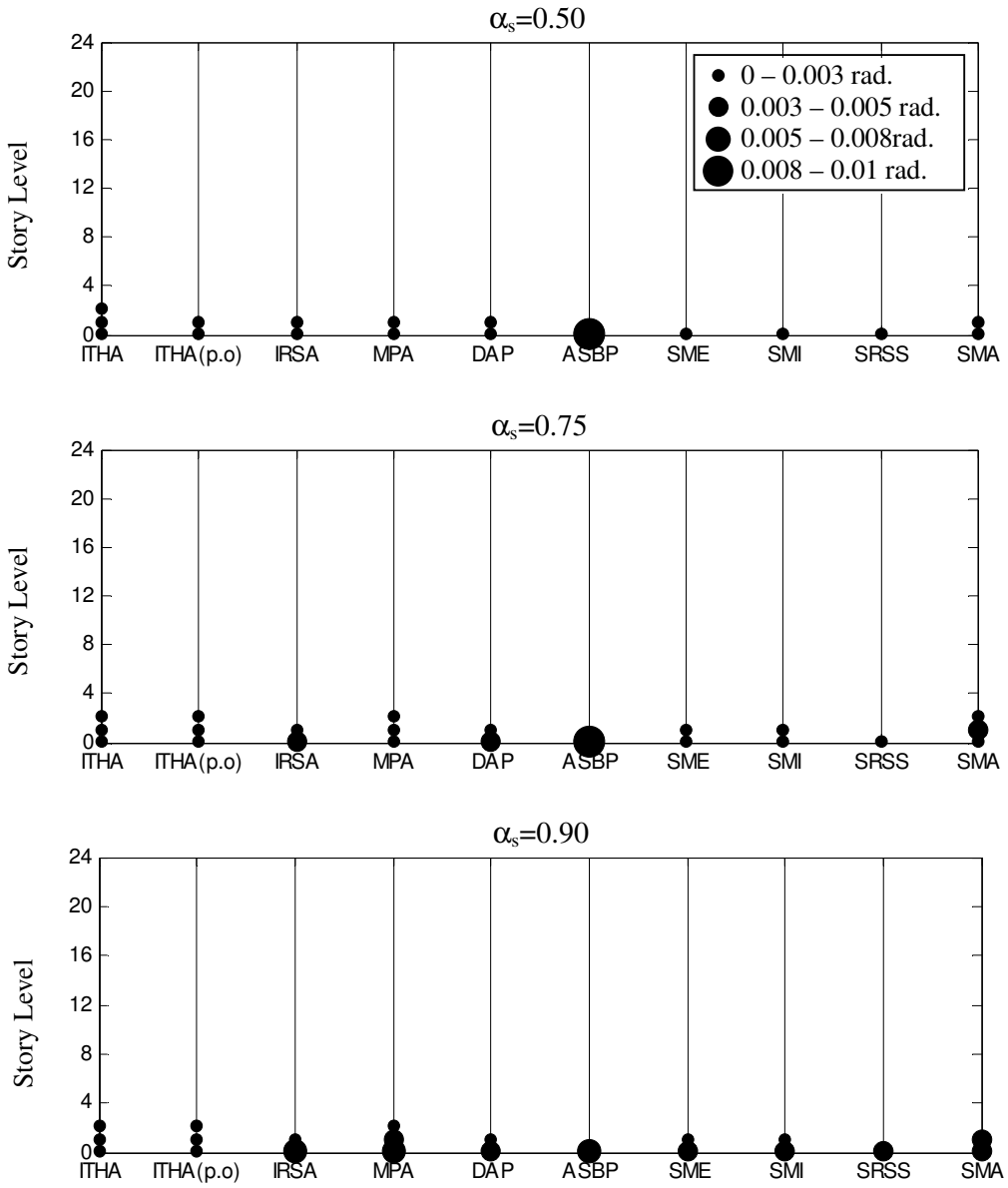

Figure 5.22. Location of plastic hinges and their magnitudes along the wall height estimated by inelastic time history analyses and nonlinear static procedures (IRSA, MPA, DAP, ASBP and four FEMA load distributions) for 24-story dual systems, each designed for α_s =0.50, 0.75 and 0.90, P-delta excluded

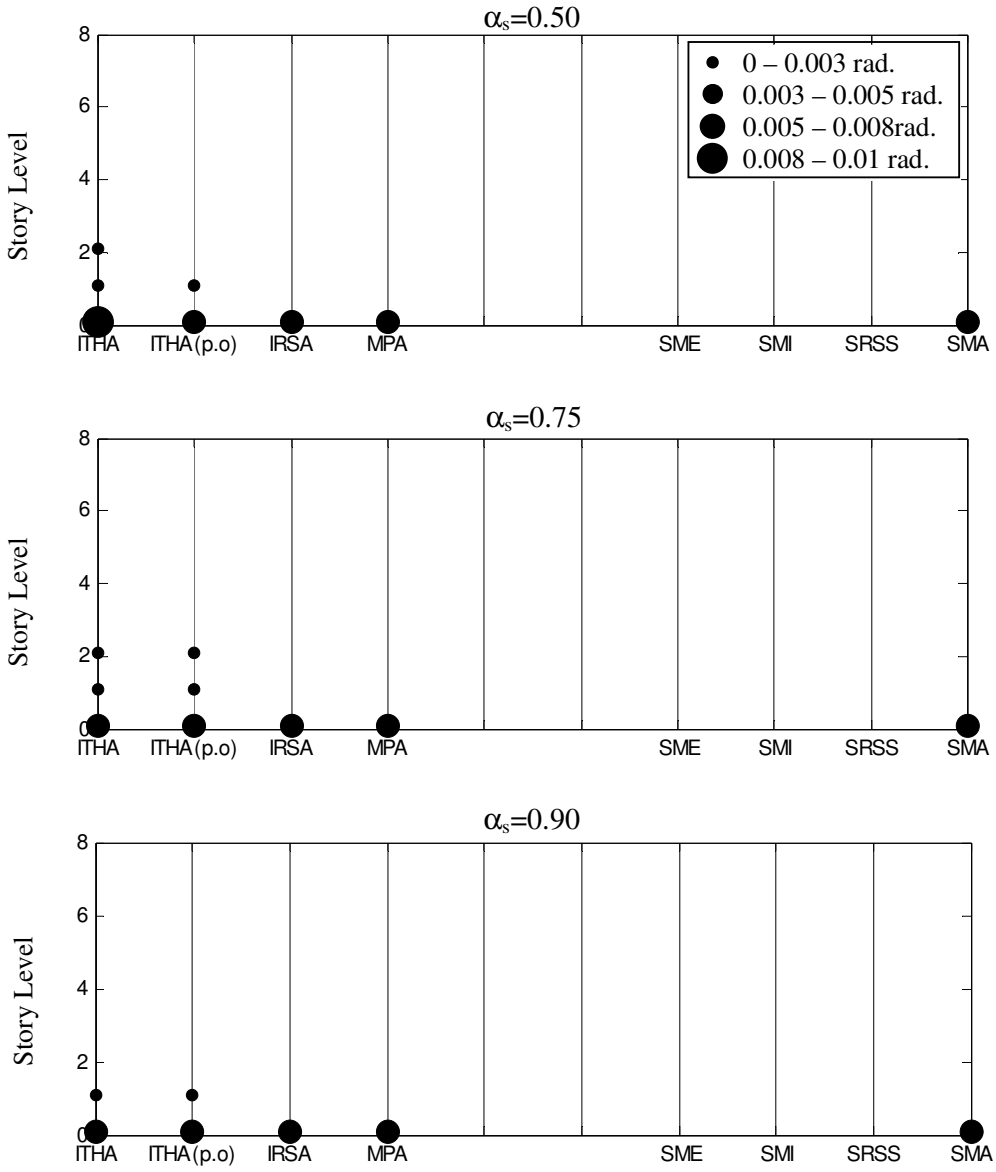

Figure 5.23. Location of plastic hinges and their magnitudes along the wall height estimated by inelastic time history analyses and nonlinear static procedures (IRSA, MPA and four FEMA load distributions) for 8-story dual systems, each designed for α_s =0.50, 0.75 and 0.90, P-delta included

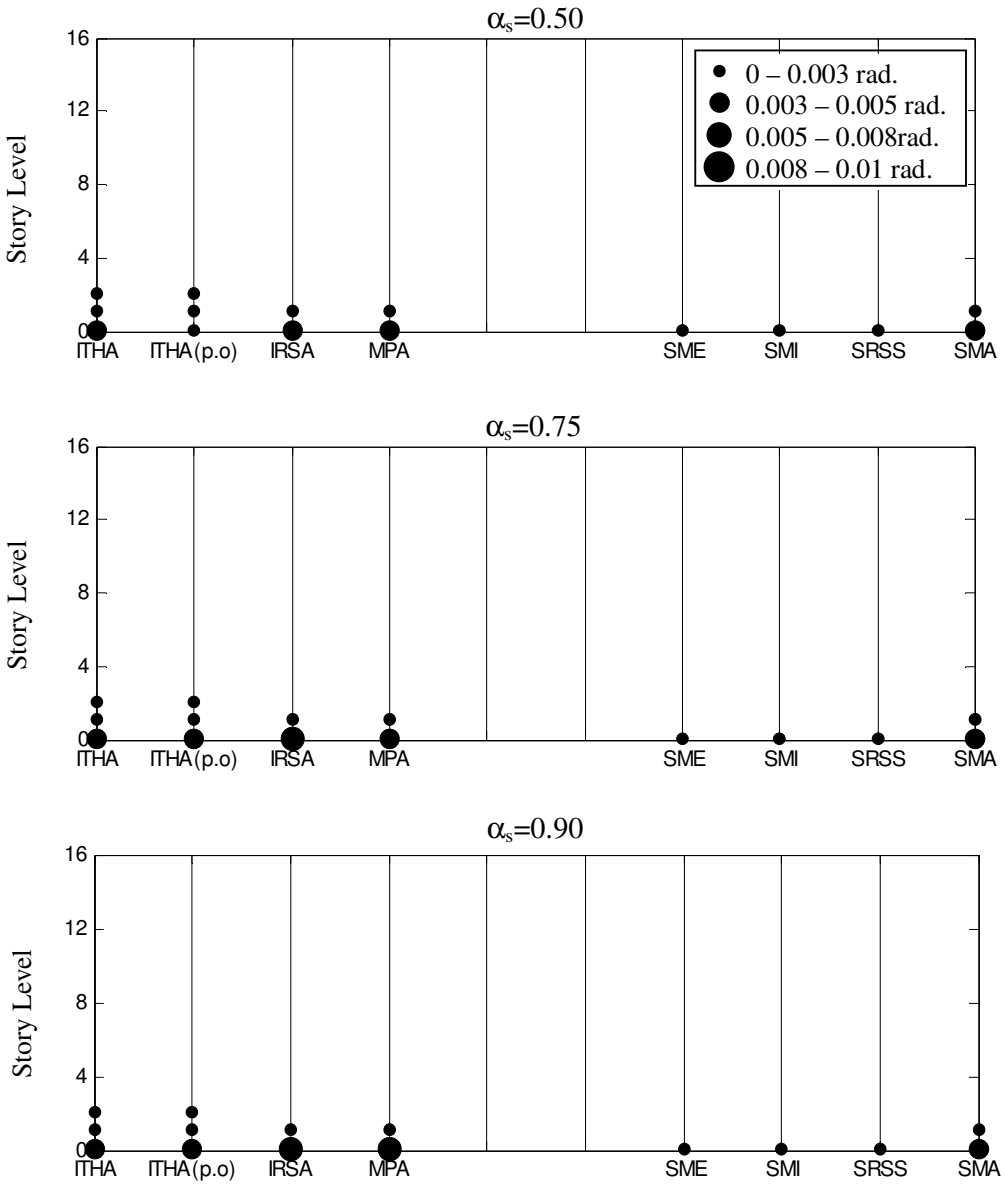

Figure 5.24. Location of plastic hinges and their magnitudes along the wall height estimated by inelastic time history analyses and nonlinear static procedures (IRSA, MPA and four FEMA load distributions) for 16-story dual systems, each designed for α_s =0.50, 0.75 and 0.90, P-delta included

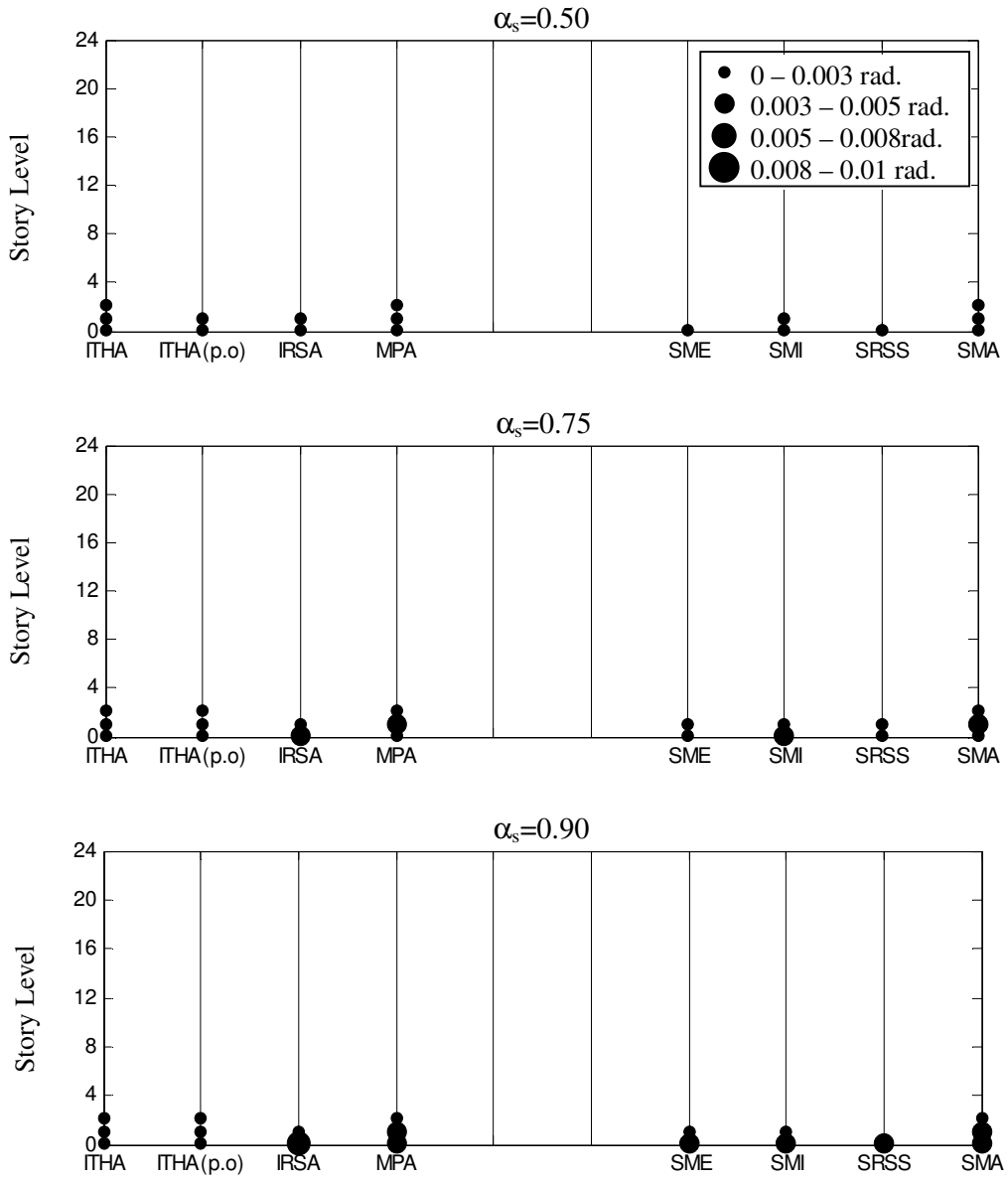

Figure 5.25. Location of plastic hinges and their magnitudes along the wall height estimated by inelastic time history analyses and nonlinear static procedures (IRSA, MPA and four FEMA load distributions) for 24-story dual systems, each designed for α_s =0.50, 0.75 and 0.90, P-delta included

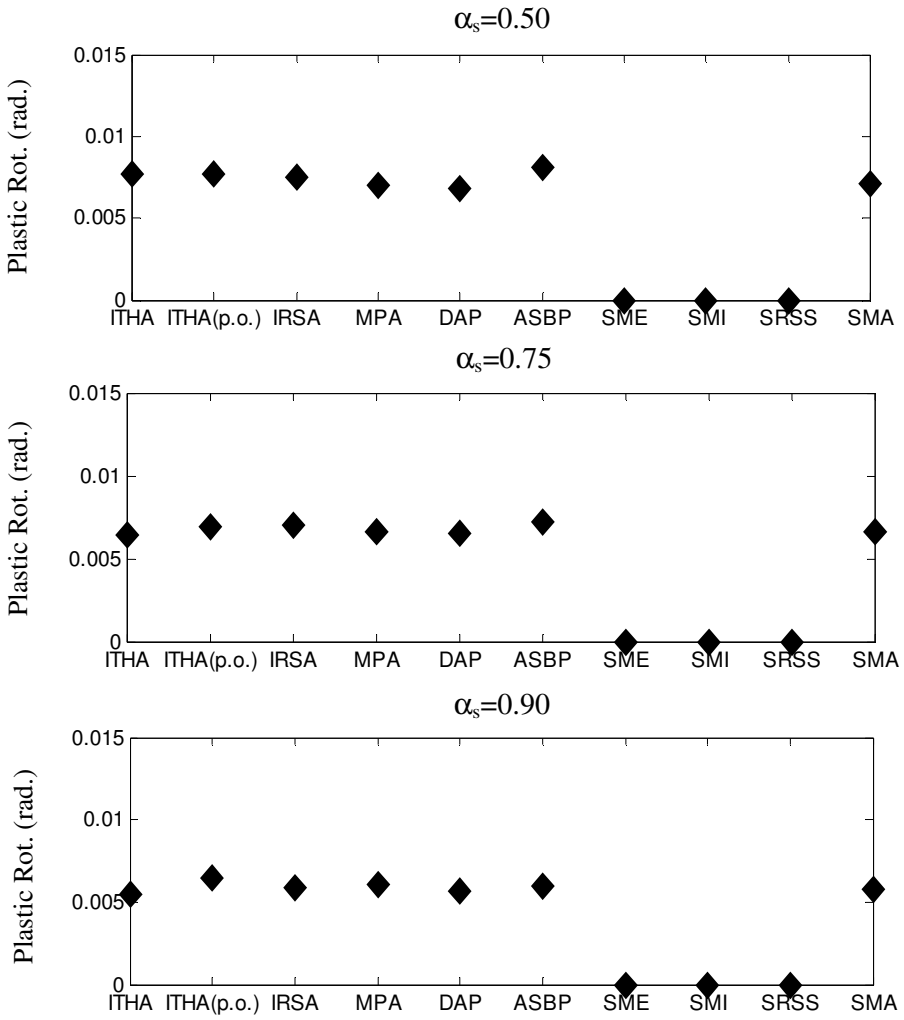

Figure 5.26. Total plastic hinge rotation at the base of the wall estimated by inelastic time history analyses and nonlinear static procedures (IRSA, MPA, DAP, ASBP and four FEMA load distributions) for 8-story dual systems, each designed for α_s =0.50, 0.75 and 0.90, P-delta excluded

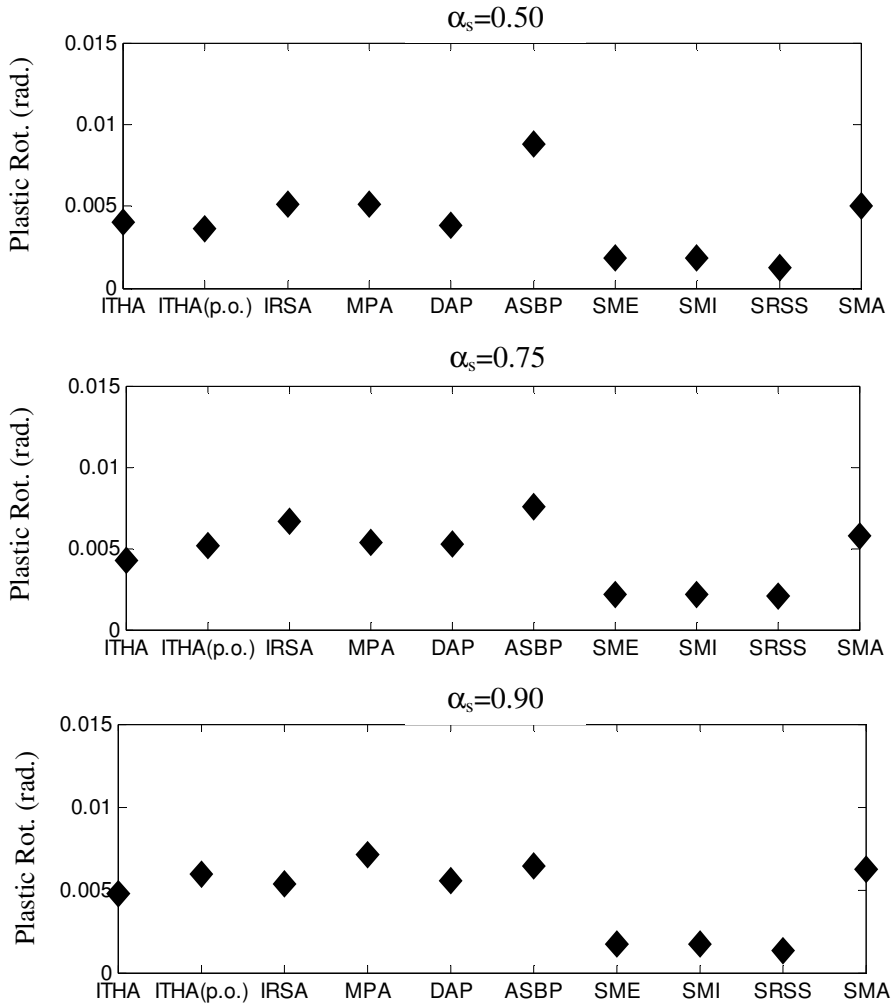

Figure 5.27. Total plastic hinge rotation at the base of the wall estimated by inelastic time history analyses and nonlinear static procedures (IRSA, MPA, DAP, ASBP and four FEMA load distributions) for 16-story dual systems, each designed for α_s =0.50, 0.75 and 0.90, P-delta excluded

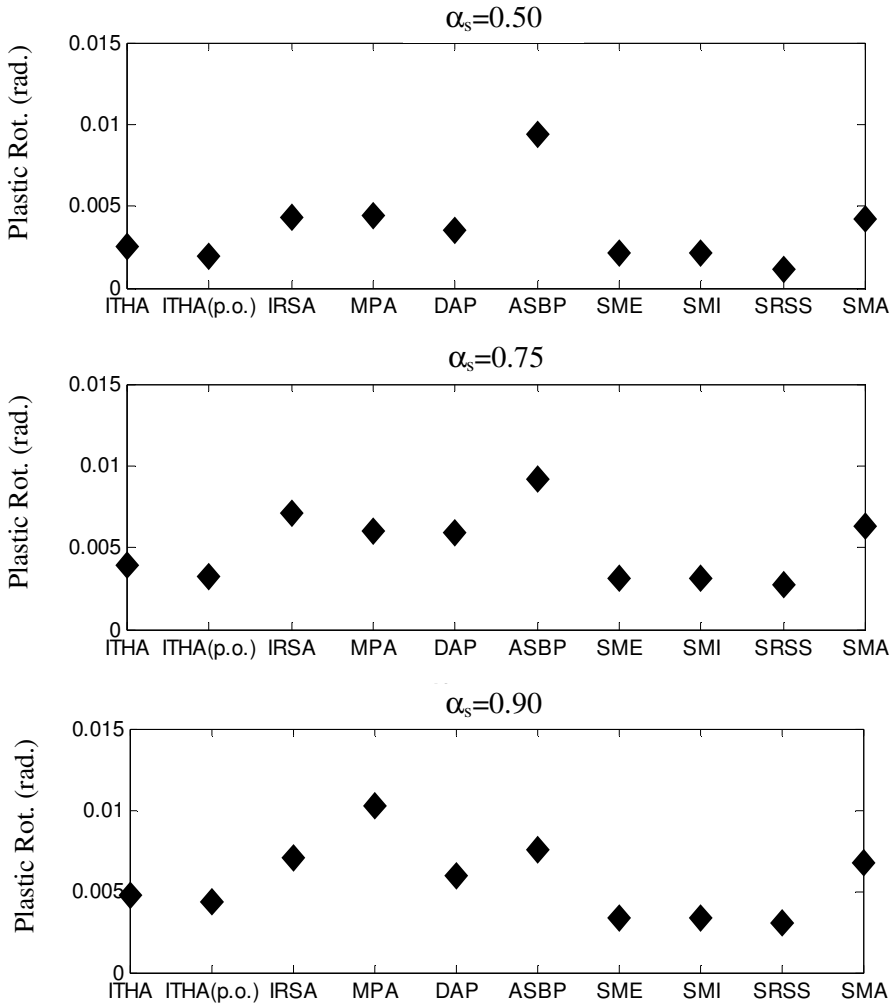

Figure 5.28. Total plastic hinge rotation at the base of the wall estimated by inelastic time history analyses and nonlinear static procedures (IRSA, MPA, DAP, ASBP and four FEMA load distributions) for 24-story dual systems, each designed for α_s =0.50, 0.75 and 0.90, P-delta excluded

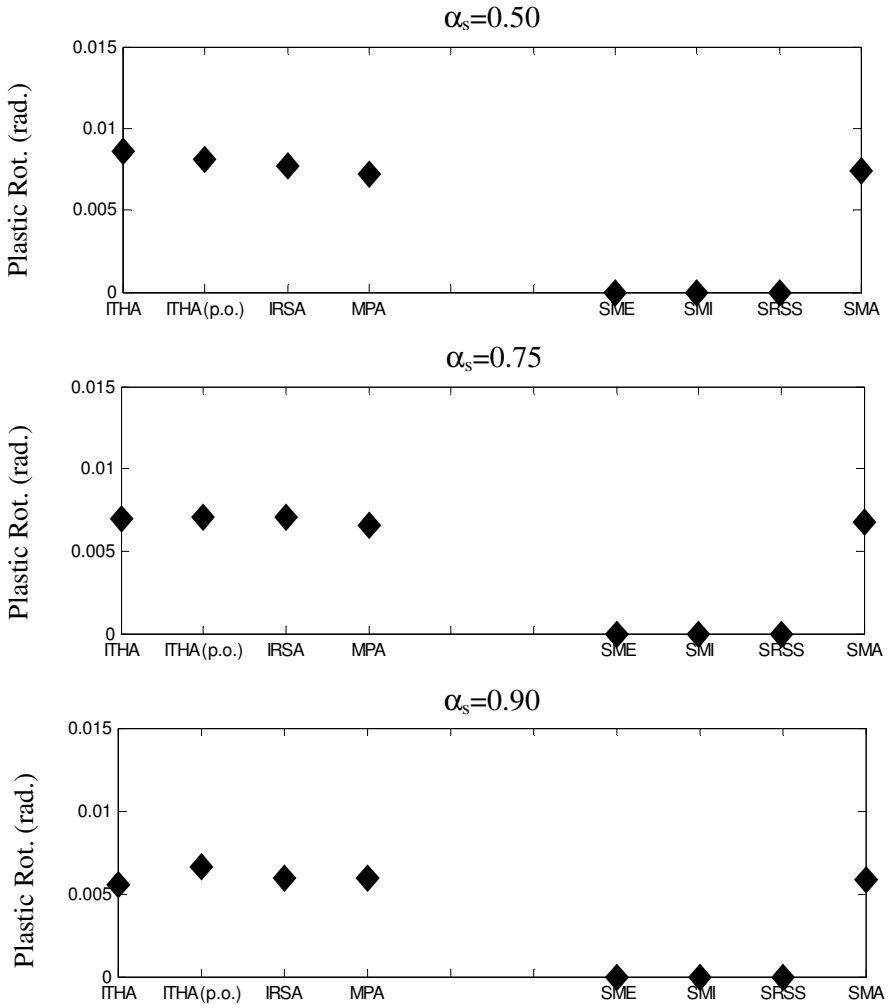

Figure 5.29. Total plastic hinge rotation at the base of the wall estimated by inelastic time history analyses and nonlinear static procedures (IRSA, MPA and four FEMA load distributions) for 8-story dual systems, each designed for α_s =0.50, 0.75 and 0.90, P-delta included

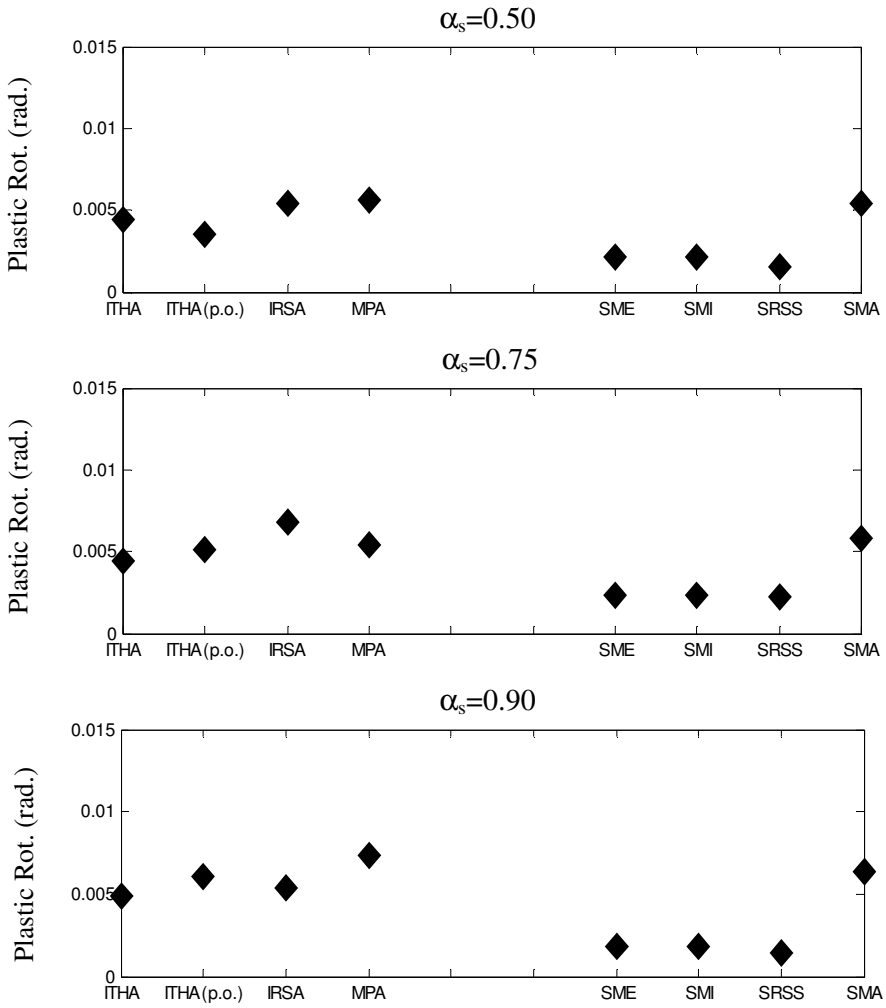

Figure 5.30. Total plastic hinge rotation at the base of the wall estimated by inelastic time history analyses and nonlinear static procedures (IRSA, MPA and four FEMA load distributions) for 16-story dual systems, each designed for α_s =0.50, 0.75 and 0.90, P-delta included

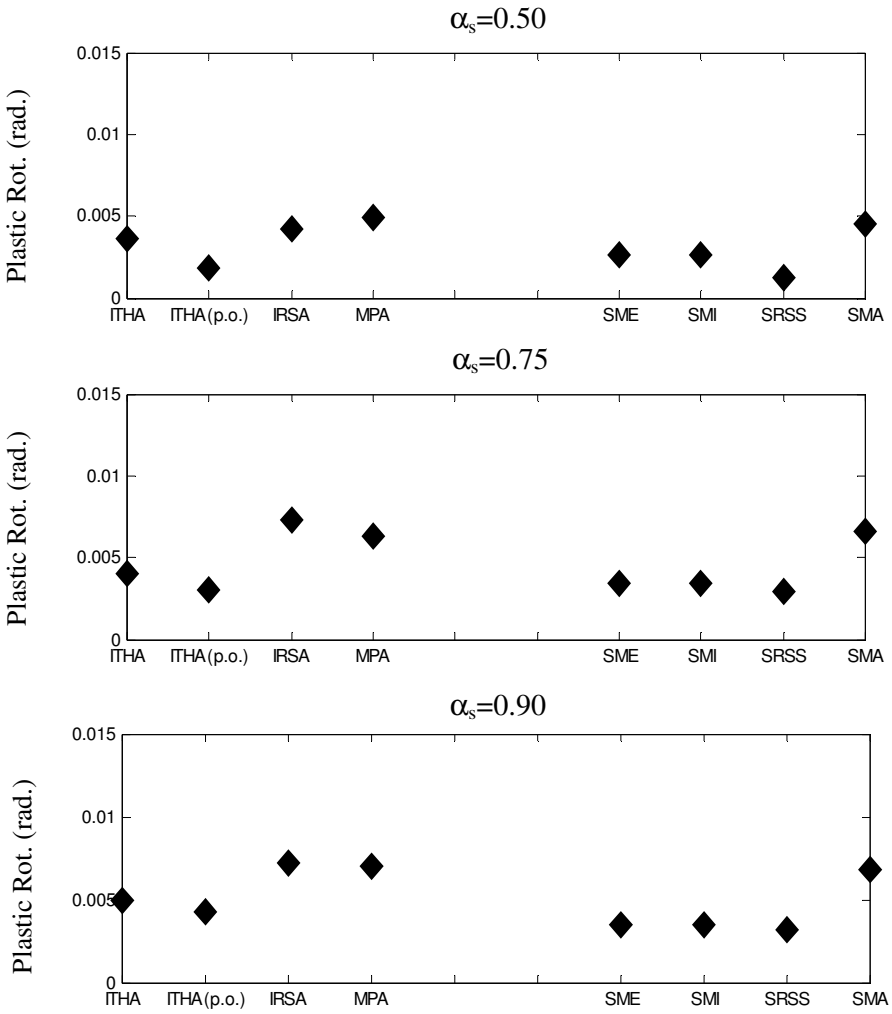

Figure 5.31. Total plastic hinge rotation at the base of the wall estimated by inelastic time history analyses and nonlinear static procedures (IRSA, MPA and four FEMA load distributions) for 24-story dual systems, each designed for α_s =0.50, 0.75 and 0.90, P-delta included

6. CONCLUSION

It has been widely recognized that definition of structural capacity and seismic demands in terms of displacement and deformation is the most effective way to control seismic design of inelastic structures. In this respect, deformation-based approach has gained a great prominence in engineering community with initial attempts, *Capacity Spectrum Method* (Freeman, 1978, 1998) and *N2 method* (Fajfar and Fischinger, 1988) to predict nonlinear seismic behavior of structures by using simplified procedures. This foregoing extensive research has formed the basis of performance based design guidelines. These guidelines present evaluation and design procedures starting from 1996 with ATC (1996) and FEMA 273 (1997) and are evolved later into a pre-standard as FEMA 356 (2000) in U.S. Finally, ASCE 41-06 has been published as a national standard for seismic rehabilitation of existing buildings. Performance based seismic engineering has been adopted also in Europe in Eurocode 8 (EN 1998-3, 2005) and in new version of Turkish Seismic Design Code (TSC, 2007).

Nonlinear static analysis formed the core analysis procedure for the above mentioned codes due to its simplicity in application and ease of evaluation of results with respect to the more complex time history analysis. However, in spite of its appealing advantages, it is widely recognized that the nonlinear static procedure recommended by FEMA 356 has still some shortcomings for high-rise structures and also for irregular low-rise structures where higher modes effects are significant. Thus, many researchers have proposed pushover analysis methods, which take into account higher mode responses, in order to increase effectiveness and the range of applicability of nonlinear static procedures.

FEMA-356 adopted a lateral load distribution proportional to story forces obtained from linear response spectrum analysis to take into account higher modes effects. The method is single-run pushover analysis with invariant single-load patterns based on combined multi-mode loading. Gupta and Kunnath (2000) have proposed simultaneous multi-mode pushover analysis with adaptive multi-modal load patterns. Relative modal contributions are scaled based on the instantaneous elastic spectral acceleration at each pushover step. Chopra and Goel (2001) in their studies have suggested a method

comprising an independent invariant modal pushover analysis-MPA, where modal response quantities are assumed to be uncoupled and combined at the last stage of pushover analysis. Incremental Response Spectrum Analysis method proposed by Aydınoğlu (2003) is basically simultaneous multi-mode pushover analysis, which perform a response spectrum analysis, considering current stiffness state at each piecewise linear pushover step. Modal scaling based on instantaneous inelastic spectral displacements (or initial elastic spectral displacements according to Equal Displacement Rule) has been adopted in order to determine relative modal contributions at each pushover step. Elnashai (2001) and Antoniou *et al*. (2002) proposed in their studies single-run pushover analysis with adaptive single-load patterns based on combined multi-mode loading. This method involves modal scaling based on instantaneous elastic spectral accelerations. Antoniou and Pinho (2004[b]) finally suggested single-run pushover analysis with adaptive single-displacement patterns based on combined multi-mode loading. This method involves modal scaling based on instantaneous elastic spectral displacements.

From theoretical perspective, all nonlinear static analysis procedures summarized above can be considered as approximate extensions of the response spectrum method to the nonlinear response analysis with varying degrees of sophistication (Aydınoğlu, 2007). All these procedures are compared on the implementation of modal scaling and demand estimation. Except Modal Pushover Analysis (Chopra and Goel, 2001), all the multi-mode pushover procedures mentioned above implement modal scaling to determine relative modal contributions in pushover analysis. Within the procedures, which implement modal scaling; Gupta and Kunnath (2000), Elnashai (2001) and Antoniou *et al*. (2002) implement modal scaling based on instantaneous elastic spectral accelerations. However, DAP (Antoniou *et al*., 2004[b]) implemented modal scaling procedure based on instantaneous elastic spectral displacement. For both instantaneous elastic spectral displacement and accelerations, P-delta effects can not be taken into account since instantaneous elastic spectral quantities are used to estimate relative modal contributions. The main differentiation comes with Aydınoğlu (2003) research where the modal scaling is based on inelastic spectral displacements (or initial elastic spectral displacements according to Equal Displacement Rule).

These methods have been evaluated on their capability in terms of estimating the seismic demand. A method developed by Elnashai (2001), DAP and FAP by Antoniou *et al.* (2004) and Gupta and Kunnath's method have limitations since they are unable to estimate seismic demands using elastic response spectrum. It should be noted that these methods can estimate seismic demands if they assume that displacement shape at each pushover step is treated as a *single-combined* mode shape, which is proposed by Casarotti and Pinho (2007). In fact it is a controversial assumption because deflected shape of a MDOF system obtained from a multi-mode pushover analysis contains higher mode effects Casarotti and Pinho are the only appliers of this proposition.

As opposed to the methods above, MPA (Chopra and Goel, 2001) and IRSA (Aydınoğlu, 2003) are the only methods that can be considered not only as demand estimation tools but also capacity estimation tools.

The motivation for discussion on pushover analysis in a theoretical framework is based on the variety of the assumptions that lie behind the methods mentioned above. All these methods try to enhance nonlinear static procedure however; an analysis and comparison of these methods in terms of their assumptions and results for practical engineering should be provided as this study aims.

Therefore, seismic demand quantities estimated by these methods should be comparatively examined. Thus, a parametric study has been carried out in order to compare the relative performance of each method with respect to inelastic time history analysis performed by using elasto-plastic and peak-oriented plastic hinge hysteresis characteristics. Frame systems and dual systems have been considered in the parametric study, which are predominantly used in the design of the reinforced concrete structures and observed in the existing building stock.

A regular moment resisting frame model with five different heights (4, 8, 12, 16 and 20 stories) has been selected for the evaluation of frame systems. In order to obtain realistic structural systems in terms of the stiffness and strength distribution, each frame system has been designed in accordance with Turkish Seismic Design Code (TSC, 2007) provisions and capacity design principles. Three ductility levels (low, medium and high)

have been adopted in the design of frames, for which strength reduction factors (R) are specified as 2, 4 and 6, respectively. Evaluation of single mode and multi mode pushover procedures for the frame systems has lead to the following conclusions:

- Story displacements obtained from ITHA and all nonlinear static analyses match fairly well in low to mid-height buildings and begin to divert as the number of stories and the ductility levels increase due to the approximation of demand estimation based on equal displacement rule. Non-adaptive single-mode or multi-mode pushover procedures (SMI and MPA) give more conservative story displacement results as compared to the adaptive single-mode or multi-mode pushover methods for all buildings.
- Consideration of only first mode is sufficient in estimating story displacements response regardless of the nonlinear static analysis procedure type and number of higher modes taken into account. This finding also supports the conclusion by Chintanapakdee and Chopra (2003), "A similar investigation comparing floor displacements... the first "mode" alone is, however, sufficient in estimating these response quantities".
- Height-wise distribution of inter-story drift ratio and plastic rotation at the central beams for low to mid-rise buildings obtained from almost all nonlinear static analyses procedures are similar to the time history analyses results. The inter-story drift ratios and plastic rotations begin to divert as the number of stories as well as the ductility levels increase at lower and middle story levels.
- ASBP tends to overestimate plastic rotation and inter-story drift demands excessively in lower and upper stories of taller frames for all ductility level due to the adoption of modal scaling procedure based on instantaneous elastic spectral accelerations.
- Multi-mode pushover analysis procedures (IRSA, DAP and SRSS), which combine multi-mode effects at each pushover step provide more consistent and accurate inter-story drift and plastic rotation estimates in the lower and middle story levels with respect to MPA.
- Multi-mode pushover analysis with single-load or single-displacement patterns based on combined multi-mode loading as implemented in DAP or SRSS can not estimate inter-story drift and plastic rotation demands accurately at the upper floors of taller buildings.

- At the upper story levels, where higher mode responses are effective, IRSA and MPA present much more accurate inter-story drift and plastic rotation estimations for R=4 and 6 as compared to the other nonlinear static procedures.
- Almost all nonlinear static procedures overestimate inter-story drift demands in the lower stories for buildings R=2 when P-delta effects are taken into account, especially for taller buildings. Analyses with P-delta effects reveal that, IRSA, MPA and SRSS are conservative at the lower and middle story level for taller buildings for R=4 and 6. MPA overestimates inter-story drift demands excessively at these story levels with respect to IRSA.
- When P-delta effects are included, ASBP and DAP cannot be performed because of the modal scaling procedures based on instantaneous elastic spectral quantities. Therefore, nonlinear static analyses including P-delta effects have been carried out only for MPA, IRSA and pushover analyses using FEMA 356 load distributions.
- P-delta effects uniformly magnifies - relative to the estimates without P-delta effect - the error rate in inter-story drift ratio and plastic rotation distributions obtained from IRSA and MPA throughout the structure. It has also been observed that frame structures considered in this study are sensitive to plastic hinge characteristics when P-delta effects are included. Both MPA and IRSA tend to deviate from inter-story drifts and plastic rotations obtained from time history analysis with peak-oriented hysteresis model. On the contrary, the effect of hysteretic plastic hinge characteristics diminishes for analyses without P-delta consideration.
- In terms of overall consistency with ITHA for elasto-plastic hysteresis or peak-oriented hysteresis model, IRSA gives more accurate and consistent inter-story drift and plastic rotation distributions throughout the structure for all buildings and ductility levels compared to other nonlinear static methods.

Dual systems with three different heights (8, 16 and 24 stories) have been selected for the evaluation of dual systems. Similar to the design objectives in the frame systems, each dual system has been designed in accordance with Turkish Seismic Design Code (TSC, 2007) provisions and capacity design principles. Three different shear wall ratios (α_s=0.5, 0.75 and 0.9) have been adopted in the design of dual systems for a fixed strength reduction factor of R=4. Evaluation of single-mode and multi-mode pushover procedures for dual systems has lead to the following conclusions:

- All multi-mode and single-mode nonlinear static analysis methods give reliable results in 8-story dual systems, where single-mode behavior is dominant in the structural response. However, discrepancy tends to increase between ITHA and nonlinear static procedures as the number of story level increases.
- For all dual systems, all multi-mode pushover procedures together with single-mode pushover methods give almost identical story displacement results. This emphasizes that considering only first mode is sufficient to estimate story displacements response as observed for the frame systems.
- P-delta effects have little influence on the seismic demands estimated by ITHA and nonlinear static procedure as compared to the analyses excluding P-delta effects due to the stiffness contribution of shear wall.
- Multi-mode pushover procedures, IRSA, DAP and SRSS, which combine multi-mode effects at each pushover step, provide better estimate of inter-story drift and plastic rotation demands in the middle and upper stories of dual systems with smaller shear wall ratio as compared to individual multi-mode pushover analysis method (MPA).
- ASBP overestimates the inter-story drift demands in the lower and upper story levels particularly for 16- and 24-story buildings due to the modal scaling procedure based on instantaneous elastic spectral accelerations.
- IRSA manages to capture variation in plastic rotation demands at the beams in 16- and 24-story buildings with a superior accuracy with respect to the other pushover analysis methods. In addition, IRSA is able to predict the location of the largest plastic rotation throughout the building.
- MPA, IRSA and ASBP capture the variation in the shear force demand reasonably well at the walls in all buildings as compared to the other nonlinear static procedures. Shear force demands predicted by DAP and SRSS are less than those obtained from the ITHA for all buildings. Therefore, multi-mode pushover procedures with invariant or adaptive single-load or -displacement patterns based on combined multi-mode loading, such as DAP and SRSS, cannot estimate accurately the variation and the amplitude of shear force demands throughout the wall.
- ASBP, MPA, IRSA and DAP are usefully conservative in estimating plastic hinge deformation at the base of the walls for 24-story dual systems. However, they give excellent result for 8- and 16-story dual systems.

- Single-mode adaptive pushover analysis can predict plastic hinge locations and plastic rotation values although singlemode is taken into account. However, invariant single-mode pushover analysis cannot estimate yielding at the base of the wall. This shows that adaptive pushover analysis technique is more reliable analysis technique than invariant pushover analysis for dual systems.

Analysis of frame and dual systems reveals the common conclusions below:

- Seismic response is specific to the strength distribution throughout the structure. It has been observed that effect of higher mode effects become less pronounced at higher story levels with increasing ductility level or strength reduction factor. Structures considered in this study have been designed as per the requirements of the Turkish Seismic Design Code (2007), including the minimum reinforcement conditions. However, it is believed that a different finding may have been obtained with a structure with a different strength distribution that allows simultaneous plastic hinge formation.
- It is observed that differences between inelastic time history analyses and non-linear static analyses in both frame and dual systems are related to the equal displacement rule, which has been utilized in estimating seismic demands for the nonlinear static procedures despite the fact that 20 ground motion records are selected rigorously.

It should be noted that two dimensional structural models with no vertical irregularities have been considered in this study, which limits the results with buildings regular in plan an elevation. Further studies comprising the effect of torsion coupled with higher mode effects is believed to give more insight to three dimensional nonlinear structural behavior.

REFERENCES

Antoniou, S., A. Rovithakis and R. Pinho, 2002, "Development and verification of a Fully Adaptive Pushover Procedure", *Proceedings of 12th European Conference on Earthquake Engineering*, London, U.K., Paper No.822.

Antoniou, S. and R. Pinho, (2004[a]), "Advantages and Limitations of Adaptive and Non-Adaptive Force-Based Pushover Procedures", *Journal of Earthquake Engineering*, 8(4), pp. 497-552.

Antoniou, S. and R. Pinho, (2004[b]), "Development and Verification of a Displacement-Based Adaptive Pushover Procedure", *Journal of Earthquake Engineering*, 8(5), pp. 643-661.

ASCE/SEI 41-06, 2007, Seismic Rehabilitation of Existing Buildings, American Society of Civil Engineers, Virginia.

ATC 40, 1996, "Seismic Evaluation and Retrofit of Concrete Buildings", Applied Technology Council, Redwood City, California.

Aydınoğlu, M.N., 2003, "An Incremental Response Spectrum Analysis Procedure Based on Inelastic Spectral Displacements for Multi-Mode Performance Evaluation", *Bulletin of Earthquake Engineering*, Vol. 1, pp. 3-36.

Aydınoğlu, M.N., 2004, "An improved pushover procedure for engineering practice: Incremental Response Spectrum Analysis (IRSA)". *International Workshop on Performance-based Seismic Design: Concepts and Implementation*, Bled, Slovenia, PEER Report 2004/05, pp. 345-356.

Aydınoğlu, M.N., 2004, "Incremental Response Spectrum Analysis (IRSA) Procedure For Multi-Mode Pushover Including P-Delta", *Proceedings of 13th World Conference on Earthquake Engineering*, Vancouver, B.C., Canada, 1-6 August, Paper No. 1440.

Aydınoğlu, M.N., 2005, "A code Approach for Deformation-Based Seismic Performance Assessment of Reinforced Concrete Buildings", *International Workshop on Seismic Performance Assessment and Rehabilitation of Existing Building*, Joint Research Centre (JRC), ELSA Laboratory, Ispra, Italy.

Aydınoğlu, M.N., 2007, "A Response Spectrum-Based Nonlinear Assessment Tool for Practice: Incremental Response Spectrum Analysis (IRSA)", *Special Issue: Response Spectra (Guest Editor: M.D. Trifunac), ISET Journal of Earthquake Technology*, 44(1), No.481, March.

Aydınoğlu, M.N. and Ü. Kaçmaz, 2002, *Strength-Based Displacement Amplification Spectra For Inelastic Seismic Performance Evaluation*, Department Report 2002/2, Kandilli Observatory and Earthquake Research Institute, Boğaziçi University, İstanbul.

Bracci, J.M., S.K. Kunnath and A.M. Reinhorn, 1997, "Seismic Performance and Retrofit Evaluation of Reinforced Concrete", *Journal of Structural Engineering*, 123 (1), pp. 3-10, January.

Casarotti, C. and R. Pinho, 2007, "An Adaptive Capacity Spectrum Method for Assessment of Bridges Subjected to Earthquake Action", *Bulletin of Earthquake Engineering*, 5(2), pp. 134–148.

Carr, A.J., 2000, "RUAUMOKO, Program for Inelastic Dynamic Analysis", Department of Civil Engineering, University of Canterbury, Christchurch, New Zealand.

Chintanapakdee, C. and A. K. Chopra, 2003, *Evaluation of the Modal Pushover Analysis Procedure Using Vertically ''Regular'' and Irregular Generic Frames*, Report No. EERC-2003/03, Earthquake Engineering Research Center, University of California, Berkeley, CA.

Chopra, A.K. and R.K. Goel, 1999, "Capacity-Demand-Diagram Methods Based on Inelastic Design Spectrum", *Earthquake Spectra* 15(4), pp. 637-656.

Chopra, A.K. and R.K. Goel, 2001, *A Modal Pushover Analysis Procedure to Estimate Seismic Demands for Buildings*, PEER Report 2001/03, Pacific Earthquake Engineering Center, University of California Berkeley.

Chopra, A.K., 2007, *Dynamics of Structures*, Prentice Hall, Upper Saddle River, NJ, USA.

CEN, 2004, Eurocode EC8, "Eurocode (EC) 8 Design of Structures for Earthquake Resistance-Part I General Rules, Seismic Actions and Rules For Buildings (EN 1998-1)", Comité Européen de Normalisation, Brussels.

CEN, 2005, Eurocode EC8, "Eurocode 8: Design of structures for earthquake resistance - Part 3: Assessment and retrofitting of buildings (EN 1998-3)", Comité Européen de Normalisation, Brussels.

Elnashai, A.S., 2000, "Advanced Inelastic Static (Pushover) Analysis for Seismic Design and Assessment", *G.Penelis International Symposium on Concrete and Masonry Structures*, Thessaloniki, 2000.

Fajfar, P. and M. Fischinger, 1988, "N-2 – A method for Nonlinear Seismic Analysis of Regular Structures", *Proceedings of 9th World Conference on Earthquake Engineering*, Tokyo, Kyoto, Japan, 2-9 August.

Fajfar, P., 2000, "A Nonlinear Analysis Method for Performance Based Seismic Design", *Earthquake Spectra*, 16(3), August, pp. 573-592.

Federal Emergency Management Agency (FEMA), 1997, "NEHRP guidelines for the seismic rehabilitation of buildings (FEMA 273)", Washington D.C.

Federal Emergency Management Agency (FEMA), 2000, "Prestandard and commentary for the seismic rehabilitation of buildings (FEMA-356)", Washington D.C.

Federal Emergency Management Agency (FEMA), 2005, "Improvement of nonlinear static seismic analysis procedures (FEMA 440)", Washington D.C.

Freeman, S.A., 1978, "Prediction of Response of Concrete Buildings to Severe Earthquake Motion", *ACI Structural Journal*, Vol. 55, pp. 589-606.

Freeman, S.A., 1998, "Development and Use of Capacity Spectrum Method", *6th U.S. National Conference on Earthquake Engineering,* Washington.

Goel, R.K. and A.K. Chopra, 2004, "Evaluation of Modal and FEMA Pushover Analyses: SAC Buildings", *Earthquake Spectra*, 20(1): pp. 225-254.

Gupta, A. and H. Krawinkler, 1998, "Effect of Stiffness Degradation on Deformation Demands for SDOF and MDOF Structures", *6th U.S. National Conference on Earthquake Engineering,* Washington.

Gupta, B. and S.K. Kunnath, 2000, "Adaptive Spectra-Based Pushover Procedure for Seismic Evaluation of Structures", *Earthquake Spectra*,16(2), pp. 367-391.

Krawinkler, H. and G.D.P.K. Seneviratna, 1998, "Pros and cons of a pushover analysis of seismic performance evaluation". *Engineering Structures*, 20(4–6), pp. 452–464.

Lawson, R.S., V. Vance and H. Krawinkler, 1994, "Nonlinear Static Pushover Analysis, Why, When and How ?", *Proceedings of 5th US National Conference on Earthquake Engineering*, Chicago, Vol. 1, pp. 283-92.

Medina, R. and H. Krawinkler, 2003, *Seismic Demands for Nondeteriorating Frame Structures and Their Dependence on Ground Motions*, John A. Blume Earthquake Engineering Center Report No. TR 144, Department of Civil Engineering, Stanford University, PEER Report 2003/15.

Miranda, E., 2000, "Inelastic Displacement Ratios for Structures on Firm Sites", *Journal of Structural Engineering*, October, 126 (10), pp.1150-1159.

Miranda, E., 2000, "Estimation of Inelastic Deformation Demands of SDOF Systems", *Journal of Structural Engineering*, September, 126 (10), pp.1150-1159.

Nassar, A.A. and H. Krawinkler, 1991, *Seismic Demands for SDOF and MDOF Systems*, John A. Blume Earthquake Engineering Research Center, Report No.95. Stanford University, CA, 1991.

Paret, T.F., K.K. Sasaki, D.H. Eilbeck and S.A. Freeman, 1996, "Approximate Inelastic Procedures to Identify Failure Mechanisms from Higher Mode Effects", *Proceedings of 11th World Conference on Earthquake Engineering*, Acapulco, Mexico, Paper No. 966.

Priestley, M.J.N., 1997, "Myths and Fallacies in Earthquake Engineering- conflict between design and reality", *Concrete International*, pp. 54-63, February.

Priestley, M.J.N., 2000, "Performance Based Seismic Design", *Proceedings of 12th World Conference on Earthquake Engineering*, New Zealand, Paper No. 2831.

Ruiz-Garcia, J. and E. Miranda, 2003, ''Inelastic displacement ratios for evaluation of existing structures", *Earthquake Engineering Structural Dynamics*, 32, pp. 1237–1258.

Sasaki, K.K., S.A. Freeman and T.F. Paret, 1998, "Multimode Pushover Procedure (MMP) – A Method to Identify the Effects of Higher Modes in A Pushover Analysis", *Proceedings of 6th U.S. National Conference on Earthquake Engineering, Seattle*, Washington.

Seneviratna, G. D. P. K., 1995, *Evaluation of Inelastic MDOF Effects for Seismic Design*, Ph.D. dissertation, Department of Civil Engineering, Stanford University.

Structural Engineering Association of California, 1995, *Performance Based Seismic Engineering of Buildings*, SEAOC Vision 2000 Committee, Sacremento.

The MathWorks Inc., 2004, MATLAB, *The Language of Technical Computing*, USA.

Turkish Seismic Design Code, 2007, “Specification for Buildings to be Built in Seismic Areas”, in Turkish, Ministry of Public Works and Settlement, Ankara, Turkey.

Celep, U.U., 2008, *Dynamic Shear Amplification in Seismic Response of Structural Wall Systems*, Ph.D. dissertation, Department of Earthquake Engineering, Boğaziçi University.

Vidic, T., P. Fajfar and M. Fischinger, 1994, “Consistent Inelastic Design Spectra: Strength and Displacement”. *Earthquake Engineering and Structural Dynamics* ,23, pp. 507-521.

REFERENCES NOT CITED

Clough, R.W. and J. Penzien, 1993, *Dynamics of Structures*, 2nd International Edition, McGraw Hill Inc., Singapore.

Elnashai, A.S. (2002), "Do we really need inelastic dynamic analysis?", *Journal of Earthquake Engineering* Vol. 6, pp. 123-130.

Goel, R.K. and A.K. Chopra, 2005, "Extension of Modal Pushover Analysis to Compute Member Forces", *Earthquake Spectra*, 21(1), pp. 125-139.

Kalkan, E. and S.K. Kunnath, 2004, "Adaptive Modal Combination Procedure for Nonlinear Static Analysis of Building Structures", *Journal of Structural Engineering*, Vol. 132, No. 11, November 1.

Kalkan, E. and S. K. Kunnath, 2006, "Assessment of Current Nonlinear Static Procedures for Seismic Evaluation of Buildings" Engineering Structures 29, pp. 305–316.

Krawinkler, H., 2006, "Importance of Good Nonlinear Analysis", *The Structural Design of Tall and Special Buildings*, Vol. 15, pp. 515-531.

Moehle, J.P., 1992, "Displacement-Based Design Of RC Structures Subjected To Earthquakes", *Earthquake Spectra* Vol. 8(3), pp.403-428.

Mwafy, A.M. and A.S. Elnashai, 2000, "Static Pushover Versus Dynamic Collapse Analysis of RC Buildings", *Engineering Structures*, 23, pp. 407-424.

Paulay, T. and M.J.N. Priestley, 1992, "Seismic Design of Reinforced Concrete and Masonry Buildings", John Wiley & Sons, New York, USA.

Senaviratna, K. and H. Krawinkler, 1997, "Evaluation of Inelastic MDOF Effects for Seismic Design", *The John A. Blume Earthquake Engineering Center*, Report No.

120, June 1997, Department of Civil and Environmental Engineering, Stanford University, CA, USA.